uOttawa

L'Université canadienne
Canada's university

FACULTÉ DES ÉTUDES SUPÉRIEURES ET POSTOCTORALES

uOttawa

L'Université canadienne
Canada's university

FACULTY OF GRADUATE AND POSDOCTORAL STUDIES

Etienne Dinel

AUTEUR DE LA THÈSE / AUTHOR OF THESIS

Ph.D. (Earth Sciences)

GRADE / DEGREE

Department of Earth Sciences

FACULTÉ, ÉCOLE, DÉPARTEMENT / FACULTY, SCHOOL, DEPARTMENT

Structural, Geochemical and Host Rock Control on Gold Mineralization in Tholeiitic Volcanic Rock of the Tisdale Assemblage, Timmins, Ontario : The Hoyle Pond Mine and the Vipond V10b Unit

TITRE DE LA THÈSE / TITLE OF THESIS

Anthony Fowler

DIRECTEUR (DIRECTRICE) DE LA THÈSE / THESIS SUPERVISOR

CO-DIRECTEUR (CO-DIRECTRICE) DE LA THÈSE / THESIS CO-SUPERVISOR

EXAMINATEURS (EXAMINATRICES) DE LA THÈSE / THESIS EXAMINERS

K. Benn (absent)

M. Hannington

J. Blenkinsop

B. Dubé

Gary W. Slater

Le Doyen de la Faculté des études supérieures et postdoctorales / Dean of the Faculty of Graduate and Postdoctoral Studies

Structural, geochemical and host rock control on gold mineralization in tholeiitic volcanic rock of the Tisdale assemblage, Timmins, Ontario; the Hoyle Pond mine and the Vipond V10b unit.

Etienne Dinel

Thesis submitted to the
Faculty of Graduate and Postdoctoral Studies
In partial fulfillment of the requirements
For the PhD degree in Earth Science

Ottawa-Carleton Geoscience Centre
Earth Sciences Department

University of Ottawa

Your file Votre référence
ISBN: 978-0-494-34125-4
Our file Notre référence
ISBN: 978-0-494-34125-4

Résumé

La mine Hoyle Pond est située à environ 15 km au nord-est de la ville de Timmins, Ontario, dans le camp aurifère de Porcupine. La mine est encaissée dans une suite de roche déformée de l'assemblage du Tisdale. Les données géochimique ainsi que l'étude structural ont permis de démontré la nature du contrôle sur la minéralisation aurifère par la roche encaissante. Les veines de quartz-carbonates aurifères de la mine Hoyle Pond sont encaissées dans une séquence de roches volcaniques homoclinales à polarité vers le sud associées avec les formations de Central et de Hershey Lake. Les roches volcaniques ont subi plusieurs épisodes de métamorphisme au faciès schistes verts dues à l'enfouissement, à la déformation tectonique et au passage de fluides hydrothermaux. Ces fluides ont été injectés pendant les épisodes de déformation D3 et D4, et associés à la formation de plis isoclinaux, de cisaillements et de failles inverses.

La zone d'altération associée à la minéralisation aurifère est enveloppée d'une zone de séricitisation qui est, à son tour, bordée par une zone d'albitisation. La zone de séricitisation est composée principalement de séricite (muscovite), de muscovite-chromifère (fuchsite), de dolomite ferrifère, d'arsénopyrite, de pyrite, de tourmaline et de graphite. L'alteration à séricite correspond également à un enrichissement en K_2O, Cr, SiO_2, CO_2, As, et S. La zone d'albitisation est composée principalement d'albite, de dolomite ferrifère et montre un enrichissement en Na_2O, CO_2 et SiO_2. De plus, un enrichissement en graphite caractérise la zone minéralisée, et résulte de réactions d'oxydation de la matière organique. Les éléments du groupe des terres rares, Al_2O_3, Zr, TiO_2 et Y, étaient relativement immobile durant le métamorphisme et la migration des fluides hydrothermaux, et ont été utilisé pour l'identification des types de roches volcaniques. Par contre, K_2O, Na_2O, Cr_2O_3, Rb, CO_2, CaO, Eu, FeO, MgO et certains éléments légers des terres rares (i.e. La) montrent une certaine mobilité.

Des réactions d'oxydoréduction sont responsables de la précipitation aurifère. Ces réactions sont le résultat d'un mélange entre fluides hydrothermaux oxydants riche en Cr^{6+}, K et Na, et des fluides réducteurs riche en complexe thiol-organo-aurifère (C_xH_x-

HS-Au), B et As. La source de l'or, de l'arsenic et du bore la plus plausible seraient les roches sédimentaires de l'assemblage de Porcupine, tandis que le Cr serait probablement dérivé de roches locales à composition mafique et ultramafique.

Deux générations de veines de cisaillement sont présentes à la mine Hoyle Pond. La première est encaissée dans des structures D3 aux contacts lithologiques, tandis que la seconde se retrouve dans des structures D4 aux contacts de coulées, ainsi que sur les deux flancs de plis isoclinaux. L'intensité de l'altération et de la déformation des roches de l'assemblage de Tisdale à la mine Hoyle Pond entraîne une certaine ambigüité quant à leur perméabilité le long des contacts lithologiques lors de la minéralisation. Cette perméabilité pourrait être de nature primaire, être le résultat d'un contraste de compétence lithologique lors de la déformation ou d'une combinaison des deux.

La formation de Vipond, plus particulièrement l'unité V10b ou "Chickenfeed" est l'hôte d'une minéralisation aurifère importante et fut longtemps interprétée comme des basaltes coussinés. Une cartographie détaillée combinée à des analyses géochimiques démontre que cette unité a une composition dacite tholéiitique et montre un faciès "lobe-coussiné" avec d'abondante hyaloclastites. Cette unité possédait une perméabilité intrinsèque élevée, une compétence et un ratio Fe/Mg élevés, ce qui en faisait un hôte idéal pour la minéralisation aurifère. À l'échelle de la région, deux types de gisement aurifère sont présents. Ceux, encaissés dans des roches volcaniques mafiques où le C (carbone) a possiblement joué un rôle dans la précipitation de l'or mobilisé par des fluides hydrothermaux, et ceux encaissés dans des roches volcaniques felsiques tholéiitique où un ratio Fe/Mg élevé a stabilisé et précipité la pyrite aurifère.

Abstract

The Hoyle Pond mine is located 15 km northeast of the city of Timmins, Ontario, in the Porcupine Gold Camp. It is hosted in deformed mafic to ultramafic volcanic rocks of the Tisdale assemblage. Geochemical data and structural analyses show interesting relations between host rock control and mineralization. The Au-bearing quartz-carbonate veins of the Hoyle Pond mine are hosted in a south-facing homoclinal sequence of stacked meta-volcanic rocks that are concordant with the Hershey Lake and Central formations of the Tisdale assemblage. The rocks were subjected to numerous sub-greenschist metamorphic events; however, detailed mapping shows that the hydrothermal mineralization took place during D3 and D4 events, and was associated with isoclinal folding, shearing, and thrusting.

The alteration associated with the gold mineralization consists of a sericite alteration, which is immediately enveloped by an albite alteration zone. The inner alteration zone is composed of sericite, Cr- mica "fuchsite", quartz, Fe-dolomite, arsenopyrite, pyrite, tourmaline and graphite, and has a concomitant enrichment in K_2O, Cr, SiO_2, CO_2, As, and S. The albite alteration zone is composed of albite, quartz and Fe-dolomite, and has an enrichment in Na_2O, CO_2 and SiO_2. In addition, carbon enrichment is also associated with mineralization. A pervasive graphite alteration envelopes the mineralization, and is the result of the oxidation of organic matter associated with Au mineralization. Rare Earth elements, Al_2O_3, Zr, TiO_2 and Y were relatively immobile with respect to alteration and can be used to identify rock type. However, K_2O, Na_2O, Cr_2O_3, Rb, CO_2, CaO, Eu, FeO, MgO and to a lesser extent La (LREE), were mobile during alteration.

Fluid mixing occurred between oxidizing fluids with soluble Cr^{6+} and other elements (e.g. K and Na), and reducing fluids carrying gold as a thiol-organic complex (Au-HS-C_xH_x), and other species, (e.g. B and As). The most plausible source of Au, As and B were the meta-sedimentary rocks of the surrounding Porcupine assemblage, whereas the Cr was likely derived from the ultramafic and mafic volcanic rocks.

Two generations of fault-fill veins are present at Hoyle Pond: those hosted in D3 structures at lithological contacts, and those associated with D4 structures and located at flow contacts and also on both limbs of isoclinal folds. Due to the intensity of alteration and deformation of the Tisdale assemblage rocks at Hoyle Pond, it remains an open question as to whether the permeability for the mineralization at flow contacts was primary in nature, the result of mechanical contrasts during deformation, or both.

The V10b or "chickenfeed" unit of the Tisdale Assemblage hosted significant gold mineralization, and was formerly thought to be composed of pillow basalt. Detailed mapping and geochemical work demonstrate that it is a pillow-lobe dacite of the tholeiitic suite associated with abundant hyaloclastite. The unit had a high intrinsic permeability, competency and Fe/Mg ratio making it an ideal host for gold. At a regional scale there are two types of Au deposits associated with tholeiitic volcanic rocks: Those hosted in mafic rocks in which C may be important in precipitating gold from hydrothermal solution, and those hosted in more felsic rocks wherein the high Fe/Mg stabilizes the formation of Au scavenging pyrite.

Acknowledgment

The project would not be a success without the support of the geology staff of the Porcupine Joint Venture, and particularly the help of Alastair Still, Ken Tylee, Erik Barr, Keith Green and Dave Gliddon. These individuals have provided their knowledge of a number of deposits in the Timmins Gold Camp, their recommendations for areas of focus of the work within the Hoyle Pond Mine, and have also provided maps, drill log, training, underground assistance and constructive criticism. I also thank David Rhys for his field trips and constructive discussions on the structural evolution of the Hoyle Pond deposit and the Timmins Gold camp. I also acknowledge a fruitful discussion with Howard Poulsen and Keith Benn for numerous discussions on Archean tectonics and many insightful reviews that considerably improved the focus and clarity of the submitted manuscripts. Ian Clark provided discussion on oxidation reactions in aqueous environment and Henri Dinel on organic geochemistry. We wish also to thank Porcupine Joint venture and Natural Science and Engineering Research Council for funding (University-Industry Grant). We thank also the Ontario Geological Survey for providing numerous geochemical analyses. We thank Tito Scaiano's and his group in the chemistry department at University of Ottawa for help with the ultraviolet absorption measurement and also Glenn Facey of the chemistry department for the NMR analysis. Peter Jones (Earth Sciences dept. Carleton University) provided Electron Micro-Probe analysis and Ron Hartree (Earth Sciences dept., University of Ottawa) provided the XRF analysis. The G.G. Hatch Stable Isotope Laboratory (University of Ottawa) provided the carbon isotopic analysis. Benoit-Michel Saumur provided able field assistant during the summer of 2004.

I sincerely thank Anthony D. Fowler for his advice, support, discussions and as a good friend through my graduate years and beyond. Thanks to John Ayer, for discussions of his views of the Abitibi architecture, geochemistry and co-supervision of the project. I thank my family and friends for there support through the challenging years. I thank my father who's been a role model in my philosophical and conquest to solve ongoing

scientific problems. Finally I thank my wife, Siba, for her support and the numerous encouragements she provided through the years of my project.

Table of Contents

List of Tables

List of Figures

List of Photos

Chapter 1.0 Introduction

My objective in writing the thesis is to better understand the geology of the Hoyle Pond Mine and provide a better understanding of the formation of Archean epigenetic gold deposits in the Abitibi greenstone belt. The geological setting of the Hoyle Pond gold mine is similar in style to other gold deposits in the Porcupine Gold camp, for example, Dome Mine, McIntyre Mine, Hollinger Mine, Buffalo-Ankerite Mine, Aunor Mine and Delnite Mine. The mineralization is generally hosted in highly deformed, sheared and folded mafic volcanic rocks of the Tisdale Assemblage (Ferguson, 1968; Pyke, 1982; and Brisbin, 1997), and associated alteration minerals. In addition, the alteration mineralogy at Hoyle Pond mine is also very common in the fore-mentioned deposits; intense carbonate alteration, sericite (muscovite), fuchsite (Cr-muscovite), albite, chlorite, graphite, tourmaline, arsenopyrite, pyrite and quartz characterize all these deposits (Brisbin, 1997; Melnik-Proud, 1992). The presence of these minerals is the result of the hydrothermal fluid alteration and regional metamorphism that affected the rocks and in some cases resulted in gold mineralization. They represent, to some extent, the footprint of the hydrothermal activity during mineralization and were investigated to better constrain the process and reactions that occurred during mineralization.

It is well known that epigenetic gold mineralization in the Abitibi greenstone belt is structurally controlled (Robert, 2001). However, this project was designed to investigate the concept of host rock control, in particular the physical and chemical properties of several key lithologies in the Timmins area.

1.1 General Overview

The Porcupine Gold Camp is situated in Neoarchean supracrustal rocks (volcanic and sedimentary) located within the western portion of the Abitibi greenstone belt (Fig. 1.1). The Abitibi belt is the world's largest Archean greenstone belt (Goodwin, 1977, Goodwin and Ridler, 1970), covering a surface area of approximately 200,000 km^2. The Abitibi greenstone belt is delimited by tectonic contacts with high metamorphic grade rocks of the Grenville Province (Proterozoic age) to the south and southeast; the Opatica subprovince to the North; and the Kapuskasing Structural Zone to the West. The Abitibi

greenstone belt rocks consist of supracrustal metavolcanic and metasedimentary rocks intruded by Archean granitic rocks, all metamorphosed from lower to upper greenschist facies and subsequently cut by Proterozoic diabase dykes.

The Porcupine gold camp is famous for its gold mines which collectively have been in continuous production since first being discovered early in the 20th century. The first gold showing in the camp was discovered in 1908 by a group of surveyors in the vicinity of Night Hawk Lake, 6km south of current location of the Hoyle Pond Mine. The discovery of the Hoyle Pond Mine is a relatively recent in the history of the area. The mine is located in Hoyle Township, within the Porcupine gold camp approximately 14km northeast of downtown Timmins, and approximately 4km north of the Pamour mine. Access to the mine is via a sinuous gravel road, the Hallnor road that passes through the coniferous forest of northern Ontario.

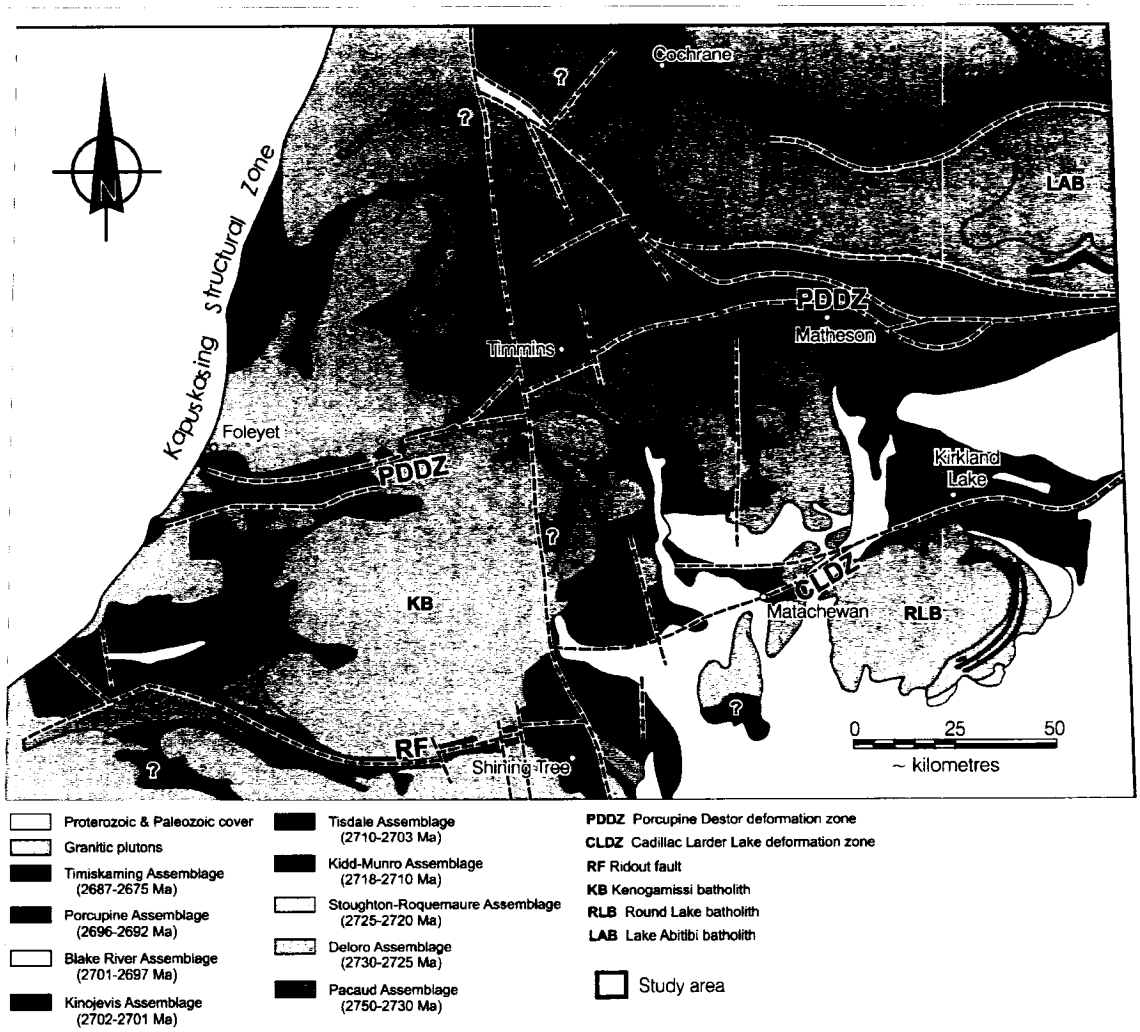

Figure 1.1 Western section of the Abitibi greenstone belt showing the distribution of the 9 volcano-sedimentary assemblages Note the location of the Hoyle Pond mine Northeast of Timmins (after Ayer et al. 2002).

1.2 History of the mine property

The Hoyle Pond discovery hole was drilled by Texas Gulf Sulfur Inc. in 1980 and development began in 1982 with the driving of a ramp. The first year of mining, in 1985, yielded 64,400 tonnes at an average grade of 13.0 gold grams per ton. The mine has been in continuous production since 1985 and was acquired by Kinross in 1993. The mine produced just over 2,000,000 oz of gold to this date. Since 1993, Kinross conducted exploration programs and underground development that added significant additional mineralization. The 1060fz, "B", "UP" and "A" veins were discovered during 1993 and a shaft was constructed along with an additional incline ramp that was built on the east side of the shaft to access the mineralization. The shaft extends to a depth of 815 meters and the development of the 1060 ramp is still today in progress at a depth below 1000m. During the summer of 2002, the Hoyle Pond Mine changed ownership to the Porcupine Joint Venture, a joint venture between Kinross Gold Corporation and Placer Dome Canada. In 2003-04, exploration was conducted to pursue mineralization in the 1060fz below the 720ml. The A vein system was proven to be rich at depth and an extension was followed through to the 980ml. The 1060fz B and UP veins were also extended to depth and a second shaft (winze) was sunk during the summer of 2005. Ore from the Hoyle Pond mine was initially processed at the Bell Creek mill, but since 2002, the ore has been processed at the Dome mine mill. In 2006, Placer Dome Canada was acquired by Goldcorp Inc.

1.3 Previous Work

The Hoyle Pond Mine is hosted in mafic-ultramafic volcanic rocks, considered to be part of the Tisdale assemblage (2710-2704 Ma, Ayer et al., 2005). This complexly deformed east-trending belt extends eastward from Tisdale Twp. into Hoyle Township and is overprinted by NE-trending asymmetric Z-folds (Fig. 1.2).

Early geological maps and reports on Hoyle Township are sparse. Rose (1924) first mapped Murphy, Hoyle and Matheson Twp and observed limited gold bearing quart-carbonate veining, but considered that the lack of porphyry intrusions was an indication of only poor economic potential. Hurst (1939) also mapped portions of the area, however,

it was not until Berry (1941) noted the presence of carbonatized pillow lavas that the area was considered prospective for economic gold mineralization. Hunt and Maharaj (1980) conducted a ground electromagnetic survey over the area and identified weak electromagnetic conductors.

Previous published geological work at Hoyle Pond mine focused on mapping the veins and describing the alteration found in pillowed Mg-tholeiitic basalts (Hodges, 1982). Downes et al. (1982), described the occurrence of unusual alteration, a graphite and carbonate alteration ("Grey Zone" alteration) associated with the Hoyle Pond Gold mineralization. Analyses conducted on graphite (Downes et al., 1982) showed that the carbon was likely organic in origin. These authors concluded that gold was possibly derived from underlying sedimentary rocks and introduced into "Grey Zone" and quartz veins through metamorphic processes.

Rye (1987) studied the geology and the geochemistry of the Hoyle Pond Mine. At that time only the north portion of the current mine was producing gold, which today coincides with the 8 to 16 vein area (see chapter 4). He described the overall volcano-sedimentary succession as an overturned sequence where carbonaceous argillites, in the 8-16 vein area, were forming the hanging wall of the deposits in shear zone contact with Mg-tholeiitic basalts corresponding to the Tisdale group. He also described gold bearing veins hosted in mafic pillowed to massive volcanic flows, in turn structurally underlain by komatiitic flows, and noted the importance of the grey zone alteration found in shear zones and its spatial association to gold mineralization. He described an alteration zonation around veins that consists of outer zones? of chlorite, paragonite, ankerite, calcite and a graphitic alteration enveloping an inner zone consisting of Fe-chlorite, muscovite, dolomite, calcite and graphite. Also he showed by mass balance calculation that the altered volcanic rocks underwent a loss of Mg, variable gains of alkali metals, silica and iron, and a large gain in Ca compared to unaltered tholeiitic rocks. Hodges (1982) also analysed the graphite by gas chromatography and determined that 22% of the carbon is organic, consisting mainly of benzene, toluene, xylene and hydrocarbon fragments, indicating a biogenic source. The most likely origin for the organic matter was

considered to be the meta-sedimentary rocks found to the north. Downes et al. (1982) and Hodges (1982) proposed that carbon was introduced by hydrothermal fluids that migrated along active shears into hydraulically brecciated tholeiitic rocks. Other studies at the Owl Creek mine (1km west of Hoyle Pond) focussed on the isotope chemistry of ^{13}C (Wilson and Rucklidge, 1986). Ratios of ^{13}C were in the range of -27 to -33.4 per mil, a very light source, and consistent with a biogenic origin. Elliot (1984) studied the geochemical, mineralogical and stable isotope of nodular pyrite in shale at Owl Creek Mine, and proposed biogenic reduction of sulphate as a source of sulphur for the sulphide minerals.

The distribution and role of carbonaceous materials in gold deposits of the Timmins gold camp has been studied by Springer (1983, 1984 a & b, 1985). She suggested that gold enrichment reflects introduction of gold and deposition in carbonaceous rocks through a process of reduction occurring in the margins of the quartz veins. King et al. (1963) observed, in graphitic shear zones associated with gold bearing veins, a dense, fully aromatic compound with 84.2% carbon and low remnant volatiles, which resembles most closely a fractionated kerabitumen. In addition, they suggested that the carbon was remobilized from black shales by hydrothermal fluids. More detailed work at Owl Creek and Hoyle Pond mine was carried out by Wilson (1986) and Wilson and Rucklidge (1984, 1986) and they concluded that the reduced carbonaceous rock was related to the gold mineralization.

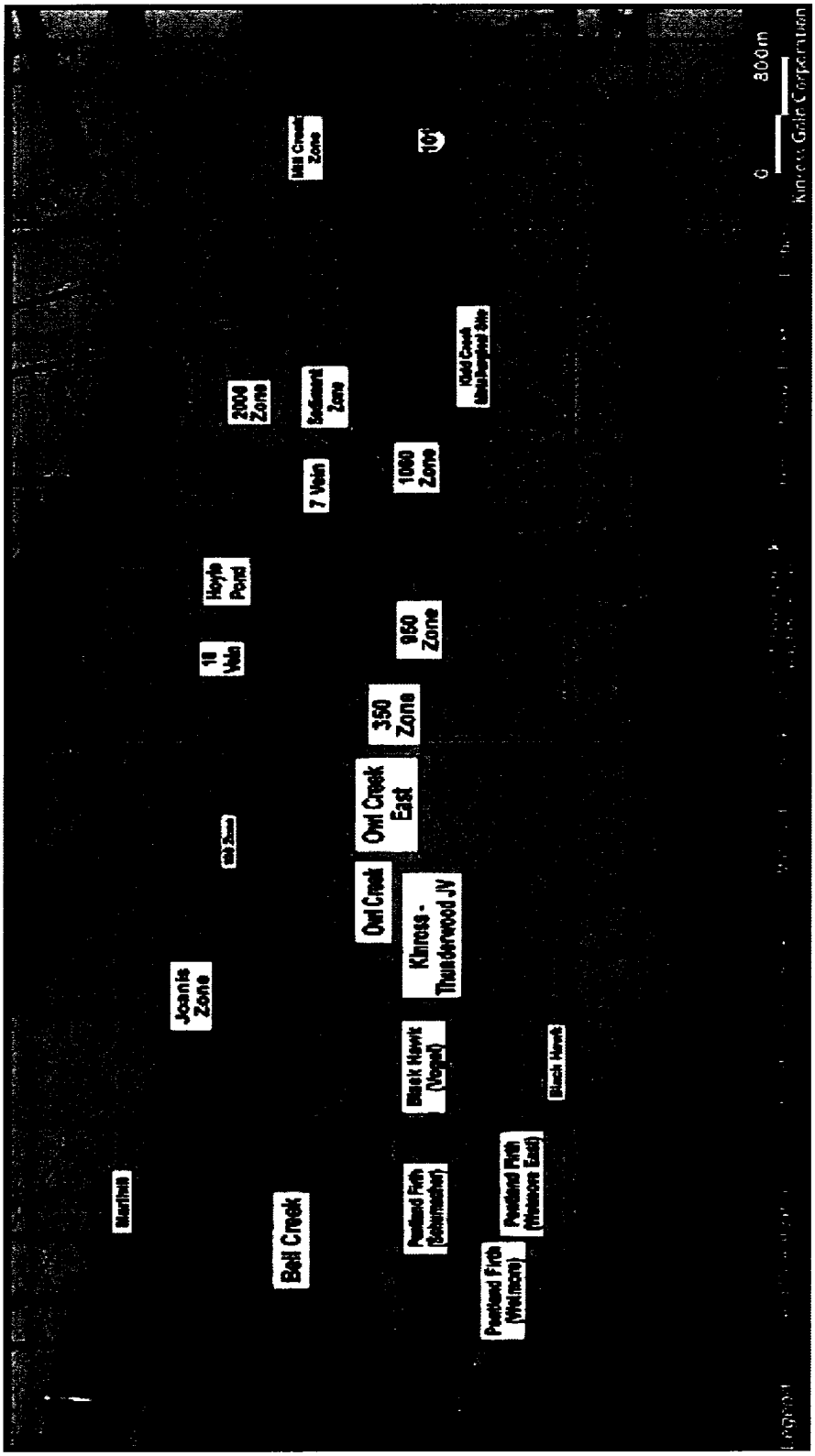

Figure 1.2 Surface Geology map of the Hoyle Pond mine area, units in green and purple represent mafic and ultramafic volcanic rocks of the Tisdale assemblage, and units in grey the sedimentary rocks of the Porcupine assemblage. These km-scale blocks of supracrustal rocks are interpreted to have been imbricated along east-trending thrust faults overprinted by northeast-trending asymmetric Z-folds.

1.4 Objectives

The main aim of this project is to identify the factors within the host rock contributing and controlling gold mineralization. Epigenetic gold mineralization is controlled principally by structures, such as shear zones (e.g. Robert and Poulsen, 2001). At the Hoyle Pond Mine the mineralization consist of free gold in quartz-carbonate veins, thus implying a structure control. However, the structures are themselves associated with primary lithological features. Thus to determine the control on gold mineralization, it is important to study the host lithologies as well as the veins. In addition to Hoyle Pond work on host rock control was also done on the V10B or so-called "chicken-feed" formation of the Vipond Formation (Tisdale Assemblage adjacent to the site of the former Vipond gold mine

Specific objectives are:

1. Determining the Hoyle Pond mine volcanic rock type based on geochemistry and lithofacies.
2. Determining the alteration mineralogy and geochemistry associated with the gold mineralization.
3. Correlation of Hoyle Pond Mine stratigraphy within the Tisdale assemblage, i.e. what formation(s) of the Tisdale assemblage are host to the Hoyle Pond mine?
4. Is there a correlation between rocks with high Fe/Mg ratio and gold mineralization, similar to the relationships determined by Ropchan et al. (2002) at the Holloway Mine, or is gold precipitation at Hoyle Pond related to other factors?
5. What are the physical properties of the host rocks? Is there a density and/or porosity control? What makes a good host rock for gold mineralization?
6. Can we determine good path finders? or fluid paths using lithogeochemistry?
7. What are the chemical reactions that caused gold to precipitate?

These questions are addressed in detail in the following chapters.

1.5 Organization

This thesis is composed of 7 chapters. Chapter 2 presents the methodology, sample preparation and laboratory analysis employed during the project. Chapter 3 focuses on the general overview of the geology of Abitibi greenstone belt and the Porcupine gold camp, wherein I summarize the 8 volcano-sedimentary rock assemblages, based on rock type, general geochemistry and geochronology. In addition, a summary description of the major structure of the Abitibi greenstone belt is also given. Chapters 4, 5 and 6 have been written as manuscripts for publication and therefore the geological descriptions are to some extent repetitive. However considerable effort has been made to minimise redundancy. Chapter 4, is written as a manuscript titled "**Litho-geochemical and stratigraphic controls on gold mineralization within the meta-volcanic rocks of the Hoyle Pond Mine, Timmins, Ontario"** (accepted by guest editor of a special volume of Economic Geology) and describes the rock units at the Hoyle Pond Mine based on field observation and geochemistry. It also details the deformation history, and describes the alteration associated with the gold mineralization, based on petrographical analysis and geochemistry. Chapter 5, also written as a manuscript is titled **"The geochemistry of the alteration at the Hoyle Pond Mine, Timmins, Ontario; Chromium and Graphite enrichment spatially associated with gold-bearing veins resulting from hydrothermal fluid mixing"**(in prep), wherein I propose a new model for the precipitation of gold based on alteration, particularly the properties of Cr and graphite associated to gold mineralization. Chapter 6 discusses the host-rock control on gold mineralization. The focus of this section is on the physical and geochemical properties of volcanic rocks that host gold mineralization. A section of this chapter is written (with Fowler and Saumur) as a manuscript and is titled **"Spherulitic aphyric pillow-lobe meta-tholeiitic dacite lava of the Timmins area, Ontario, Canada: A new Archean facies and its implications for lode-gold mineralization"** (under revision in the special volume of Economic Geology) and describes the lithofacies, geochemical properties of a marker horizon for gold exploration in the Porcupine gold camp. Chapter 7 concludes the thesis and provides a list of contributions.

1.6 Co-authorship

Chapters 4, 5 and 6 have been written as manuscript format for publication. Numerous co-authors have participated in the elaboration of the papers. They provided supervision, instruction, interpretation roles and commented on initial drafts of the manuscripts. In addition, some have helped with funding of analytical work. As a senior author, I have been responsible of the drafting, writing, editing and primary interpretation of data and observation and submission of manuscript to journals. The paper in chapter 6. represents a joint effort with Fowler and B.Sc. student Saumur. I was involved in the field work, supervision of the B.Sc. thesis and was also responsible for the interpretation of the geochemical data. Saumur was responsible for the detailed mapping, sampling, petrography and the construction of the viscosity model. Fowler initiated the project, provided the crystallization model, and did much of the writing. List of co-authors and theirs affiliations, as well as journals to which manuscripts have been, or will be submitted, follows.

Chapter 4: 2007, accepted by guest editor, Economic Geology. Co-authors Dr Anthony D. Fowler, University of Ottawa, Ottawa, Ontario, K1N 6N5; John Ayer, Ontario Geological Survey, Sudbury, Ontario, P3E 6B5; Alastair Still, Ken Tylee and Erik Barr, Goldcorp, Timmins, Ontario, P0N 1H0.

Chapter 5, 2007, in prep, Mineralium Deposita, Co-authors Dr. Anthony D. Fowler, University of Ottawa, Ottawa, Ontario, K1N 6N5.

Chapter 6, 2007, submitted, 4/06 and received back for revision 1/07. The paper is currently under revisions and will be re-submitted 3/07 , Economic Geology, Co-authors, Benoit-Michel Saumur and Dr. Anthony D. Fowler, University of Ottawa, Ottawa, Ontario, K1N 6N5.

Chapter 2.0 Methodology

This chapter covers the different methods used during the project, from mapping to laboratory analysis. The first part of the chapter focuses of the mapping and sampling used to determine the lithology, structure and alteration. The second part consists of a description of the sample preparation and laboratory analysis completed on the samples. Finally, the last section covers the various statistical analyses utilized for the interpretation of the geochemical database.

2.1 Mapping

During the summers of 2003 and 2004, 4 levels in the mine were mapped in detail. No outcrop is exposed at Hoyle Pond as it is covered by 20-30m of overburden. Mapping was completed by underground access, sampling, drill core logging and core sampling. The 440meter level (ml) was first investigated during the summer of 2003, focusing on a north-south cross section in order to define the rock units, structure and stratigraphy of the mine (see generalized geological map, Fig. 2.1). During the summer of 2004, reconnaissance mapping was completed on the 720ml to determine the continuity of the stratigraphy at depth. Detailed mapping was also completed on the 880ml, along the north-south 1060 cross-cut to understand the origin and kinematics of the 1060 fault zone. In addition, I mapped and sampled the ~400ml (Hoyle Pond mine 3 level), to help define the upper level extensions of the north volcanic package in the mine and to observe the correlation between vein emplacement and lithological contacts. Mapping and sampling in this area was restricted as the result of limited access underground.

Other methods of mapping consisted of logging diamond drill core to study rock units, alteration and mineralizations. The various mafic volcanic rock types, high-Mg and Fe rich tholeiitic basalts cannot be discriminated by observation of drill core, although ultramafic volcanic rocks can mapped in comparison to mafic volcanic. In addition, some alteration can be identified from drill core by staining of carbonates (potassium ferro-cyanide) or by modal observation.

2.2 Sample distribution

Figure 2.1 illustrates the various rock units and structures of the mine, details on sample locations are listed in appendix II and on maps of the 440ml and 720ml (appendix III). The sampling was strategic, focusing on two objectives: first, the identification of the rock units, and second, characterization of the alteration. On the 440ml samples were collected from units that appeared to have variations in morphology, mineral assemblages or lithofacies (in older sections of the mine accumulated grime could not be removed despite washing with a degreasing agent). Also samples were collected from the 440ml, 950 zone South Volcanic Package (SVP) and the 16 Vein area North Volcanic Package (NVP), at an interval of 1m so as to detail the chemistry and mineral variation approaching gold bearing quartz-carbonate veins, and also to characterize the alteration patterns. Samples were collected on the 720ml to correlate with the stratigraphy of the 440ml. The focus of the 1m interval sampling on the 720ml, was the 1060 fault zone (1060fz) and its numerous gold bearing veins (B1N, B1, B1S and B3 veins, see Fig. 2.2) A total of 112 samples were collected along 3 cross sections, across 4 principal veins (B1N, B1, B1S and B3 veins, see Fig. 2.2) of the main ore body, the 1060fz, to define the stratigraphy and document the mineral and chemical alteration in the ore zones and also characterize the correlations of gold bearing veins to lithology contacts.

In total ~500 samples were collected, 355 were analyzed for whole-rock geochemistry (major oxide and trace elements) from the Hoyle Pond 3 Level (220ml), the 440ml, the 720m level and the 880m level and drill core, 350 polished thin sections were made for petrography and electron microprobe analyses. From the 355 chemical analyses, 112 analyses were from the 1060fz, for defining the alteration pattern on the 720m level ore zone. In addition, similar analyses were conducted in other areas of the mine, 50 from the 1060fz 880ml, ~40 from the 440m level 950 zone and ~100 from the Hoyle Pond vein area (13-14-15-16 veins) on the 440m level (Fig. 2.1) and on the 3 level (~400ml). Geochemical results are provided in Appendix II.

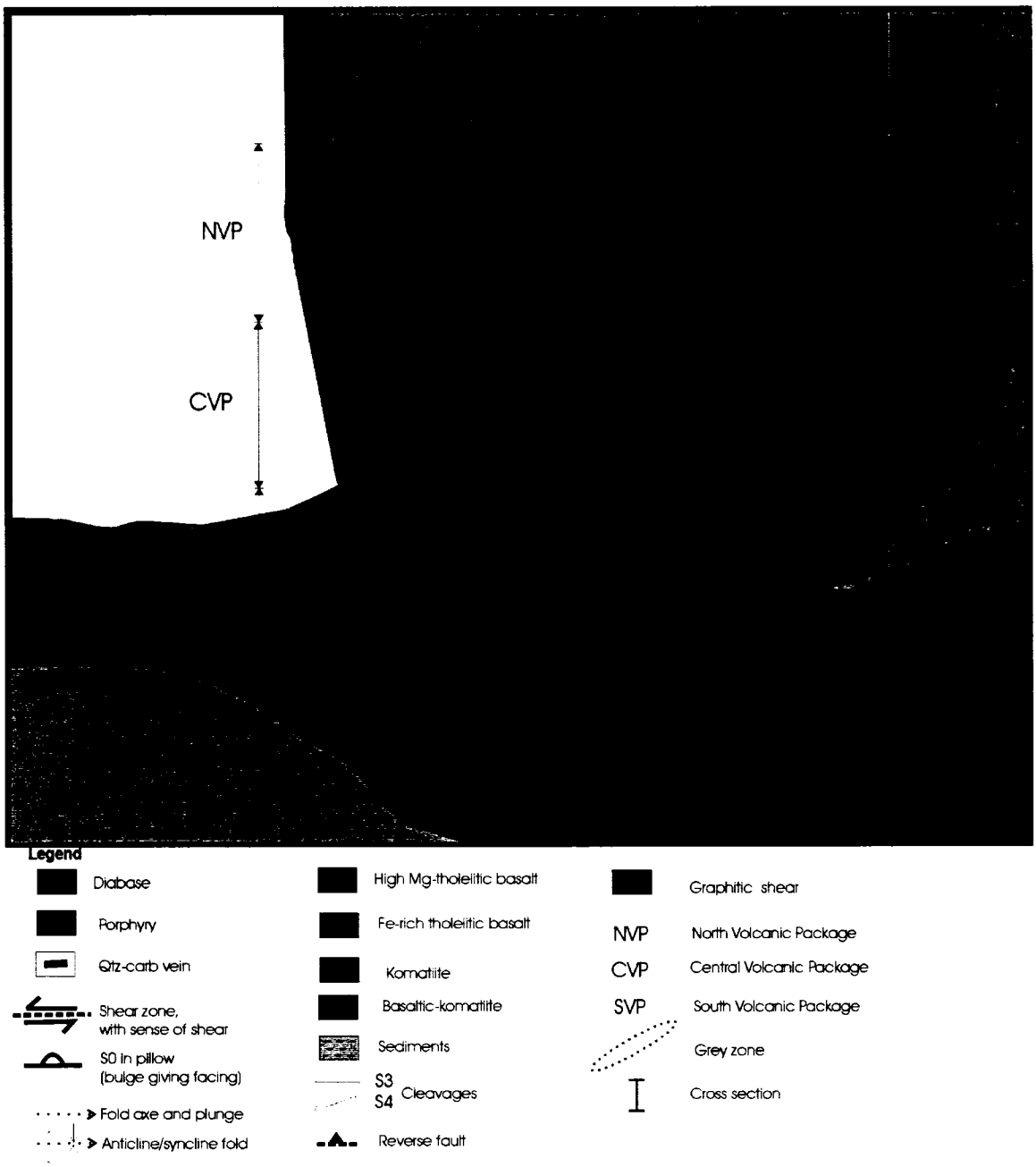

Figure 2.1 Geological map of the Hoyle Pond Mine, compiled from the 440 ml and 720 ml levels maps showing the distribution and structural pattern of the rock units. Certain veins and mineralized zones are labeled using the mine convention e.g. 950 stands for 950 zone, I-beams indicate detailed traverse areas across veins and the large stratigraphic cross sections, the rectangle shows location of figure 2.2 (see Dinel et al. accepted by guest editor, Chapter 4).

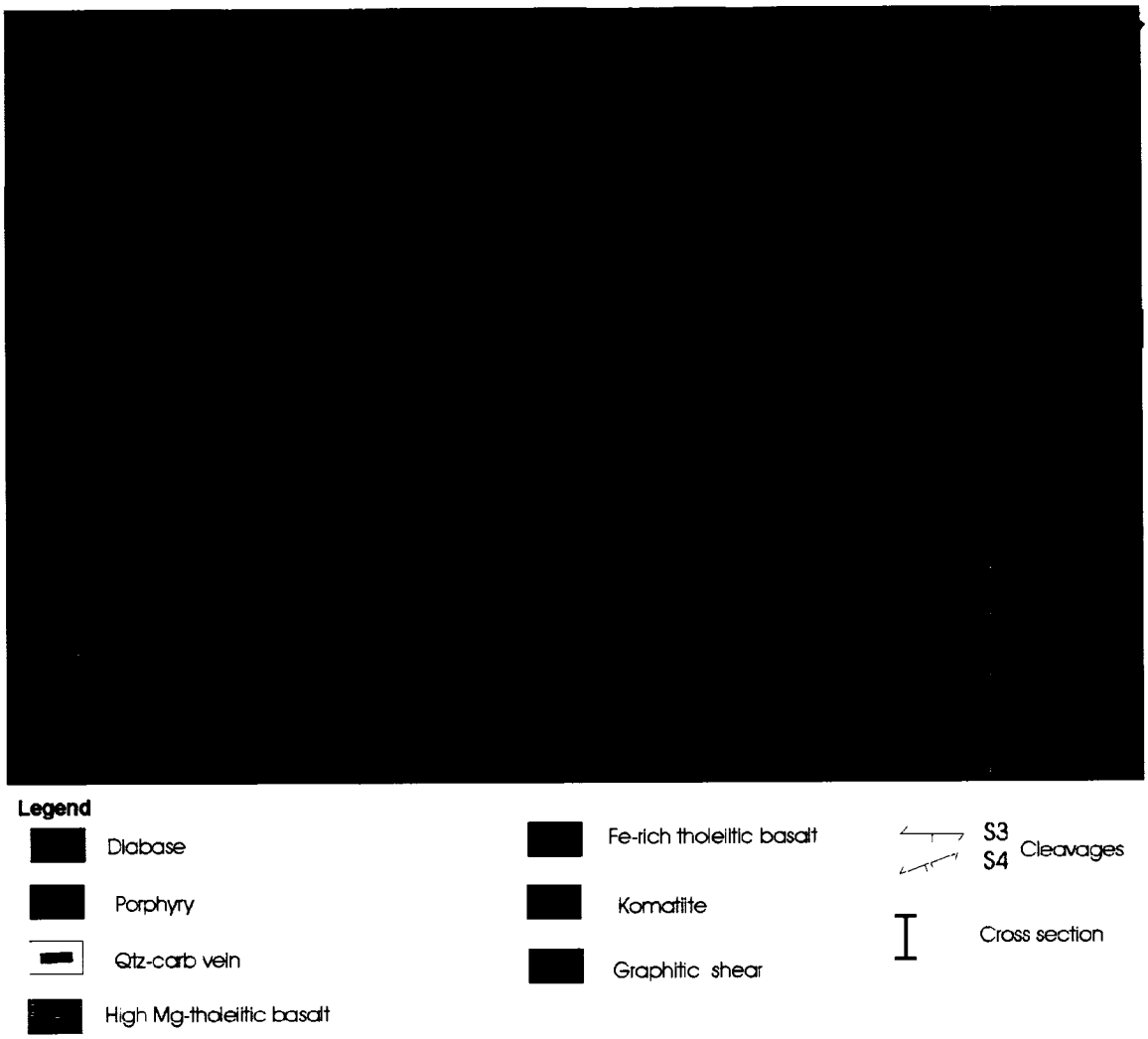

Figure 2.2 Geological map extracted from figure 2.1 showing the distribution of the B1, B1N, B1S, B3 vein in the 1060fz (720ml). I-beams, showing where detail mapping and sampling through the mineralization zones, was completed.

2.3 Sample preparation and laboratory analysis

The samples collected were cleaned of all blast powder and washed through a sieve. Small cm size blocks were cut for thin sectioning selected on the basis of texture and/or structure. For geochemical analyses the samples were crushed using a steel plate Jaw Crusher, to less than ~1cm fragments and finally pulverized to a very fine powder using a porcelain shatter box. In 2003 the Ontario Geosciences Lab executed all the sample preparation (160 samples). For logistical reasons the 2004 samples (195 samples) were all prepared at the University of Ottawa. X-ray fluorescence analysis were completed on fused disks composed of 1g of sample mixed with 4g of flux, which consist of 78.53% lithium tetraborate ($Li_2B_4O_7$) and 21.47% lithium metaborate fused in platinum crucibles. The lithium metaborate and lithium tetraborate are non-oxidizing fluxes (Chao and Sanzolone, 1992).

For the organic matter analysis, the samples needed supplementary preparation consisting of removing all silica from the sample by hydrofluoric acid, followed by drying at room temperature and sodium hydroxide extractions. For chromium analyses, magnetic separation of Cr-muscovite was executed with a Frantz iso-dynamic separator.

Laboratory analysis

The major oxides were analysed using a Philips 2400 spectrometer controlled by the software XRF SuperQ. The method used for determination of iron (XRF) did not discriminate the Fe^{2+} and Fe^{3+} oxidation state, but determined total iron content as Fe3+. However, ferrous iron was determined by the modified Wilson (1960) technique (Whipple 1974). It requires adding ammonium meta-vanadate to the samples to oxidize all the Fe^{2+} and hydrofluoric acid (HF) to the solution for 24hours, to permit sample dissolution. HF is a weak, non-organic acid that utilizes the complexing ability of F^- to breakdown the silicate mineral lattice. Subsequently boric acid (to neutralize the HF), phosphoric/sulphuric and ferrous ammonium sulphate solution were added to the solution. Barium diphenylamine p-sulphonic acid is used as indicator in the solution and Potassium Dichromate is used as a titrant. The total volume of titrant added is proportional to volume of ferrous iron in the solution and used to calculate the proportion of Fe^{2+} and Fe^{3+}.

The trace elements were analyzed by means of an Inductively Coupled Plasma Mass Spectrometer (ICP-MS) at the Ontario Geoscience Laboratories after the rock powder had been digested for 14 days in a closed beaker using the following acids; hydrochloric, hydrofluoric, perchloric and nitric acids (Tomlinson et al., 1999). This method proves to be the most efficient digestion process. The analyses were conducted using an Elan 9000 ICP-MS with sample introduction by solution nebulisation using a cross-flow nebuliser, Ryton Scott-type double pass spray chamber, alumina injector, and Pt cones.

Analyses were carried out in peak hopping mode, with 5 sweeps per replicate and 8 replicates per analysis. The isotopes used for each element, including the Ru and Re internal standards, along with the dwell times per isotope, are summarized in the following table.

Element	Isotope	Dwell Time (μs)	Element	Isotope	Dwell Time (μs)
Rb	85	20	Gd	160	50
Sr	86	20	Tb	159	50
Y	89	20	Dy	163	50
Zr	90	20	Ho	165	50
Nb	93	20	Er	167	50
Cs	133	50	Tm	169	100
Ba	135	20	Yb	173	75
La	139	20	Lu	175	75
Ce	140	20	Hf	178	100
Pr	141	20	Ta	181	150
Nd	143	20	Th	232	20
Sm	147	50	U	238	35
Eu	151	50			

Table 2.1 ICP-MS dwell time for particular isotopes.

The instrument is calibrated after every 30 samples by analyzing a matrix-matched blank and 100 ppb multi-elemental solutions and interpolating the calculated sensitivities between calibration blocks as a function of analysis number. An instrument control solution is analyzed every few samples to monitor instrumental performance.

Data are removed from the instrument as raw intensity data as ASCII text files and are processed off-line using customized in-house Visual Basic programs. These programs parse the data, normalize the intensities to the internal standard, perform a background subtraction (determined from a blank matrix-matched solution), correct for oxygen-based interferences, before calculating the variation in sensitivity through the run and the concentrations for each sample based on the mass of sample used (0.200 ± 0.01 g), the volume of the sample after digestion (100mL), and any additional dilutions applied (normally 1:10).

Carbon Isotopes were measure by Vario EL III (Elementar, Germany) and DeltaPlus IRMS (ThermoFinnigan, Germany) to define the ^{13}C ratios, at the G.G. Hatch isotope

laboratory of the University of Ottawa. Traces of organic matter were isolated by NaOH extraction (hydrolization of organic matter) of the graphite. Analyses were conducted using a spectrophotometer to verify if traces of organic matter were present, by measuring the absorption of light in the ultraviolet wavelength range. To detail the organic matter present, we conducted a NMR (Nuclear Magnetic Resonance) analysis at the University of Ottawa, using a Bruker ASX 200 using a 7mm triple resonance CPMAS probe in double resonance mode. The spectrum was acquired with ramped cross polarization, magic angle spinning and high power proton decoupling. The data were collected over 57 hours, with proton pulse at 3.9 microseconds interval at 90°, with a contact time of 10 milliseconds and relaxation time of 2 seconds.

Geochronology

Two age dating methods were employed, organic matter was dated using carbon isotope dating (^{14}C) executed at the IsoTrace laboratory facility at the University of Toronto. In addition, U/Pb dating on zircons from two samples was done using a Thermal Ionization Mass Spectrometer at the Jack Satterly laboratory at the University of Toronto (see Ayer et al. (2005) for details).

2.4 Statistical analysis

In order to evaluate errors 3 samples were analysed in repetition (5 times) (in blind fashion) and 2 blank samples were analysed (clear quartz crystals) to identify contaminants. In addition data were provided by the laboratory on analyses of standards. The error was calculated with a confidence interval of 95% using the method of Kretz (1985). The error in the major oxides is less than 0.5% of the reported value and for trace elements, less than 10%.

In addition to graphical methods to study the geochemical distributions, Principal Component Analysis (PCA) was employed to treat sample independently. Because there are 355 samples, each having ~50 analyses, it is impractical to thoroughly search the data set for inter-element correlation using binary or ternary plots; hence PCA was implemented in order to examine the set as a whole. The PCA is a multivariate technique for examining relationship among several quantitative variables. The method reduces the dimensionality of the dataset into a vector space so as to identify meaningful variations and identify the chemical tendency of the sample populations. All PCA analyzes were calculated in ppm with oxygen anions removed so as to correlate independent variables. Each principal component is a linear combination of the original variables with coefficients equal to eigenvectors of the covariance matrix. The eigenvectors are taken as unit-normalized values. The principal components are sorted by ascending order of the eigenvalues, which are equal to the variance of components. The first principal component has the largest variance of any unit-length linear combination of the observed variables and the last one has the smallest variance of the linear combination of the original variables. The eigenvectors are orthogonal, so the principal components represent jointly perpendicular directions through the space of the original variables. The software SYSplus was used to calculate the covariance matrices and the vectors, and present the data in the form of a binary plot. PCA were performed with SYSplus, and the interpretation was in accord with the conceptual approach of Gabriel (1971) and Jolicoeur and Mosimann (1960).

Chapter 3.0 Regional and Hoyle Pond Geology

The Neoarchean Abitibi Greenstone Belt, part of the Superior Province in the Canadian Shield, is unique amongst greenstone belts of the Canadian Shield as it is composed of a large proportion of supracrustal relative to intrusive rocks (e.g. Goodwin and Ridler, 1977). Moreover it is the largest greenstone belt in the world, has a generally low metamorphic grade, contains a diversity of mineral deposit types, and is one of the best documented greenstone belts in the world.

3.1 Geology of Abitibi greenstone belt

The belt extends east-west for more than 800km, from northern Québec to northern Ontario (see Fig. 3.1). It consist primarily of metavolcanic, metasedimentary and metagranitic rock that range in age from 2750-2660Ma. The belt is bounded to the north by the Neoarchean plutonic and metasedimentary rock of the Opatica subprovince (Card and Ciesielski, 1986), to the south by the Neoarchean metasedimentary rock of the Pontiac subprovince, to the southeast by high-grade gneisses and granitoids of the Grenville Province that were deformed by northwest directed thrusting during the MesoProterozoic (e.g. Wynne-Edwards, 1972; Sangster and Bourne , 1982; Carr et al., 2000) and finally to the west by the Kapuskasing Structural zone, a Paleoproterozoic crustal-scale overthrust (Percival and Card, 1983, 1985).

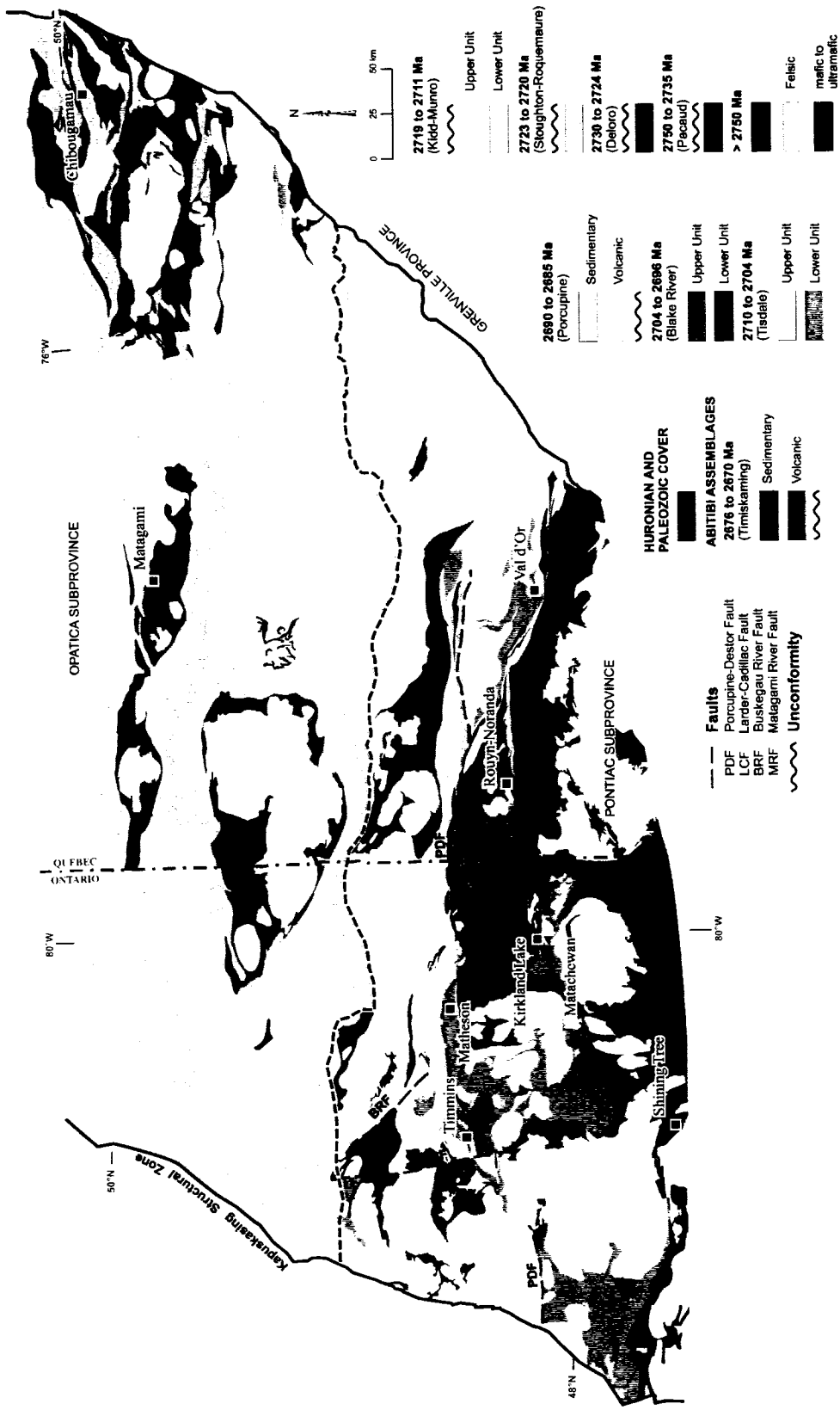

Figure 3.1 Geological Map of the Abitibi Greenstone Belt. Notice the distribution of the 8 volcano-sedimentary rock assemblages (from Thurston et al., under revision).

3.1.1 Abitibi greenstone belt Assemblages

The Abitibi Greenstone belt greenstone belt has been subdivided into two zones. The northern belt consists of abundant tonalite-trondjemite-granodiorite (TTG) intrusions, large anorthosite complexes, interspersed with volcanic rocks of greenschist or higher grade regional metamorphism (Dimroth et al., 1983). The southern belt is characterized by fewer TTG intrusions, and abundant ultramafic to felsic flows of greenschist or lower regional metamorphic grade (Dimroth et al., 1983). The belt is crosscut by numerous east-west trending deformation zones, including the Porcupine Destor Deformation Zone (PDDZ) and the Cadillac Larder Lake Deformation Zone (CLLDZ) in the south. These shear zones can extend for more than 400km and are spatially associated with the major gold deposits in the Abitibi greenstone belt (Robert, 2001).

In Ontario the Abitibi greenstone belt was subdivided into 52 assemblages by Jackson and Fyon (1991) based on the concept that many of these assemblage represented different allochthonous microplates that were accreted together to form the Abitibi subprovince. Similarly accretion of the northern and southern parts of the Abitibi across the PDDZ representing a plate tectonic "suture zone" was proposed by Mueller et al., (1996). Ayer et al. (2002, 2005) revised the stratigraphy of the Abitibi into belt-wide autochthonous assemblages based on over 200 high precision U-Pb zircon geochronological analyses (Ayer et al., 2002, 2005) and were subsequently subjected to tectonic deformation (folding and faulting) (see Fig. 3.1). The 8 assemblages described below are described by their geochemical signatures and facies characteristics.

Pacaud Assemblage

The Pacaud assemblage represents the oldest assemblage in the Abitibi greenstone belt, and ranges from about 2750 to 2735 Ma (Ayer et al., 2002). It is mainly observed in outcrop on the margins of large intrusive batholiths (Fig. 3.1) (e.g. Kenogamissi and Round Lake batholith) and is estimated to be 5 km thick. The assemblage consists predominantly of tholeiitic mafic to intermediate flows, calc-alkaline felsic to intermediate volcanic rocks, minor ultramafic and felsic volcanic rocks and local lenses

of sulpfide-facies iron formation adjacent to batholiths (e.g. Round Lake) (Lawton, 1959; Ayer et al., 2002, Ayer et al., 2005).

Pristine outcrops of the Pacaud are observed in the Shinning Tree area where it is in contact with the overlying Deloro assemblage. The geochemical signature suggests that the tholeiitic volcanic rocks are high-Fe and high-Mg basalts (Oliver et al., 2000) and chemically similar to those of the Kidd Munro and Tisdale assemblages (discussed below). The Pacaud tholeiitic volcanic rocks have slightly depleted LREE (Light Rare Earth Element, La, Ce, Pr, Nd, Pm, Sm) and unfractionated HREE (Heavy Rare Earth Element, GD, Tb, Dy, Ho, Er, Tm, Yb, Lu). The chondritic normalized La/Yb ratio ranges from 0.6-1.5 and there is a slight depletion in HFSE, Nb and Ti. Oliver et al., (2000) proposed that the Pacaud was formed due to an up-welling mantle plume which triggered moderately high degrees of partial melting in enriched spinel lherzolite mantle.

Deloro Assemblage

The Deloro assemblage is a very extensive regional stratigraphic package of rocks, with consistent age and maximum thickness of 5 km. It ranges in age from approximately 2730 to 2724 Ma (Ayer et al., 2002) and is best exposed in the Shaw Dome area, southeast of Timmins. It consists primarily of pillowed, commonly amygdaloidal and plagioclase-phyric, calc-alkaline basalt and andesite with local mafic tholeiitic volcanic rocks. In addition, Pyke (1982) has observed a thin layer of ultramafic komatiite flows in the Peterlong Lake area South of Timmins thought to be at the base of the Deloro assemblage, although it is not exposed in the Timmins area. In the Shining Tree area the base of the Deloro consists of extensive units of chert breccia. The central portion of this assemblage consists of approximately 3 km of calc-alkaline basalts and andesites that are overlain by pyroclastic rocks. The upper section of the assemblage is dominated by calc-alkaline rhyolitic to dacitic tuff and lapilli tuff. A thin layer of banded iron formation (BIF) overlies the uppermost section and caps the Deloro stratigraphy (Pyke, 1982). The assemblage is also found typically in the margins of large batholiths where it conformably overlies the Pacaud assemblage. The upper sequence of the Deloro is conformably overlain by the rocks of the Stoughton-Roquemaure volcanic rocks.

However, in the Porcupine gold camp, the Deloro assemblage is overlain unconformably by the Tisdale assemblage (described below).

The Deloro volcanic rock's geochemistry indicates predominantly calc-alkaline major element affinities with high degree of LREE fractionation ($(La/Lu)_{CN}$ approximately (5-50) and pronounced Nb and Ta depletion (Dostal and Mueller, 1996; Oliver et al., 2000; Lafrance et al., 2000). Dostal and Mueller (1997) suggest based on the geochemical signatures that the magmatism was subduction-related arc basalts and back-arc basin basalts.

Stoughton-Roquemaure Assemblage

The Stoughton-Roquemaure age ranges from 2723 to 2720 Ma and largely consists of tholeiitic mafic volcanic rocks, local ultramafic and felsic volcanic rocks with a maximum thickness of about 12km. Dostal and Mueller (1997) described the base of the Stoughton-Roquemaure as being composed of tholeiitic basalts, basaltic-komatiites and komatiites. Locally, minor felsic lapilli tuffs volcanic flow crop out at its base. Jensen and Langford (1985) described the Stoughton-Roquemaure volcanic rocks south of the Lake Abitbi Batholith as being composed of komatiite and basaltic komatiite, high-Mg and high-Fe tholeiites, finely layered chert, iron formation and felsic tuff horizon. These units were intruded by coarse grained gabbroic, peridotitic and dunitic intrusions.

The Stoughton-Roquemaure tholeiitic volcanic rocks are MORB-like, with chondritic normalized La/Yb ratio of 0.8 to 2.4, slight negative Eu anomalies, near chondritic Nb/La ratios, and depleted ε_{Nd} values (+2.5-+4.7, no errors reported) thus reflecting derivation from primitive mantle (Dostal and Mueller, 1997; Barrie, 1999). The komatiites have depleted ε_{Nd} values (+2.5 - +5.6; Stone et al., 1995; Dostal and Mueller, 1997) and comprise a gradation from Al-depleted komatiites to Al-undepleted komatiites, suggesting mixing between depleted mantle source regions (Sproule et al., 2002). It is suggested that the komatiites are derived from a garnet-harzburgite or –peridotite mantle source where partial melting commenced at a higher pressure (greater depth) than for the Kidd Munro and Tisdale Komatiites (discussed below). The petrogenesis model for the

Stoughton-Roquemaure komatiites suggest a mantle plume rising beneath an arc (the Deloro Ass.) with the basalts produce from the cooler plume head at a shallower depth (Dostal and Mueller, 1997). The basal contact of the Stoughton-Roquemaure appears to be conformable with the Deloro volcanic rocks east of Lake Abitibi in Québec, but south of Kirkland Lake the Stoughton-Roquemaure overlies the Pacaud assemblage. This 20Ma age difference is expressed by an unconformity, and could mean that the Deloro volcanic rocks do not extend uniformly throughout the Abitibi.

Kidd Munro Assemblage

The Kidd Munro assemblage ranges in age from 2719-2710 Ma and conformably overlies the Stoughton-Roquemaure. The Kidd Munro extends from Loveland Twp. (northwest Timmins) to Stoughton Twp. (75km east of Matheson) and into Québec with a maximum thickness of approximately 5km (Fig. 3.1). Some Kidd Munro age volcanic rocks were observed south of the Shining Tree area. It is subdivided into a lower sequence and an upper sequence based on the geochemical signature of the volcanic rocks.

The lower sequence is largely dominated by intermediate to felsic calc-alkaline volcanic rocks. Calc-alkaline intermediate to felsic volcanic rocks have ε_{Nd} values from 2.4 to 3.3 reflecting their derivation from depleted mantle (Ayer et al., 2002). The upper sequence is dominated by tholeiitic mafic and komatiitic rocks with localized flows of tholeiitic felsic volcanic rock and graphitic sedimentary units. In the east, the basal contact of the upper sequence appears to be conformable with the calc-alkaline volcanic rocks of the lower sequence, thus in the west the basal unit is in a faulted contact with the younger rocks of the Porcupine assemblage (described below) and the upper margins lie in faulted contact with rocks of the Timiskaming assemblage (described below). Tholeiitic basalts are MORB-like with flat REE patterns at 10-20 times chondrites values and flat primitive mantle normalized patterns (Barrie, 1999). The komatiites define a bimodal Al_2O_3/TiO_2 population with both aluminium depleted komatiites (Al_2O_3/TiO_2 approximately 10) and aluminium undepleted komatiites (Al_2O_3/TiO_2 approximately 22) (Sproule et al., 2002).

Tisdale Assemblage

The Tisdale assemblage consists of an extensive terrain of ultramafic-mafic to intermediate volcanic rocks (see Fig. 3.1) that range in ages from 2710 to 2704 Ma (Ayer et al. 2002).

Locally, the Tisdale assemblage was previously subdivided into different groups such as the Northern, Central, Vipond and Gold Center (Jones 1948). Today's classification, subdivides it into 4 formations, the Hershey Lake, Central, Vipond and Gold Center formations (Ferguson, 1968, Pyke 1982) and will described in detail below. In the Timmins area, the upper Tisdale is unconformably overlain by the Porcupine assemblage decribed in detail in the next section.

Blake River Assemblage

The Blake River assemblage is best preserved in the east central part of the South Abitibi Greenstone Belt (see Fig. 3.1), between the PDDZ and the CLLDZ in the Blake River syncline, east of Sheraton Twp and into Québec. The Blake River assemblage consists of an amalgamation of two previous assemblages the lower portion was formerly the Kinojevis assemblage (Ayer et al. 2002) and the upper portion, the Blake River assemblage.

The lower portion of the Blake River assemblage consists of volcanic rocks that range in age from 2704 to 2701 Ma (Ayer et al., 2005). Previously identified as the Kinojevis, the rocks consist predominantly of tholeiitic mafic volcanic rocks to tholeiitic felsic volcanic rocks and locally turbiditic metasedimentary rocks. The basal contact conformably overlies the Tisdale assemblage and is truncated to the north by the PDDZ and to the south by the CLLDZ. Ropchan et al. (2002) have identified local andesite, dacite and rhyolite volcanic flows in the upper sequence. Subsequently minor clastic sedimentary horizons were observed locally. The thickness of the lower portion is estimated at 6km based on seismic data. The lower portions are composed of high-Mg tholeiitic basalt and Fe-tholeiitic basalt and show general upward iron enrichment (Fowler and Jensen, 1989). Chondritic normalised patterns of the volcanic rock are flat and show an enrichment in

more evolved units, which in turn have greater Eu depletions. Fowler and Jensen (1989) suggest that the assemblage evolved by fractional crystallization of olivine, pyroxene and Fe-Ti oxides. In addition, they suggest that a plume dominated of mid-oceanic ridge to explain the upward iron enrichment of tholeiitic andesite, dacite and rhyolite, similar to what observed in Iceland. Basal tholeiitic basalt and upper sequence tholeiitic rhyolitic flows yield ε_{Nd} values of 2.7 and 3.3 respectively (Ayer et al., 2002).

The upper portion ranges in age from 2701 to 2696 Ma (Ayer et al., 2005) and consists of calc-alkaline basaltic and andesitic volcanic flows with local bi-modal tholeiitic basalts and rhyolites, and felsic to intermediate coherent flows and pyroclastic volcanic flows. The thickness of the upper portion is very ambiguous, Verpaelst et al. (1995) estimated 10-12km based on seismic synthesis, Calvert and Ludden (1999) interpret that this part of the Abitibi greenstone belt is overlain by 19km of volcanic rocks, based again on seismic profiles. Jackson et al., (1995) identified concave reflective profiles coinciding with the basal contact of the upper section on the Ontario side resulting in an estimate of the upper portion of the Blake River of 5-6 km. Geochemically, the upper portion's calc-alkaline suites display moderately fractionated LREE ($(La/Yb)_{CN}$ approximately 2-5) with no evidence of iron enrichment (Ayer et al., 2002), similar to rock observed in modern subduction zones. The tholeiites have MORB-like REE pattern with slight Eu negative anomalies. It is suggested that the suite of tholeiitic rocks formed in a back-arc environment (Laflèche et al., 1992).

Porcupine Assemblage

The Porcupine assemblage consists of dominantly metasedimentary rocks that range in age from 2690 to 2685 Ma (Ayer et al., 2005) (Fig 3.1). The assemblage is composed primarily of sandstone, siltstone and mudstones as incomplete Bouma sequences that were deposited in a distal to deep marine environment, by turbidity currents (Born, 1995). The Porcupine metasedimentary rocks are in part restricted to a long corridor north of the PDDZ from Bristol Twp., west Timmins to Guibord Twp, representing a distance of approximately 110km and another 150km into province of Québec (Brisbin, 1997). In addition, we can observe in map pattern (Figure 1.2) that km-scale blocks, of the Tisdale,

Kidd Munro and Stoughton-Roquemaure assemblage, are imbricated by thrust faults into rocks of the Porcupine. The Porcupine assemblage is subdivided into 4 different formations in the Timmins area; the Krist, the Hoyle, the Beatty and the Whitney formation. They are classified based on their sedimentary facies and discussed in detail in the following sections.

Timiskaming Assemblage

The Timiskaming assemblage consists of dominantly metasedimentary rocks ranging in age from 2676 to 2670 Ma (Ayer et al., 2005). The assemblage is restricted to a narrow corridor of clastic metasedimentary rocks along the major deformation zone, the PDDZ in Timmins and Matheson, and the CLLDZ from Kirkland Lake extending into Québec (see Fig. 3.1). In Timmins area, the assemblage consists of a corridor that extends from Bristol Twp. to Stock Twp. The Timiskaming is mainly composed of polymictic conglomerate, sandstone, deposited in subaerial fan, fluvial and deltaic environments (Mueller et al., 1994; Born, 1995). Locally felsic calc-alkaline pyroclastic and volcanoclastic rocks are observed in the Timmins area and Kirkland Lake area. The Timiskaming rocks of the Timmins area will be discussed in detail below.

Intrusion framework

In general five types of intrusion are observed in the southern part of the Abitibi greenstone belt. The first two belong to a group of regional scale felsic to intermediate batholiths and mafic to ultramafic intrusions ranging from 2745 Ma to 2696 Ma and 2740 to 2700 Ma in age. They are interpreted to represent synvolcanic intrusions (Ayer et al., 2005). The felsics to intermediates intrusions are part of the TTG suites (trondjemite-tonalite-granodiorite) (Polat and Kerrich, 2001). The second group consist of mafic and ultramafic intrusions ranging in composition from gabbro to peridotite (Houlé et al., under revision; Sproule et al., 2002; Ayer et al., 2005) and are dominantly coeval with the Tisdale assemblage but may also be correlative to other volcanic rock such as the Kidd-Munro and Blake River (Ayer et al 2002, 2005).

The third type of intrusion consists of syntectonic plutons and numerous smaller porphyry intrusions ranging in age from 2695 to 2670 Ma (Ayer et al., 2005). The early group consist of 2695 to 2685 Ma intrusions of tonalite, granodiorite, diorite and feldspar-quartz porphyries. They vary from massive to foliated and are present as stocks near larger older batholiths (e.g. Round Lake batholith). In the Timmins area, most syntectonic intrusion range in age from to 2691 to 2687 Ma and help to constrain timing of deformation and mineralization. The later group of syntectonic intrusion range in age from 2680 to 2672 Ma, and are thus broadly coeval with the Timiskaming assemblage. They occur in the vicinity of the PDDZ and LLCDZ and are typically alkalic in composition, consisting of monzonite, syenite and albitite.

The fourth group represent late tectonic intrusions that range in age from 2670 to 2660 Ma, typically massive they commonly are found within the large batholiths and consist of biotitic granite, pegmatite and muscovite granite.

A fifth intrusion type, of minor importance in the Abitibi greenstone belt, consists of Proterozoic age diabase dyke swarms. The southwest-northeast oriented Abitibi diabase dyke swarm is composed of equigranular plagioclase and orthopyroxene and yields an U/Pb age of 1141Ma +- 1 (Krogh et al., 1987),whereas, the north-south oriented

Matachewan diabase dyke is composed of plagioclase and orthopyroxene with distinctive glomeroporphyritic plagioclase and yield an U/Pb age of 2473 Ma +16/-9 (Heaman, 1997).

3.1.2 Stratigraphy of the Porcupine Gold camp

The geology of the Porcupine Gold camp is composed of 4 distinct volcanic assemblages (Fig. 3.2). These are the Deloro, Tisdale, Porcupine and the Timiskaming assemblages defined by their geochronological age (U/Pb TIMS), lithofacies, tectonic affinity and geochemical signatures (Fig. 3.3). All the rock types in the camp are metamorphosed to at least the lower greenschist facies; however for simplicity from hereon the prefix "meta" will be omitted.

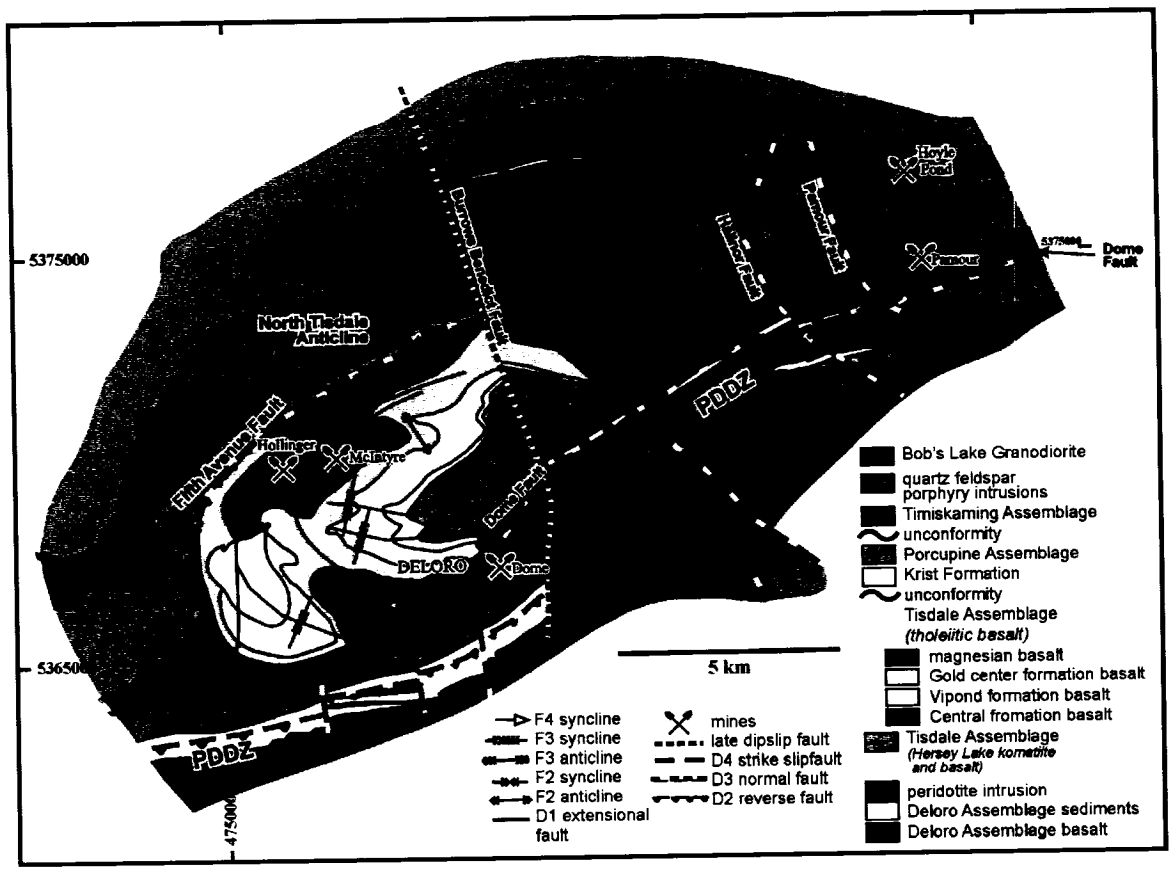

Figure 3.2 Geological map of the Timmins gold camp, notice the distribution of the volcano-sedimentary rock assemblages, and the folding complexity of the area. Four deformation events are illustrated on the map which resulted in 4 different generations of folds as interpreted by Bateman et al., 2005.

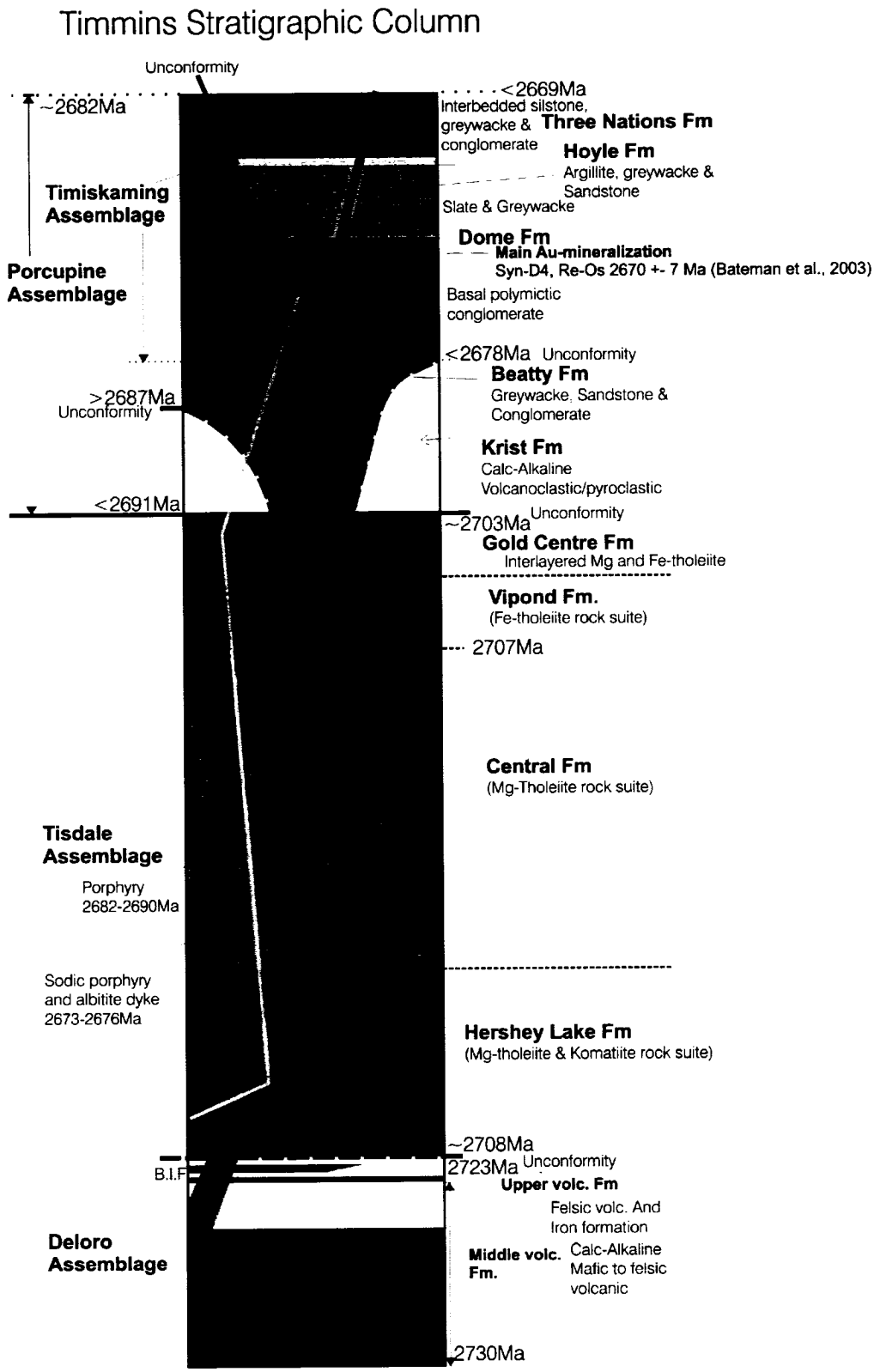

Figure 3.3 Stratigraphic column of the Timmins Area, illustrating the field and structural relationship between the 4 main volcano-sedimentary assemblages and age constraints of the stratigraphic units (modified from Barr, internal company report, 2005).

Deloro Assemblage

To recapitulate, the Deloro assemblage is the lowermost stratigraphic unit observed in the vicinity of the Timmins Gold Camp (Fig. 3.3). It ranges in age from approximately 2730 to 2724 Ma (Ayer et al., 2002) and is restricted to the area south of the PDDZ. Here it consists of mafic to felsic calc-alkaline volcanic rocks. The uppermost part of the assemblage also contains regionally extensive oxide iron formation units (BIF). The assemblage thickness is estimated to be up to about 5 km, and is disconformably or unconformably overlain by the volcanic rocks of the Tisdale assemblage.

Tisdale Assemblage

The Tisdale assemblage is mainly composed of mafic volcanic rocks of the tholeiitic suite, with some komatiitic and locally intermediate to felsic volcanic rocks (see Chapter 6) (Fig. 3.3). It ranges in age from 2710 to 2704Ma (Ayer et al., 2005). The maximum apparent thickness of the Tisdale assemblage in the Porcupine camp is 3440m (Brisbin, 1997), measured in northeastern Tisdale Township, between the axis of the North Tisdale anticline and the upper contact with the Krist formation. Some authors have reported that the Porcupine Destor Deformation Zone (PDDZ) is located at the base of the Tisdale assemblage (Pyke, 1982). However, field mapping by Dinel and others (Vaillancourt et al., 1999) show that the location of the PDDZ is neither restricted to the base of the Tisdale assemblage nor is it a unique fault surface. Instead it is a large (100 to 500m) corridor of ductile deformation overprinting the contact. The Tisdale assemblage is an important unit for gold exploration (Dunbar, 1948), because the majority of the economic deposits are contained within it, particularly the Central and Vipond formations. The Tisdale Group was subdivided into 4 formations by Ferguson (1968), Dunbar (1948) & Jones (1948).

Hershey Lake Formation

At the base of the Tisdale assemblage, the Hershey Lake formation is composed of mainly Mg-rich mafic volcanic (high-Mg tholeiitic basalts) and komatiite lava flows. The estimated thickness is approximately 600m (Brisbin, 1997), on the south limb of the North Tisdale anticline. This formation is dominantly composed of intercalated

polysutured ultramafic and pillowed mafic flows along the North side of the PDDZ in northern Deloro Twp (Pyke, 1982; Brisbin 1997) and southeastern Tisdale Twp.

The ultramafic flows are described as komatiite and basaltic komatiite based on the geochemical criteria of Arndt (1975) and on the Jensen Cation plot (Jensen, 1976). Geochemicaly the komatiites have a flat REE pattern with chondrite ratios <7. Their MgO content varies from 10-18 w%, for basaltic komatiite, >18 w% for komatiite. In the field the ultramafic flows of the Hershey Lake formation can be distinguished from the mafic flows by their color index. Komatiites are dark grey, on fresh surfaces and have an orangey (buff-tan) color on weathered surfaces. Also, they can also be distinguished because the komatiites often have polygonal suturing. In addition, some komatiite flows have spinifex textures and joint-like structures caused by serpentinization. Talc and carbonate alteration are distinctive.

The basaltic komatiites are intercalated with komatiites and tholeiitic mafic flows and are present as various facies, such as massive flows, pillowed flows and flow breccias. In general they can be distinguished from komatiites (>18% MgO) in the field as they tend to lack prominent spinifex textured olivine and they generally have less serpentine.

The tholeiitic mafic volcanic rocks within the Hershey Lake formation are identical to those of the overlying Central formation and are distinguished from them only in that they are intercalated with ultramafic flows.

Central Formation

The Central formation (Fig. 3.3) is approximately 450m (Brisbin, 1997) thick and is mainly composed of mafic volcanic flows, intercalated massive, pillowed and pillow breccia flows. On average the pillows are 1m by 0.5m in size in section with selvages 1-5 cm thick. The rocks of the Central formation are high-Mg tholeiites very similar to the Hershey Lake Fm. rock, except they do not have intercalated ultramafic volcanic rocks. Some variolitic rocks are present locally, and the upper contacts of some of the variolitic flows are characterized by beds of black argillites or cherty clasts.

Pyke (1982) described the composition of the mafic volcanic flows of the Central formation, as forming a continuum from magnesium tholeiitic basalts through iron tholeiitic basalts on the basis of the Jensen Cation Diagram. The increase in iron content is reflected in the dark green color of these flows relative to the light green color of the Mg tholeiites.

Vipond Formation

The Vipond formation (Fig. 3.3) is characterized by very distinctive high-Fe tholeiitic variolitic pillowed mafic volcanic flows and variolitic hyaloclastic mafic flows which are intercalated with massive mafic flows and carbonaceous argillite. The Vipond formation is a key marker in the gold camp; a majority of deposits in the Timmins Gold Camp are spatially associated with the Vipond fm. (Brisbin, 1997). The Vipond formation as been thoroughly studied and several flows have been identified which are key for stratigraphic correlation in the camp.

> The 99 Flow is the basal unit of the Vipond fm overlying the Central Fm. It is typically a dark green, fine grained, massive, leucoxene-bearing mafic flow characterized by interflow argillites that intermittently occur at its lower and upper contacts. The C17 unit is a carbonaceous argillite that locally underlies the 99 flow. The V7 unit is a laminated argillite and greywacke unit that locally overlies the 99 flow, and contains graphite and some breccia fragments.
>
> The V8 is the most prominent rock unit on Ferguson's (1968) geological map containing variolitic pillow flows. The unit is dominantly High Fe-tholeiites, with various textures, from massive flows and spherulitic pillow flows. The spherulites can vary from chloritic to albite and are concentrated in pillow rims. The V9 is a grey to black argillite unit containing graphite with some breccia fragment that locally overlies the V8.

Overlying the V8 is the V10 unit. It is of intermediate composition and is dominated by volcanic fragmental rocks locally with pillowed, lobe and breccia facies (V10B) (Dinel et al., under revision, see chapter 6). The breccia facies have been called "chicken feed" or broken varioles (Brisbin, 1997).

Gold Centre Formation

The Gold Centre formation (Fig 3.3) is the uppermost volcanic sequence of the Tisdale assemblage and is dominated by massive leucoxene-bearing flows and associated pillowed and pillow breccia (Brisbin, 1997).

Tisdale sedimentary rocks

The Tisdale assemblage is a volcanic sequence interlayered with sparse carbonaceous argillites. In addition, two interflow units are described by Mason et al. (1988). They consists of 5-30 m thick units of interbedded wackes and argillites with basal matrix supported oligomictic conglomerate, intercalated with lower Tisdale strata mafic and ultramafic volcanic flows.

Porcupine Assemblage

The Porcupine assemblage is mainly composed of wackes, local polymictic conglomerate, siltstone and mudstone. The basal unit of the Porcupine assemblage consists of calc-alkaline felsic pyroclastic termed the Krist formation which unconformably overlies the Tisdale volcanic rock. Buffam (1948) reported: "This unconformity is well preserved in the Moneta Mine area where it is reported that the volcanic pyroclastic rocks overly the mafic sequence with mark angularity". Geochronology has shown a crystallization age of the Krist formation at 2687.5 Ma (Ayer et al. 2005). The porphyry intrusions (discussed below) in the Timmins area are identical in age and geochemistry with that of the Krist formation indicating there are subvolcanic intrusions (MacDonald and Piercey 2005). The Beatty formation, which consists of a turbiditic sedimentary sequence within the core of the Porcupine syncline, overlies the Krist formation (Fig. 3.3). Around the periphery of

the Tisdale assemblage in the Timmins are the turbiditic sedimentary units of the Hoyle formation. The Hoyle is time equivalent with the Beatty formation, but is more extensive, extending from the Bristol Twp. in the west to Guibord Twp in the east. The Hoyle formation lies north of the PDDZ and unconformably overlies numerous older volcanic rocks of the Tisdale and Kidd Munro assemblages. The Whitney formation consists of a turbiditic sequence south of the PDDZ in Whitney and Cody Twp. The Whitney formation occurs in the core of a synclinal fold immediately overlying the Krist formation on the west limb and the Tisdale assemblage on the east limb of the fold.

Timiskaming Assemblage

The Timiskaming assemblage in the Timmins area is mainly confined to narrow units of polymictic conglomerates and sandstone and some local volcaniclastic rock. To the South the assemblage is truncated by the PDDZ and to the north by an angular unconformity with rocks of the Porcupine and the Tisdale assemblages. The assemblage consists of polymictic, poorly sorted conglomerate and sandstone deposited in sub-aerial alluvial-fan, fluvial and deltaic environments (Jackson et al., 1994; Mueller et al. 1994). The clasts consist of cobbles and pebbles of granitic rocks and pebbles of ultramafic, mafic to felsic volcanic rocks, banded iron formation (jasperoid clasts) and some fragments of quartz-carbonate veins, supported by fine-grained sandstone. In some locations the sandstone is finely laminated with cross stratification having dune-scale wavelengths.

Brisbin (1997) described the Timiskaming Group (now part of Timiskaming assemblage) as a partially preserved sequence of clastic sedimentary rocks that unconformably overlie folded sedimentary and volcanic rocks. The Timiskaming extends easterly to Stock Township where it is truncated by the PDDZ. The lowermost portion of the assemblage is called the Dome formation and is composed of turbidites interbedded with argillites, wackes and polymictic conglomerate approximately 400m thick. This unit is overlain by the Three Nations formation composed of cross stratified sandstone, conglomerates and turbidites. The conglomerates are again polymictic, poorly sorted, massive and poorly bedded.

Albitite dykes are found locally cutting early phases of gold mineralization associated with disseminated Cu and Mo (e.g. McIntyre Mine). These dikes are coeval with the Timiskaming assemblage (Ayer et al 2005).

3.1.3 Structural Evolution

The Timmins gold camp is marked by at least 6 deformation events, D1-D6 (Bateman et al. 2005 and Bleeker, 1995). The first two events D1 and D2 are marked by folding, and angular unconformities with local developed fabric, but fabric associated with these events were not observed at the Hoyle Pond Mine. D1 deformation was related to plutonism, uplift and early folding and is most evident in map pattern within the Porcupine camp wherein the Tisdale contact with the unconformably overlying Porcupine assemblage rocks locally represents a low angle erosional surface in which the Vipond and Gold Centre formations (and most likely the overlying 2703-2696 Ma Blake River assemblage) have been removed (Fig. 3.2, Bateman et al., 2005). D2 deformation resulted in east-west trending folds and thrust faults (see Fig. 3.2) evident in the Tisdale and Porcupine assemblages locally truncated by an angular unconformity between the Porcupine and Timiskaming assemblages which is preserved in outcrop in South Porcupine (Bateman et al., 2005). D3 is represented by east-west-trending isoclinal folds with a steeply dipping axial planar S3 foliation, parallel to lithological contacts. Bateman (2005) relates the timing of D3 to be syn to post Timiskaming. D4 is also recognized as a steeply dipping foliation, S4, oriented ~060-070°, approximately 15 degrees counterclockwise to S3 and is axial planar to isoclinal 1st order F4 folds near the 1060fz of the Hoyle Pond Mine and also to second order asymmetric F4 folds. The intersection lineation of the S3 (east-west) and S4 (ENE-WSW) appears to be sub parallel to the mineralization plunge at the Hollinger-McIntyre deposits (Melnik-Proud, 1992) and also at Hoyle Pond mine. The D5 event is represented by a moderately dipping crenulation cleavage S5 with two general strikes; 045° and 335°. The crenulation cleavage S5 is axial planar to asymmetric Z-folds and S-folds. The D6 event is only visible on vertical surfaces as a sub-horizontal crenulation cleavage axial planar to mm to m scale sub-horizontal folds (Dinel, 2001). D5 and D6 represent slight rotation of the stress field.

The major shear zones in the area are expressed by corridors of intense foliation. In the Timmins area the PDDZ is proximal to a number of the major gold deposits and represents a corridor of intense deformation that is commonly the locus of tight to isoclinal folding. The Hollinger-McIntyre and the Dome mines occur on distinct deformation zones representing sub-parallel splays.

3.1.4 Regional metamorphism

The metamorphic grade in the Timmins area generally ranges from upper to lower greenschist facies. All the volcano-sedimentary rocks in the Timmins area were subjected to greenschist facies metamorphism, with amphibolite facies in the vicinity of some of granitic plutons (Thompson, 2005). It has been argued and discussed that the regional metamorphism in the area is syn-deformation and peaked during D3 and D4 (Thompson, 2005). However, if previous greenschist metamorphism occurred prior to this one, it would be very difficult to differentiate them. However, metamorphic overprinting provides evidence that more than one metamorphic event occurred. Throughout the area, undeformed volcanic rocks generally consist of a mineral assemblage of albite-chlorite with porosity infilling by calcite with minor quartz and chlorite. Delicate primary volcanic textures such as spherulites, perlitic fractures and spinifex-textured olivine are commonly well preserved. The chlorite is pervasive but does not define a tectonic fabric. In shear zones (e.g. PDDZ) and zones of mineralization (e.g. 1060fz), the metamorphic mineral assemblage is also composed of chlorite-albite; however the carbonate is typically composed of dolomite-ferroan-dolomite and ankerite. Typically the preferred orientation of chlorite defines the deformation induced petrofabric and primary textures are overprinted or obliterated. Moreover, these rock contain unfoliated chlorite-rich microlithons enveloped by a cleavage domain defined by a preferred alignment of chlorite and other minerals. One could argue that the chlorite observed in the cleavage domains is simply reoriented chlorite crystals.

We suggest there is evidence for more than one stage of greenschist metamorphism; a passive greenschist metamorphic event associated with volcanism and burial (e.g. the Tisdale assemblage formation) followed by the regional scale fabric forming event. Indeed Thompson (2005) shows a first stage of burial metamorphism and greenschist metamorphism of the Tisdale rocks prior to 2685Ma and a second main stage metamorphic event after 2774Ma i.e. post-Timiskaming sediment deposition. Powell et al. (1995) suggest that regional metamorphism post-date major deformation zone (e.g. PDDZ), metamorphic grade being continuous across structures and post 2674 Ma in the Rouyn-Noranda area of Québec.

3.2 Economic Geology of the Porcupine Gold camp

Gold production in the Timmins camp started in the early 1900's (Bachmann, 2005). The discovery of gold was made by a group of surveyors cutting an east-west baseline from Matheson to Timmins which today would correspond to highway 101. E.M. Burwash and W.A. Parks recorded gold showings in exposed quartz veins on a portage route from the Matagami River to Whitney Twp. After this discovery, numbers of prospectors searched the boreal forest of the Timmins area. The big gold rush started after the discovery of gold in the Kirkland Lake area. The discovery of a gold rich dome shape white quartz veins in 1909, by Jack Wilson, W.S. Edwards and Dr. T.N. Jamieson, led to the opening of the Dome mine recently stop their underground production (1909-2005) and recently re-opened (2006). At approximately the same time Benny Hollinger and Alex Gilles discovered a gold showing west of the Wilson crew, on Hollinger Hill where mineralization was also observed in quartz vein. This area would later be the site of the famous Hollinger and McIntyre Mines. The Hollinger-McIntyre deposits were in constant production from 1910 to 1970 and produced most of the gold mined in the Timmins Gold camp. In addition to having produced gold the McIntyre mine also produced significant amount of silver, copper and molybdenum. Since then numbers of gold producing mines operated during the 20th century, the following tables detail the years of production and metals extraction.

Mine Name	Township	Years in Producion	Tons milled	Oz. Au	Au (Kg)	Grades (oz/t.)	Grades (g/t.)
Ankerite/March	Deloro	1926-35	317,769	61,039	1,730.46	0.19	5.39
Aquarius	Macklem	1984, 1988-1989	139,634	27,117	768.77	0.19	5.39
Aunor Pamour (#3)	Deloro	1940-1984	8,482,174	2,502,214	70,937.77	0.3	8.51
Banner	Whitney	1927-28,-33,-35	315	670	18.99	0.13	3.69
Bell Creek	Hoyle	1987-91, 92-94	576,017	112,729	3,195.87	0.196	5.56
Bonetal	Whitney	1941-1951	352,254	51,510	1,460.31	0.15	4.25
Bonwhit	Whitney	1951-54	200,555	67,940	1,926.10	0.34	9.64
Broulan Porcupine	Whitney	1939-53	1,146,059	240,660	6,822.71	0.21	5.95
Broulan Reef Mine	Whitney	1915-65	2,144,507	498,932	14,144.72	0.23	6.52
Buffalo Ankerite	Deloro	1926-53,78	4,993,929	957,292	27,139.23	0.19	5.39
Cincinnati	Deloro	1914, 1922-24	3,200	736	20.87	0.23	6.52
Concordia	Deloro	1935	230	16	0.45	0.07	1.98
Coniaurum/Carium	Tisdale	1913-18, 1928-61	4,464,006	1,109,574	31,456.42	0.25	7.09
Crown	Tisdale	1913-21	226,180	138,330	3,921.66	0.61	17.29
Davidson-Tisdale	Tisdale	1918-20, 1988	53,221	2,438	69.12	0.26	7.37
Delnite	Deloro	1937-64	3,847,364	920,404	26,093.45	0.2	5.67
Open pit		1987-88	56,067	3,602	102.12	0.77	21.83
Desantis	Ogden	1933, 39-42, 61-64	196,928	35,842	1,016.12	0.18	5.10
Dome	Tisdale	1910-2004	91,717,560	15,256,616	432,525.06	0.165	4.68
Faymar	Deloro	1940-42	119,181	21,851	619.48	0.18	5.10
Fuller (Vedron)	Tisdale	1940-44	44,028	6,566	186.15	0.15	4.25
Gillies Lake	Tisdale	1921-31, 35-37	54,502	15,278	433.13	0.28	7.94
Goldhawk	Cody	1947	636	53	1.50	0.08	2.27
Open pit		1980	40,000	3,967	112.46	0.1	2.84
Hallnor (Pamour#2)	Whitney	1938-68, 81	4,226,419	1,690,560	47927.38	0.4	11.34
Hollinger-Schumacher	Tisdale	1915-18	112,124	27,182	770.61	0.24	6.80
Hollinger	Tisdale	1910-68	65,778,234	19,327,691	547940.04	0.29	8.22
Pamour Timmins Prop.	Tisdale	1976-88	2,615,866	182,058	5,161.34	0.07	1.98
Hoyle-Falconbridge	Whitney	1941-44, 46-49	725,494	71,843	2,036.75	0.1	2.84
Hoyle Pond	Hoyle	1985-today	4,920,817	1,900,943	53,891.73	0.385	10.91
Hugh-Pam	Whitney	1926, 48-65	636,751	119,604	3,390.77	0.19	5.39
Marlhill	Hoyle	1989-91	156,800	30,924	876.70	0.199	5.64
McIntyre Pamour Schumacher	Tisdale	1912-88	37,634,691	10,751,941	304,817.53	0.29	8.22
ERG tailing recovery		1988-89	2,549,189	18,260	517.67		0.00
Mclaren	Deloro	1933-37	876	201	5.70	0.23	6.52
Moneta	Whitney	1938-43	314,829	149,250	4,231.24	0.47	13.32

Naybob (Kenilworth)	Ogden	1932-64	304,100	50,731	1,438.22	0.17	
							4.82
Nighthawk	Macklem	1995-99	1,479,607	175,803	4,984.02	0.12	3.40
Owl Creek	Hoyle	1981-89	1,984,400	236,880	6,715.55	0.12	3.40
Pamour #1 (incl pits 3, 4 & 7) Hoyle	Whitney	1936-99	45,795,863	4,078,525	115,626.18	0.09	
							2.55
Pamour (other sources)	Whitney	1936-99	7,416,634	676,645	19,182.89	0.091	
							2.58
Paymaster	Deloro	1915-19, 22-66	5,607,402	1,192,206	33,799.04	0.21	5.95
Porcupine Lake (Hunter)	Whitney	1937-40, 44	10,821	1,369	38.81	0.13	
							3.69
Porcupine Peninsula	Cody	1924-27, 40, 47	96,688	27,354	775.49	0.27	
							7.65
Preston	Tisdale	1938-68	6,284,405	1,539,355	43,640.71	0.24	6.80
Preston NY	Tisdale	1933	2,800	153	4.34	0.05	1.42
Preston/Porcupine Pet	Deloro	1914-15	NA	314	8.90		
							0.00
Preston/Porphyry Hill	Deloro	1913-15	46	312	8.85	6.78	
							192.21
St.Andrew Goldfields-Stock	Stock	1989-94, 2000	815,429	129,856	3,681.42	0.16	
							4.54
Tisdale Ankerite	Tisdale	1952	14,655	2,236	63.39	0.15	4.25
Tommy Burns/Arcadia	Shaw	1917	21	14	0.40	0.28	
							7.94
Vipond	Tisdale	1911-1941	1,565,218	414,367	11,747.30	0.26	7.37
Total				64,831,953	1,837,985.87	average grade	9.62

Table 3.1 Past and present gold mines in the Timmins gold camp, from Atkinson et al., 2005

The Hollinger mine is hosted in complexly folded and sheared south facing mafic volcanic rocks of the Vipond and Central formations in the Tisdale assemblage (Bateman 2005) (Fig. 3.2), intruded by younger lens-shaped foliated quartz-feldspar porphyry. The gold mineralization is found in quartz veins, stringer lodes, stockworks and in pyritized wall rock (0.5m to 25m wide) (Jones 1948) on the south limb of the Hollinger anticline. The mineralization is reported to be hosted in shear zones in part emplaced at flow contact of various rock types (Brisbin, 1997). The volcanic rocks at the Hollinger mine consist of massive flows and associated pillowed and hyaloclastic breccias. Compositionally the rocks at the base consist of high-Mg tholeiitic basalts of the Central formation overlaid by the Fe-rich tholeiitic basalts (Brisbin, 1997) and dacitic flows (Jones, 1948, Dinel et al., under revision, see chapter 6). Interbedded graphitic materials interpreted to be interflow sediments (Brisbin, 1997) are observed locally.

The Hollinger mine gold bearing veins are hosted in highly hydrothermaly altered volcanic rocks. The alterations consist of carbonate and white micas (Jones, 1948) and where the veins are hosted in the porphyries, intense sericitic alteration was present with some carbonate alteration. Brisbin (1997) describes the veins wall rock alterations of the Hollinger-McIntyre mines as zones of intense sericite alteration, ankerite-dolomite and pyrite. In addition, he describes a paragenetic sequence consisting of an early albitization and silicification followed by sericitization and carbonatization. He also describes that where the sericite alterations was less intense, the albite-quartz alterations is preserved and the rocks have a hard, bleached and silicified appearance. Brisbin also observed two generations of carbonate, pre and syn-mineralization.

The McIntyre Mine (Fig. 3.2) is interpreted to represent the eastern extension of the Hollinger mine, and the two are often discussed as the Hollinger-McIntyre system. The McIntyre mine is hosted in folded mafic to intermediate volcanic, part of the Gold Centre, Vipond and Central formation and numerous small-scale lens-shape quartz-feldspar porphyries. In general the style of mineralization and alteration is similar to the Hollinger mine described above. However, Melnik-Proud (1992) suggested that sericite alteration occurred pre-deformation such that the rocks competency was increase by favouring the loci of shear zones. In addition, another style of mineralization was described at McIntyre mine, which consist of gold mineralization associated with disseminated pyrite (Hurst, 1935) in the host rock.

Bateman et al. (2005) indicate that quartz-carbonate-Au veins at the Hollinger-McIntyre deposit comprise the biggest single concentration of gold (~1000 tonnes) in the Timmins-Porcupine camp. Cu-Au-Ag-Mo mineralization are crosscut by narrow ankerite-quartz veins that are in turn crosscut by quartz-ankerite-albite-scheelite-tourmaline-sulfides-tellurides-gold (Wood et al., 1986). Wall rock alteration consists of sericite-ankerite-rutile-chlorite-sulfides. Maximum dimensions of the mineralized zone are 500 m width x >5000 m length x 2400 m depth, with individual veins over 300 m long. Vein arrays strike northeast and north-north east. In the vein arrays, the main foliation (here inferred

to be S3) is rotated in the same manner as veins in the core of the array (Burrows et al., 1993; Rhys, 2003), and hence the veins are interpreted as syn D3. Vein geometries and kinematic indicators show that veins were formed and deformed in a sheared zone with right lateral – oblique movement dominant over left lateral movement (Burrows et al., 1993; Rhys, 2003). Early tourmaline veins show chocolate-tablet boudinage (Burrows et al., 1993). These veins thus record formation during shortening-to-right-lateral transpression, as was interpreted from camp-scale structures. The "main-stage" quartz-gold veins were interpreted (Mason and Melnik, 1986) as the outermost zone of a porphyry-type hydrothermal system with a porphyry Cu core. Ages refute this: the 2688±2 Ma Pearl Lake porphyry (Corfu et al., 1989; Burrows et al., 1993) is cut by the 2672.8±1.1 Ma (TIMS U-Pb on zircons) albitite dike, which is mineralized by molybdenite dated by the Re-Os method at 2672±7 Ma (Ayer et al., 2004) in the Cu-Au-Ag-Mo McIntyre mineralization, which in turn is cut by "main-stage" veining.

The Dome Mine is located 4km south east of the Hollinger-McIntyre mines (Fig. 3.2). It is hosted in various rock types; mafic to intermediate volcanic rock, sedimentary rocks (Porcupine and Timiskaming assemblage) and younger quartz-feldspar porphyries. The volcanic rock consists of mafic to intermediate volcanic rocks. Holmes (1948) reported andesitic and dacitic flows, which could corresponds to what Dinel et al. (under revision, see chapter 6) described in the Vipond formation, the V10b unit. Jones (1992) described the volcanic rocks of the Dome mine area to represent a north facing sections forming the north limb of the South Tisdale anticline or alternatively the south limb of the Porcupine syncline; and is part of the Central and Vipond formation. The volcanic rocks consist of Mg tholeiitic basalts of the Central and Fe-rich tholeiites of the Vipond formation. The upper contact of the volcanic rocks is marked by a 10m thick section of carbonaceous sediments. To the south, the volcanic sequence is bound by the "Sedimentary Trough" which is composed of Porcupine assemblage sediments and some local polymictic Timiskaming assemblage conglomerate.

The mineralization style at Dome mine was classified into two types: "Ankerite veins" which consist of en echelon ankerite-quartz veins with some minor arsenopyrite and

tourmaline, and the "Dacite ore" which consists of en echelon quartz veins within lenticular ore bodies with mineralized wall rock (Jones, 1992). In addition, Moritz and Crocket (1991) reported gold-bearing quartz-fuchsite veins in highly carbonatized rock in contact with sediments. The bulk of the mineralization is said to be located in the unconformity at the contact of the volcanic rock sequence and the sediments. The volcanic rock alteration associated with mineralization is described by Moritz and Crocket (1991), and consists of intense carbonate alteration (ferroan-dolomite), clinochlore, pyrite and quartz, with accessory rutile and fuchsite (Cr-muscovite).

The Aunor, Buffalo Ankerite, and Delnite mine are located 5km south of Timmins. They form a linear band of deposit on the interpreted location of the PDDZ. Two main rock types are observed in the area, the ultramafic volcanic rock to the Hershey Lake formation, at the base of the Tisdale assemblage in shear contact with Timiskaming assemblage polymictic conglomerate. The mineralization is mainly found in quartz-carbonate fault-fill and extensional veins, and some reported disseminated Au mineralization has been reported (Fyon and Crocket, 1980). The alteration is characterized by intense carbonatization, pyritization, and local sericite in the vicinity of veins.

3.2.1 Structural control on gold mineralization

The Timmins gold camp bedrock geology is best described by Ferguson (1968), Pyke (1982) and Brisbin (1997). The Porcupine camp was subjected to multiple generation of deformation that folded and sheared the rocks at various intensities. Deformation zones (fault or shear zone) are the loci of the majority of Au deposits in the Timmins area and throughout the Abitibi Greenstone Belt (Pyke, 1982). In particular, in the Timmins area, the Au deposits are spatially associated with the Porcupine Destor Deformation Zone (PDDZ) corridor; 1st order and second order splays of the PDDZ are the loci of major Au deposits. The locations of the 2nd order deformation zones are in part associated with the folding event in the area. Often gold-bearing shear zones occur on the limbs of isoclinal folds (Dinel et al., accepted by guest editor) or in cores of folds (Ropchan et al., 2002). For example, the Dome mine is spatially associated with the Dome Fault which is parallel

to, but located about 1 km northwest of the PDDZ. The Hollinger-McIntyre mine are associated with the Hollinger Fault, which also striking paralle to the PDDZ, but is located about 5 km northwest (Bateman 2005). This structure was interpreted by Bateman et al (2005) to be a hanging wall anticline related to a series of south-dipping thrusts panels, all rooted within the PPDZ at depth and associated with D2 south-side dip-slip movement on the PDDZ.

3.3 Geology of the Hoyle Pond mine

The Hoyle Pond mine is located in Hoyle Twp., hosted within a km-scale east west striking panel of mafic and ultramafic volcanic rocks of the Tisdale assemblage (Fig. 3.2), bounded to the north, east and south by meta-sediments of the Porcupine assemblage (Rye, 1987) (Fig. 3.4). The volcanic rocks are in faulted (thrust) contact with south-facing wackes and siltstones of the Porcupine assemblage to the north; and by discordance (a fault or an unconformity) with south facing sediments, (siltstones & greywackes) also of the Porcupine assemblage to the south. The volcanic rocks have been overprinted by an asymmetric km-scale Z-fold and have been intruded by quartz-feldspar porphyries, and quartz porphyries as well as two Matachewan diabase dikes of Proterozoic age. The mine stratigraphy was previously believed to be within an anticlinal structure having ultramafic volcanic rocks in its core (Pressaco, 1999). In this study, the stratigraphy has been subdivided into three volcanic sequences, the North, Central and South volcanic packages (NVP, CVP and SVP). Below we detail the petrography of the volcanic rocks utilizing this nomenclature i.e. North, Central and South Volcanic packages. Later we correlate these packages within the overall stratigraphic framework of the Tisdale assemblage in the Timmins area. The distinction between rock types has been aided by geochemical analyses.

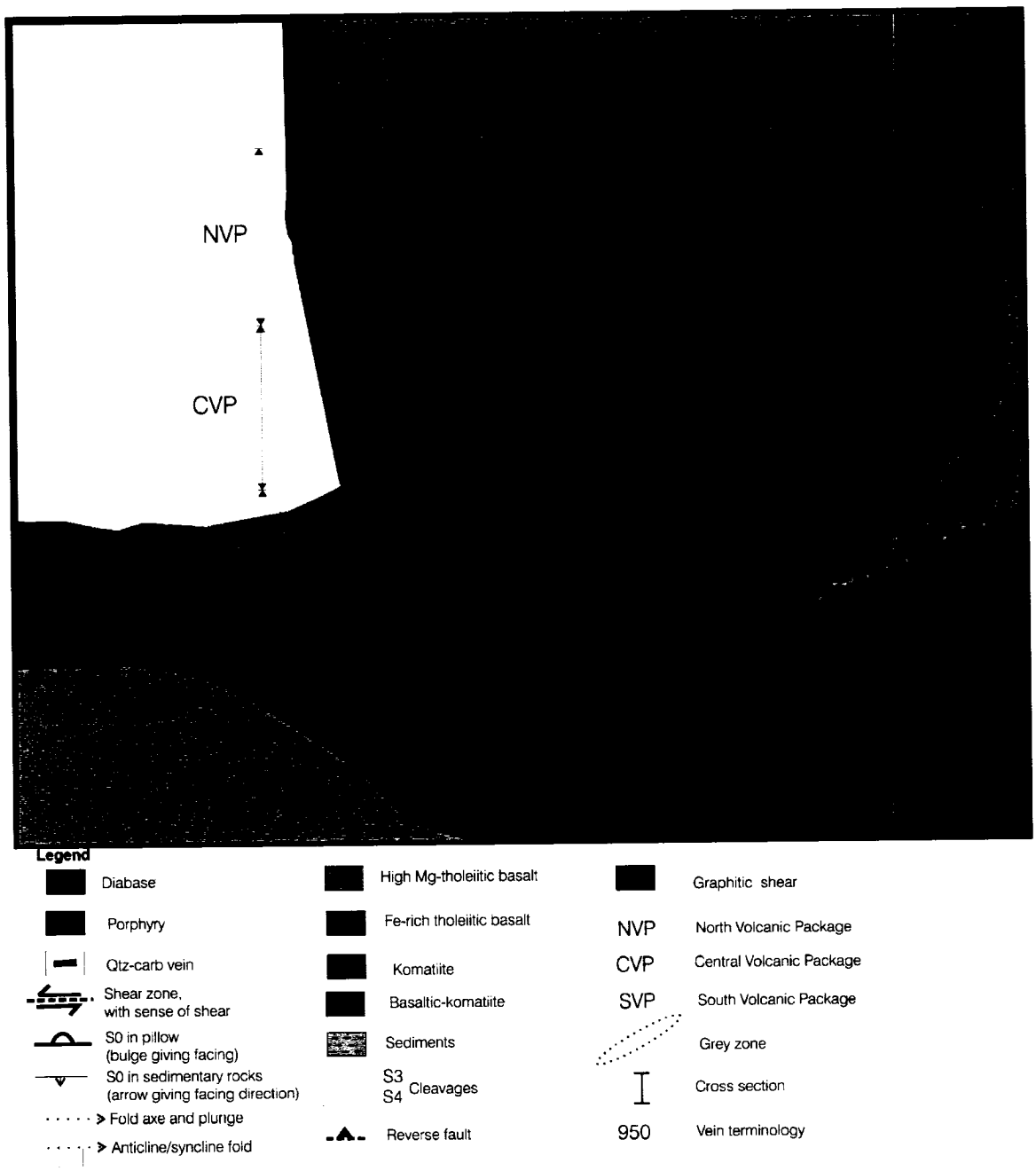

Figure 3.4 Geological map of the Hoyle Pond mine (Dinel et al., accepted by guest editor, chapter 4).

3.3.1 Hoyle Pond volcanic packages

North Volcanic Package

The NVP consists of interbedded mafic and ultramafic volcanic rocks (Fig. 3.4). The rocks are dominated by massive flows and associated pillowed flows and locally flow and pillow breccias (Photo 3.1. and 3.2). The pillows vary in size from 5m to 1.5m, and are generally undeformed, however in proximity to shear hosted veins they are stretched vertically and flattened by ~50%. In general pillows are characterized by a pale apple-green color, and a very fine-grained groundmass. On level 3 of the mine, variolitic pillow flows and pillow breccias were observed. Variolitic pillows exhibit leucocratic globular bodies, mm scale (2-5mm) that are aligned and form bands along pillow margins. In some pillows the varioles are concentrated into domains which at the macroscopic-scale appear to be single large varioles. The pillow breccia's fragments are amoboedal in shape varying in size from 5cm to 25cm with mm size "varioles" that are concentrated in sinuous bands and truncated by the pillow selvages (Photo 3.3). The "varioles" have very diffuse and undistinguishable rims and do not resemble the Vipond formation V8 flow, with its discrete cm-size varioles found in concentric bands in pillow margins. Rye (1987) reported that the pillow sequence in the North volcanic package at Hoyle Pond had facing direction to the north, however recent observation of pillows from the 720m level demonstrate a series of pillow flows having south facing directions, thus showing consistent facing with the Porcupine sediments bounding the volcanic stratigraphy at the mine to the north and south.

Petrographic examination of these rocks shows that the varioles are very fine, 2-5mm spherulites having diffuse edges that blend with the groundmass. They are albitized and contain patches of titanite. Pervasively albitized rocks have fan-like albite in micro-lithons with spherulitic extinction. The mineral assemblage of the mafic rocks is dominated by chlorite, albite, carbonate, hydrothermal quartz, sericite, local graphite and some opaque minerals: chiefly minor iron oxides, pyrite and traces of chalcopyrite. Locally, sericite is concentrated along the cleavage domains.

A striking feature is the presence of the so called: ''Grey Zone'' alteration consisting of a very-fine grained dark grey to black pore-filling material composed of graphite, with minor sericite, ferroan-dolomite, plus disseminated pyrite and chalcopyrite. The graphite is conspicuous in zones of increased porosity. This alteration is best observed in samples taken to the surface because there is little contrast between it and the mafic rocks. It occurs in what was originally porous rock, and appears to be restricted to certain lithofacies (typically flow breccias, hyaloclastites, and pillow breccias) and by structures such as shear zones. Several Grey zones are identified (Fig. 3.4); they strike ~070^0 and are commonly spatially associated with Au-rich quartz veins. The origin of the graphite is believed to be organic, (Downes, 1982 & Rye, 1987). More details are provided on this alteration type in the geochemistry section below.

The ultramafic units in the NVP are characterized by dark grey to black aphanitic rocks with a soapy-soft cleavage. Fresh surfaces may have a very granular texture consisting of coarse grained porphyroblasts of euhedral dolomite. In addition the ultramafic volcanic rocks may contain minor chlorite, some disseminated quartz crystals, and iron oxides. On the 440ml, in the 16 vein area (see NVP section on Fig. 3.4), metamorphism has achieved upper greenschist facies metamorphic conditions over a 20m section consisting of actinolite, minor albite and chlorite (Photo 3.4). This is the only location in the mine where actinolite was observed.

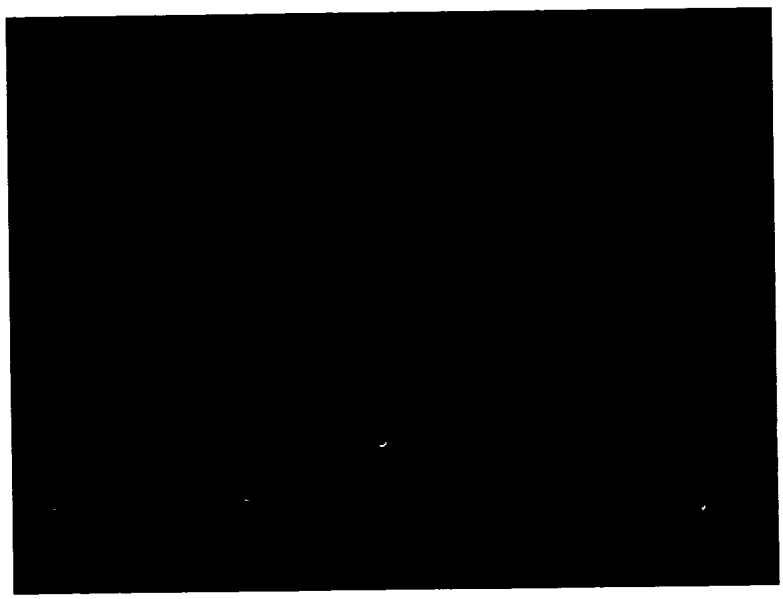

Photo 3.1 NVP mafic pillow flow, with younging direction to the southeast (Left hand side of picture), rebar for scale ~ 4 inch.

Photo 3.2 NVP flow top breccia, notice the various angular pale coloured clasts.

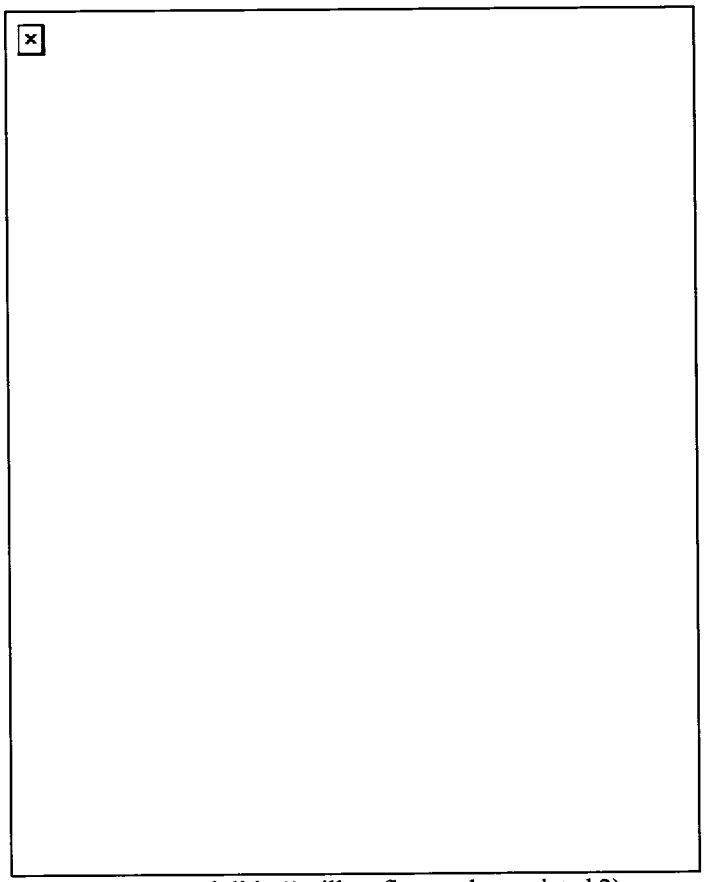

Photo 3.3 NVP, variolitic 1) pillow flow and associated 2) pillow breccia.

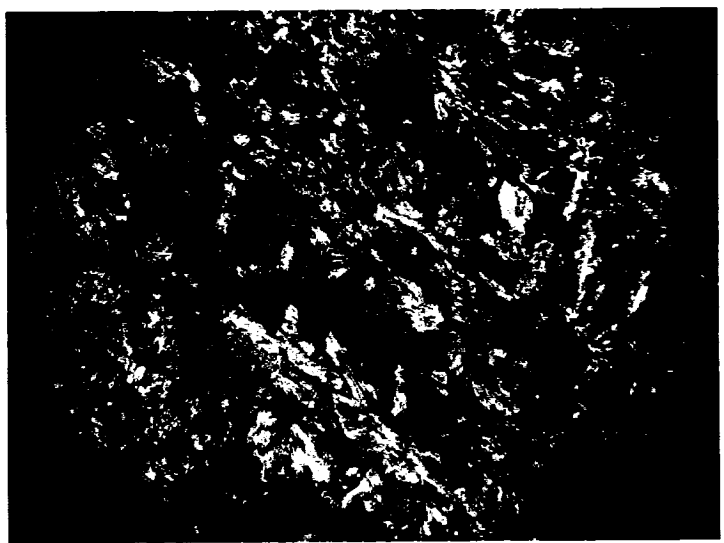

Photo 3.4 NVP, ultramafic volcanic rock, metamorphic actinolite and chlorite crystals, f.o.v ~4 mm.

Central Volcanic Package

The Central Volcanic package (CVP) (Fig. 3.4) consists of a sequence of interbedded komatiite (typically>18 wt% MgO) and basaltic komatiites (12-18 wt% MgO) approximately 200m in apparent thickness and composed of talc schist, talc chlorite schist to chlorite schist. The contacts between the basaltic komatiites and komatiites are gradational and commonly have been overprinted by strong carbonate alteration (dolomite to ferroan-dolomite), and deformation which resulted in the generation of an intense fabric and associated quartz-carbonate stringer zones.

The basaltic komatiites are characterized by carbonatized fine-grained to medium-grained dark green to black chlorite schists with minor talc. The mineral assemblage is dominated by chlorite, talc, dolomite, hydrothermal quartz, iron-titanium oxides, coarse grained (1-2mm) carbonate porphyroblasts and locally Cr-micas, actinolite and traces of pyrite.

The komatiites are altered to talc-chlorite schist to talc schist. Their color varies from dark grey-black, to cream grey-beige due to carbonatization. The mineral assemblage is dominantly talc, minor chlorite, dolomite, hydrothermal quartz, iron titanium oxides and locally serpentine. In some thin sections, the Fe-Ti oxide crystals form ring-like structures typical of relict olivine and are interpreted to represent the remnants of olivine cumulate zones (Photo 3.5). The ultramafic volcanic rock sequence consists of undifferentiated massive flows with pillows facies recognized in drill core (Photo 3.6), no spinifex textures were observed. The rocks are stratiform, and have conformable to gradational contacts. Based on their conformable setting, pillows and knowledge of the Tisdale assemblage elsewhere in the camp, we interpret their emplacement as flows.

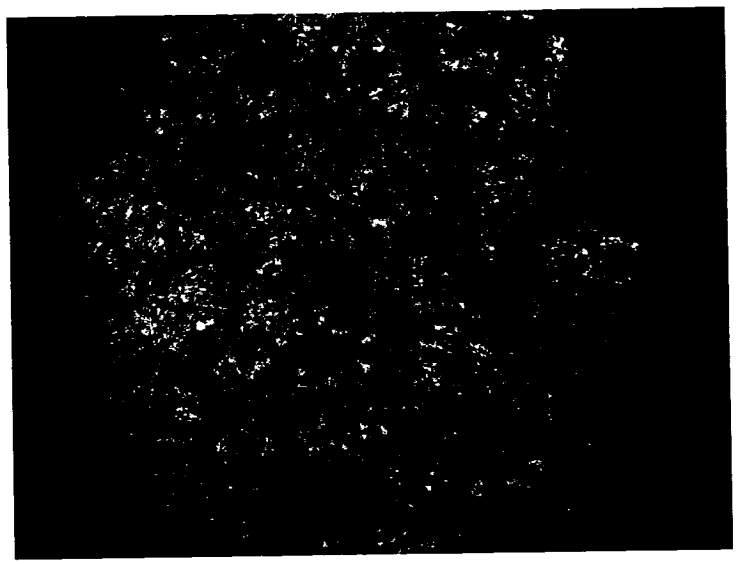

Photo 3.5 CVP, remnant of olivine crystals cumulate textured, now altered to talc and magnetite crystals forming rims, f.o.v. ~4mm

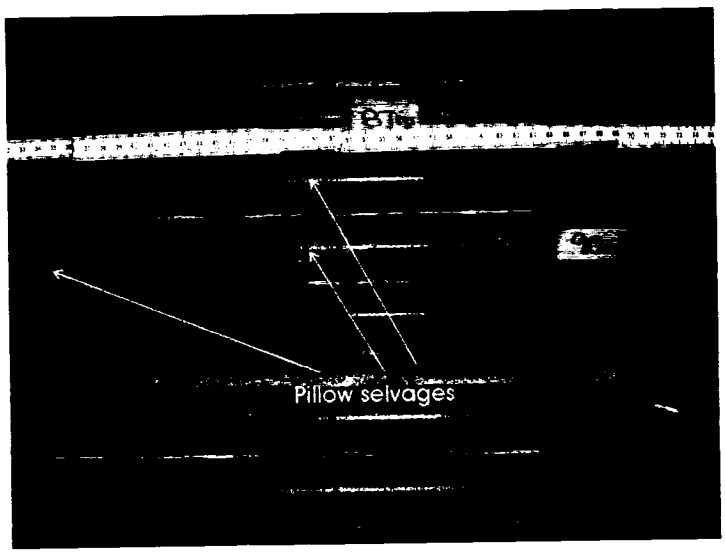

Photo 3.6 CVP, ultramafic volcanic pillow flow, notice the pillow selvages on the core, strongly altered to dolomite

South Volcanic Package

The SVP is in general more foliated than the NVP and the CVP. The fabric is pervasive and becomes more intense near the 1060 fault zone (1060fz). In addition the SVP rocks have been significantly carbonatized. They are composed of high-Mg tholeiitic basalts interbedded with iron-rich tholeiitic basalt units, as recognized on the 720m level (Fig. 3.4).

Iron-rich tholeiitic basalts comprise a unit that is approximately 10m thick with undifferentiated lithofacies possibly as a result of the amount of superimposed strain. In hand sample the rock is a dark green, fine to medium grained, chlorite schist with varying intensity of carbonate alteration. The mineral assemblage defining the iron-rich tholeiitic basalts is chlorite, quartz, titanite, sericite, ferroan dolomite, K feldspar, pyrite, iron-titanium oxides and local graphite. The contact relationship with the high-Mg tholeiitic basalts is interpreted to be sharp and is in most cases marked by a zone of quartz-veining, Cr-muscovite and sericite (muscovite) alteration (Photo 3.7).

The high-Mg tholeiitic basalts are approximately 30-40m thick flows. It is impossible to distinguish the high-Mg tholeiites from the Fe-rich tholeiites without the use of geochemistry (see below). The high-Mg basalts consist of pale to dark green, medium to coarse grained chlorite schist with variable alteration. Litho-facies includes massive flows, pillow flows with some pillow breccias and flow top breccias. The pillows and breccia clasts in the 1060fz are stretched vertically, parallel to the intersection lineation S3-S4. The size of the pillows varies from 5m to 2m in the pillow flows and .1m to 3m in the pillow breccias, with thin (1-4 cm) pillow selvages. The mineral assemblage in the high-Mg tholeiites is dominantly chlorite with minor albite, quartz, dolomite to ferroan-dolomite, sericite, Cr-muscovite (fuchsite), K-feldspar, local graphite and local abundant pyrite and chalcopyrite. The mineralogy in the ore zone is dominated by dolomite, local sericite, "fuchsite", graphite and albite (see below section on vein description). In general the carbonate alteration is pervasive and observed throughout the whole package. The intensity of the carbonate, sericite and "fuchsite" alteration increases locally and is most intense in the 1060fz in the vicinity of veins and lithological contacts.

Photo 3.7 SVP, contact relationship between the interbedded high-Mg tholeiitic basalt and Fe-rich tholeiitic basalt in the 1060fz. The majority of the gold bearing veins are located in similar contact relationship.

3.3.2 Other Rock types

Some younger intrusive rocks intrude the SVP, quartz-feldspar porphyries (QFP) and quartz porphyry sericite schist (QP). The QP sericite schist was observed in drill core and underground on the 600-620m UP/splay level and on 720m level. It is a 2-4m thick body conformable with volcanic stratigraphy over a strike length of 200 m and is composed of ~5% quartz phenocrysts, with some local fuchsitic clasts and a strongly developed cleavage defined by sericite. In thin section, the quartz phenocrysts are embayed, a dissolution texture typical of felsic volcanic rocks or shallow intrusive rock. A sample submitted for U-Pb zircon dating yielded a discordant age of 2687.6 ± 2.2 Ma (TIMS) (Ayer et al. 2005). Although originally thought to be a volcanic unit because of its conformable nature, based on the 2710-2704 Ma age of the Tisdale assemblage, we now conclude that the QP is a sill-like, generation of porphyry.

The QFP's cross-cut the stratigraphy, are moderately foliated and have very weak to nonexistent metamorphic halos. They are composed of 30-40% feldspar phenocrysts (albite) varying in size from 5cm to 1.5cm, ~5% quartz phenocrysts varying in size from 2mm to 5mm and a trachytic texture defined by an alignment of feldspar phenocrysts. The emplacement of the intrusive QFPs is likely post-D3 but pre-D4; because they lack the penetrative S3 fabric yet possess the S4 fabric, whereas the mafic volcanic rock hosting the QFPs outside the 1060 fz posses both, S3 and S4 fabric. Zircons extracted from a sample on the 620m level gave an U-Pb concordant emplacement age of 2684.4 ± 1.9 Ma (TIMS), but also contained inherited zircons with an age of 2695.2 Ma (Ayer et al. 2005). The ages of the QP and QFP are overlapping if we consider the uncertainties of the age data. However, cross cutting relationship between the QP and QFP and the structural observations are strong geological evidence of a time gap between the formations of the two intrusive events.

A graphitic unit is also present within the SVP (Fig. 3.4). It consists of a 2 to 10m wide corridor composed of 80-90% graphite, "nodular" pyrite, and sericite-carbonate fine stringers that are very similar to the "grey-zones" associated with areas of increased

porosity in the NVP described above. Downes (1982) previously reported a graphitic argillite unit at the contact between the high-Mg tholeiitic basalts and Fe-rich tholeiitic basalts. However, mapping on the 440m level demonstrates that this graphitic unit locally cross-cuts the SVP stratigraphy in the 950 zone, whereas elsewhere it appears conformable (Fig. 3.4). However, it is likely that deformation associated with the D4 event transposed the unit into apparent conformity in proximity to the 1060fz. Given the cross-cutting nature of the unit we do not interpret it to be an argillite unit, instead we interpret it to be a relict porous zone, possibly a fault or shear zone, into which fluid migrated and deposited graphite, pyrite, sericite and carbonates. This unit is pre- to syn-D3, and was later refolded by D4 in the 1060fz. Previous work (Downes, 1982) described the presence of sedimentary bedding, and interpreted the unit as being interflow sediments. Petrographic examination during this study demonstrates that the "bed-like" features represent aligned boudins of quartz –carbonate-sericite veinlets. Disseminated graphite is found up to tens of meters of the 1060fz and is conspicuous in zones of increased porosity as in-fillings within volcanic flow breccias and shear zones in Fe-rich and high-Mg tholeiitic basalts.

The youngest rock units in the mine are Proterozoic Matachewan diabase dikes. The dikes strike north-south, but locally deviate in the 1060fz (Fig. 3.4). The dikes cross cut all geological units in the 1060fz and all deformation fabrics. The diabase consists of plagioclase- and pyroxene with some minor epidote and magnetite. The units have a blocky jointing pattern with grain size ranging from fine-grained at the contacts to medium-grained in the central zones. No evidence of contact metamorphism was observed associated with the dike.

3.3.3 Structures

The mine stratigraphic sequence was previously described as occurring within an antiform fold having a central ultramafic volcanic core flanked by mafic volcanic rocks (Rhys, 1999). The fold was interpreted as an F1 isoclinal fold, characterized by a pervasive foliation S1, axial planar to F1 folds and sub parallel to S0. S1 is refolded at the mine scale by the ~070 fabric S2 axial planar to isoclinal F2 folds observed in the 1060fz (fault zone) which is the locus of the main mineralization in the mine (Rhys, 1999). For this study the structural interpretation has changed to fit the deposit into the regional scale structural scale evolution (Bleeker et al., 1999, Bateman et al., 2005) such that fabric previously termed S1 is now identified as S3 and the former S2 as S4. Fabric associated with D1 and D2 deformations are not observed at the mine scale. The mineralization at Hoyle Pond is sub parallel to the intersection lineation of S3-S4 in the 1060fz. D5 is locally observed as a crenulation cleavage, S5, oriented approximately north-south and axial planar to small scale asymmetric fold. D6 is visible in the 1060fz as a sub-horizontal crenulation cleavage associated with cm to m-scale asymmetric folds and kink bands, indicative of a vertical displacement.

The relationship among stratigraphy, structures, petrofabrics, metamorphic minerals, porphyry intrusions, veins and alteration minerals were studied to establish a paragenetic sequence and alteration paragenetic sequence at the Hoyle Pond mine (see Fig. 3.5). The mineralization at Hoyle Pond is interpreted to be syn to late D4, because the main mineralization is sub-parallel D4 structures (SVP). The D3 event in Hoyle Pond is different to the D3 described in Bateman et al, 2005. D3 is constrained between 2687.6 Ma (age of QP) and 2684.4Ma (age of the QFP), which is pre-Timiskaming and may reflect heterogeneous deformation of the Porcupine gold camp. All the alteration minerals observed (i.e. graphite, sericite, fuchsite, albite, arsenopyrite, pyrite, dolomite and ferroan-dolomite) are also interpreted to be syn to late D4 with no evidence for pre-mineralization alteration.

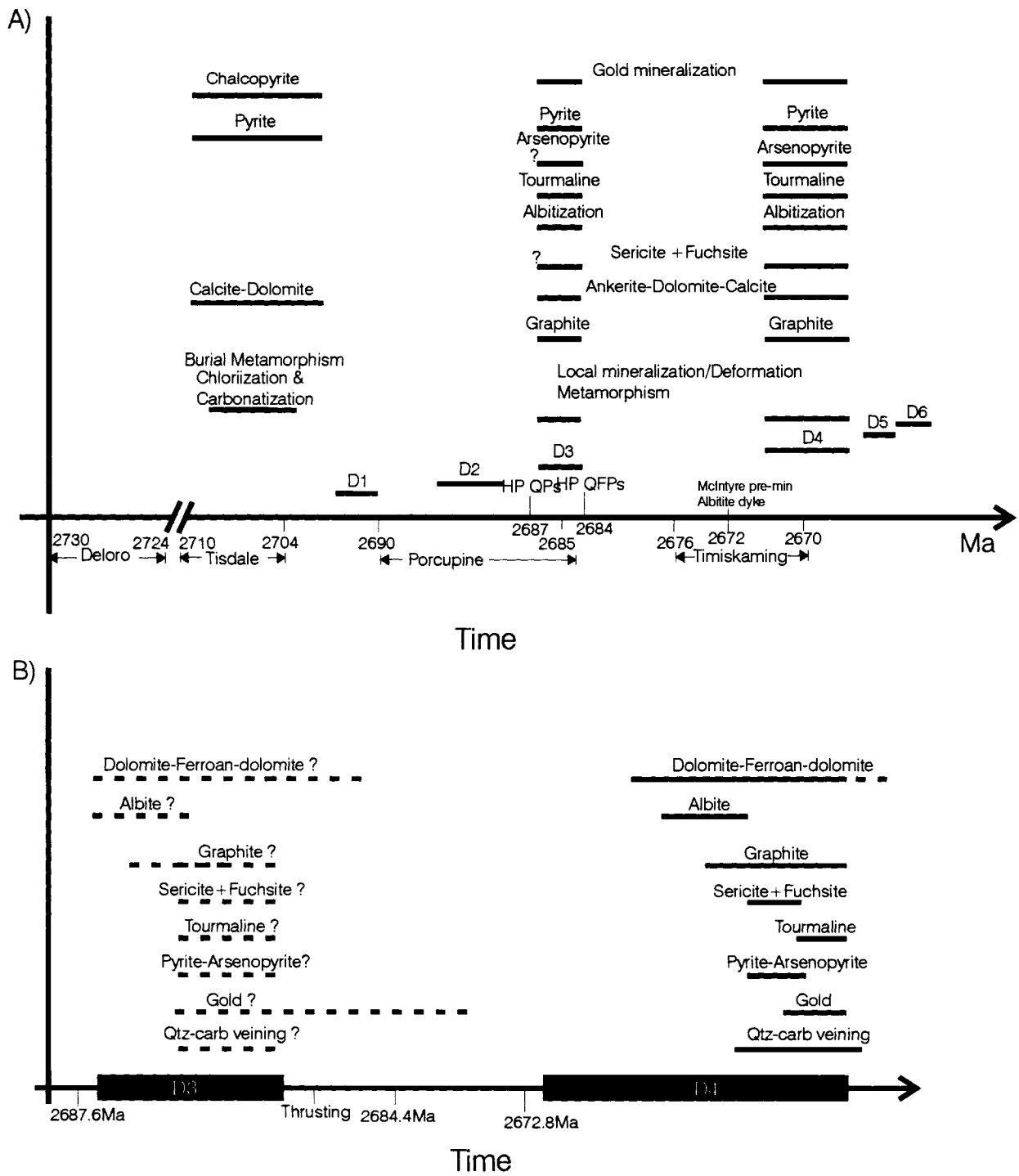

Figure 3.5 A) Para genetic sequence of deformation, alteration and mineralization vs. time based on Bateman et al. 2005, B) Para genetic alteration sequence vs. time in relation to porphyry intrusion ages in the mine sequence and generation of tectonically induced fabrics (from Dinel et al., accepted by guest editor).

3.3.4 Vein descriptions

The Hoyle Pond mine vein styles vary from extensional with a massive appearance, to fault-fill veins that occur as either sheeted, boudinaged, or massive veins. The extensional veins generally have a linear or sigmoidal shape and cross cut the fabric at high angles. They are generally massive veins composed of white to greyish quartz with local pyrite along the wall rock-vein contact. Locally some extension veins have a black appearance, due to graphite and/or tourmaline-filled fractures. The fault-fill veins generally have a more diverse mineralogy consisting of massive, white to grey quartz, with interstitial tourmaline and/or stylolitic chlorite and locally muscovite or Cr-muscovite. Other fault-fill veins are mainly composed of massive white quartz and are commonly associated with variable concentrations of graphite in the wall rock selvages. Mineralization in the Hoyle Pond vein systems consists of free gold ranging from micron size specks to medium-large (cm-scale) flakes found along stylolites or randomly distributed in massive veins, to thick mm-cm scale gold veinlets (Photo 3.8).

In the 1060fz, two types of veins are present. The fault-fill veins, the B1 and B3 group (B1N, B1S...) consist of veins parallel to the fabric S4 and are observed at the contacts between high-Mg and Fe-rich tholeiitic basalts on the limb of isoclinal F4 folds. The extensions veins (UP veins) consist of veins intersecting the S4 fabric and are sigmoidal in shape. However, the vein emplacement is generally at the contact of the mafic volcanic rocks of the SVP and the ultramafic volcanic rocks of the CVP. Outside of the 1060fz, in the SVP, the 950 veins and the A veins have similar style. They are sigmoidal in shape in part parallel to fabric and in part intersecting the fabric. We suggest that they were formed and rotated during D4. The 950 vein has a sub-horizontal component possibly representing a similar system to the "#7 veins" which are a group of shallow dipping (sub horizontal) extensional veins. These lie in the F4 syncline of the NVP and may represent some vertical displacement during D4. The "A" vein consists of a north striking vein, emplaced in the SVP that in part lies on the short limbs of F4 asymmetric Z-folds and propagates into the fold hinges to terminate in the ultramafic volcanic rock of the CVP. At the northern tip of the "A vein" the UM vein is observed, possibly consisting of a D4 structure lying on the long limb of the F4 Z-fold, at the contact of the mafic volcanic

(SVP) and the ultramafic volcanic (CVP). However, no veins are completely hosted in ultramafic volcanic rocks, likely due to its ductile nature.

The NVP hosts the veins were first mined out, and the mine vein terminology classifies them as the "#8 vein"to"#16 veins". In general, these fault-fill veins are mostly observed at the contacts of volcanic flows. However, it is not unusual to observe an extensional vein connecting fault-fill veins of two separate lithological contacts. These extensional veins show evidence of sinistral rotation. The fault-fill veins are parallel to S3 fabric. At first, I interpreted that it reflected a D3 mineralization thus suggesting a pre-Timiskaming event (Fig. 3.5). However, this interpretation is unlikely, because there is no evidence in the PGC for pre-Timiskaming gold mineralization. In addition, a 15 million year gap between the two mineralization events, producing exactly the same alteration minerals, with exactly the same chemistry is improbable. It is proposed that one mineralization event occurred late during D4 and that fluids migrated into previously formed D3 structures.

The timing of alteration minerals with respect to vein formation and gold precipitation appears to be syn-mineralization as indicated by alteration halos which are parallel and enveloped without intersecting the veins. Alteration minerals are found in the S3 and S4 fabrics and envelop the veins. Muscovite and Cr-muscovite are observed in the cleavage domains parallel and immediately surrounding the Au bearing quartz shear veins, and are also observed in some veins as stylolites. This zone is termed the Sericite Alteration zones and is also composed of Fe-dolomite, minor pyrite, tourmaline and graphite. In addition, extension veins developed during D4 have a similar alteration. The Sericite Alteration Zone is enveloped by a halo rich in albite, chlorite, Fe-dolomite and is termed the Albite alteration zone. No cross cutting relationship were observed between the Sericite alteration zone and the Albite alteration zone. However, locally observed albite rich lithons intersected by sericitic cleavage, suggesting that the albite alteration may have formed pre-sericite alteration. The pervasive Fe-Dolomite alteration is observed overprinting S4 and dislocated by S4 which is interpreted to represent different stages of

reactivation during D4. The graphite alteration is pervasive in the gold mineralization zones and is observed in the S4 fabric surrounding the veins.

The Gold mineralization at Hoyle Pond Mine is interpreted to have been formed late during D4. Gold rich mineralizing fluids migrated in previously formed D3 structures.

Photo 3.8 Gold flake in the gold bearing vein of the 440ml 950 zone

Chapter 4.0 Geochemistry of the volcanic rock at Hoyle Pond Mine

This chapter is written in the format of a manuscript accepted by the guest editor submitted to the Economic Geology Journal. The paper discussed primarily the geochemical signature of the volcanic and the alteration patterns associated to mineralization at Hoyle Pond mine. A summary is provided in the paper.

The following paper "**Litho-geochemical and stratigraphic controls on gold mineralization within the meta-volcanic rocks of the Hoyle Pond Mine, Timmins, Ontario"** by Dinel et al., (accepted by guest editor) discusses primarily the geochemical signature of the volcanic rock of the Hoyle Pond mine and the alteration associated to mineralization. Those who have read the previous chapter 1-3, may continue the reading at the page 95 (Mine Geology section).

4.1 Litho-geochemical and stratigraphic controls on gold mineralization within the meta-volcanic rocks of the Hoyle Pond Mine, Timmins, Ontario

Etienne Dinel[a], Anthony D. Fowler[a], John Ayer[b], Alastair Still[c], Ken Tylee[c] and Erik Barr[c]

a) University of Ottawa, Department of Earth Sciences, Ottawa-Carleton Geoscience Centre
b) Ontario Geological Survey, Precambrian Science Division
c) Porcupine Joint Venture, Hoyle Pond Mine, Timmins, Ontario

Abstract

The Hoyle Pond gold deposit is hosted in complexly deformed mafic-ultramafic volcanic rocks of the Hershey Lake and Central formations (Tisdale Assemblage) in the Porcupine Gold Camp, located approximately 15km north-east of Timmins in the Abitibi greenstone belt. The deposit is hosted within a homoclinal sequence of south facing stacked volcanic flows of high-Mg tholeiitic basalt, basaltic komatiite and komatiite flows, and interbedded high-Mg tholeiitic basalt and Fe-rich tholeiitic basalts. The bulk of the gold mineralization was emplaced at lithological contacts along late shear zones associated with isoclinal folding and thrusting. The mineralization is characterized by micron size to cm size, free gold flakes or veinlets in quartz-carbonate (dolomite and ferroan-dolomite) shear and extension vein arrays. At the mine scale a broad carbonate alteration is evident. Two alteration zones were mapped at the meter scale: an inner sericite alteration zone composed of sericite (muscovite), fuchsite (Cr-muscovite), quartz, arsenopyrite, pyrite, ferroan-dolomite, dolomite, graphite plus tourmaline, and an outer albite alteration zone consisting of albite, quartz, ferroan dolomite and dolomite.

Geochemical analyses of 355 samples show that the REE, Zr, Al_2O_3, TiO_2 and Y were largely immobile during alteration and mineralization. CO_2, K_2O, Na_2O, Cr_2O_3, Rb, As, B, SiO_2, CaO and on occasion Fe_2O_3, FeO and MgO, were mobile during alteration and mineralization. The chromium enrichment is not primary and is interpreted to have been caused by remobilization (as Cr^{6+}) from ultramafic rocks during mineralization. In addition, an intense graphite alteration, originally derived from organic matter and now associated with mineralization, is present in zones that were porous and permeable at the time of mineralization. In common with other mesozonal orogenic gold deposits, gold was most likely transported as a thio complex (Au HS). The Cr enrichment in the wall rock indicates that Cr was mobile most likely as Cr^{6+} . Oxidising species such as Cr^{6+}, reduced organic matter and Au-HS cannot coexist in the same fluid, implying that more than one fluid was involved in the mineralization/alteration. Thus it is postulated that reactions between reducing and oxidizing fluids reduced Cr^{6+} to Cr^{3+}, oxidized the organic matter to form graphite, oxidized sulphur to form sulphides, and precipitated Au. Reducing fluids rich in boron, arsenic, organic matter and Au were likely generated from sedimentary rocks (Porcupine Assemblage?) at depth and expelled during orogenesis into

syn-deformation structures within overlying volcanic rocks where they mixed with oxidizing fluids containing Cr, K_2O, SiO_2, Na_2O and CaO.

Introduction

The Hoyle Pond mine is located 15 km east of downtown Timmins and 3 km north of the Pamour mine in the Porcupine Gold Camp of the Archean Abitibi Subprovince in the Superior Province, northern Ontario (Fig. 4.1). The discovery hole was drilled by Texas Gulf in 1980 and the mine has been in constant production since 1985. The mineralization is associated with fault-fill and extensional quartz-carbonate veins along second order shear zones and faults spatially related to the Porcupine-Destor Deformation zone (PDDZ). It is hosted by ultramafic and mafic meta-volcanic rocks of the Tisdale Assemblage (2710-2704Ma, Ayer et al., 2005), which is subdivided in the mine into three volcanic packages, namely, the north, the central and the south volcanic packages (NVP, CVP and SVP respectively) (Fig. 4.2). Prior to 1994, most of the ore was mined from the Hoyle Pond zone (13-14 and 16 veins) in mafic rocks of the NVP. Subsequently, in 1994, with the discovery of the 1060 zone, the A-vein zone and the 7-veins zone, the main focus of production switched to the SVP. Currently, production comes predominantly from the A vein and the 1060 fault zone, which extend vertically to depths of greater than 1000m.

The main goals of the paper are to characterize the geology (stratigraphy, structural geology, alteration, and mineralization) of the Hoyle Pond deposit and more importantly to identify critical host rock chemical and physical factors that contributed to the localization of gold mineralization. The geology of the Hoyle Pond deposit is compared to other deposits in the Timmins Porcupine camp and these results are integrated into a model describing the structural and hydrothermal evolution of the Hoyle Pond mine.

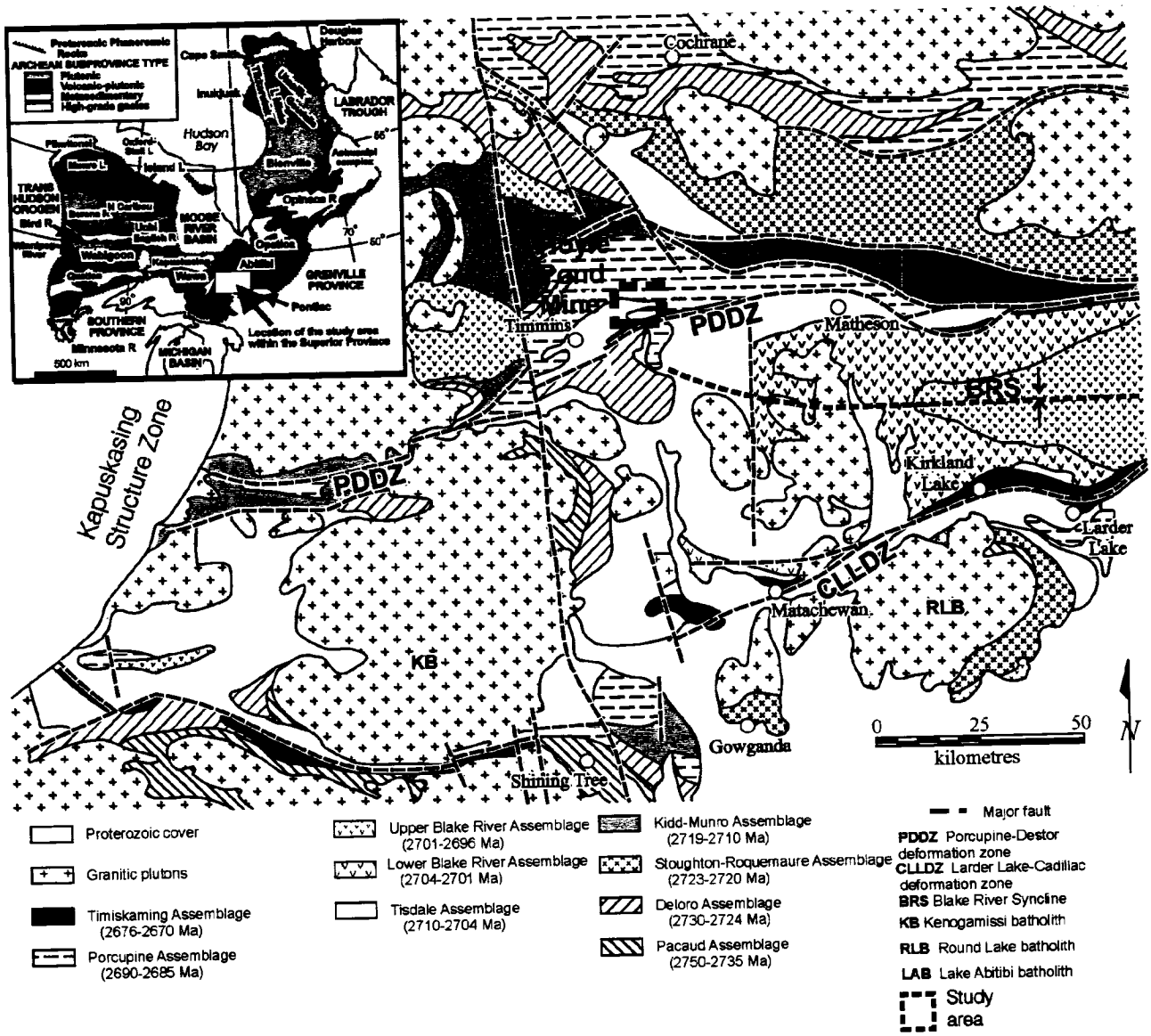

Figure 4.1 Geological map of the Abitibi Greenstone Belt illustrating the 9 volcano-sedimentary rock assemblages as defined by Ayer et al. (2005). The Hoyle Pond Gold Mine is located in the Tisdale Assemblage of the Abitibi South Volcanic zone and the mine area is outlined by dash line box.

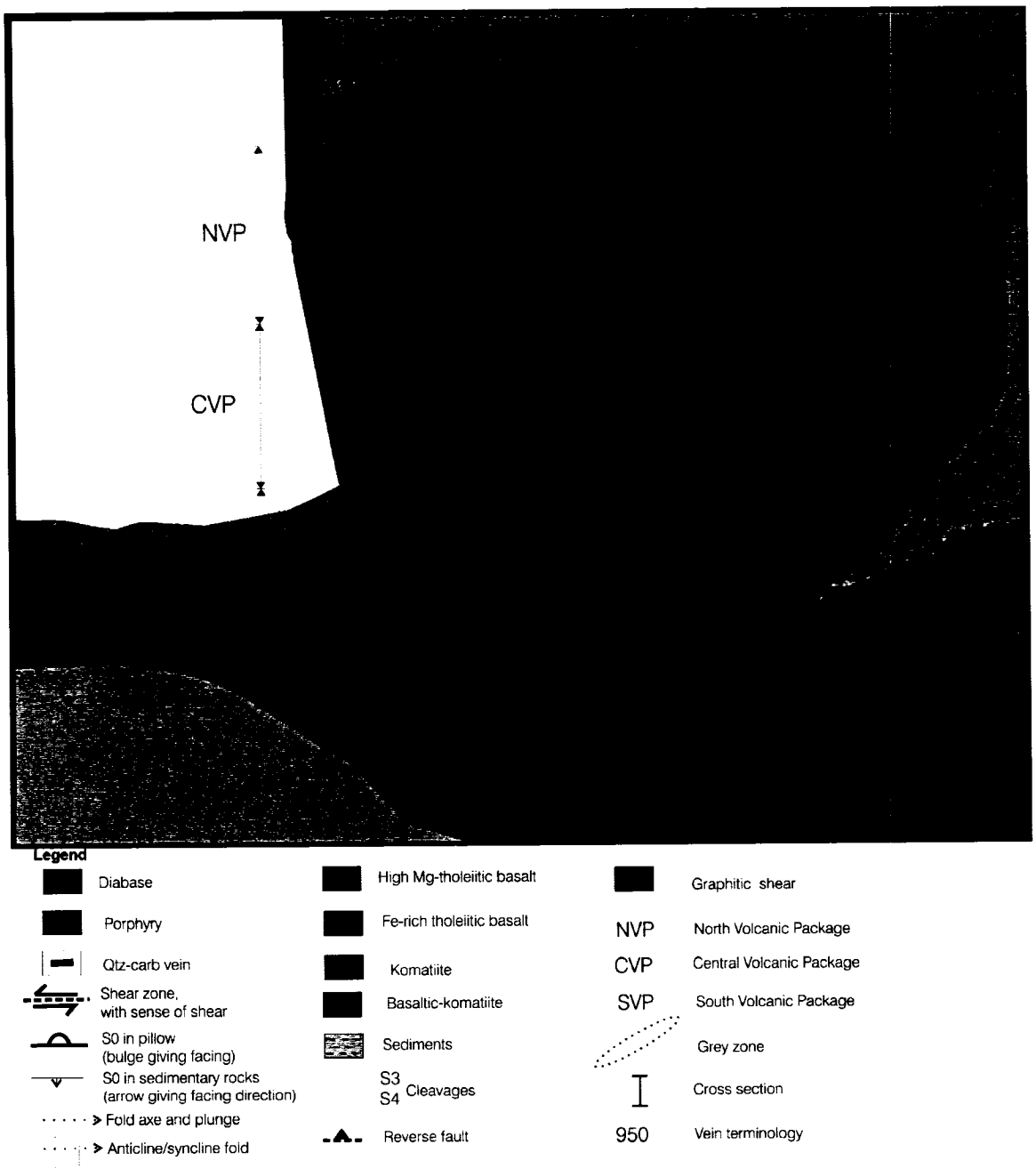

Figure 4.2 Simplified geological map of the Hoyle Pond mine, compiled from the 440 and 720 ml maps. Certain veins are labeled using the mine convention e.g. "A" vein. "I-beams" indicate traverses made across veins. Note that in the western portion of the SVP, the graphitic unit transects the stratigraphy.

Methodology

Mapping

Four levels in the mine were mapped for the project. The two main levels, the 440 meter level (ml) and 720 ml, were investigated to define the stratigraphy of the mine (Fig. 4.2) and to verify the continuity of the stratigraphy vertically. In addition two levels were investigated: the 880ml 1060 cross-cut to understand the origin of the 1060 fault zone and the ~400ml (Hoyle Pond mine 3 level) to determined the control on emplacement of the mineralization in the NVP.

Sampling, sample preparation, and laboratory analysis

Close to 500 samples were selected for rock identification and characterization of the alteration. 355 samples were analyzed for whole-rock geochemistry (major oxides and trace elements) from the 3 Level (400ml) #16 vein zone, the 440ml 950 zone and #16 vein zone, the 720ml 1060 zone, the 880ml 1060 zone and drill core. Analytical data and locations are given in appendix II.

The samples were cleaned of all blast powder and carefully cleaned of vein material prior to crushing. One half of the sample was kept as a reference and the other half was used for thin sections and geochemical analysis. Major elements and trace elements were analyzed by XRF and ICP-MS, respectively, at the University of Ottawa, Ottawa, Ontario, and Ontario Geoscience Laboratories, Sudbury, Ontario. Methods used for determination of iron (XRF, XRD, ICP-MS) do not discriminate the Fe^{2+} and Fe^{3+} oxidation state, but measure the total iron content as Fe^{3+}. Ferrous iron was determined by the modified Wilson (1960) technique (Whipple 1974). Analyses of alteration minerals were done using the electron microprobe at Carleton University, Ottawa, Ontario. Carbon isotopes were measured by Vario EL III (Elementar, Germany) and DeltaPlus IRMS (ThermoFinnigan, Germany) at the University of Ottawa to determine the relative and absolute isotopic ratios of $\delta\ ^{13}C$. Organic matter in graphite was extracted from the powdered rock samples by NaOH hydrolisation and was analysed using a spectrophotometer which measures the absorption of light in the ultraviolet wavelength range. To characterize the type of organic matter present, a NMR (Nuclear Magnetic

Resonance) analysis was done at the University of Ottawa, using a Bruker ASX 200 with a 7mm triple resonance CPMAS probe in double resonance mode.

The error in the major oxides is less than 0.5% of the reported value and for trace elements, less than 10%. The error was calculated with a confidence interval of 95% using the method of Kretz (1985) on lab standards and on three blind samples analysed five times in repetition. Two blank samples were analysed to identify contaminants.

Regional geological setting

Archean bedrock geology of the Timmins Gold camp consists of 4 distinct supracrustal units identified as the Deloro, Tisdale, Porcupine and the Timiskaming assemblages. These assemblages are cut by different suites of intrusions (Fig. 4.3A), which are defined by their geochronological age (U-Pb TIMS), tectonic affinity and geochemical signatures. The Tisdale and Porcupine Assemblages are the only assemblages present at Hoyle Pond and are described below.

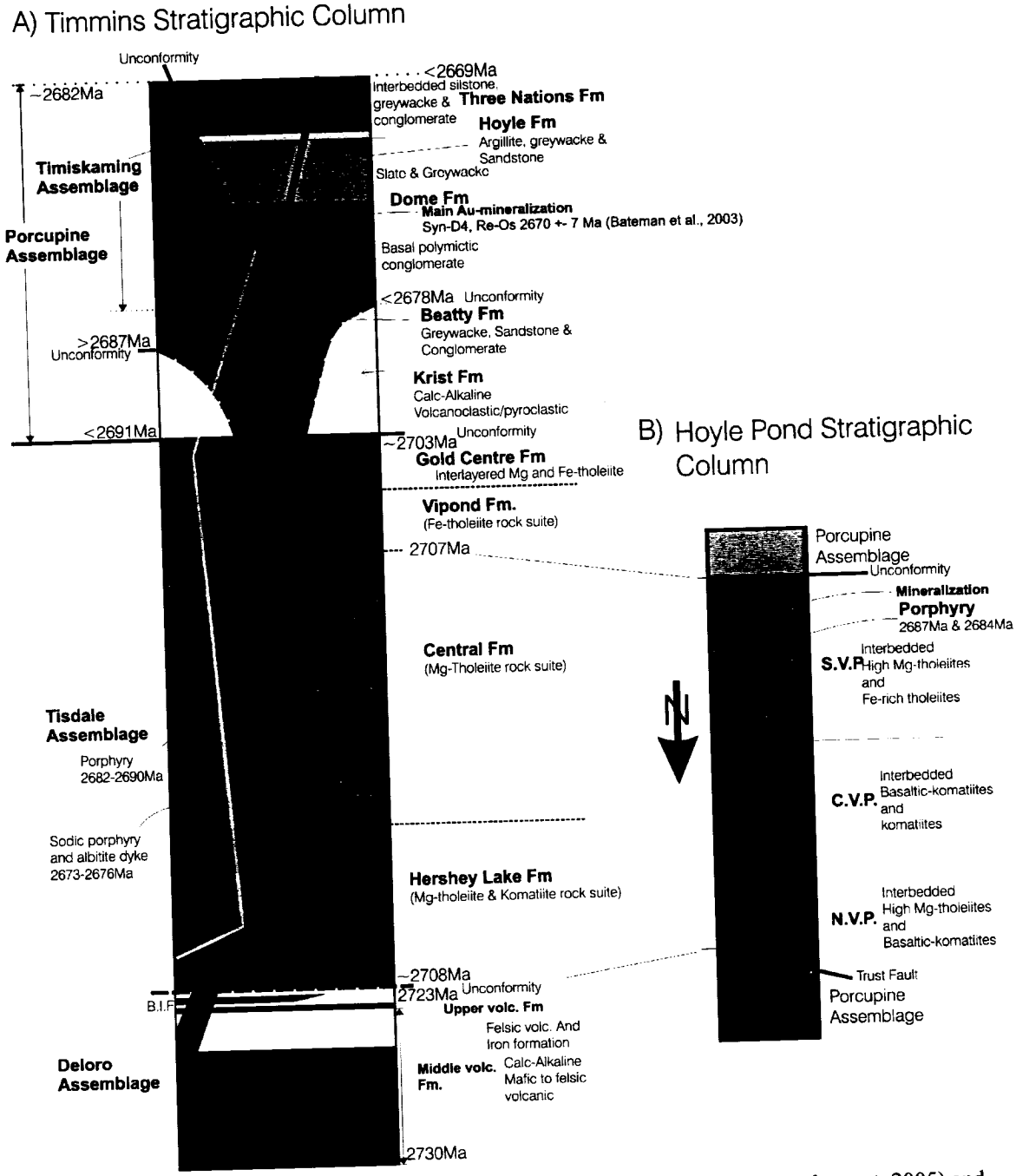

Figure 4.3 Timmins area (A) stratigraphic column (modified from Barr, PJV internal report, 2005) and Hoyle Pond mine (B) stratigraphic column, SVP (South Volcanic Package), CVP (Central Volcanic Package), and NVP (North Volcanic Package). The mine rocks are within the Hershey Lake and Central formations of the Tisdale assemblage.

Tisdale Assemblage

The Tisdale Assemblage is mainly composed of mafic tholeiitic volcanic rocks intercalated with ultramafic and felsic volcanic rocks and of felsic calc-alkaline volcanic rocks (Fig. 4.3A) ranging in age from 2710 to 2704 Ma (Ayer et al., 2005). South of the PDDZ, the Tisdale Assemblage unconformably overlies the Deloro Assemblage. The maximum apparent thickness of the Tisdale Assemblage is 3440m as measured in the north-eastern part of the Tisdale Township between the axis of the North Tisdale anticline and its upper contact with the Krist formation (Brisbin, 1997). Previous authors interpret the base of the Tisdale Assemblage to be within the Porcupine Destor Deformation Zone (PDDZ) (Pyke, 1982). However, field mapping by Dinel and others (Vaillancourt et al., 2001, Bateman et al. 2005) show that the location of the PDDZ is neither restricted to the base of the Tisdale Assemblage, nor is it a discrete fault surface. Instead it is a large (100 to 500m) corridor of deformation overprinting the unconformity. The Tisdale Assemblage (formerly a group) is subdivided into 5 formations (Ferguson 1968, Dunbar 1948 and Jones 1948), two of which, the Central and Vipond Formations, host the majority of the economic deposits. The formations are briefly described below in ascending stratigraphic order.

Hershey Lake Formation

The Hershey Lake Formation consists mainly of high-Mg tholeiitic basaltic pillowed flows, basaltic komatiitic, and komatiitic flows. It has an apparent thickness of ~600m (Brisbin, 1997).

The ultramafic flows have MgO contents of 10w%-18w% and >18 w% and are classified as basaltic komatiite and komatiite, respectively, based on the geochemical criteria of Arndt (1975). They have flat REE patterns with chondrite ratios <7. In the field, the ultramafic flows of the Hershey Lake Formation can be distinguished from the mafic flows by their color index and characteristic polygonal jointing. Komatiites are dark grey on fresh surfaces and have an orange-brown color on weathered surfaces. In addition, some komatiite flows have spinifex textures, are altered to talc and carbonate, and cut by serpentine infilled fractures. The tholeiitic mafic volcanic rocks within the Hershey Lake

Formation occur as massive and pillowed flow and differ from similar flows in the overlying Central Formation by their association with ultramafic flows.

Central Formation

Pyke (1982) described the composition of the mafic volcanic flows of the Central Formation as a continuum from magnesium tholeiitic basalts through iron tholeiitic basalts. The Central Formation is approximately 450m thick (Brisbin, 1997) and is mainly composed of mafic, locally variolitic, massive and pillowed flows with pillow top breccias. Pillows have 1-5 cm thick selvages and an average size of 100cm by 50 cm in plan view. The rocks of the Central Formation are in general high-Mg basalts intercalated with beds of black argillites or siltstones with cherty clasts.

Vipond Formation

The Vipond Formation is characterized by very distinctive high-Fe tholeiitic variolitic pillowed mafic and intermediate volcanic flows (Dinel et al., under revision, see chapter 6) and by variolitic hyaloclastic mafic flows intercalated with massive mafic flows and carbonaceous argillite.

Gold Centre Formation

The Gold Centre Formation is the uppermost formation of the Tisdale Assemblage. It is dominated by green, fine-to medium-grained, massive, leucoxene-bearing mafic flows (likely tholeiitic basalts) and calc-alkaline mafic to felsic volcanic rocks (Brisbin, 1997).

Porcupine Assemblage

The Porcupine Assemblage ranges in age from 2690 to 2685 Ma and unconformably overlies the Tisdale assemblage in the Timmins area (Ayer et al., 2005). It is composed of siltstone, mudstone and sandstones with local polymictic conglomerate, in conformable contact with calc-alkaline felsic volcanic rocks of the Krist Formation at the base of the assemblage (Fig. 4.3A). The turbidites have Bouma sequence subdivisions indicating distal deposition from turbidity currents in a shelf like environment (Born, 1995). It is a very extensive assemblage, occurring north of the PDDZ from Bristol Township to Matheson, over a distance of approximately 60 km.

Regional Major structures

The Porcupine-Timmins gold camp is deformed by at least 6 deformation events, D1-D6 (Bateman et al. 2005, Bleeker, 1999). The first two events D1 and D2 are not observed at Hoyle Pond and will not be discussed further. D3 is represented by east-west-trending isoclinal folds with a steeply dipping axial planar S3 foliation parallel to lithological contacts. D3 is either syn- or post-deposition of the Timiskaming assemblage (Bateman 2005). D4 produced a steeply dipping foliation, S4, oriented ~060-070°, ~15 degrees counterclockwise to S3. S4 is axial planar to isoclinal F4 folds, which characterized in Hoyle Pond, the northern margin of the 1060 fault zone (fz). The intersection lineation of S3 (E-W) with S4 (ENE-WSW) appears to be subparallel to the plunge of ore zone at the Hollinger-McIntyre deposit (Melnik-Proud, 1992) and Hoyle Pond mine. The D5 event is represented by a moderately dipping crenulation cleavage S5 with two general strikes: 045° and 335°. S5 is axial planar to asymmetric Z-folds and S-folds. D6 structures are observed on vertical surfaces as a sub-horizontal crenulation S6 cleavage axial planar to mm to m scale subhorizontal folds (Dinel, 2001).

The major shear zone in the Timmins area, the PDDZ is a high-strain corridor with intense foliations, characterized by tight to isoclinal F4 folds. The Hollinger-McIntyre and Dome mine occur on structures that are subparallel splays of the PDDZ.

Mine Geology

The volcanic belt is bounded on all sides by meta-sedimentary rocks of the Porcupine Assemblage (Rye, 1987) (Fig. 4.2). The volcanic rocks at the mine are thrust-bounded to the north by south facing greywackes and siltstones of the Porcupine Assemblage and are bounded to the south by a discordance (either a fault or unconformity) at their contact with south facing siltstones and greywacke also of the Porcupine Assemblage (2690-2685Ma, Ayer et al., 2005). The volcanic rocks are intruded by quartz-feldspar porphyries and quartz porphyries (Fig. 4.2).

The volcano-sedimentary rocks in the Hoyle Pond area were subjected to greenschist facies regional metamorphism (e.g. Thompson, 2005). Throughout the area, undeformed

and deformed volcanic rocks are composed of an albite-chlorite mineral assemblage, the pores spaces of which (clast interstices and vesicles) have been filled with calcite, minor quartz and chlorite.

Meter-scale sampling facilitated relatively precise determination of "immobile" elements with respect to alteration by use of isocon diagrams (Grant, 1986) comparing numerous samples heuristically to identify the least altered samples. The elements Al, Ti, HREE, Zr, and Y, and to a lesser extent LREE, are "immobile" (see Fig. 4.4) consistent with previous work by Michard et al. (1983,1987), Michard and Albarède (1986) and Michard (1989), Kerrich et al.(1999) and Wyman (2003). REE chondritic normalized plots (Sun and McDonough, 1989) and various trace element ratios plots were used to help discriminate rock types and to compare the stratigraphy of the Hoyle Pond with formations within the Tisdale assemblage.

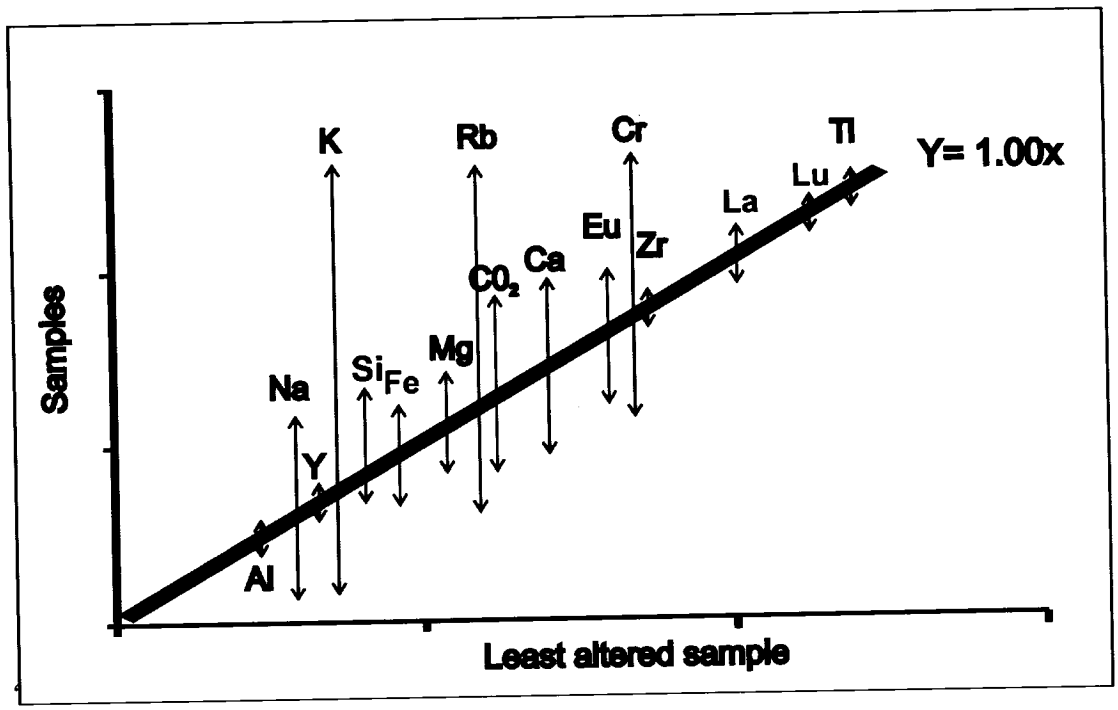

Figure 4.4 Schematic summary using the isocon diagram method of Grant (1986), of altered sample on the SVP 720ml 1060fz, demonstrating the mobility of some trace elements (ppm) and major oxides (w%), the abscissa represents least altered sample and the ordinate ore zone sample.

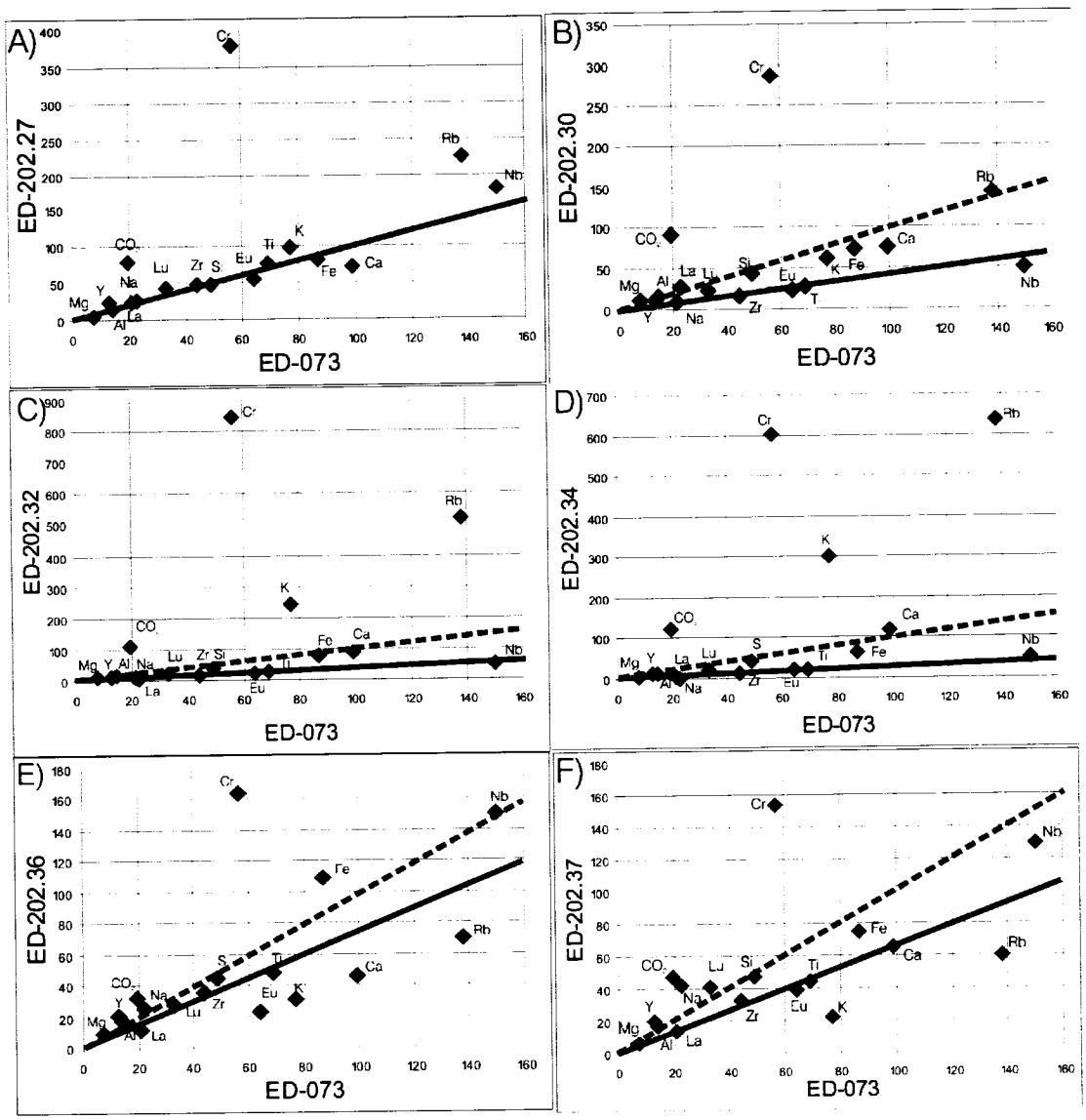

Figure 4.5 Isocon diagram plot of samples collected in the 1060fz B3 vein area (see Figure 5.2 and appendix III),. Figures 5.5-A to F are from samples at different distances from veins. The samples represented by isocon A and B are located 3 and 2 m respectively south of the B3 vein, in the albite alteration zones (see below), whereas the samples represented by isocons C and D occur within a stockwork zone and in the sericite alteration zones (see below) enveloping the B3 vein. The samples represented by isocon E and F are 3 m and 4 m from the stockwork zone respectively, north of the B3 stockwork zone, in the albite alteration zone. The major oxides are in wt % and trace elements in ppm. Each variable have been multiplied by a factor: Al = Al_2O_3 wt % x 1, Mg = MgO wt % x 1, Ti = TiO_2 wt % x 100, Zr = ppm x 1, Na = Na_2O w% x 10, K = K_2O w% x 100, Ca = CaO w% x 10, Rb = ppm x 10, Eu = ppm x 100, Cr = ppm x 1, Y = ppm x 1, La = ppm x 10, Lu = ppm x 100, Lu = ppm x 100, Fe = FeO w% x 10, Nb = ppm x 100, Si = SiO_2 w% x 1. The major oxides are label as elements in the figure. Two curves are plotted on the isocon diagrams. The dashed lines represent a curve y=x, along which all the immobile elements should plot if no alteration affected the samples. The solid line correlates identified immobile elements and its slope is less than expected demonstrating the concentration of the immobile elements have been diluted by a mass gain in mobile elements.

North Volcanic Package

The NVP consists of interbedded mafic and ultramafic volcanic rocks (Fig. 4.2). The mafic rocks are dominated by pillowed flows, pillow breccias, and locally massive coherent flows (Photo 4.1 and 4.2). The pillows vary in size from 50cm to 1.5m. They are generally undeformed and south-facing outside of shear zones, consistent with the facing direction of the Porcupine meta-sedimentary rocks bounding the mine stratigraphy to the north and south (cf. Rye, 1987). Rye (1987) reported that the pillow sequence in the NVP at Hoyle Pond faces to the north. They are characterized by a pale apple-green color and a very fine-grained groundmass. On level 3 of the mine, variolitic pillow flows and pillow breccias were observed. Variolitic pillows exhibit leucocratic mm scale (2-5mm) globular bodies which are aligned and form bands along pillow margins. Fragments in the pillow breccia are amoboedal in shape and vary in size from 5cm to 25cm with mm size varioles that are concentrated in sinuous bands and are truncated by the pillow selvages (Photo 4.2)

The mafic rocks are composed of chlorite, albite, carbonate, hydrothermal quartz, sericite, local graphite and some opaque minerals, chiefly minor iron oxides, pyrite and traces of chalcopyrite. Locally, sericite is concentrated along cleavage domains. In thin section the varioles appear as very fine, 2-5mm spherulites that have diffuse edges that blend with the groundmass. They are albitized and contain patches of titanite. Pervasively albitized rocks have fan-like albite in micro-lithons with spherulitic extinction.

The ultramafic rocks are dark grey to black aphanitic rocks with coarser grained dolomite porphyroblasts and a soapy-soft cleavage. They locally contain minor chlorite, some disseminated quartz crystals, and iron oxides.

Although FeO and MgO were mobile we use the Jensen Cation Plot because of its widespread use in studies of volcanic rocks of the area. The mafic rocks plot mostly in the high-Mg tholeiitic field with some samples appearing in the calc-alkaline basaltic field (Fig. 4.6). The high Mg-tholeiitic basalt's geochemical signatures can be identified by their generally flat to slightly concave REE patterns (Fig. 4.7). The HREE (Gd, Dy, Er, Yb, Lu) are in general slightly more enriched than the LREE (La, Ce, Nd, Sm). They

have flat to shallow negative sloped LREE (La-Sm) varying from 8 to 14 times chondrites and gently positive sloped HREE varying from 12 to 20 times chondrites. The La/Lu and Ce/Yb chondritic normalized ratios range from 0.2-0.8 and 0.3-0.8 respectively. Although most samples have negative Eu anomalies, others have positive Eu anomalies. The positive Eu anomalies may represent the deposition of carbonate minerals from relatively Eu-rich fluids in carbonate minerals (Michard and Albarède, 1986).

In contrast, the basaltic komatiites REE (Fig. 4.7) chondritic ratios are below 10 times chondrite and show convex REE patterns with enriched HREE compared to LREE. The normalized LREE abundance vary from 5.5 to 7.5 times chondrites and the normalized HREE abundance vary from 8.0 to 9.5 times chondrites. Eu anomalies vary from slightly positive to slight negative. The La/Lu and Ce/Yb chondritic normalized ratios range from 0.4-0.8 and 0.5-0.8 respectively.

Photo 4.1 NVP high-Mg tholeiitic basalts pillow flow (3 level). Looking east, younging direction to the south.

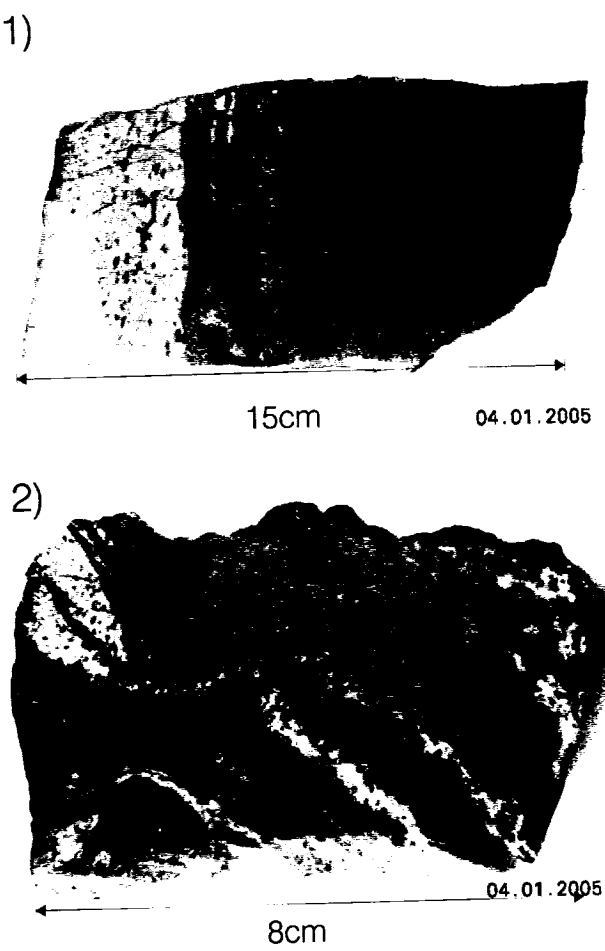

Photo 4.2 NVP high-Mg tholeiites as 1) Variolitic pillow flow and 2) pillow breccias with flow banding.

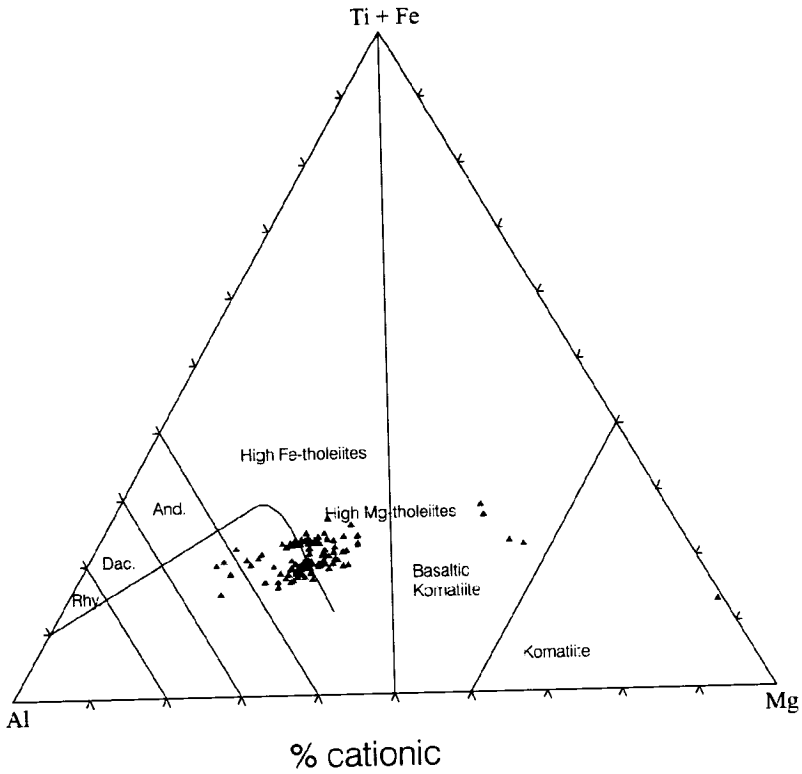

Figure 4.6 Jensen Cation plot (Jensen, 1976) of the NVP volcanic rocks which plot in the field of high-Mg tholeiitic basalts and basaltic komatiites.

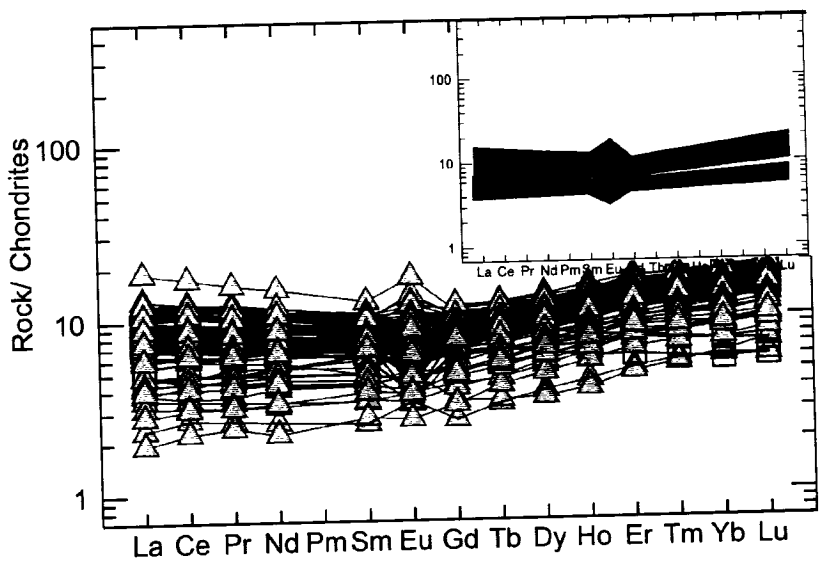

Figure 4.7 Chondritic normalized REE pattern of the NVP high-Mg tholeiitic (triangles) basalts and basaltic komatiites (square). The inset shows the approximate range of the normalized REE abundance of the high-Mg tholeiitic basalts (green) and basaltic komatiites (blue).

Central Volcanic Package

The Central Volcanic package (CVP) (Fig. 4.2) consists of a sequence of interbedded komatiite (typically>18 wt% MgO) and basaltic komatiites (12-18 wt% MgO) (Fig. 4.8) approximately 200m in apparent thickness. The contacts between the basaltic komatiites and komatiites are gradational and are commonly overprinted by strong carbonate alteration (dolomite to ferroan-dolomite) and deformation, which resulted in the generation of an intense fabric and associated quartz-carbonate stringer zones.

The basaltic komatiites are characterized by carbonatized fine-grained to medium-grained dark green to black chlorite schists with minor talc. The mineral assemblage is dominated by chlorite, talc, dolomite, hydrothermal quartz, iron-titanium oxides, coarse grained (1-2mm) carbonate porphyroblasts and locally Cr-micas, actinolite and trace pyrite.

The komatiites are altered to talc-chlorite schist to talc schist. Their color varies from dark grey-black, to cream grey-beige due to carbonatization. The mineral assemblage is dominantly talc, chlorite, dolomite, hydrothermal quartz, iron titanium oxides and locally serpentine. In some thin sections, the Fe-Ti oxide crystals form ring-like structures typical of relict olivine and are interpreted to represent the remnants of olivine cumulate zones (Photo. 4.3).

With one exception, all of the CVP specimens have REE less than 10 times chondrite (Fig. 4.9). The HREE patterns have less curvature than the LREE and a slight decrease in concentration from Dy to Lu. Some samples have slight positive Eu anomalies, whereas the majority have small negative Eu anomalies. There is a continuum in REE concentrations from komatiites to basaltic komatiites. The komatiites have normalized LREE abundance varying from 1.5 to 3.5 times chondrites and normalized HREE abundance varying from 3.0 to 5.5 times chondrites. The La/Lu and Ce/Yb chondritic normalized ratios range from 0.3-1.0 and 0.3-1.2 respectively. The basaltic komatiites have normalized LREE of 4.0 to 8.0 times chondrites and normalized HREE abundance from 6.5 to 10 times chondrites. The La/Lu and Ce/Yb chondritic normalized ratios range from 0.4-0.8 and 0.5-0.9 respectively.

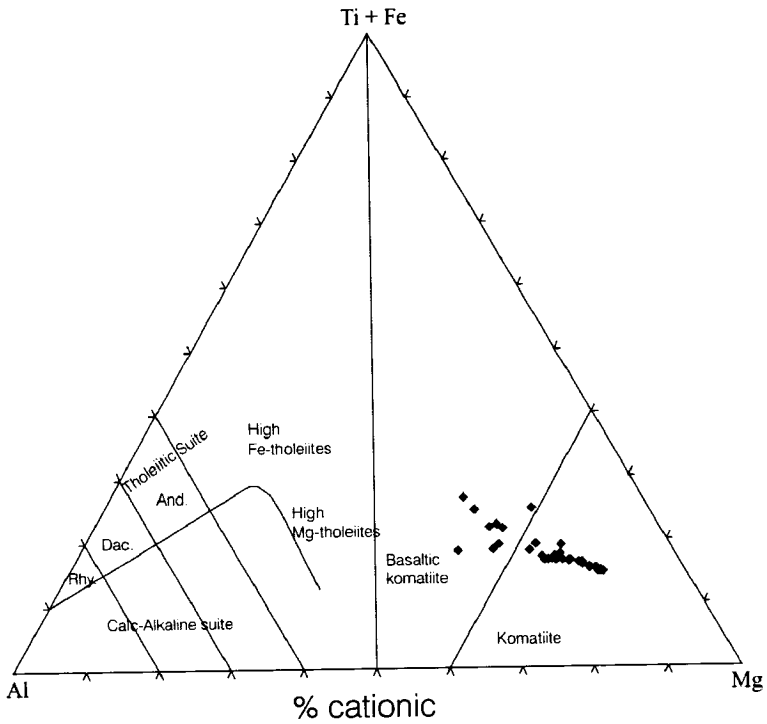

Figure 4.8 Jensen Cation plot (Jensen, 1976) of the CVP volcanic rocks, komatiites and basaltic komatiites.

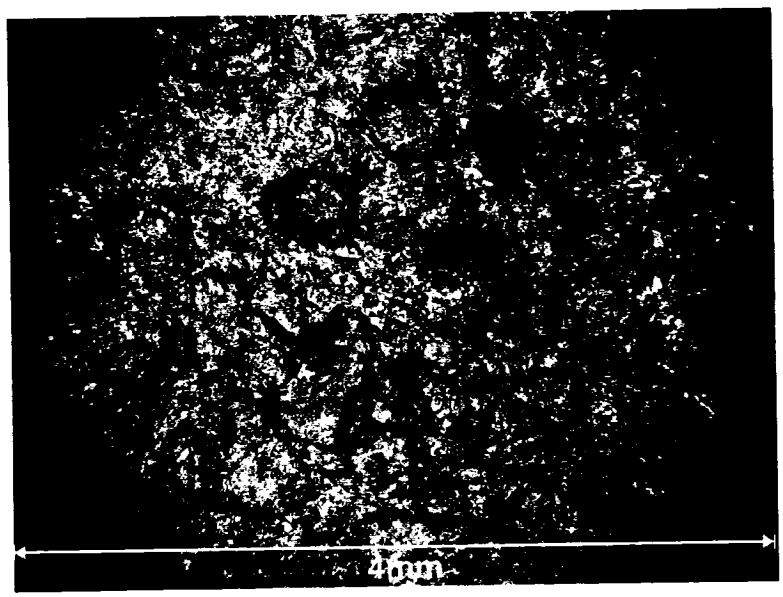

Photo 4.3 Komatiitic flow, altered to talc, and iron-titanium oxides that rim relict cumulate crystals of olivine (fov~4 mm).

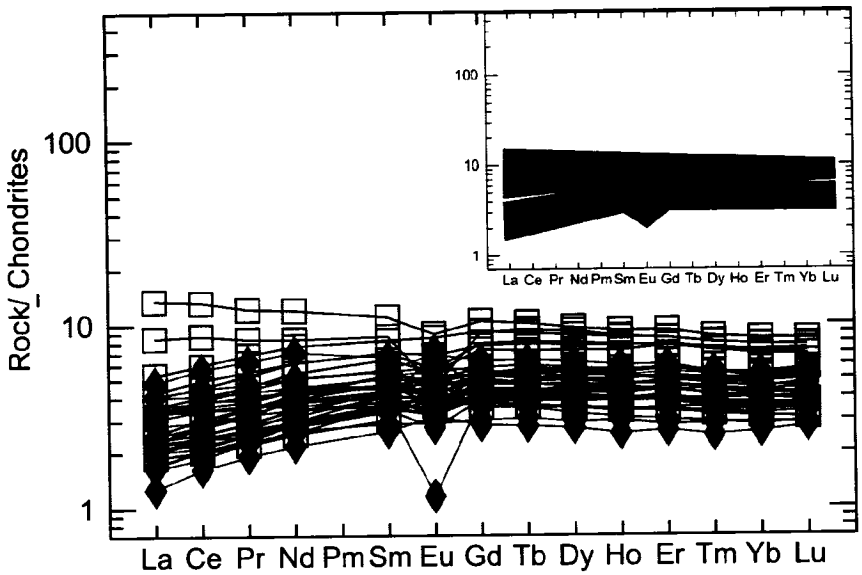

Figure 4.9 Chondritic normalized REE pattern of the CVP volcanic rocks, komatiites (diamonds) and basaltic komatiites (square). The inset shows the approximate range of the normalized REE abundance of the komatiites (pink) and basaltic komatiites (blue).

South Volcanic Package

The SVP rocks are strongly carbonatized basalts that are generally more foliated than rocks of the NVP and CVP. They occur as pale to dark green ~10-40 m thick massive to pillowed flows with local flow top breccias, which were deformed to coarse-grained chloritic schist. Their mineralogy consist of chlorite, quartz, titanite, sericite, carbonate (calcite, dolomite and ferroan-dolomite), K feldspar, pyrite, iron-titanium oxides and, locally graphite.

The SVP rocks can be differentiated based on their geochemistry as high-Mg, Mg-rich and Fe rich tholeiitic basalt units (Fig. 4.2). The composition of the carbonate mineral differs in the Fe-rich tholeiitic basalts compared to the two other units; it is more enrich in Fe and consists of ferroan dolomite. In addition, the High-Mg and Mg tholeiitic basalts show slight modal increase in pyrite and chalcopyrite. Contacts between the three units are sharp and marked by quart-veining and Cr-mica and sericite alteration (Photo 4.4). The basalts of the SVP are ~10-40m thick massive to pillowed flows with local pillow and flow top breccias. They are pale to dark green and occur as a medium to coarse grained chlorite schist. The pillows and breccia clasts in the 1060fz are stretched vertically, parallel to the S3-S4 intersection lineation.

The three compositional groups are observed on the Jensen Cation plot (Fig. 4.10), REE chondritic normalized plot (Fig. 4.11) and ratio plot (Zr/Al_2O_3 vs. TiO_2/Al_2O_3) (Fig. 4.12). The Fe-rich tholeiitic basalts are characterized by their relatively high chondritic ratios and concave LREE to HREE pattern with HREE slightly more enriched than LREE. The normalized LREE abundance varies from 15-30 times chondrites and the normalized HREE abundance varies from 20-30 times chondrites (Fig. 4.11). The La/Lu and Ce/Yb chondritic normalized ratios range from 0.4-0.8 and 0.5-0.9 respectively. The Mg-tholeiitic basalts have similar slopes as the Fe-rich tholeiitic basalts and high-Mg tholeiitic basalts but have intermediate REE concentrations. The LREE ratios vary from 6.0 to 11 times chondrites and the HREE ratios vary from 8.0 to 15 times chondrites (Fig. 4.11). The La/Lu and Ce/Yb chondritic normalized ratios range from 0.4-0.9 and 0.5-0.9 respectively. On the Jensen Cation Plot, the Mg-tholeiites are identical to the other Mg-basalts observed in the NVP. The high-Mg tholeiitic basalts have similar REE slopes as

the other two basalts type but they are characterized by lower REE chondritic ratios, normalized LREE abundance that vary from 2.2 to 4.7 times chondrites and normalized HREE abundance that vary from 7.0 to 11 times chondrites (Fig. 4.11). The La/Lu and Ce/Yb chondritic normalized ratios range from 0.3-0.7 and 0.3-0.7 respectively.

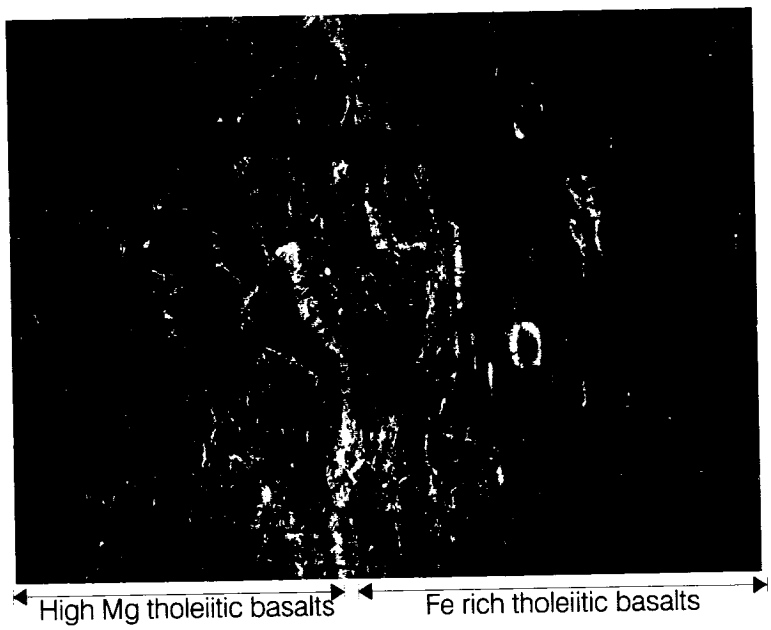

Photo 4.4 Underground photo of the contact between the Fe-rich tholeiitic basalts (left) and high-Mg tholeiitic basalts (right). 5-10cm quartz-carbonate veins with sericite-fuchsite alteration halo are at the contact between the two rock types.

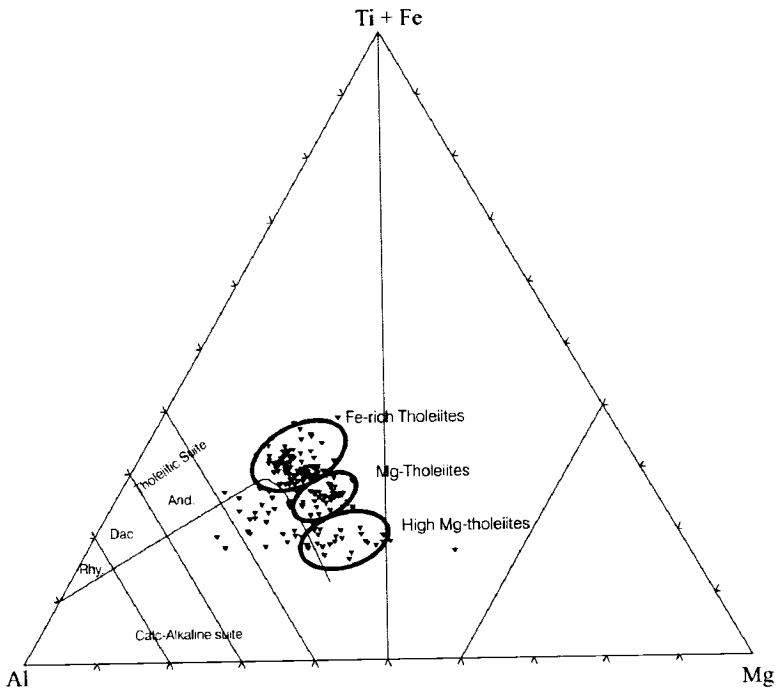

Figure 4.10 Jensen Cation plot (Jensen, 1976) of the SVP volcanic rocks, Fe-rich tholeiitic basalts, Mg tholeiitic basalts and high-Mg tholeiitic basalts.

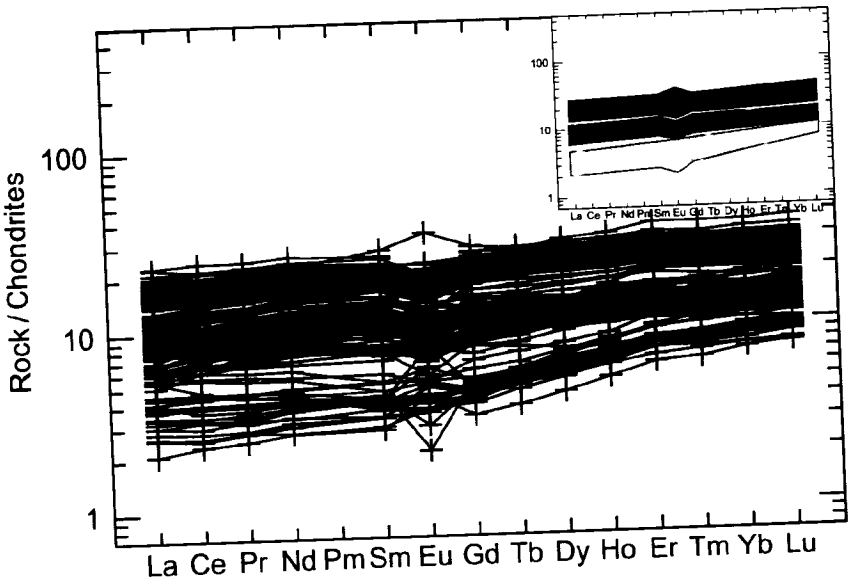

Figure 4.11 Chondritic normalized REE pattern of the SVP volcanic rocks, Fe-rich tholeiitic basalts, Mg tholeiitic basalts and high-Mg tholeiitic basalts. The inset shows the approximate range of the normalized REE abundance of the Fe-rich tholeiitic basalts (dark green), Mg tholeiitic basalts (very light green) and high-Mg tholeiitic basalts (intermediate green).

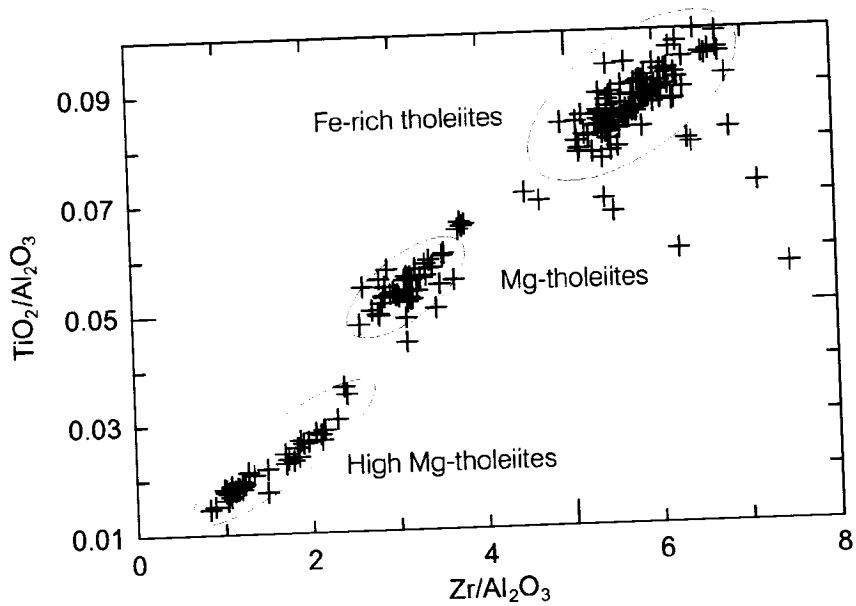

Figure 4.12 Ratio plot of the SVP, TiO_2/Al_2O_3 vs. Zr/Al_2O_3, differentiating the 3 volcanic rock types, Fe-rich tholeiitic basalts, Mg tholeiitic basalts and high-Mg tholeiitic basalts.

Other Lithologies

Younger quartz-feldspar porphyries (QFP) and quartz porphyry sericite schist (QP) cut the SVP. The QP is a 2-4m thick, 200 m long, sericitized and foliated sill composed of ~5% quartz phenocrysts, with rare fuchsitic altered clasts. The QP is intersected by dominant S3 fabric and folded by D4. In thin section, the quartz phenocrysts have an embayed dissolution texture typical of felsic extrusions or shallow intrusions. It has a U-Pb zircon discordant age of 2687.6 ± 2.2 Ma (TIMS) (Ayer et al. 2005).

The QFPs cut across stratigraphy. They are moderately foliated by S4 and they have very weak to no metamorphic halos. They are composed of 30-40% albite phenocrysts (5mm to 1.5cm) and ~5% quartz phenocrysts varying in size from 2mm to 5mm within a matrix composed of very-fine-grained quartz, albite and muscovite. They have a trachytic texture defined by an alignment of feldspar phenocrysts. Zircons extracted from a sample from the 620m level returned an U^{207}/Pb^{206} concordant crystallization age of 2684.4 ± 1.9 Ma (TIMS), but the sample also contains inherited zircon with an age of 2695.2 Ma (Ayer et al. 2005).

The quartz-feldspar porphyry and the quartz porphyry have very similar composition. The two porphyries have identical REE chondritic normalized pattern - a LREE (18-25 times chondrite) to IREE negative slope and IREE to HREE flat pattern (1 time Chondrite) (Fig. 4.13).

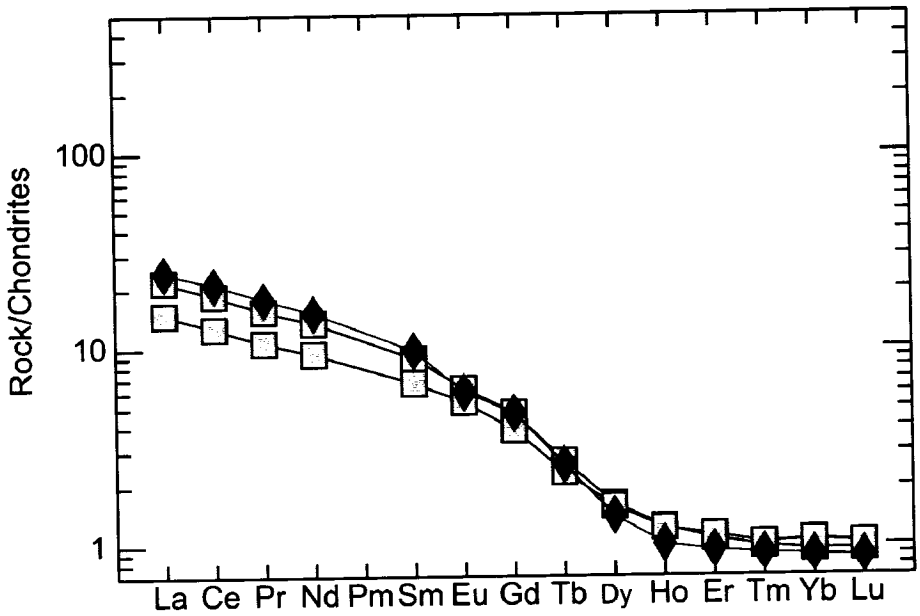

Figure 4.13 Chondritic normalized REE pattern of the felsic intrusive Quartz-Feldspar (squares) and Quartz (diamonds) porphyry.

Structure

The mine stratigraphy consists of a south facing homoclinal sequence of stacked volcanic rocks, previously interpreted to be an anticlinal fold cored by ultramafic volcanic rocks. The volcanic rocks are foliated by a dominant S3 (Fig. 4.14) fabric parallel to bedding that strikes generally eastward. Although not visible at the mine scale, the S3 fabric is interpreted to be associated to isoclinal F3 folds. When compared to the Porcupine gold camp deformation history, the Hoyle Pond mine main fabric (S3) is comparable to what Bateman et al. (2005) describes as S2. If correct, this would indicate that the S3 fabric described by (Bateman et al., 2005) is not observed at the mine (see table 4.1) and restricted to the PDDZ. S3 is refolded at the mine scale by D4. The S4 fabric trends ~070 (Fig. 4.2) and is axial planar to isoclinal F4 folds in the 1060 fault zone and to Z-shaped F4 folds, northwest of the 1060fz (see Fig. 4.2 and 4.15). The F4 fold hinges plunge approximately 075° to the northeast and parallel to the locally observed stretching lineation (L4) and parallel to the shoot (ore zone plunge) of the mineralization in the 1060Fz. D5 and D6 (Fig. 4.14) have affected the stratigraphy at the centimetre and metre scale. Since it is a minor component in the genesis of the deposits it will be ignored in the following pages.

The timing of D3 event is constrained between 2687.6 ± 2.2 Ma and 2684.4 ± 1.9 Ma. The QPs are pre-D3, and are foliated by S3, the QFPs are post-D3 and pre-D4, because. One would consider the age of the QFP and QP to be identical when comparing the uncertainties on the ages. However, the geological evidence is strong, where the QP's are deformed by D3 and D4, possessing S3 and S4 fabric, whereas the QFP's are only deformed by D4 within and external to the 1060fz where they lack the penetrative S3 fabric yet possess the S4 fabric. This geological cross cutting relationship clearly shows a time interval existed between inrusion of the QP and QFP.

The loci of the mineralization in the 1060fz are coincident with the contacts of the various lithologies on the limbs of the isoclinal F4 folds (1060fz). The 1060fz (shear zone) is a corridor of intense deformation, where S4, oriented ~070°, is very penetrative and acted as a shear foliation.

The sequence of deformation, alteration and mineralization events is shown in figure 4.16 and 4.17. The albite and carbonate porphyroblasts present in microlithons are dissected and in their wall rocks, which also contain pyrite at vein contacts. by a cleavage defined by muscovite, Cr-muscovite, with minor quartz and graphite (Photo 4.5), thus demonstrating the existence of an earlier albite-carbonate alteration. Locally, Fe-dolomite porphyroblast are dislocated and overprinted by S4 fabric, indicating a reactivation during D4. Graphite alteration is visible in fault-fill, extension veins and, both alteration halos enveloping the gold bearing veins (eg. Albite and Sericite Alteration Zones, see below), in former wall rock interstices (Photo 4.6), within flow top breccias and hyaloclastite, and along stylolites and cleavages. The tourmaline is present in stylolites and in the fault-fill veins and extensional veins as coarse euhedral grains. Needles of arsenopyrite occur in the veins

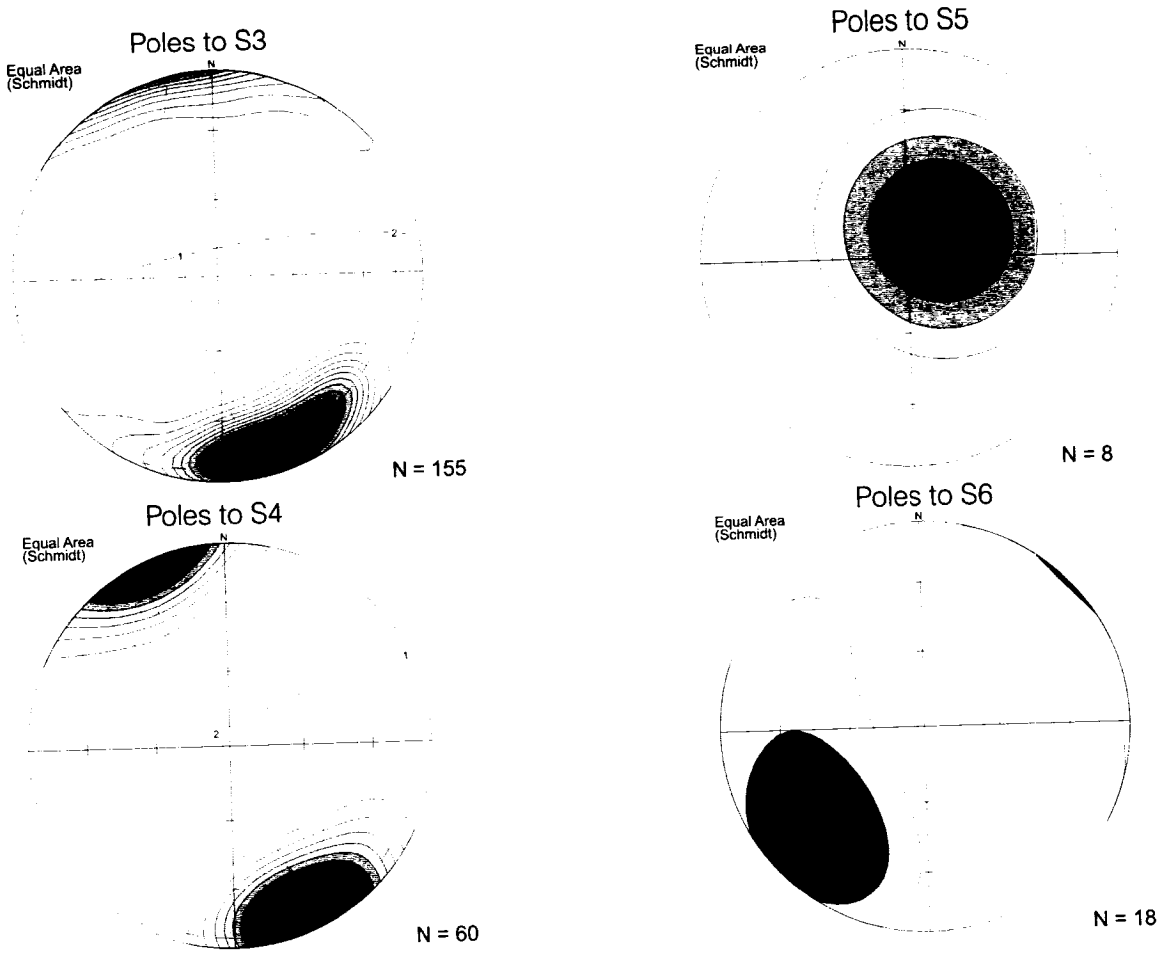

Figure 4.14 Lower hemisphere equal area projections of poles to S3, S4, S5 and S6.

Rhys (2003b) interpretation			Bateman et al., (2005)		Dinel et al.
Age (Ma)	lithologies	Deformation events	Age (Ma)	lithologies	deformation events	Deformation events
2730-2725 2708-2700 2700- ~2690	Deposition of the Deloro assemblage Deposition of the Tisdale assemblage	**D1a** : Northwest trending folds, no foliation developed or preserved.	2730-2723 2708-2703	Deposition of the Deloro assemblage Deposition of the Tisdale assemblage	**D1**: extensional-uplift event, no foliation associated. Tisdale-Porcupine unconformity.	**D1** : No fabric observed at the mine.
~2691- ~2680	Deposition of the Porcupine assemblage		2691- ~2682	Deposition of the Porcupine assemblage	**D2**: Isoclinal folds (e.g. North Tisdale Anticline, Porcupine Syncline) and late thrust event (Tisdale thrust over Porcupine). Early dip-slip faulting in the Destor-Porcupine deformation zone.	**D2**: No fabric observed at the mine (based on Rhys, 2003a, internal company report).
~ 2680- ~2675		**D1b**: West-northwest trending isoclinal folds lacking axial planar cleavage, modificationof D1a folds.				**D3**: East-west isoclinal folds with axial planar cleavage parallel to bedding, possible late gold mineralization (2687>D3>2684). Late D3 Thrust, Tisdale on Porcupine.
~2675- ~2672		Destor-Porcupine fault system, early faulting, >10km sinistral strike slip displacement, north side down.	2678-2669	Deposition of the Timiskaming assemblage + albitite dyke at McIntyre Mine (~2672Ma)	**D3**: folding (e.g. South Tisdale anticline) and axial planar cleavage S3 dominant penetrative fabric in Timmins (oriented 281°) post 2677Ma, result of oblique-slip movement along major deformation zones. Gold mineriization associated with D3.	
~2674- ~2672	Deposition of the Timiskaming assemblage + albitite dyke		> 2669		Formation of the Dome Fault. **D4**: isoclinal folding and S4 axial planar cleavage oriented 070° strong, restricted to the Timiskaming syncline. Dip-slip movement associated to D4 faults. Associated to gold mineralization.	**D4**: penetrative S4 fabric oriented 070°, axial planar to isoclinal folds and gold mineralization associated with D4.
~2672-?2643		**D2** + regional metamorphism: penetrative S2. east-southeast cleavage. Late gold mineralization.			**D5**: constrictional strain, observed west of Porcupine syncline, forming very stretched pillows, prominent where the Destor-Porcupine fault deflects. **D6**: Flat-lying crenulation cleavage. **D7**: north-northeast striking kink and chevron folds, steeply dipping axial planar cleavage.	**D5**: Northest crenulation cleavage associated to small scale Z-folds and conjugate kinks. **D6**: sub-horizontal crenulation cleavage axial planar to broad open fold (vertical displacement along S4).
		D3: Spaced S3 foliation east-southeast cleavage, continuation of sinistral displacement. **D4**: late retrograde deformation, north-northeast crenulation cleavage and conjugate kinks. **D5**: shallow southwest dipping crenulation cleavage.				

Table 4.1 Comparison of the chronology of deformation event in the Porcupine gold camp from different authors.

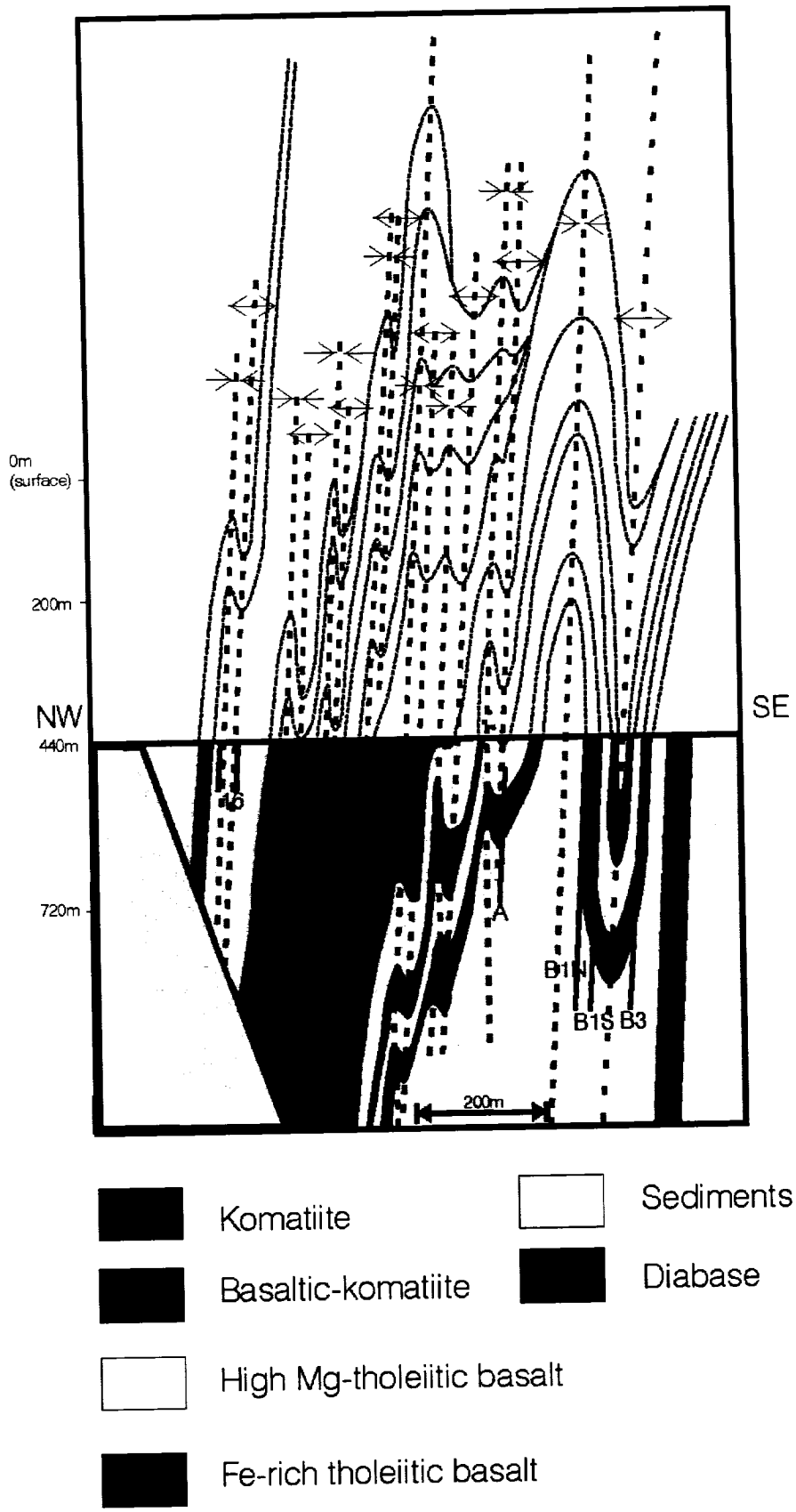

Figure 4.15 Vertical section of Hoyle Pond mine along NW-SE section with projection of F4 folds to and above surface.

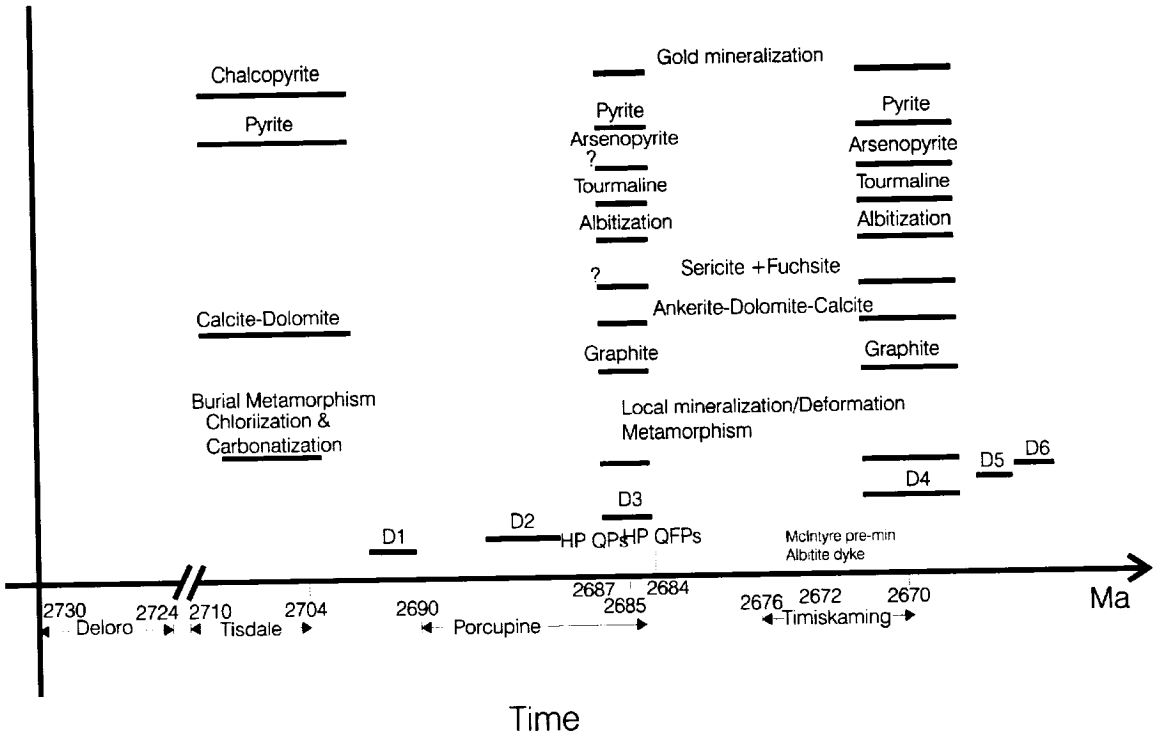

Figure 4.16 Paragenetic sequence of deformation, alteration and mineralization vs. time based on Bateman et al. (2005) and field observation at Hoyle Pond mine.

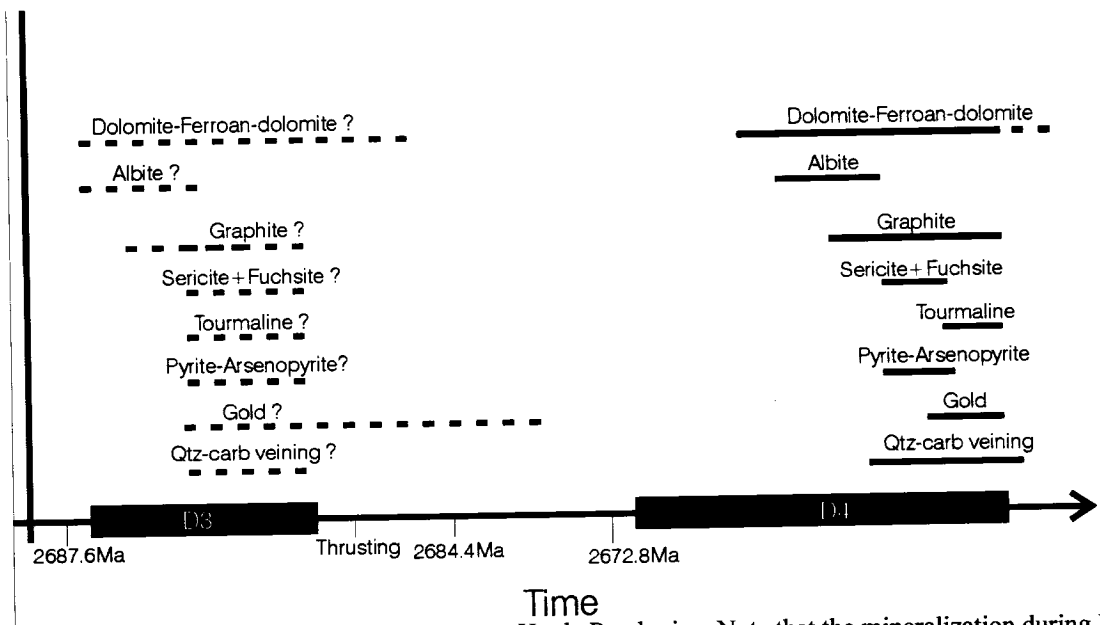

Figure 4.17 Paragenetic alteration sequence at Hoyle Pond mine. Note that the mineralization during D4 is similar to what is observed elsewhere in the PGC.

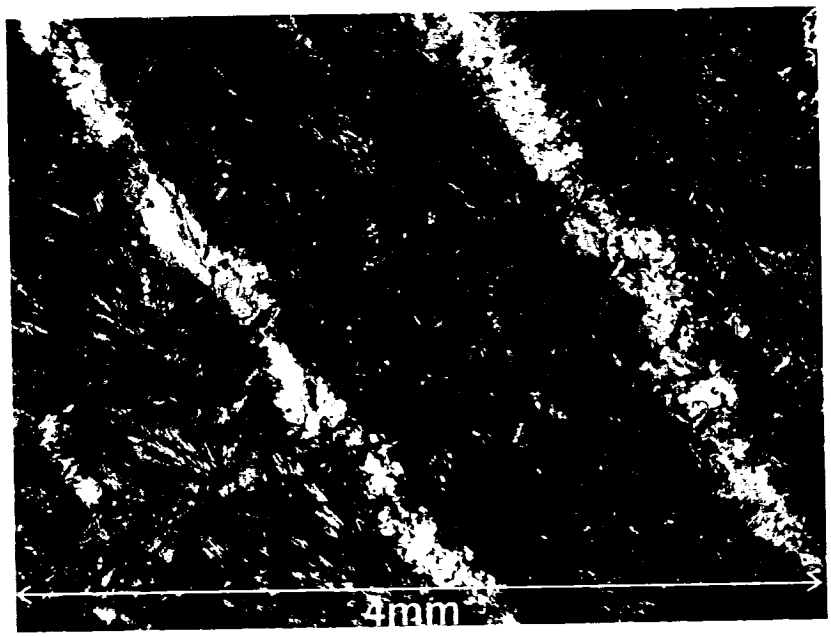

Photo 4.5 Spherulitic textures in albitized microlithons cut by S4 cleavage consisting of muscovite, Cr-muscovite and Fe-dolomites, crossed polars, showing albite is pre-sericite alteration.

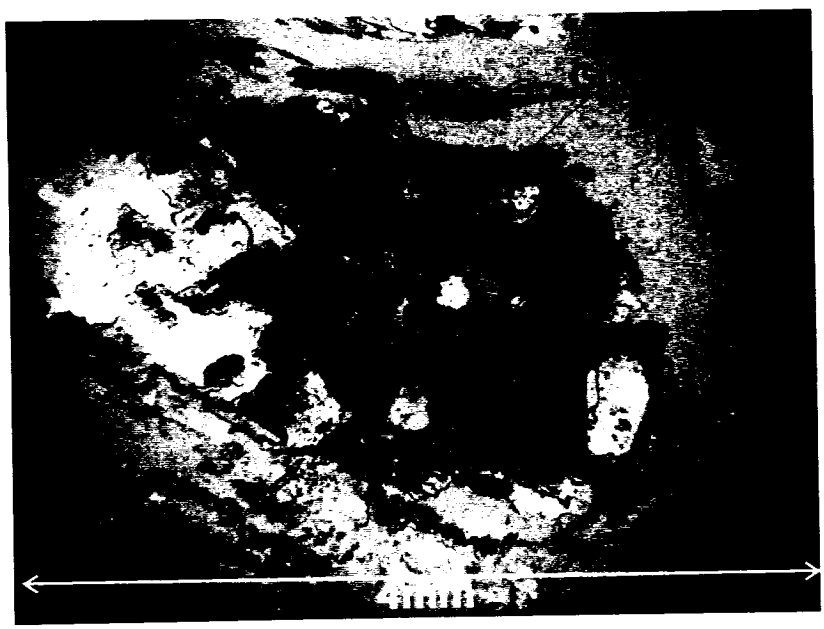

Photo 4.6 Graphite alteration in zone of increase porosity in a brecciated clast, natural light.

Vein descriptions

Both extensional and fault-fill veins are observed at Hoyle Pond. The extensional veins are straight to S-shaped, cut across the foliations S3 and S4 at high angles and have a general sinistral rotation. They are generally massive and composed of white to greyish quartz, with local pyrite along the wall rock-vein contact. Locally some extension veins have a black appearance due to graphite and tourmaline-filled fractures. The fault-fill veins are generally oriented ~070^{0} and have a more diverse mineralogy consisting of massive white to grey quartz, with interstitial tourmaline and/or stylolitic chlorite and locally muscovite or Cr-muscovite. Other fault-fill veins are mainly composed of massive white quartz and are commonly associated with variable concentrations of graphite in the wall rock selvages. In the NVP, the fault-fill veins, e.g. #13 vein, are parallel to S3, however in the SVP, the fault-fill veins are parallel to S4.

Gold mineralization

Fault-fill and extensional veins contains free gold flakes ranging in size from micron to 2 cm size flakes found along stylolites in the veins or are randomly distributed in massive veins as thick mm-cm gold veinlets, in fault-fill and extension veins. No economic concentrations of disseminated gold have thus far been reported in the wall rock to the veins at Hoyle Pond.

Mine Alteration

Three traverses that intersect the B1N, B1 and B3 veins on the 720ml were mapped and sampled. The timing of alteration mineral formation with respect to vein development and gold mineralization appears to be syn-mineralization as indicated by alteration halos which symmetrically envelope the veins without intersecting them. Three alteration zones were identified, mapped, and sampled during the study: an inner sericite zone surrounding the veins, an outer albite zone, and a graphitic alteration zone (Grey zone). The alteration minerals are sericite, fuchsite (Cr-muscovite), K-feldspar, albite, carbonates, graphite, chlorite, tourmaline, pyrite and arsenopyrite. In general, carbonate alteration is pervasive and observed throughout the mine. The intensity of carbonate, sericite and "fuchsite" alteration increases locally and is best developed in the 1060fz in the vicinity of veins.

Mobile elements

The mobile elements have been identified using the method of Grant (1986). On isocon diagrams (Fig. 4.5_{A-F}) shows two curve, a solid and a dashed line. The dashed line expresses y=x, where one would expect that all the immobile elements to plot if no alteration would have affected the country rocks. However, the immobile elements plots below the dashed line, coinciding with the solid line. The diminution of the solid line slope is consistent with lower concentration of immobile elements in the altered sample . This behaviour reflects an addition of mobile elements such as K_2O, CO_2, Rb, Cr, SiO_2, CaO and Na_2O and consequently a dilution of the immobile element. That dilution of immobile elements occurred due to flooding by hydrothermal minerals and shifting the isocon line (solid line). The isocon diagrams (Fig. 4.5_{2-6}) show that K_2O, Na_2O, Cr_2O_3, Rb, CO_2, CaO, Eu, FeO, MgO and to a minor extent La (LREE) were all mobile to a varying degree. On the Jensen Cation diagram, high Mg-tholeiitic basalts are displaced toward aluminum and into the calc-alkaline field (Fig. 4.6) due to the mobility of MgO and FeO (i.e. a loss of FeO and MgO relative to Al_2O_3).

Sericite Alteration Zone

The sericite alteration zone consists of enrichment in muscovite, Cr-muscovite, calcite, dolomite and ferroan-dolomite, graphite, plus microcrystalline alkali-feldspar, local acicular arsenopyrite and anhedral to euhedral pyrite (Photo 4.5). Typically, the sericite zones extend 4-6m from the veins and range in color from pale grey, to light beige, to light yellow and possess a weak to strong pale grey sericitic cleavage (S3 and/or S4). The extent of the alteration appears to be dependant on the host rock composition, as the most significant enrichment in mobile elements is in high-Mg tholeiitic basalts. K_2O, Rb, As and S concentrations increase adjacent to veins (fig. 4.18 B & C). The enrichment in Rb is identical to that of K_2O (Fig. 4.5_{1-6}) and reflects a substitution of K by Rb in the crystal lattice of sericite and alkali feldspars. Sericitic alteration and element enrichment and depletion can be observed at lithological contacts where no veins are present.

A)

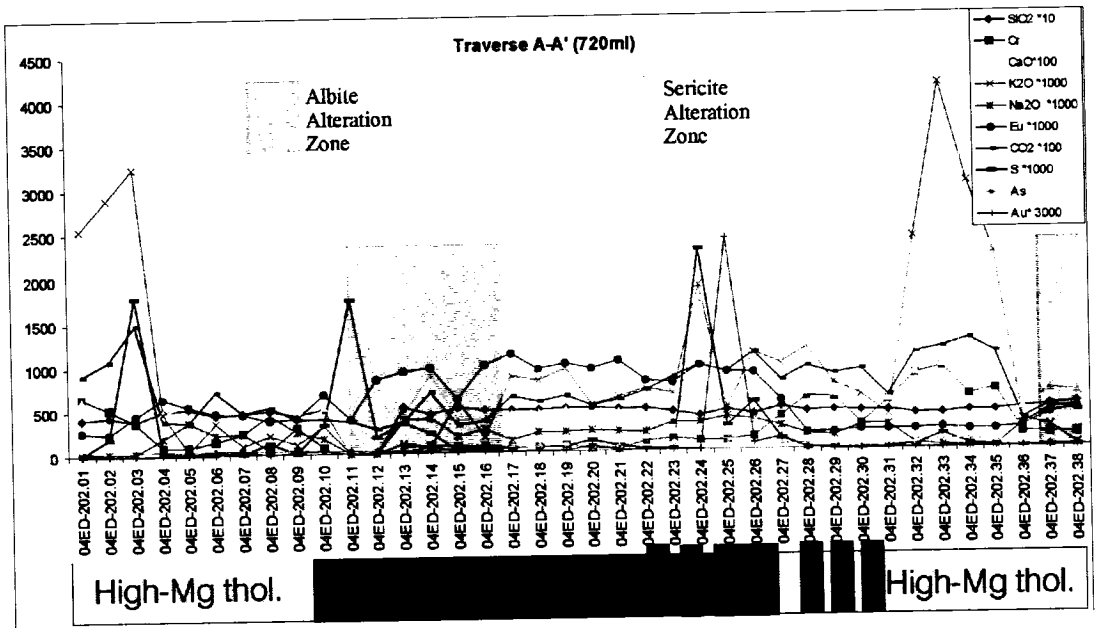
Traverse A-A' (720ml)
Albite Alteration Zone
Sericite Alteration Zone
SiO2 *10
Cr
CaO*100
K2O *1000
Na2O *1000
Eu *1000
CO2 *100
S *1000
As
Au* 3000
High-Mg thol.
High-Mg thol.

B)

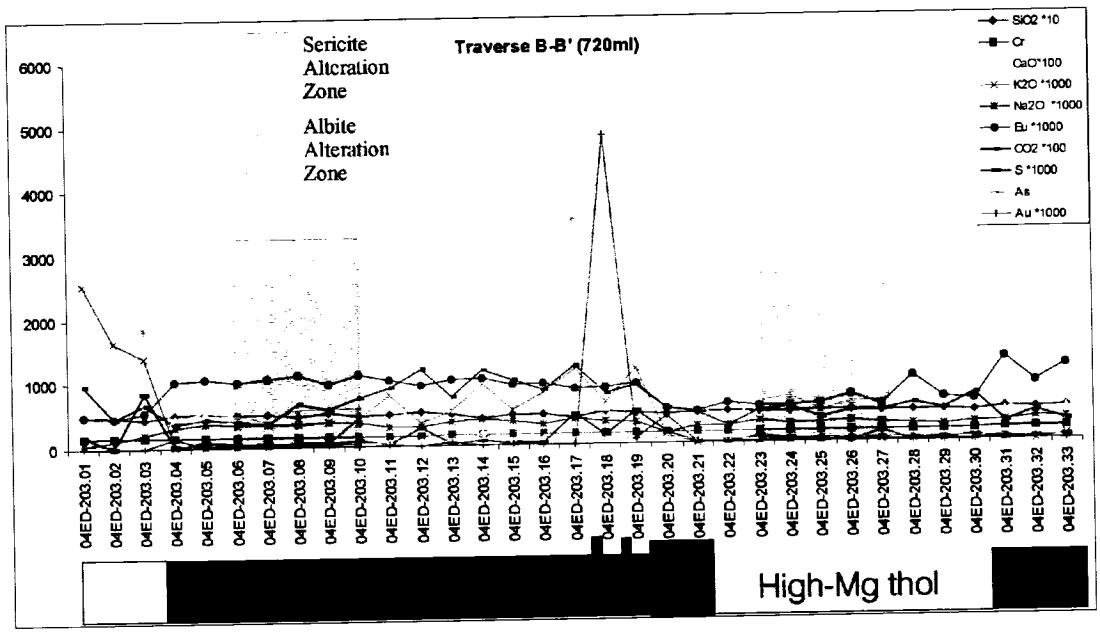
Traverse B-B' (720ml)
Sericite Alteration Zone
Albite Alteration Zone
SiO2 *10
Cr
CaO*100
K2O *1000
Na2O *1000
Eu *1000
CO2 *100
S *1000
As
Au *1000
High-Mg thol

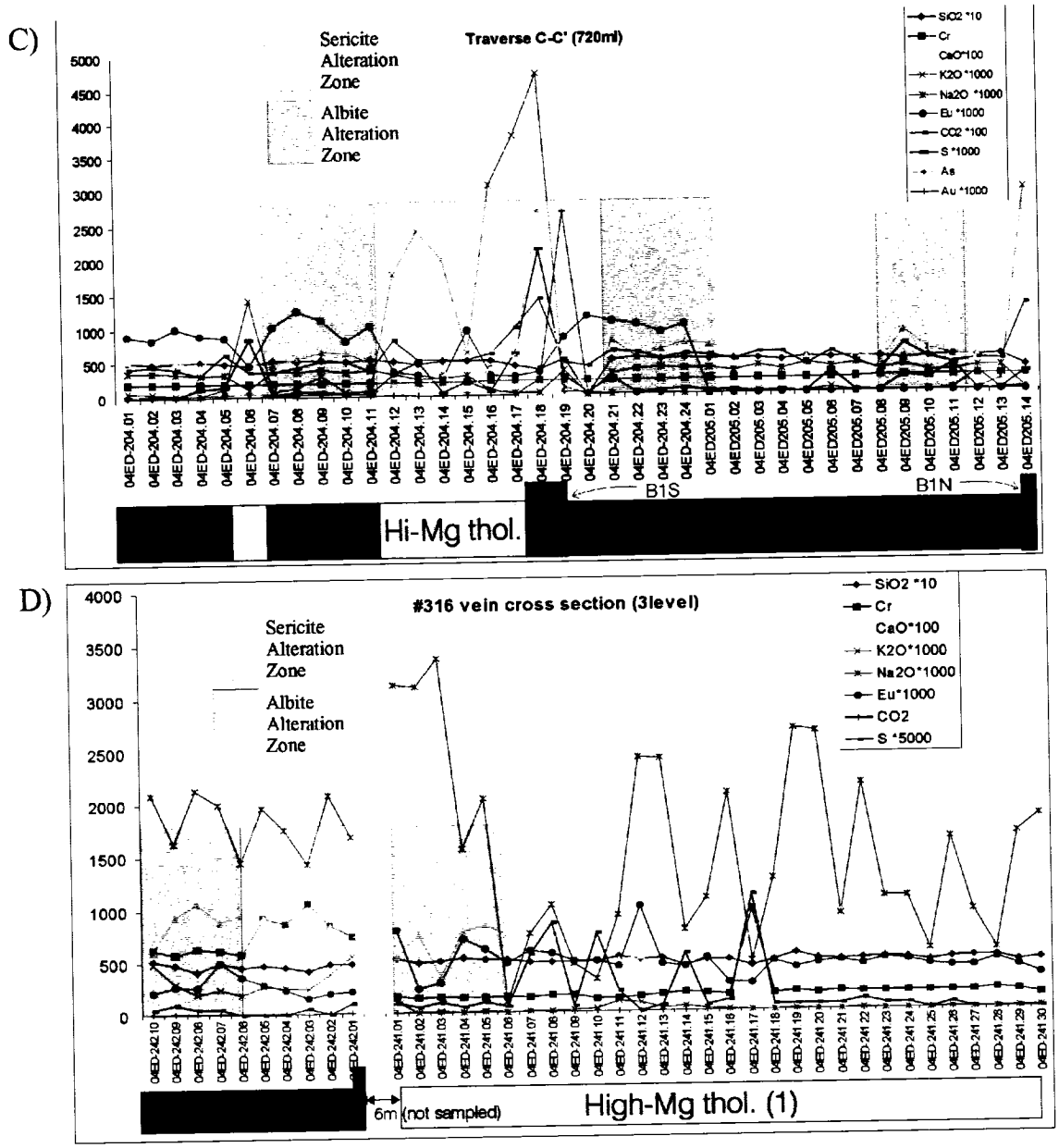

Figure 4.18 A), B) and C) Enrichment and depletion plot of trace and major elements along three traverses (A-A', B-B', C-C') on the 720ml. The traverses cut across the stratigraphy folded by F4 along the 1060fz.D) A fourth traverse cut across the 3level #16 vein. Samples along the four traverses were taken at 1m intervals. Ordinate axes represents the element w% or ppm times a factor: SiO_2 = w% x 10, Cr = ppm, CaO = w% x 100, K_2O = w% 1000, Na_2O = w% x 1000, Eu = ppm x 1000, CO_2 = w% x 100, S = w% x 1000, As = ppm, Au = ppm x 1000.

Chromium enrichment

Chromium content increases in close proximity to veins and is found in muscovite (Table 4.2), and Cr-micas replacing Al in the octahedral site of the crystal lattice (Deer, Howie & Zussman, 1992). Chromium contents in tholeiitic basalts of the area are generally on the order of 150 to 250ppm similar to oceanic crust (Faure, 1998). In proximity to the quartz-carbonate gold bearing veins, chromium concentration increases by a factor of 6 to reach levels of 1200ppm. We note that the nickel concentration and the Mg# do not follow the chromium trend and reject the idea that the chromium enrichment is a primary igneous feature. Moreover the isocon diagrams (Fig. $4.5_{1\text{-}6}$) clearly show Cr enrichment. Moritz and Crocket (1991) and McCuaig and Kerrich (1998) also noted fuchsite-rich quartz veins at the Dome Mine in Timmins and suggested that Cr could be mobile.

Albite alteration zone

These zones envelop the sericite alteration and are best observed in thin section. They consist of a fine-grained apple-green groundmass with albite porphyroblasts and spherulitic textured secondary albite overgrowing chlorite (Photo 4.7). REE chondritic normalized (e.g. Fig. 4.7) patterns of albitized rocks have negative Eu anomalies that are likely due to the loss of Ca and Eu in the transformation of Ca-plagioclase to albite (e.g. Fowler and Doig, 1983). The Na enrichment decreases approaching the vein and is replaced by an increase in K_2O-sericite alteration. The albite alteration zones can be difficult to identify due to the number of overlapping alteration halos around veins and the fact that mineralization is dominated by sericitic alteration.

Graphitic alteration ("Grey Zone")

Grey zone alteration trends roughly 070° and commonly cut across the stratigraphy (Fig. 4.2) and are parallel to the sericite and albite alteration zones. The grey zones extend for several hundred meters along strike, and range from 0.5 to 20m in thickness. This alteration is commonly centered on quartz-carbonate veins, and is associated with coarse brecciation and a modal increase in graphite, pyrite and globular pyrite, calcite, dolomite and ferroan-dolomite. Drilling shows that the grey zones form anastamosing three dimensional networks surrounding lenses of less altered rock (Rye, 1987). They are commonly spatially associated with Au-rich quartz veins. In the 1060fz, the graphite

enrichment is found in the vicinity of veins and it correlates with the zone of intensive shear mapped by Rhys (unpublished company report, 2003).

Graphite is thought to be organic in origin (Downes et al. 1982 & Rye, 1987). Downes et al. (1982) did gas chromatograph analyses of samples, which showed peaks corresponding to C-H bonds as well as toluene and xylene structures. This indicated the presence of highly condensed aromatic polymers. Hodges (1982) showed that 22% of reduced carbonaceous material at Owl Creek is organic. Samples were collected from the graphitic shear on the 440m level and were analysed for ^{13}C concentration. Results were in the range of -24 to -27 per mil. This indicates a very light fraction of carbon, likely caused by a fractionation process. Thus the carbon isotopic signature could have resulted from fractionation of either mantle or atmospheric C. Further analyses were conducted to test if the carbon was primitive or had a biological signature. Spectrophotometry showed a strong absorption peak at 280nm (Fig. 4.19), indicating the presence of lignoid molecules (Farmer and Morrison, 1960; Sapek et al., 1980). Nuclear Magnetic Resonnance (NMR) analyses showed peaks corresponding to complex aromatic molecules, possibly cyclic molecules demonstrating a biological source for the carbon.

Carbonate Electron Micro-Probe data

Sample	203-17-1	203-17-3	203-17-6	203-17-7	204-07-1	204-07-3	204-07-4	70-1	70-2	70-4	77-1-2	204.05-2-1
CaO	28.75	28.95	28.56	27.5	56.33	57.87	55.65	56.34	57.97	57.53	57.46	57.11
FeO	17.36	17.62	18.75	17.19	0.99	0.92	0.88	0.38	0.02	0.09	0.96	1.13
MnO	0.35	0.46	0.42	0.4	1.02	0.92	0.99	1.72	0.07	0.09	0.53	0.68
MgO	10.33	10.15	8.88	9.75	0.41	0.41	0.37	0.23	0	0	0.37	0.39
SrO	0.01	0.02	0	0	0.04	0	0	0	0	0	0	0
BaO	0	0.1	0	0.1	0.07	0.08	0.01	0.05	0	0	0	0.02
CR_2O_3	0.03	0.02	0.02	0.02	0.02	0.03	0.03	0.03	0.03	0.03	0.03	0.03
TOTAL	56.83	57.32	56.63	54.96	58.88	60.23	57.93	58.75	58.09	57.74	59.35	59.36

Cr-Muscovite Electron Micro-Probe data

Sample	115-01-1	115-01-2	115-01-3	115-01-4	115-01-5	115-02-1	115-02-2	115-03-1	115-04-1	115-04-1	115-04-2	115-04-3
SiO_2	48.49	48.07	48.42	47.76	48.34	48.17	48.42	48.28	48	48.75	48.04	48.66
Al_2O_3	32.59	32.78	32.99	33.46	30.91	31.85	32.39	32.25	32.77	32.88	32.58	31.88
TiO_2	0.36	0.34	0.4	0.38	0.34	0.37	0.43	0.22	0.34	0.37	0.32	0.35
Cr_2O_3	1.19	1.18	0.52	1.45	2.77	1.92	1.71	1.97	1.54	1.59	0.98	1.77
V_2O_3	0.09	0.09	0.12	0.08	0.11	0.09	0.09	0.06	0.07	0.09	0.1	0.09
FeO	0.9	0.77	0.96	0.86	0.92	0.99	1	0.97	0.92	1.02	1.23	1.17
MgO	1.63	1.48	1.48	1.29	1.55	1.6	1.51	1.52	1.45	1.5	1.54	1.61
MnO	0.02	0.03	0.02	0	0	0	0	0.03	0	0	0	0.03
K_2O	10.82	10.78	10.74	10.67	10.77	10.8	10.85	10.55	10.83	9.81	10.68	10.82
CaO	0	0	0	0.02	0.02	0	0.01	0.01	0.01	0	0.05	0.03
Na_2O	0.29	0.32	0.28	0.37	0.29	0.24	0.29	0.35	0.4	0.29	0.38	0.3
BaO	0.19	0.26	0.2	0.33	0.23	0.23	0.19	0.29	0.26	0.26	0.22	0.26
Cl	0.01	0.01	0	0	0	0	0	0	0	0	0	0
F	0	0	0.15	0.11	0.17	0.1	0.07	0.09	0.1	0.11	0.11	0.09
Total	96.58	96.11	96.28	96.78	96.42	96.36	96.96	96.59	96.69	96.67	96.23	97.06

Sample	115-04-4	119-01-1	119-01-2	119-01-3	119-02-0	119-02-3	119-03-1	119-03-2	119-03-3	119-04-1	119-04-2	119-04-3
SiO_2	48.18	47.93	48.19	48.01	48.02	48.01	47.76	48.3	47.62	47.78	47.37	48.31
Al_2O_3	33.2	34.79	34.91	35.52	33.34	33.7	34.08	32.89	32.3	35.8	34.78	35.97
TiO_2	0.32	0.18	0.15	0.11	0.25	0.3	0.22	0.26	0.23	0.09	0.21	0.15
Cr_2O_3	0.93	1.17	1.11	1.01	1.33	1.22	1.91	1.99	2.29	0.33	0.87	0.9
V_2O_3	0.09	0.12	0.1	0.12	0.1	0.13	0.07	0.1	0.06	0.11	0.08	0.1
FeO	0.78	0.6	0.55	0.44	0.86	0.82	0.58	0.74	0.75	0.39	0.63	0.43
MgO	1.43	0.95	0.93	0.68	1.26	1.39	0.97	1.31	1.2	0.8	0.99	0.69
MnO	0	0	0.04	0.01	0.04	0	0.01	0	0	0	0.03	0
K_2O	10.72	10.02	10.24	10.04	10.46	10.19	10.38	10.19	10.08	10.03	9.82	9.18
CaO	0	0.01	0.03	0.01	0.09	0	0	0.01	0.06	0.09	0.46	0.03
Na_2O	0.34	0.51	0.38	0.53	0.49	0.41	0.5	0.4	0.48	0.49	0.6	0.58
BaO	0.29	0.14	0.13	0.16	0.28	0.19	0.17	0.12	0.19	0.11	0.12	0.14
Cl	0	0	0	0	0	0.01	0.01	0.03	0.01	0.01	0.01	0.02
F	0.06	0.08	0.07	0.11	0.08	0.06	0.09	0.13	0.12	0.25	0.02	0.07
Total	96.34	96.5	96.83	96.75	96.6	96.43	96.75	96.47	95.39	96.28	95.99	96.57

Sample	116A-1-1	116A-1-2	116A-2-1	116A-2-2
SiO_2	48.79	48.55	49.61	48.49
Al_2O_3	31.73	31.1	31.51	33.26
TiO_2	0.25	0.39	0.41	0.18
Cr_2O_3	1.41	1.49	1.4	1.03
V_2O_3	0.07	0.05	0.03	0.07
FeO	0.67	0.83	0.71	0.64
MgO	1.56	1.9	1.89	1.25
MnO	0	0.03	0	0
K_2O	10.45	10.57	10.78	10.57
CaO	0	0	0	0.03
Na_2O	0.25	0.23	0.23	0.22
BaO	0.17	0.12	0.07	0.13
Cl	0	0	0	0
F	0.08	0.14	0.14	0.21
Total	95.43	95.4	96.78	96.08

Table 4.2 Electron Micro-probe data for carbonate and Cr-muscovite, major oxide express in weight %.

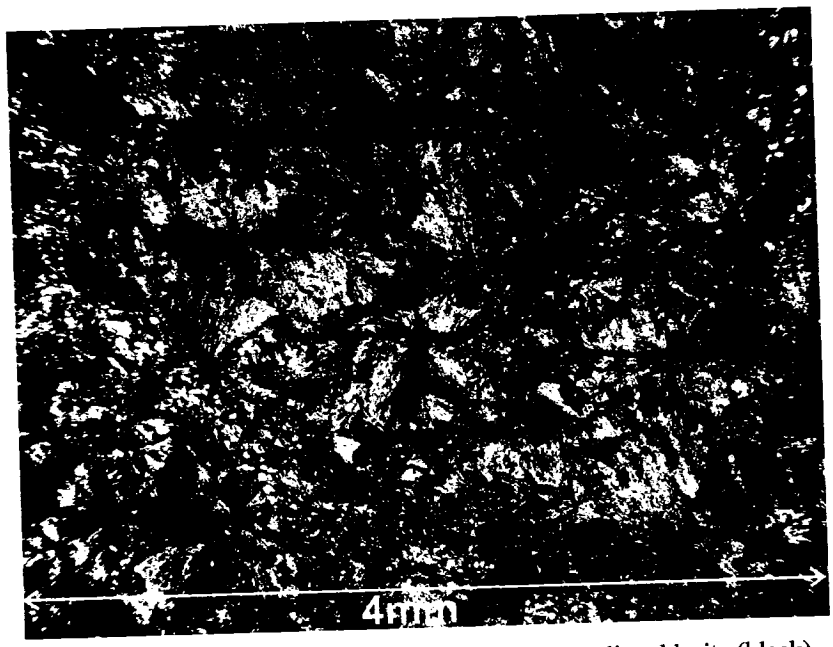

Photo 4.7 Secondary spherulitic albite overprinting earlier chlorite (black), crossed polars.

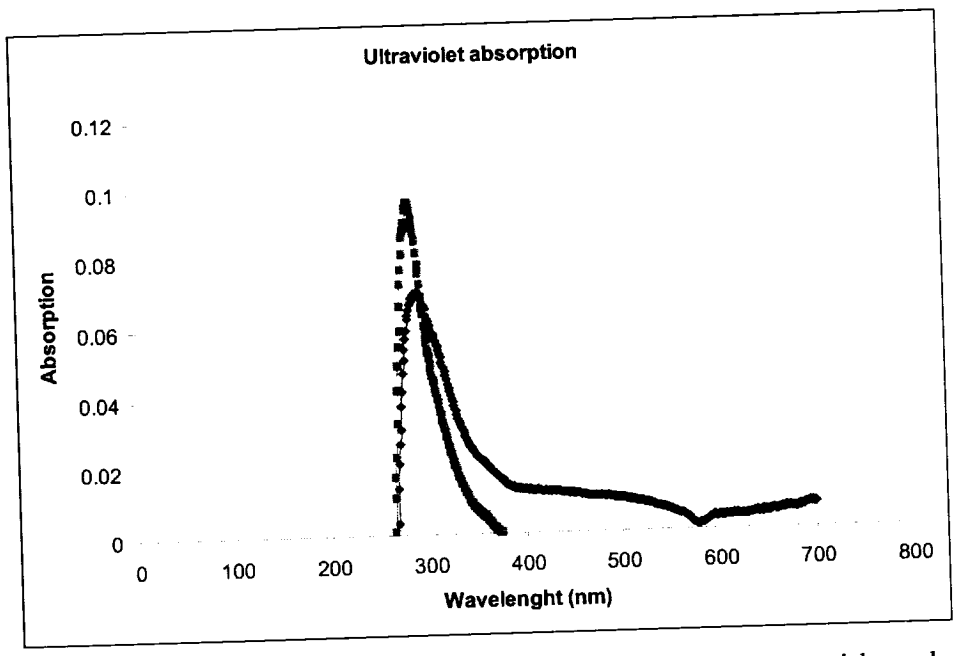

Figure 4.19 Ultraviolet absorption spectrophotometry plot for graphitic material samples on the 440 and 720ml.

Carbonate alteration

The carbonate alteration is developed over and beyond the mine area. Two type of carbonate alteration are observed, an early one consisting of deformed calcite crystals in amygdules and pillow selvages and a later one consist of porphyroblasts of dolomite and ferroan-dolomite overprinting and dislocated by S4 fabric. Figures 4.18 (A,B,C & D) illustrate a significant enrichment in CO_2 in the Mg-rich rocks of the 1060fz in comparison to the Fe-rich tholeiitic basalts.

Silica alteration

Silica alteration is observed in thin section as stringers and patches of anhedral quartz and resulted in dilution of immobile elements (Fig. $4.5_{1\text{-}6}$). This alteration is less marked in the Fe-rich tholeiitic basalts than in the Mg-rich volcanic rocks.

Alteration paragenetic sequence

The various alterations enveloping the Au mineralization can be dissected chronologically (Fig. 4.17) based on cross cutting relationship. Generally the Fe-carbonate (dolomite and ferroan-dolomite) alteration is observed in both sericite and albite alteration zones. It can be observed locally overprinting and/or dislocated by the S4 fabric. The albite alteration zone consists of albite and Fe-carbonate porphyroblasts with associated chlorite-rich-cleavage. The transition between the albite and sericite alteration is gradual. In the transition zone, albite porphyroblasts are observed as lithons intersected by sericite cleavage (Photo 4.5). The sericite alteration zone mineralogy consists of sericite, fuchsite, Fe-dolomite and graphite. The Cr content fluctuates through the zone and generally increases toward the veins. The sericite alteration zone also contains intimately associated pyrite formed syn-sericite alteration. The tourmaline and arsenopyrite are both observed in the vein and therefore are interpreted to be syn-mineralization. The graphite alteration, termed "grey zone alteration", is observed in both alteration zones. It is visible in the cleavage associated with chlorite and the sericite. The "grey zone" is also observed cross cutting the stratigraphy in interclasts, pores spaces and in voids of pillow margins. In addition the grey zone rock also occur within the graphitic unit observed in the SVP, cross cutting the stratigraphy, but not the mineralization. It is

also observed in the NVP migrating from the interpreted thrust fault into the volcanic rocksy of the mine.

Principal Component analysis

Two statistical methods were used for analysis of the database. The probability of error by Kretz (1985) was employed, but because the variables are statistically dependant, Principal Component Analysis (PCA) was used to reduce the dependencies. In addition, the large data base, 355 samples, each having ~50 elements, it is impractical to search for inter-element correlation using binary or ternary plots; hence principal component analysis (PCA) was implemented in order to examine the data set as a whole. All PCA analyses were calculated in ppm and oxygen anions were removed so as to correlate independent variables. The software SYSplus was used to calculate the covariance matrices, the vectors, and to present the data in the form of a binary plot. Results were interpreted in accordance with the concepts described in Gabriel (1971) and Jolicoeur and Mosimann (1960).

The statistical method (PCA) was employed to further investigate the inter-element correlations observed through visual inspection of geochemical plots. We focus on two aspects, mobile elements and oxides (Ca, K, Na, Si, As, Au, Cr, Eu, Rb, CO_2, La and S) and the immobile elements (Zr, Al, Ti, Ce, Nd, Sm, Gd, Dy, Er, Yb and Lu). Figure 4.20 is a PCA plot of principal components 1 and 2 which express 79% percent of the sample population, based on the cumulative proportion of the covariance. The numbers represent the sample value in terms of Principal component 1 and 2. On the plot the vectors expressing K_2O and Cr are opposite to Na_2O (oxygen anion has been removed for statistical analysis) which confirms that Na and K have antithetic behaviour. A line passing through the vector origin represents a resultant, which consists of a vector summation of principal components 1 and 2. It shows that data from specimens having completely different composition can behave similarly. We can compare these samples by drawing a projection line (drawn perpendicular to the resultant) and passing through individual samples. The intercept on the resultant defines clusters of samples having different chemical compositions, but overall similar behaviour. We observed that samples defined by SiO_2 vectors have a similar tendency as samples defined by K_2O vectors,

coinciding with the enrichment in K_2O and SiO_2 in the sericite alteration zone. In addition, samples defined by CaO vectors have similar tendencies to those defined by Na_2O, interpreted as these are the products of albitization of Ca-plagioclase. For example, sample #22 is defined by the K_2O vector and sample #110, by SiO_2. Their normal projections to the resultant do correlate, and although their chemistry is different, they behave similarly.

Figure 4.21 is a PCA plot expressing the variability of the immobile elements. This represents a bias representation but confirms that there is very little variability between these elements across all rock types; the results show the cumulative proportion of the covariance is 99% (i.e. component 1 and 2 represent 99% of population). The plot defines three distinct clusters: a first, the behaviour of which is expressed by TiO_2, forms an elongate cluster consisting of the Fe-rich tholeiitic basalts found in the 1060fz. At the opposite end of the TiO_2 vector, we observe clusters forming two groups, one closer to the origin (0,0), which consist of the Mg-tholeiitic basalts and another, away from origin, the high-Mg tholeiitic basalts. These three clusters show, purely in a statistical manner, the classification of rock types. In addition, the technique indicates that Al_2O_3 and TiO_2 are the two elements which distinguish the various rock types in the SVP. The correlation of the three rock types on the resultant also shows that they have similar behaviour.

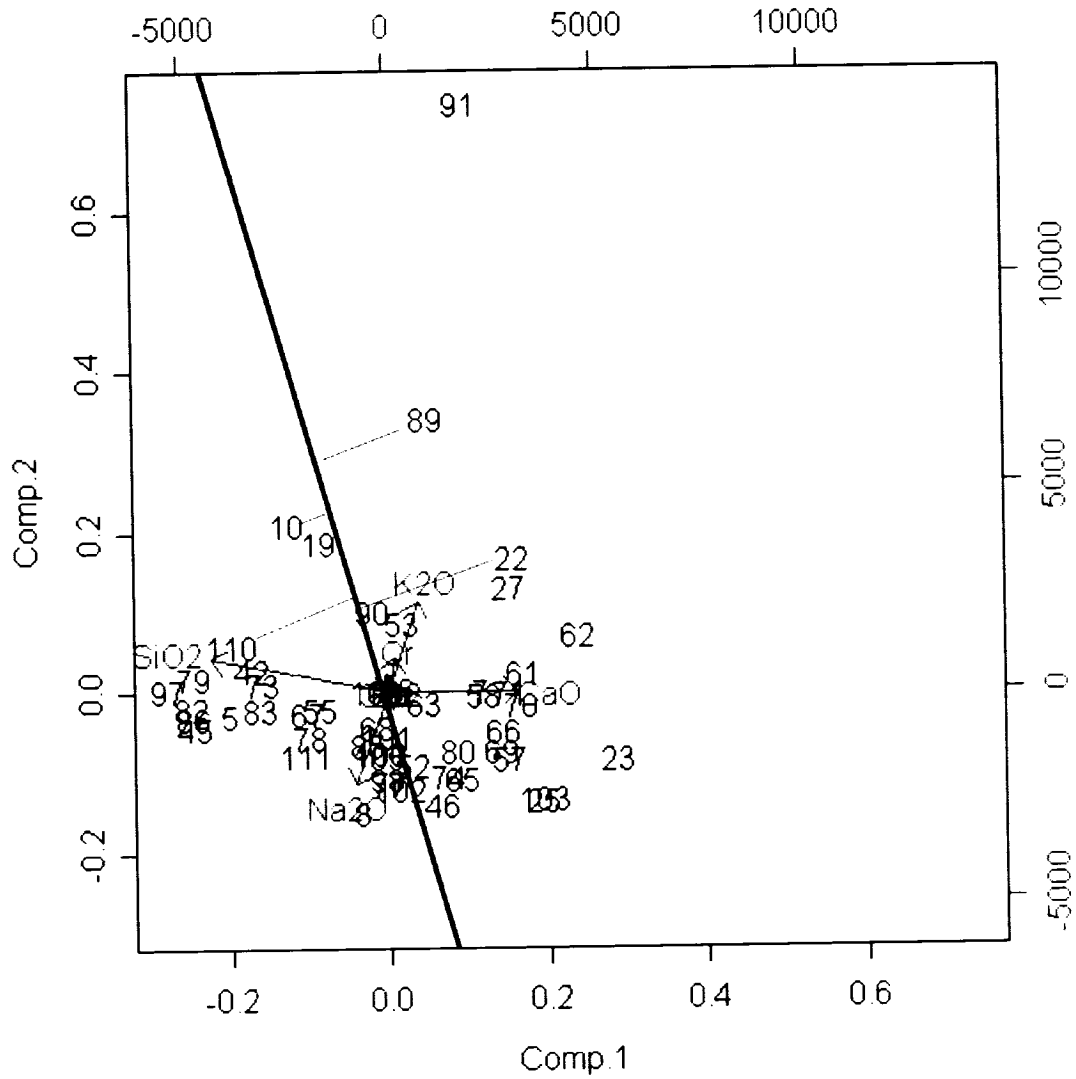

Figure 4.20 Principal component analysis (PCA) plot showing behavior of the samples defined by Component 1 and 2 of the mobile elements, SiO_2, K_2O, CaO, Na_2O, Cr and Rb vector. The values express from -0.2 to 0.6 on the abscissa and ordinate represents the eigenvector value. The two other axes with value spreading from -5000 to 10000 represent covariance value in the matrice. Note, a resultant curve has been drawn through the origin. This resultant is a summation of all vectors in the matrice and permits to do comparison between samples. For example, sample 22 and 110, two samples that are define by different vector, meaning it as a different composition, on the resultant have a very similar behaviour. Which indicates that the two samples although different when compared to each other, are alike in the database. Note that the vectors are express as major oxides on the figure, however, the oxygen has been removed for calculation.

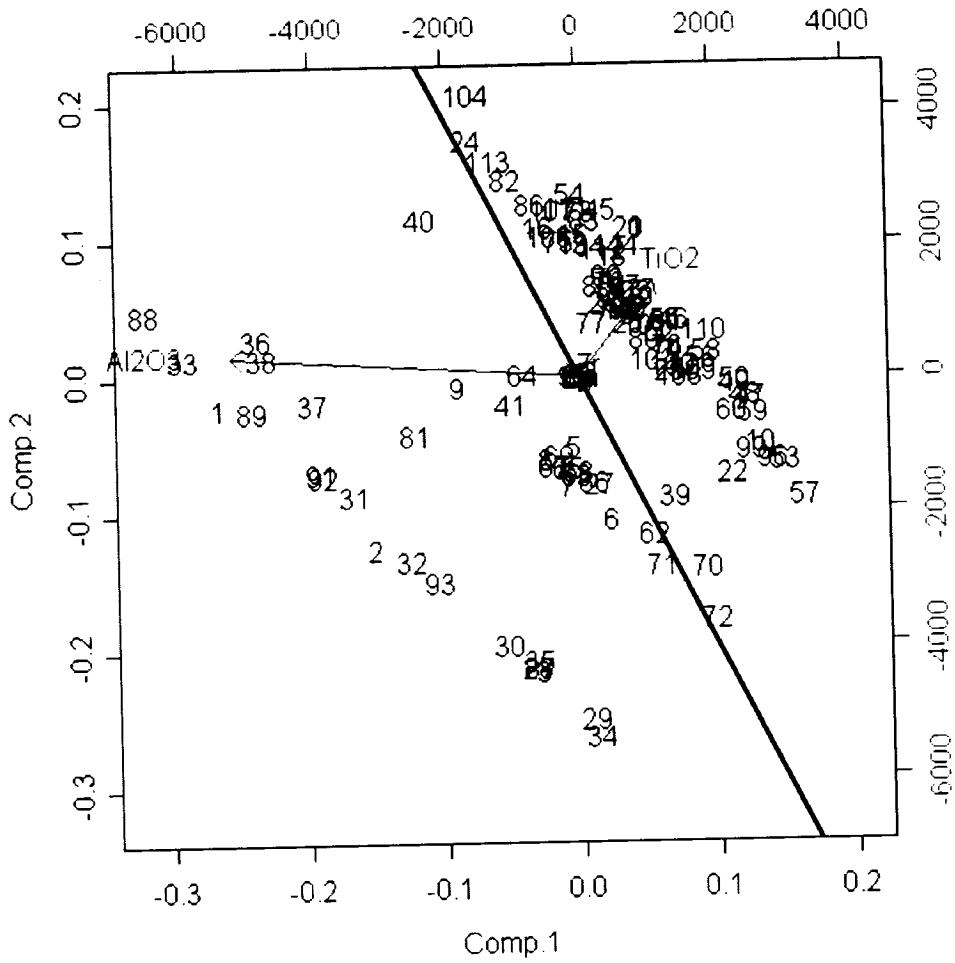

Figure 4.21 Principal component analysis plot showing behaviour of the sample defined by the immobile elements, TiO_2, Al_2O_3, Zr, Yb, and REE, vectors defining the SVP. Note, that the TiO_2 and Al_2O_3 vectors have greater amplitude and best define the populations. The values express from -0.3 to 0.2 on the abscissa and ordinate represents the eigenvector value. The two other axes with value spreading from -6000 to 4000 represent covariance value in the matrice. Note that the vectors are express as major oxides on the figure, however, the oxygen has been removed for calculation.

Interpretation

The geochemical signatures of the volcanic rocks at the mine have been compared with a geochemical database of over 1000 analyses from the Timmins area (provided by the Porcupine Joint Venture). This comparison shows that the Hoyle Pond volcanic rocks are geochemicaly correlative (Fig. 4.23 and 4.24) with the Hershey Lake and Central Formations (Fig. 4.3B). They have similar immobile element chemistry, specifically TiO_2/Al_2O_3 and Zr/Al_2O_3 ratios indicating the SVP has very similar geochemistry to the Central Formation whereas the NVP and CVP correlate with the Hershey Lake formation.

The dominant foliation (S3) formed during north-south compression, after the deposition of the Tisdale and Porcupine Assemblage. S2 and S3 have an average orientation of 075/84 and 281/84 respectively in the Timmins area (Bateman et al., 2005). At Hoyle Pond, S3 is sub-parallel to lithological contacts and interpreted to be axial planar to F3 isoclinal folds. The thrust fault observed at the northern contact of the NVP formed late during the D3 event. Mineralization began during the D3 event as a result of the migration of fluids along the D3 thrust fault which resulted in the formation of extensional veins normal to S3 and fault-fill veins sub parallel to S3 (e.g. #13-#14-#15-#16 veins). However, it is possible that mineralization in the NVP could have formed during D4 and infilled older D3 structures. D4 resulted in localized isoclinal folding and in the formation of a pervasive 070° S4 foliation containing the majority of the gold-bearing veins in the 1060fz area. These fault-fill and extensional veins (e.g. B1, B1N, B1S, B3, UP etc) likely formed by flexural shear along the limbs of isoclinal F4 fold (Fig. 4.2). Figure 4.15 illustrates the relationships of F4 1st order folds with mineralization.

Mineralization in the Hollinger-McIntyre deposits is syn-D4 and it overprints an albitite dyke dated at 2672.8 ±1.1 Ma (TIMS, U/Pb zircon; Ayer et al., 2005). We suspect that mineralization at Hoyle Pond mine was coeval with that of the Hollinger-McIntyre system. We postulate that sedimentary rocks were buried during D3 folding and thrusting, were heated, and fluids expelled from these rocks migrated along permeable D3 structures (Fig. 4.25). These processes were likely repeated during the D4 event.

Gold mineralization is coeval with wall rock alteration. The mineralization is surrounded by muscovite and Cr-muscovite alteration which in turn is surrounded by albite alteration. The so called "Grey zone" alteration described by Downes (1982) is caused by an addition of graphite to pore-spaces. The source of the organic matter was most likely from sedimentary rocks, as were also As and B. For instance, marine sediments, mudstone and deep-seated clay generally contain significant amount of As and B (Faure, 1998). The most plausible sedimentary source would have been the Porcupine Assemblage rock surrounding the mine volcanic rock sequence.

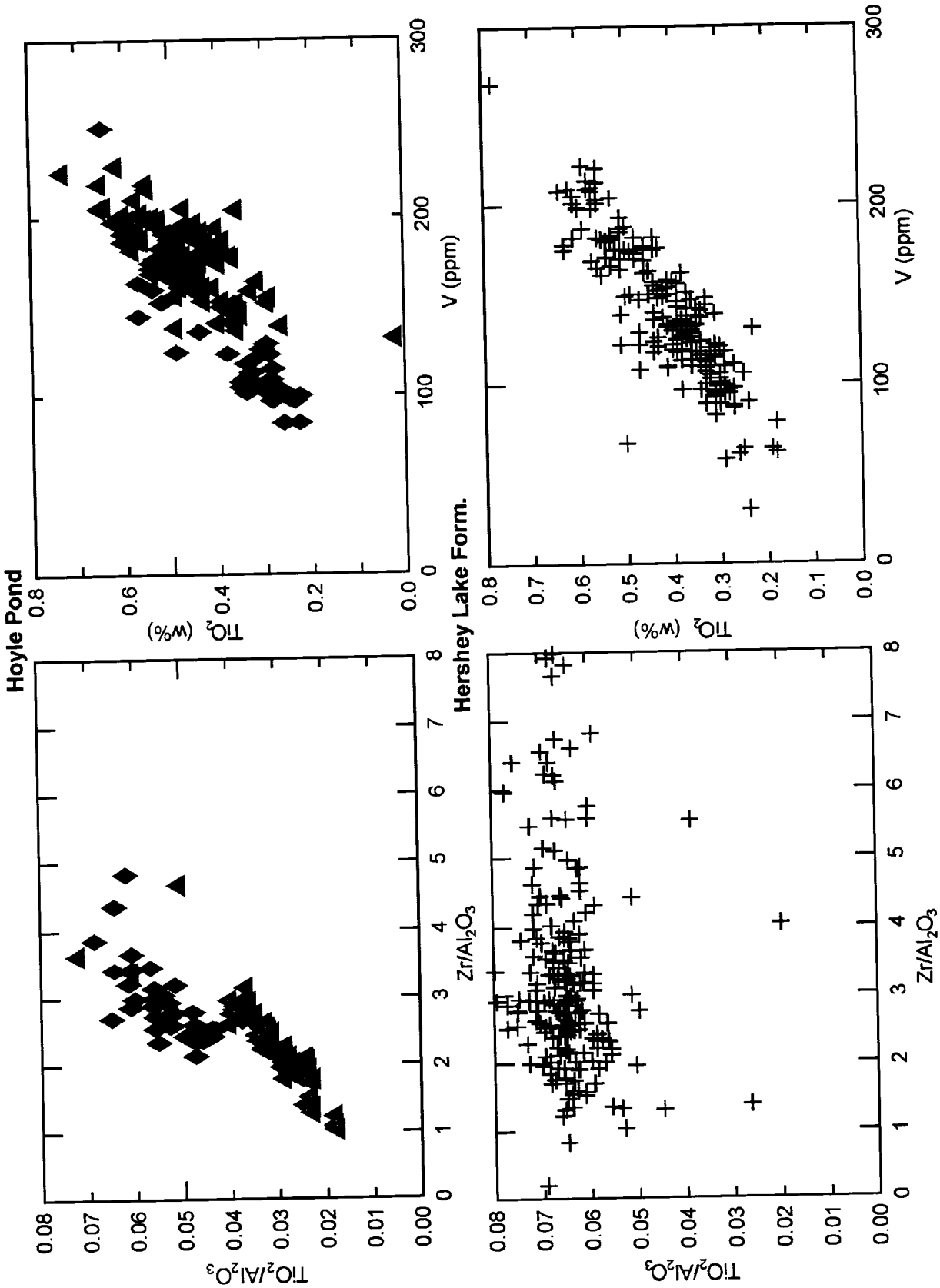

Figure 4.23 Trace element comparison of the NVP (triangle) and CVP (diamonds) at Hoyle Pond mine with the Hershey Lake formation of the Tisdale assemblage.

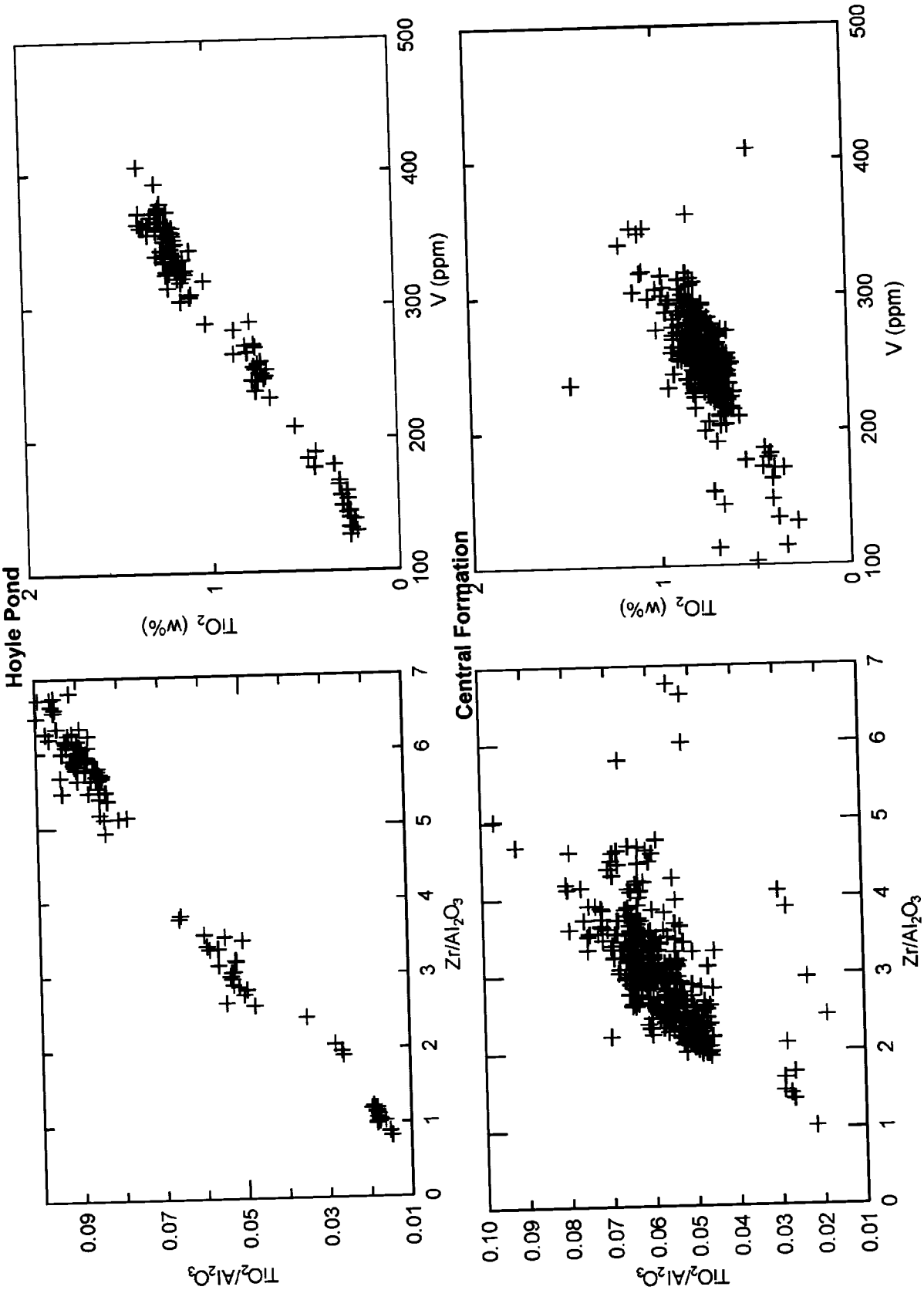

Figure 4.24 Trace element comparison of the SVP (cross) at Hoyle Pond mine with the Central formation of the Tisdale assemblage.

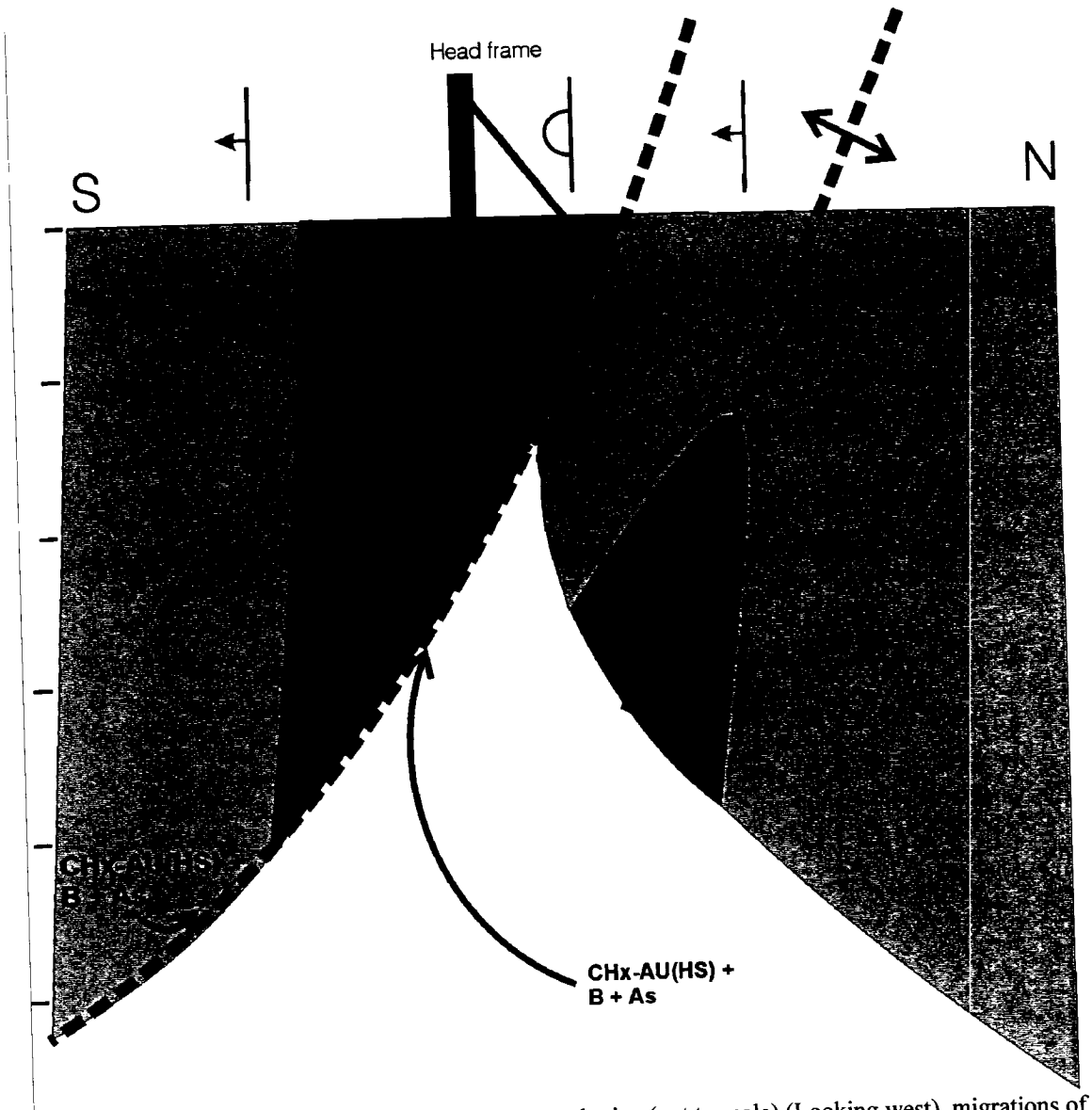

Figure 4.25 North-south vertical sketch of Hoyle Pond mine (not to scale) (Looking west), migrations of fluids during D3 and D4 demonstrating possible source of Au, organic matter and Cr^{6+}.

Role of Chromium

The enrichment in Cr (Fig. 4.18 A and D) demonstrates that chromium was mobile during hydrothermal activity. The notion of mobility of chromium in hydrothermal systems appears to have been largely ignored. However it has been studied extensively as a result of its toxicity in groundwater systems. Chromium is generally found as a trivalent (Cr^{3+}) or hexavalent ion (Cr^{6+}). Cr^{3+} is immobile, but when oxidized to Cr^{6+} it becomes highly mobile under various ranges of pH and temperature. The oxidation efficiency of Cr^{3+} to Cr^{6+} increases with increasing temperature and pressure in aqueous solution (Henry, 2000) from 67% at 197°C to 95% at 347°C (Anderson, 1975). The latter temperature is similar to estimated temperatures for auriferous hydrothermal fluids in the Abitibi Greenstone Belt (e.g. Olivo and William-Jones, 2002). Cr^{3+} can be easily oxidized to Cr^{6+} by manganese\iron oxides or by hydroxide (Richard et al., 1991; Böhm and Fisher, 2004). Potassium and sodium salts of chromate (CrO_4^{2-}) are freely-soluble over the pH range of 1-14 (Nieboer et al., 1988). It is therefore proposed, consistent with the correlation of K and Cr observed in the alteration halos surrounding the veins, that the association can be explained by the oxidation of Cr^{3+} to Cr^{6+} and transportation in the fluid with K^+.

The enrichment of Cr in the wall rock is possibly due to the reduction of Cr^{6+} and precipitation of Cr^{3+} in the mineral phase. The most efficient reduction agents are dissolved Fe II ions (Sass and Rai, 1987), Fe^{2+} sulfides (pyrite), thiol, hydrogen sulfides and organic matter (Zouboulis et al., 1995, Thornton and Amonette, 1999, Kim et al. 2001, Szulczewski et al. 2001). Thiol complexes (e.g. $Au-(HS)^-$) are often cited as the agents by which gold is transported in hydrothermal solutions that produced many Au deposits (e.g. Seward, 1973, Ropchan et al 2002 and Böhlke, 1989). Thus Cr^{6+}, a strong oxidant, and Au-thiol complexes and organic matter cannot coexist in the same fluid. This was not tested at pressure and temperature existing during greenschist metamorphism, therefore we propose that more than one fluid was involved, and postulate that fluid mixing processes were responsible for Au-precipitation at Hoyle Pond. Gold at the Hoyle Pond Mine was likely transported as an organo-thiol-complex in a fluid, which mixed with an oxidizing fluid transporting Cr^{6+}, forming graphite, pyrite, arsenopyrite, tourmaline, muscovite, Cr-muscovite and precipitating gold.

Discussion

Vein systems (e.g. 1060fz) at Hoyle Pond are emplaced at contacts between different rock units. Similarly in the Hollinger and McIntyre system, Melnik (1992) and Brisbin (1997) observed that a majority of veins were located at flow contacts. This raises the possibility that units with primary porosity, such as interstices in flow breccias, could have been preferred hosts for hydrothermal mineralization due to increased of porosity and increased surface area for geochemical reactions. Alternatively porosity may have been developed at contacts during faulting or shearing as a result of the competency contrast between adjacent units. The alteration patterns observed at Hoyle Pond mine are consistent with the alteration associated with mineralization at the Hollinger-McIntyre deposit (Brisbin, 1997; Melnik-Proud, 1992) and also in Archean "intrusion related" gold deposits (Robert, 2001).

At Hoyle Pond, the majority of Au mineralization is hosted in D4 structures. Indicating the existence of post-Timiskaming assemblage Au mineralization. However, there is Au mineralization hosted in D3 stuctures which is interpreted to have formed during D4 and migrated into previously formed D3 structures. We have no evidence to constrain the end of D4, but F4 folds and fabric (S4) are found within Timiskaming sedimentary units with a maximum depositional age of 2670 Ma (Ayer et al 2005).

Regionally, Au-bearing quartz veins in the Timmins area are parallel to a prominent 070° fabric which may suggest that the two are related. At Hoyle Pond, fabrics do not intersect Au-bearing quartz veins and the boudinage of the veins is interpreted to have formed as part of the shear-veining process associated with the D4 event. Across the Timmins area it is difficult to decipher the timing of the various generations of fabrics because they do not have a constant dip, hence fabrics having the same strike but opposing dips in adjacent outcrops may have been interpreted as the result of different deformation events. Structural complications are on-going problems that still needs to be resolved.

Conclusion

Geochemical data and facing direction determinations demonstrate that the NVP and SVP are not equivalent, indicating that the three volcanic packages represent a south facing homoclinal sequence which was previously thought to be an anticline fold cored by ultramafic volcanic rocks. The stacked volcanic rocks at Hoyle Pond correlate with the Hershey Lake and Central Formations of the Tisdale Assemblage.

The high-Mg tholeiitic basalts are significantly more enriched in mobile elements (e.g. CO2 and CaO) than Fe-rich tholeiitic basalts, suggesting that the high–Mg tholeiitic basalt was more prone to reaction with the hydrothermal fluid concording to what Bohlke (1989) observed. The hydrothermal mineralizing fluid was injected during isoclinal folding , D4 and migrated into D3 structures. Mineralized fault-fill veins were emplaced in shear zones located at lithological contacts. One generations of fault-fill veins are present at Hoyle Pond; in the NVP, fault-fill veins are hosted in D3 structures, and in the SVP, more precisely the 1060fz, the fault-fill veins formed during D4.

Analyses of geochemical data show that the REE, Al, Zr, Ti and Y were relatively immobile during alteration. The alteration associated with Au-bearing quartz-carbonate veins is zoned and consists of an inner sericite alteration, and an outer albite alteration zone. Carbonate alteration is ubiquitous. The sericite alteration zone is composed of muscovite, Cr- muscovite "fuchsite", quartz, carbonate, arsenopyrite, pyrite, tourmaline and graphite and it shows has a concomitant enrichment in K_2O, Cr, SiO_2, CO_2, As, and S. The albite alteration zone is composed of albite, quartz and carbonate and shows enrichment in Na_2O, CO_2 and SiO_2.

Cr is significantly enriched proximal to mineralized veins and was likely introduced by an oxidized fluid in the mobile hexavalent state whereas gold and carbon were likely transported in reduced fluids. Thus it is hypothesized that a reduced C, B, As, Au bearing fluid mixed with an oxidized fluid carrying Cr, precipitating gold. Trace concentrations of organic matter preserved as graphite alteration and enrichment of As and B suggests that gold was derived from a sedimentary source, most likely the subjacent Porcupine assemblage sedimentary rocks.

We postulate that sedimentary rock (eg.Porcupine Assemblage) were transported to depth by burial, folding and thrusting, and fluids were expelled and migrated along D3 and D4 structures (thrust faults). These reduced fluids were focussed into porous and permeable volcanic rocks and mixed with locally derived oxidized Cr-bearing fluids to precipitate gold. The hydrothermal fluids circulation was reinitiated during D4. However, it is possible that the bulk of the mineralization is syn-D4 and was locally injected in previously formed D3 structures.

Chapter 5.0 Gold transportation and precipitation model

This chapter is written as a manuscript which is in preparation for submittal to Mineralium Deposita. It principally discusses the alteration geochemistry and proposes a model for transportation and precipitation of gold at Hoyle Pond. A summary is provided in the paper.

This section discussed the contribution of chrome and organic matter in the transportation and precipitation of gold and suggests a new interpretation and approach to understanding the precipitation of gold. The paper is entitled "**The geochemistry of the alteration at the Hoyle Pond Mine, Timmins, Ontario; Chromium and Graphite enrichment spatially associated with gold-bearing veins resulting from hydrothermal fluid mixing**" To avoid repetition, readers of the previous chapters can continue reading from the section on the **style of vein mineralization** (p.146).

5.1 The geochemistry of the alteration at the Hoyle Pond Mine, Timmins, Ontario; Chromium and Graphite enrichment spatially associated with gold-bearing veins resulting from hydrothermal fluid mixing

Dinel E., and Fowler A.D.

Ottawa-Carleton Geoscience Centre, Earth Science Department, University of Ottawa.

Abstract

Chromium mobility is relatively poorly documented in research on gold deposits. This paper presents the evidence for Cr mobility and its addition to wall rocks hosting gold mineralization at the Hoyle Pond mine. Our data indicates that there is a modal increase in muscovite and Cr-muscovite associated with sericite alteration zones surrounding the gold-bearing veins. Cr^{6+} is a mobile species in aqueous solutions and its best known reducing agents are organic matter, thiol complexes, and Fe II. We interpret that gold was most likely mobilized by Au-thiol complexes and organic matter (Au-HS-C_xH_x). At least two fluids were involved in the mineralization processes; a reducing fluid that mobilized gold along with organic matter, As and B; and an oxidizing fluid which mobilizing Cr^{6+}. Analyses conducted on graphite samples from mineralized zones have shown trace amounts of complex organic aromatics. This suggests gold, organic matter, B and As were derived from metasediments buried to depth by folding and thrusting. The gold would have been leached from the sediments by a reducing fluid containing dissolved organic matter. The gold precipitated during D3 and D4 deformation by interacting with an oxidizing fluid containing Cr derived from ultramafic and mafic metavolcanic rocks in the mine stratigraphy. Fluid mixing involving oxidation-reduction reactions best describes the evolution of hydrothermal systems in which an oxidizing fluid with soluble Cr^{6+} along with other alkaline elements, such as K, Na, interacts with a reducing fluid carrying organic matter, a Au-thiol complex, B and As. The fluid interaction resulted in reduction of Cr^{6+}; oxidation of organic matter and a thiol-complex to form graphite and CO_2; release of S and As to form arsenopyrite and pyrite; and finally precipitation of gold.

Introduction

The Hoyle Pond mine is located 15 km northeast of downtown Timmins and 3km north of the Pamour mine, Northern Ontario, on the eastern fringe of the Porcupine Gold Camp (Fig. 5.1). The mineralization consists of gold bearing fault-fill and extensional quartz-carbonate veins hosted in a volcanic sequence of interbedded ultramafic and mafic metavolcanic rocks of the Abitibi greenstone belt (Dinel et al., accepted by guest editor), part of the Tisdale Assemblage (2710-2704Ma, Ayer et al., 2005), which extends eastward from Tisdale Twp. into Hoyle Township. The Hoyle Pond mine volcanic stratigraphy correlates with the Hershey Lake and Central formation, defining the base of the Tisdale assemblage within the Porcupine gold camp.

The aim of this paper is to characterize the wall rock alteration zones associated with the mineralization and document the geochemical properties of particular elements (chromium and carbon) in order to depict the chemical reactions that led to Au precipitation. The Grant (1986) isocon diagram method was used in which relatively unaltered samples are compared to altered samples to determined mobile and immobile elements. We herein propose a fluid mixing model in which a reduced organic matter-Au-As-B-S rich fluid derived from deeply buried metasedimentary rocks reacted with an oxidizing K-Na-Cr-Si-HCO_2 fluid during D3 and D4.

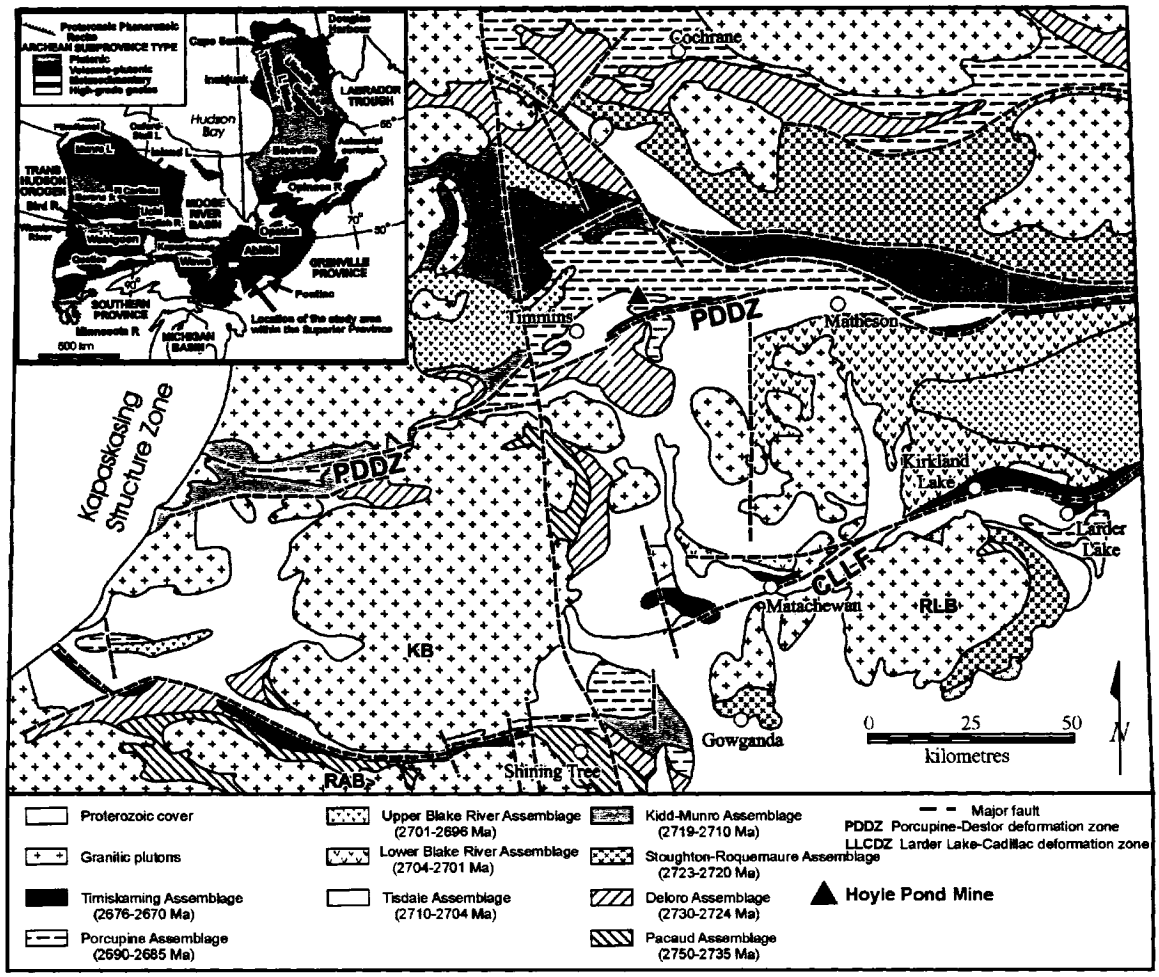

Figure 5.1 The Abitibi greenstone belt, location of the Hoyle Pond Mine, the various patterns symbolized the locations of various rock assemblages.

Methodology

Sampling and Analysis

Underground mapping was conducted (Dinel, in prep) in order to define the mine stratigraphy, structure, mineralization and alteration types. Sample preparation methods are detailed in Dinel (in prep). Sampling at 1 m intervals was executed along 3 transects, intersecting the B1, B1N, B1S and B3 veins (720 meter level) over distances of about 40 m in order to characterize the alteration mineralogy and geochemistry associated with the mineralization. A total of 250 samples were collected in the vicinity of gold bearing veins. Each sample was analysed for major oxides at the XRF facility at the University of Ottawa, and trace elements at the Ontario Geological Survey Laboratories in Sudbury. The samples covers 4 mineralization zones, the 720 ml (meter level) 1060fz (fault zone), the 950-440ml, the #16 vein on the 3 level (~400ml) and 440ml (Fig. 5.2 and appendix III).

The error in the major oxides is less than 0.5% of the reported value and for trace elements, less than 10%. The error was calculated with a confidence interval of 95% using the method of Kretz (1985) on lab standards and on three blind samples analysed five times in repetition. Two blank samples were analysed to identify contaminants. In addition, Principal Component Analysis (PCA) was employed to investigate inter-elements correlations.

Mine Geology

Based on work reported in Dinel et al., (accepted by guest editor), the Hoyle Pond gold deposit is hosted in south facing homoclinal sequences of stacked volcanic rocks part of the Hershey Lake and Central formation at the base of the Tisdale Assemblage, which ranges in age from 2710 to 2704Ma (Ayer et al., 2005). The volcanic sequence at the mine has been subdivided into 3 volcanic packages; the North Volcanic Package (NVP), the Central Volcanic Package (CVP), and the South Volcanic Package (SVP). In general, the volcanic sequence consists of interbedded komatiites, basaltic-komatiites and high Mg-tholeiitic basalts, in the NVP (Rye, 1987); interbedded basaltic-komatiites and komatiites in the CVP; and the SVP is composed of interbedded high Mg-tholeiitic basalts and Fe-rich tholeiitic basalts (Fig. 5.2). These rock units are overprinted by carbonate alteration at the regional scale and "Grey Zone" (graphite) alteration along the mineralized veins (Pressacco, 1999, Downes, 1982 and an inner sericite alteration zone and an outer albite alteration zone enveloping the gold bearing veins. The bulk of the current gold production and reserves are located in the SVP and the NVP.

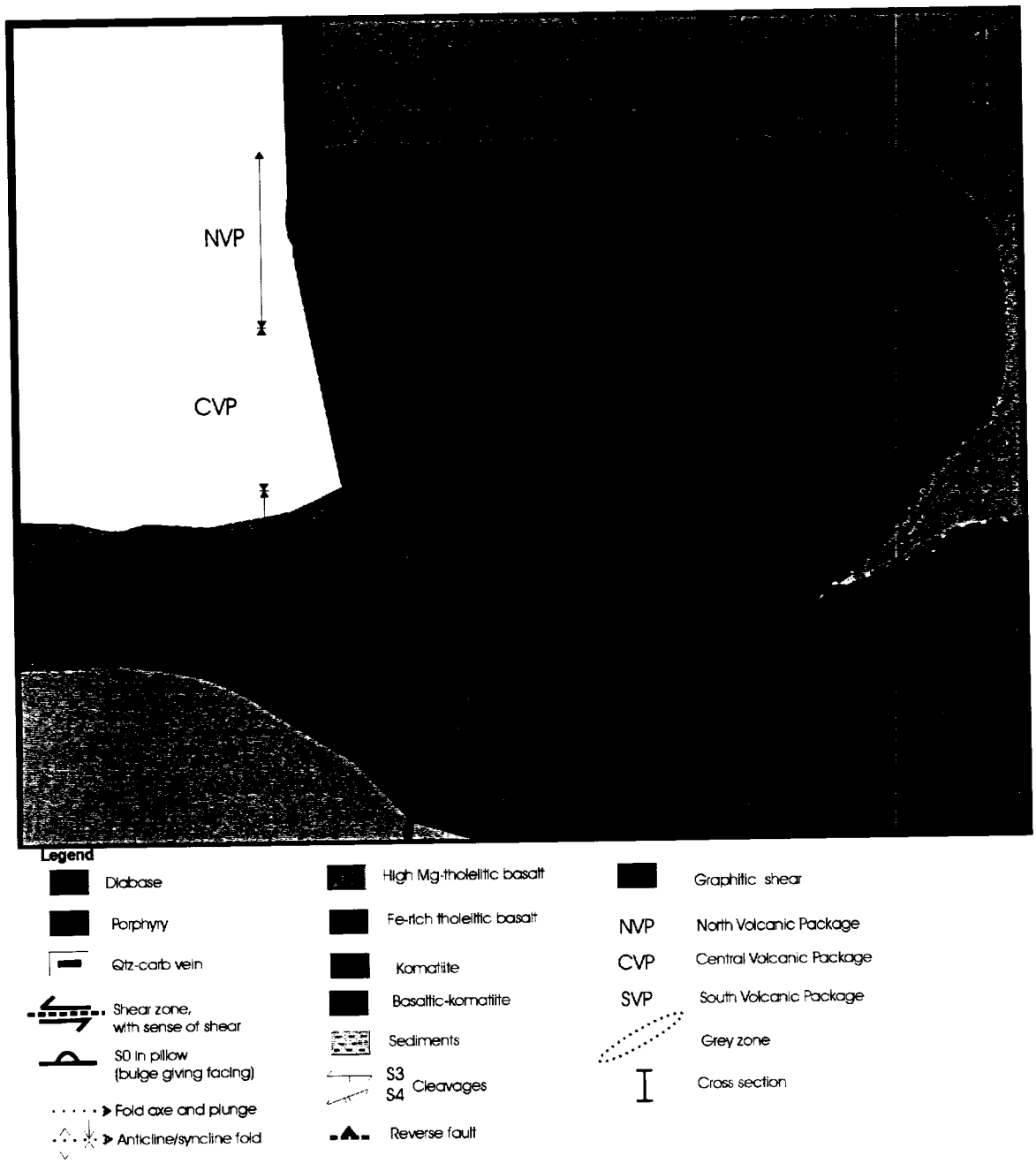

Figure 5.2 Hoyle Pond mine geological compilation of the Hoyle Pond mine 440ml and 720ml maps.

Structures

The volcanic rock of the Porcupine Gold Camp was subjected to 6 deformation event (Bateman et al., 2005, Dinel et al. accepted by guest editor, see chapter 4). Fabric related to the first two deformation event, D1 and D2, were not observed at the mine. The mine volcanic rocks are foliated by a dominant S3 fabric parallel to bedding that strikes generally eastward. S3 is refolded at the mine scale by D4. The S4 fabric trends ~070 (Fig 5.2), is axial planar to isoclinal F4 folds (e.g. 1060fz), and Z-shaped F4 folds to the northwest of the 1060fz (see Fig. 5.2). The timing of D3 deformation is constrained between a U-Pb zircon age of 2687.6 ± 2.2 Ma for a porphyry sill containing both S3 and S4 and 2684.4 ± 1.9 Ma for a QFP intrusion which lacks S3 fabric yet processes the S4 fabric (Dinel et al., accepted by external editor, see chapter 4). The 1060fz (shear zone) is a corridor of intense deformation, where a penetrative S4 parallel cleavage oriented ~070° formed by shear strain. The S4 foliation observed in the mine is interpreted to be equivalent to the S4 fabric observed in the Porcupine gold camp in proximity to the Porcupine-Destor Deformation Zone (PDDZ) as described by Bateman et al. (2005).

Styles of vein mineralization

Auriferous veins at Hoyle Pond vary from extensional with a massive appearance, to fault-fill veins that occur as either sheeted, boudinaged, or massive types. The extensional veins are linear to S-shaped, cut across S3 and S4 at high angles and in general have experienced some sinistral rotation. They are typically composed of massive white to greyish quartz, locally with pyrite (<5%) along the vein contacts. Locally the extension veins are black as the result of abundant graphite and tourmaline-filled fractures. The fault-fill veins are generally oriented ~070° and have a diverse mineralogy consisting of massive white to grey quartz, with interstitial tourmaline and/or stylolitic chlorite and locally muscovite or Cr-muscovite. Other fault-fill veins are mainly composed of massive white quartz and are commonly associated with variable concentrations of graphite in the vein selvages. In the NVP, the fault-fill veins (e.g. #16 vein) are parallel to S3 fabric, however in the SVP, the fault-fill veins are parallel to S4 fabric. Mineralization in the 1060fz is typically coincident with the contacts between lithological units occurring on the limbs of isoclinal F4 folds.

Mineralization in the Hoyle Pond vein system consists of free gold ranging from micron size specks to flakes of mm-cm size occurring along stylolites or randomly distributed gold in massive veins, and finally as thick mm-cm gold ribbons (Photo 5.1). No economic concentrations of disseminated gold mineralization have been reported in the wall rock. The gold mineralization event in the NVP and SVP is temporally associated with deformation event, D3 and D4 (Dinel et al., accepted by guest editor).

Photo 5.1 Au mineralization in quartz-carbonate vein, pencil for scale.

Alteration Patterns and Mobile Elements

At Hoyle Pond mine, the auriferous quartz-carbonate veins are enveloped by zones of alteration. These alteration zones differ in terms of their mineralogy and chemical signatures in comparison to rocks distal to the mineralization. However, some trace elements did remain immobile thus allowing for discrimination of rock-types (Dinel et al., accepted by guest editor). Figure 5.3 demonstrates, in a qualitative fashion that the elements K, Cr, Rb, Na, S, Ca, CO_2, and Eu were mobile and to a lesser extent that Fe, Mg and LREE, were also mobile during hydrothermal alteration. In addition, the alteration is also associated with increased concentration of C (in graphite), B (in tourmaline) and As (Dinel et al., accepted by guest editor). Al, Ti, Zr, Yb, and REE were relatively immobile. Figure 5.4 depicts the generalized alteration trend in the vicinity of the Au-bearing veins. Typically, an inner sericite alteration envelope immediately adjacent to the veins contains enrichment of K, Cr and As. The outer albite alteration envelope is enriched in Na. There are also two generations of carbonate alteration, an early widespread calcite alteration occurring in hyaloclastite breccias, pillow margin and amygdules, and a later dolomite to Fe-dolomite alteration spatially restricted to the auriferous quartz-carbonate veins and locally with strongly foliated rocks (Dinel et al., accepted by guest editor, see chapter 4). We interpret the early carbonate alteration to be related to volcanic deposition and burial metamorphism and the latter dolomitic alteration to hydrothermal alteration during mineralization (Dinel et al., accepted by guest editor, see chapter 4).

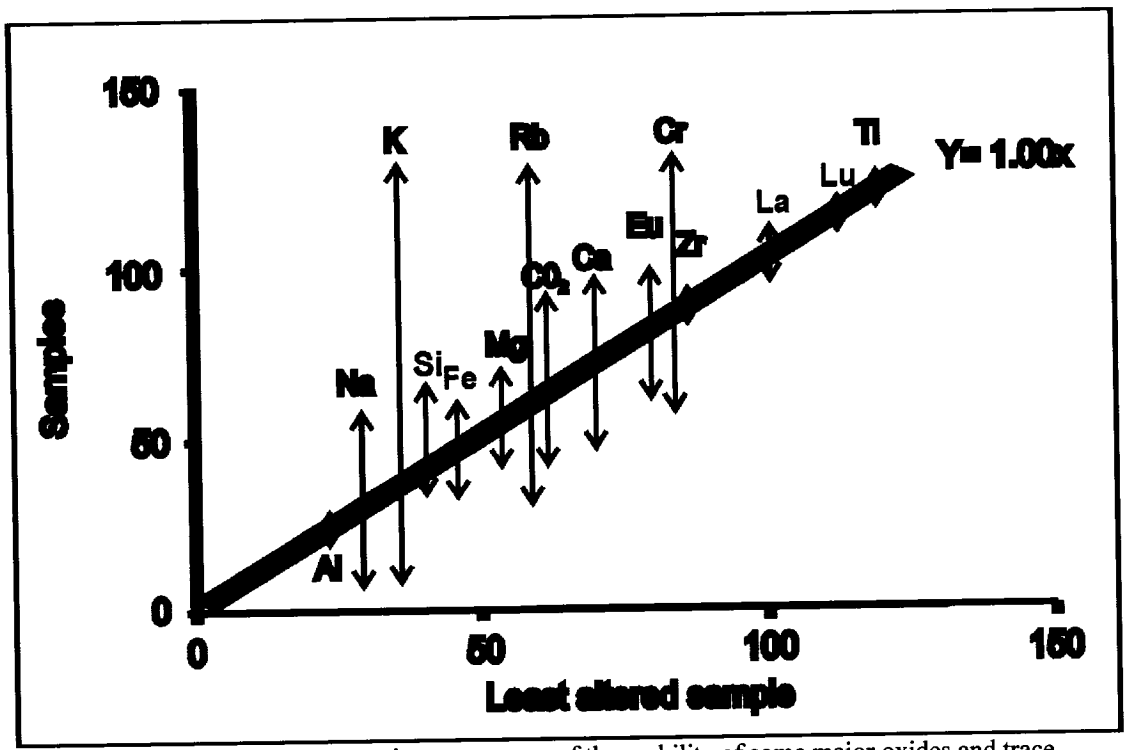

Figure 5.3 Isocon diagram expressing a summary of the mobility of some major oxides and trace elements based on Grant (1986).

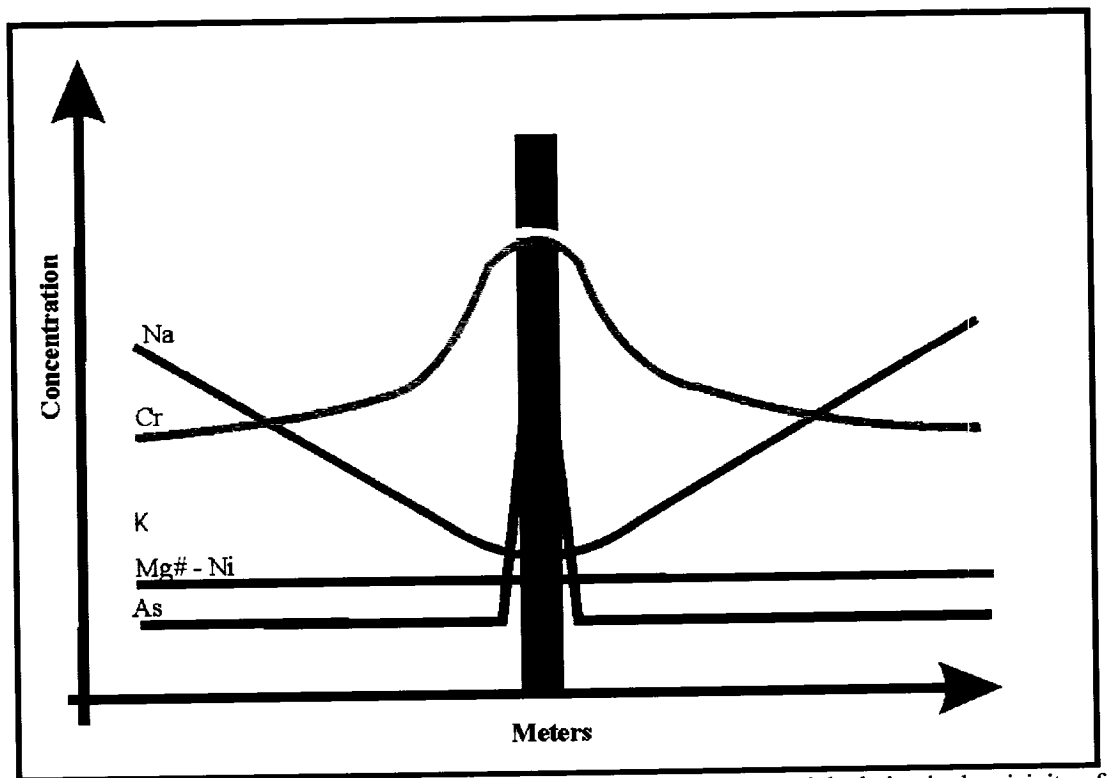

Figure 5.4 Alteration geochemistry model of some element enrichment and depletion in the vicinity of Au bearing veins.

Sericite Alteration

Sericite alteration occurs as 2m to 5 m thick selvages surrounding mineralized veins. Sericite alteration consists of muscovite (10-20%), Cr-muscovite (5-40%) (Photo 5.2), minor arsenopyrite (<2%), pyrite (<5%) and graphite (1-15%) in a pale greyish light yellow coloured rock with a weak to strong cleavage. The alteration zone has undergone enrichment of K, Rb, Cr, As, B, CO_2 and Si (Dinel et al., accepted by guest editor, see chapter 4) and is thus consistent with the data of Davies et al. (1982) reported in the Porcupine gold camp. This type of alteration is also associated with chromium enrichment (discussed below). The muscovite crystals are aligned parallel to the veins and are interpreted to be syn-mineralization. In addition to surrounding veins, sericitic alteration also occurs at some lithological contacts (Dinel et al., accepted by guest editor, see chapter 4) where veins are not present. Cr-muscovite (fuchsite) alteration is common in many gold mineralization zones (Photo 5.3) in the Timmins area and other localities in the Abitibi greenstone belt, e.g. Kirkland Lake and Matheson area (Kerrich and Hodder 1982).

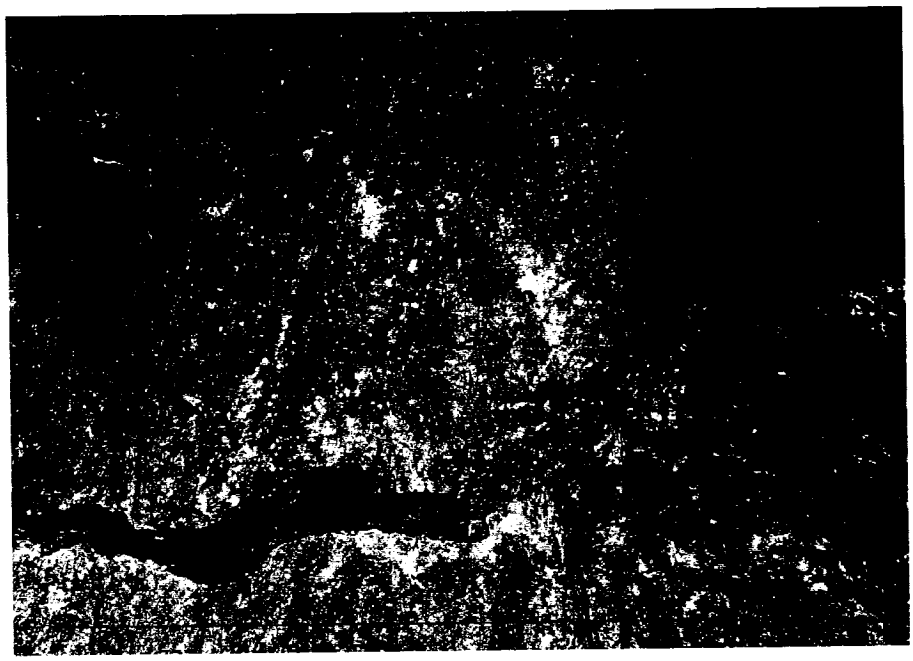

Photo 5.2 Cr-muscovite rich bands in foliated mafic volcanic rock of the SVP, looking east (440 ml cross cut).

Photo 5.3 Cr-muscovite alteration in the wall rock of gold-bearing vein (A vein, 720ml) (hammer handle for scale).

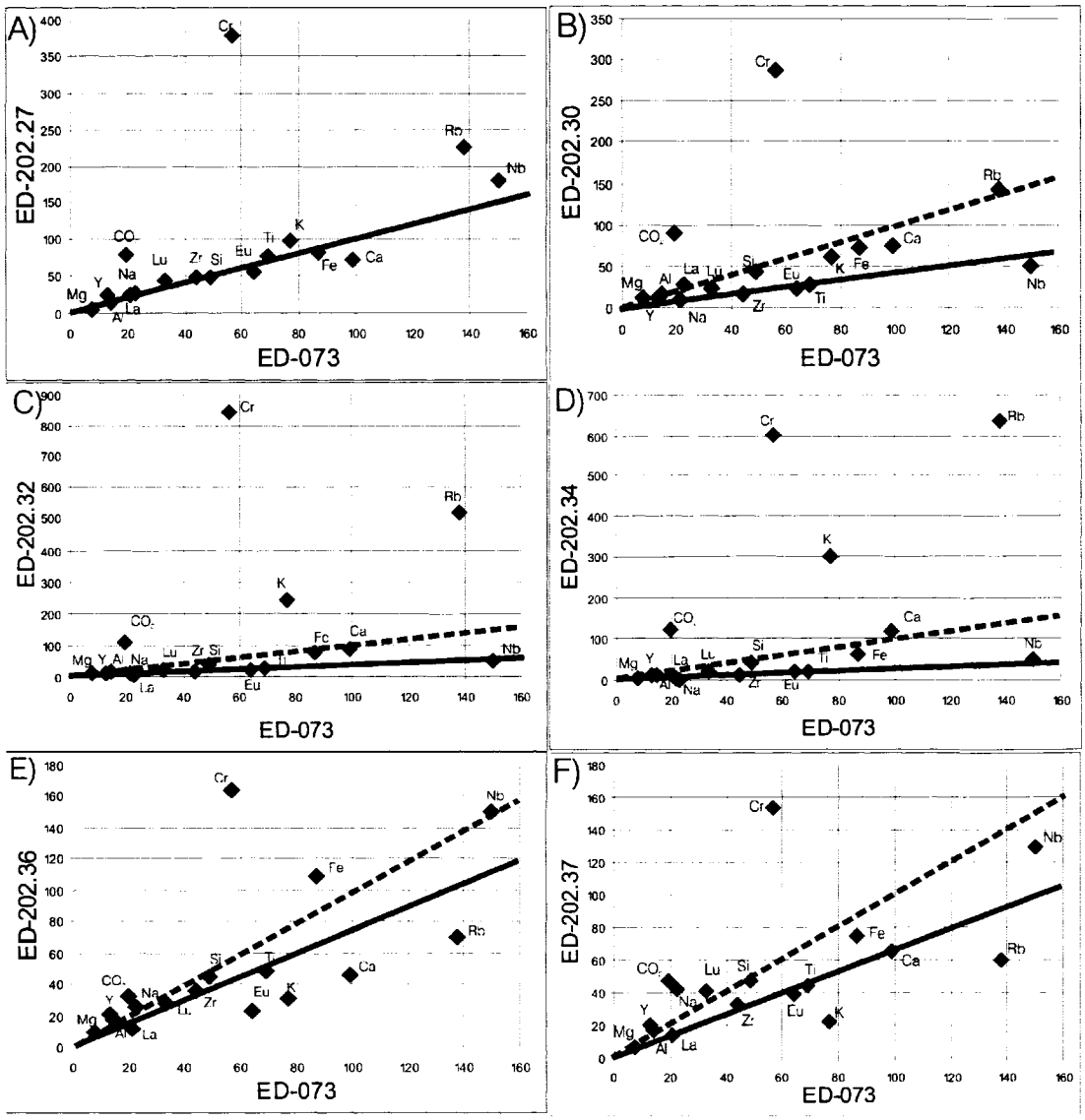

Figure 5.5 Isocon diagram plot of samples collected in the 1060fz B3 vein area (see Figure 5.2 and appendix III),. Figures 5.5-A to F are from samples at different distances from veins. The sample represented by isocon A is located 3m from the B3 vein, the sample represented by isocon B is located 2 m from stockwork zone, whereas the samples represented by isocons C and D occur within a stockwork zone immediately north of the B3 vein. The samples represented by isocon E and F are 3 m and 4 m from the stockwork zone respectively. The major oxides are in wt % and trace elements in ppm. Each variable have been multiplied by a factor: Al = Al_2O_3 wt % x 1, Mg = MgO wt % x 1, Ti = TiO_2 wt % x 100, Zr = ppm x 1, Na = Na_2O w% x 10, K = K_2O w% x 100, Ca = CaO w% x 10, Rb = ppm x 10, Eu = ppm x 100, Cr = ppm x 1, Y = ppm x 1, La = ppm x 10, Lu = ppm x 100, Lu = ppm x 100, Fe = FeO w% x 10, Nb = ppm x 100, Si = SiO_2 w% x 1. The major oxides are label as element in the figure.

Chromium enrichment

Our data demonstrates that enrichment in chromium is also associated with enrichment of K and Rb in close proximity to the B3 and B1 veins in both high Mg-tholeiitic and Fe-rich tholeiitic basalts (Fig. 5.5_{a-f}). This sympathetic correlation is also observed in the Principal Component Analysis plot (Fig. 5.6), where the covariance vectors of Cr, K and Rb have similar orientations (Dinel et al. accepted by guest editor, see chapter 4). Chromium is found in the octahedral site of muscovite (Table 5.1) replacing Al (Deer et al., 1992). Elsewhere in the Timmins gold camp (i.e. Buffalo Ankerite and Beaumont deposits), Cr-rich tourmaline occurs in the quartz-carbonate veins (King and Kerrich 1989a), thus indicating Cr was a constituent of the hydrothermal fluids. In addition, analysis on quartz-carbonate veins hosted in mafic volcanic and sedimentary rocks by Kerrich and Hodder (1982) shows Cr contents ranging from 150 to 1800 ppm, whereas typical Cr contents in tholeiitic basalts range from 150 ppm to 250 ppm (Faure, 1998). In proximity to gold-bearing veins at Hoyle Pond, the Cr content of basalts increases by a factor of 5 to reach levels greater than 1200 ppm accompanied by an apple green colouration. The lack of accompanying increases in MgO and Ni contents (Fig. 5.4) indicates the Cr enrichment is the direct result of remobilization of Cr by hydrothermal fluids and not igneous fractionation processes.

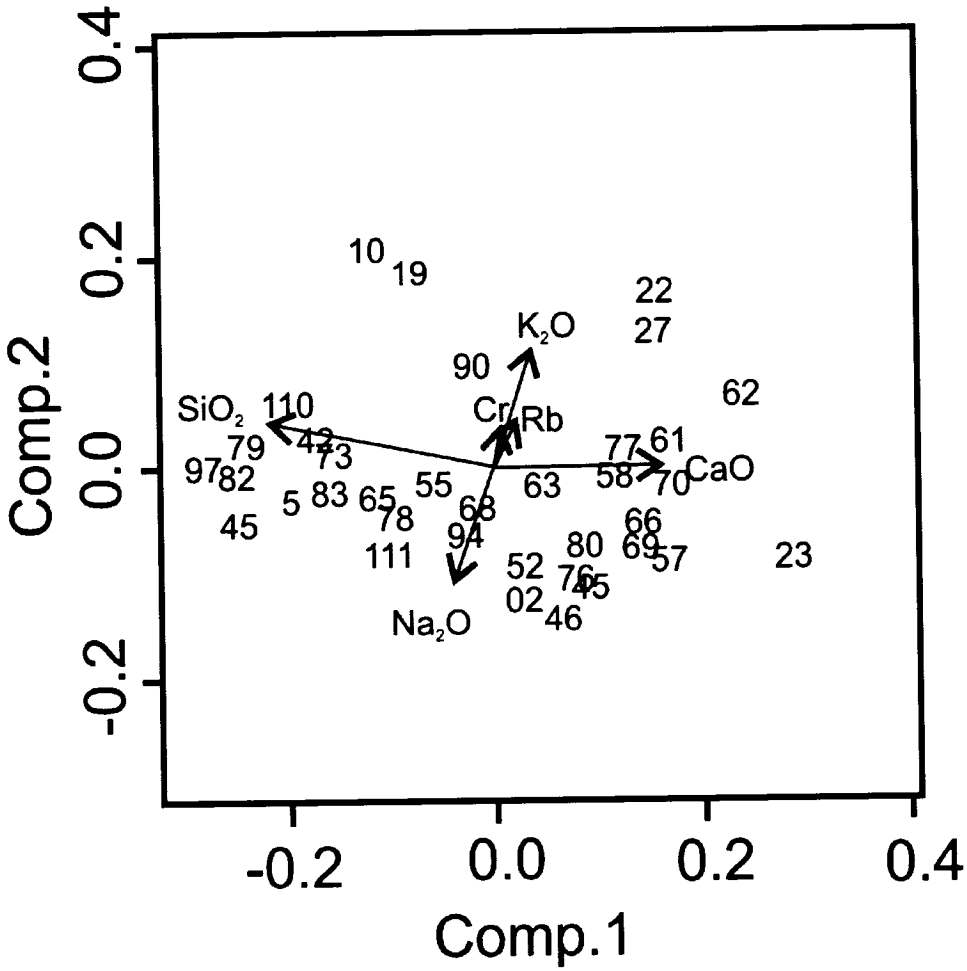

Figure 5.6 Principal component analysis plot of the covariance (comp1 vs. comp2) of mobile elements showing the Cr-K_2O sympathetic behaviour and Na_2O and K_2O antithetic behaviour.

Table 5.1 Cr-muscovite Electron Micro-Probe analysis and mineral calculation.

	115-01-1	115-01-2	115-01-3	115-01-4	115-01-5	115-02-1	115-02-2	115-03-1	115-04-1	115-04-1	115-04-2	115-04-3	115-04-4	116A-1-1	116A-1-2	116A-2-1	116A-2-2	119-01-1	119-01-2	119-01-3	119-02-0
SiO_2	48.49	48.07	48.42	47.76	48.34	48.17	48.42	48.28	48	48.75	48.04	48.66	48.18	48.79	48.55	49.61	48.49	47.93	48.19	48.01	48.02
Al_2O_3	32.59	32.78	32.99	33.46	30.91	31.85	32.39	32.25	32.77	32.88	32.58	31.88	33.2	31.73	31.1	31.51	33.26	34.79	34.91	35.52	33.34
TiO_2	0.36	0.34	0.4	0.38	0.34	0.37	0.43	0.22	0.34	0.37	0.32	0.35	0.32	0.25	0.39	0.41	0.18	0.18	0.15	0.11	0.25
Cr_2O_3	1.19	1.18	0.52	1.45	2.77	1.92	1.71	1.97	1.54	1.59	0.98	1.77	0.93	1.41	1.49	1.4	1.03	1.17	1.11	1.01	1.33
V_2O_3	0.09	0.09	0.12	0.08	0.11	0.09	0.09	0.06	0.07	0.09	0.1	0.09	0.09	0.07	0.05	0.03	0.07	0.12	0.1	0.12	0.1
FeO	0.9	0.77	0.96	0.86	0.92	0.99	1	0.97	0.92	1.02	1.23	1.17	0.78	0.67	0.83	0.71	0.64	0.6	0.55	0.44	0.86
MgO	1.63	1.48	1.48	1.29	1.55	1.6	1.51	1.52	1.45	1.5	1.54	1.61	1.43	1.56	1.9	1.89	1.25	0.95	0.93	0.68	1.26
MnO	0.02	0.03	0.02	0	0	0	0	0.03	0	0	0	0.03	0	0	0.03	0	0	0	0.04	0.01	0.04
K_2O	10.82	10.78	10.74	10.67	10.77	10.8	10.85	10.55	10.83	9.81	10.68	10.82	10.72	10.45	10.57	10.78	10.57	10.02	10.24	10.04	10.46
CaO	0	0	0	0.02	0.02	0	0.01	0.01	0.01	0	0.05	0.03	0	0	0	0	0.03	0.01	0.03	0.01	0.09
Na_2O	0.29	0.32	0.28	0.37	0.29	0.24	0.29	0.35	0.4	0.29	0.38	0.3	0.34	0.25	0.23	0.23	0.22	0.51	0.38	0.53	0.49
BaO	0.19	0.26	0.2	0.33	0.23	0.23	0.19	0.29	0.26	0.26	0.22	0.26	0.29	0.17	0.12	0.07	0.13	0.14	0.13	0.16	0.28
Cl	0.01	0.01	0	0	0	0	0	0	0	0	0	0	0	0	0	0	0	0	0	0	0
F	0	0	0.15	0.11	0.17	0.1	0.07	0.09	0.1	0.11	0.11	0.09	0.06	0.08	0.14	0.14	0.21	0.08	0.07	0.11	0.08
H2O	4.5515	4.52863	4.47387	4.49898	4.43019	4.4758	4.5242	4.49669	4.4948	4.52307	4.4741	4.51152	4.51767	4.47644	4.43131	4.50551	4.44595	4.5413	4.56208	4.54546	4.51392
total	101.06	100.567	100.682	101.207	100.779	100.76	101.41	101.015	101.11	101.121	100.63	101.5	100.786	99.8349	99.7597	101.214	100.454	100.97	101.321	101.224	101.042
Si	3.1929	3.18121	3.19463	3.14683	3.21353	3.1935	3.1859	3.18934	3.1689	3.19515	3.1826	3.20398	3.178	3.24087	3.2369	3.25389	3.19888	3.13866	3.14467	3.13132	3.16346
Al	0.8071	0.81879	0.80537	0.85317	0.78647	0.8065	0.8141	0.81066	0.8311	0.80485	0.8174	0.79602	0.822	0.75913	0.7631	0.74611	0.80112	0.86134	0.85533	0.86868	0.83654
Tetra	**4**	**4**	**4**	**4**	**4**	**4**	**4**	**4**	**4**	**4**	**4**	**4**	**4**	**4**	**4**	**4**	**4**	**4**	**4**	**4**	**4**
Al	1.7219	1.73777	1.75975	1.74498	1.63515	1.6819	1.6976	1.70004	1.7184	1.73483	1.7264	1.67779	1.75881	1.72476	1.68049	1.68952	1.7847	1.82351	1.82938	1.86155	1.75189
Ti	0.0178	0.01692	0.01985	0.01883	0.017	0.0184	0.0213	0.01093	0.0169	0.01824	0.0159	0.01733	0.01588	0.01249	0.01956	0.02023	0.00893	0.00887	0.00736	0.0054	0.01239
Cr	0.0596	0.05943	0.02611	0.07271	0.14015	0.0969	0.0856	0.09905	0.0774	0.07931	0.0494	0.0887	0.04669	0.07128	0.07561	0.06989	0.05171	0.05831	0.05513	0.05014	0.06668
V	0.0048	0.00478	0.00635	0.00423	0.00586	0.0048	0.0047	0.00318	0.0037	0.00473	0.0053	0.00475	0.00476	0.00373	0.00267	0.00158	0.0037	0.0063	0.00523	0.00627	0.00528
Fe	0.0496	0.04261	0.05296	0.04738	0.05114	0.0549	0.055	0.05358	0.0508	0.0559	0.0681	0.06442	0.04302	0.03721	0.04627	0.03894	0.0353	0.03285	0.03001	0.024	0.04737
Mg	0.16	0.14602	0.14557	0.12671	0.15361	0.1581	0.1481	0.14969	0.1427	0.14657	0.1521	0.15804	0.14062	0.15448	0.18885	0.18481	0.12294	0.09274	0.09047	0.06612	0.12375
Mn	0.0011	0.00168	0.00112	0	0	0	0	0.00168	0	0	0	0.00167	0	0	0.00169	0	0	0	0.00221	0.00055	0.00223
Oct.	**2.0148**	**2.00921**	**2.01171**	**2.01485**	**2.00291**	**2.015**	**2.0124**	**2.01815**	**2.0099**	**2.03957**	**2.0173**	**2.0127**	**2.00978**	**2.00395**	**2.01515**	**2.00496**	**2.00729**	**2.02259**	**2.01979**	**2.01402**	**2.00959**
K	0.9088	0.91001	0.90388	0.89677	0.91327	0.9133	0.9106	0.88899	0.912	0.82015	0.9025	0.90877	0.90197	0.88543	0.89893	0.90191	0.88947	0.83698	0.85237	0.83529	0.87898
Ca	0	0	0	0.00141	0.00142	0	0.0007	0.00071	0.0007	0	0.0035	0.00212	0	0	0	0	0.00212	0.0007	0.0021	0.0007	0.00635
Na	0.037	0.04106	0.03581	0.04726	0.03738	0.0308	0.037	0.04482	0.0512	0.03685	0.0488	0.0383	0.04348	0.03219	0.02973	0.02925	0.02814	0.06475	0.04807	0.06702	0.06258
Ba	0.0049	0.00674	0.00517	0.00852	0.00599	0.006	0.0049	0.00751	0.0067	0.00668	0.0057	0.00671	0.0075	0.00442	0.00313	0.0018	0.00336	0.00359	0.00332	0.00409	0.00723
Inter.	**0.9507**	**0.95781**	**0.94486**	**0.95397**	**0.95806**	**0.9501**	**0.9532**	**0.94203**	**0.9706**	**0.86368**	**0.9606**	**0.95589**	**0.95294**	**0.92205**	**0.93179**	**0.93295**	**0.92308**	**0.90602**	**0.90586**	**0.9071**	**0.95514**
F	0	0	0.03129	0.02292	0.03574	0.021	0.0146	0.0188	0.0209	0.0228	0.023	0.01874	0.01251	0.0168	0.02952	0.02904	0.04381	0.01657	0.01444	0.02269	0.01667
Cl	0.0011	0.00112	0	0	0	0	0	0	0	0	0	0	0	0	0	0	0	0	0	0	0
OH	1.9989	1.99888	1.96871	1.97708	1.96426	1.979	1.9854	1.9812	1.9791	1.9772	1.977	1.98126	1.98749	1.9832	1.97048	1.97096	1.95619	1.98343	1.98556	1.97731	1.98333
total	**2**	**2**	**2**	**2**	**2**	**2**	**2**	**2**	**2**	**2**	**2**	**2**	**2**	**2**	**2**	**2**	**2**	**2**	**2**	**2**	**2**

Silica enrichment

Enrichment in silica is evident in wall rock samples as fine-grained quartz within the rock matrix, and as a slope change in the isocon diagrams (Fig 5.5 C & D). On isocon diagrams, immobile elements plot on a line with a slope = 1, unless there has been a net change in mass (Grant, 1986). As demonstrated in figure 5.5 straight line relationships with slopes of less than 1 indicate addition of SiO_2 and CO_2 and other mobile elements which resulted in a dilution effect for the immobile elements (Ti, Lu, Zr and Y).

Grey zone alteration (Graphite)

Grey zone alteration is commonly centered on auriferous quartz-carbonate veins which trends 070° and cut stratigraphy (Downes et al., 1982; Dinel et al., accepted by guest editor). Drilling has shown that the grey zones form an anastamosing network surrounding and overlapping lenses of sericite alteration (Rye, 1987). They represents enrichment in graphite, minor pyrite, carbonates, and sericite and predominantly occur in volcanic lithofacies with good original porosities, such as flow breccias, hyaloclastite breccias, pillows selvages and associated pillow breccias, and in later developed porous zones such as faults and shear zones along cleavages. Graphite enrichment also occurs at the north contact between the Tisdale and Porcupine assemblages which is interpreted to be the locus of a thrust fault (Fig. 5.2). All of the above observations indicate that the graphite alteration resulted from mobilization of carbon compounds.

Origin of the Grey Zone alteration (Graphite)

Graphite samples from Hoyle Pond mine grey zone alteration was first analysed by gas chromatograph (Downes, 1982) to determine the nature of the carbon. The data contained peaks corresponding with those expected for C-H bonds as well as toluene and xylene structures indicating the presence of highly condensed aromatic polymers. The oxidation of such organic matter would form free carbon, in other word graphite and a gas phase (e.g., CO). King et al., (1963) and Springer (1985) reported organic matter in graphitic sediments in the form of complex organic molecules such as hydrocarbons and kerabitumens. MacDougall and Hancock (1981) demonstrate that organic matter-bearing cyanide solutions have the capacity to scavenge metals into aqueous solution and to mobilize gold. As solution temperatures increase will result in the formation of graphite

flakes and the organic matter loses its capacity to absorb resulting in precipitation of gold (Springer, 1983). This process is very similar to the cyanide solution method used to extract gold from the ore by the mining industry.

In order to investigate the organic geochemistry of the carbon-rich material further analysis were conducted with a spectrophotometer under ultraviolet light. Samples collected from the graphitic shear on the 440m level were concentrated using a NaOH extraction and analysed using a spectrophotometer, to measure ultra-violet light absorption at various wavelengths of 280, 360, 480 550 and 660λ, from infra red to ultraviolet. The results show an absorption peak around 280 nm (Fig. 5.7), which corresponds to a trace fraction of organic matter (Farmer and Morrison, 1960, Sapek et al., 1980). In order to test for contamination (i.e. the introduction of anthropogenically derived organic matter) we analysed a sample for radio-carbon ^{14}C. The analyses yielded an age date of 39 950 +/- 660 years with a confidence interval of 68.3%. This indicates contamination and that the carbon in the sample is a mixture of modern day ^{14}C and Archean carbon (i.e. no ^{14}C). Given that the half life of ^{14}C is 5700 years we calculate that the age of ~40000 years represents a contamination of Archean carbon by approximately 0.5 wt % modern carbon.

We have also analysed the carbon for its organic matter content by Nuclear Magnetic Resonance (NMR) with a peak corresponding to those of complex organic aromatic molecules at 127.77 ppm (parts per million at 16.5 GHz) (Fig. 5.8) (Ashworth et al., 1985). In addition, a hydrogen spectra attained by NMR shows distinct traces of C-H bonding suggesting that the C-H bounds were from organic matter (Fig. 5.9) (Ashworth et al., 1985). Peaks in the range of 0 to 15 ppm usually suggest protons (H+) bound to aromatic molecules (Ashworth et al., 1985). In addition, samples were analysed for ^{13}C isotopic signatures; the results indicate fractionation of ^{13}C, in the range of -25 to -28 per mil suggest a reduced sedimentary rock (Rye, 1987) and suggest that it could be derived from organic matter. The presence of multiple peaks corresponding to various carbon-based molecules demonstrates with confidence that the degree of contamination is minimal.

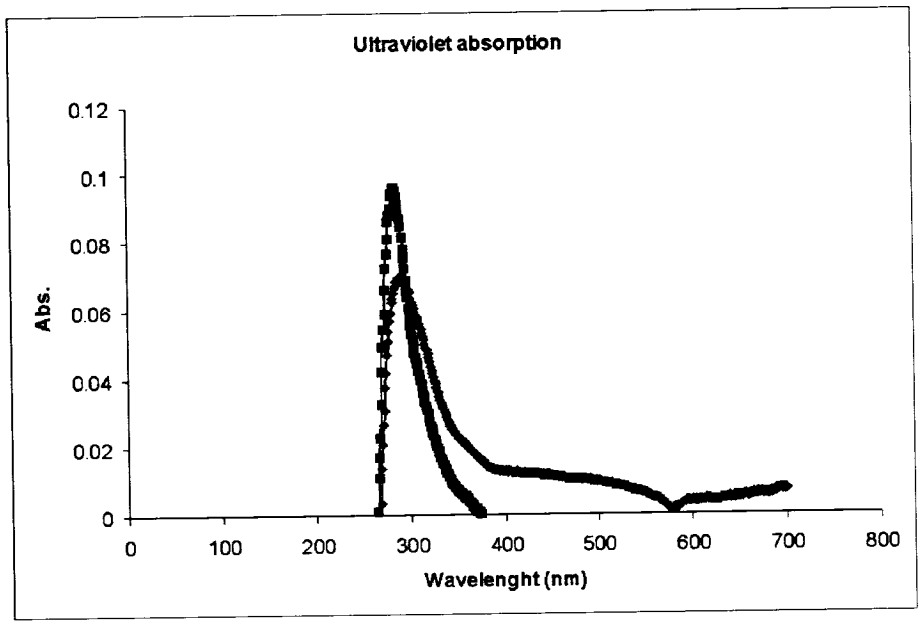

Figure 5.7 Ultraviolet absorption spectrophotometry plot for graphitic material samples on the 440 and 720ml.

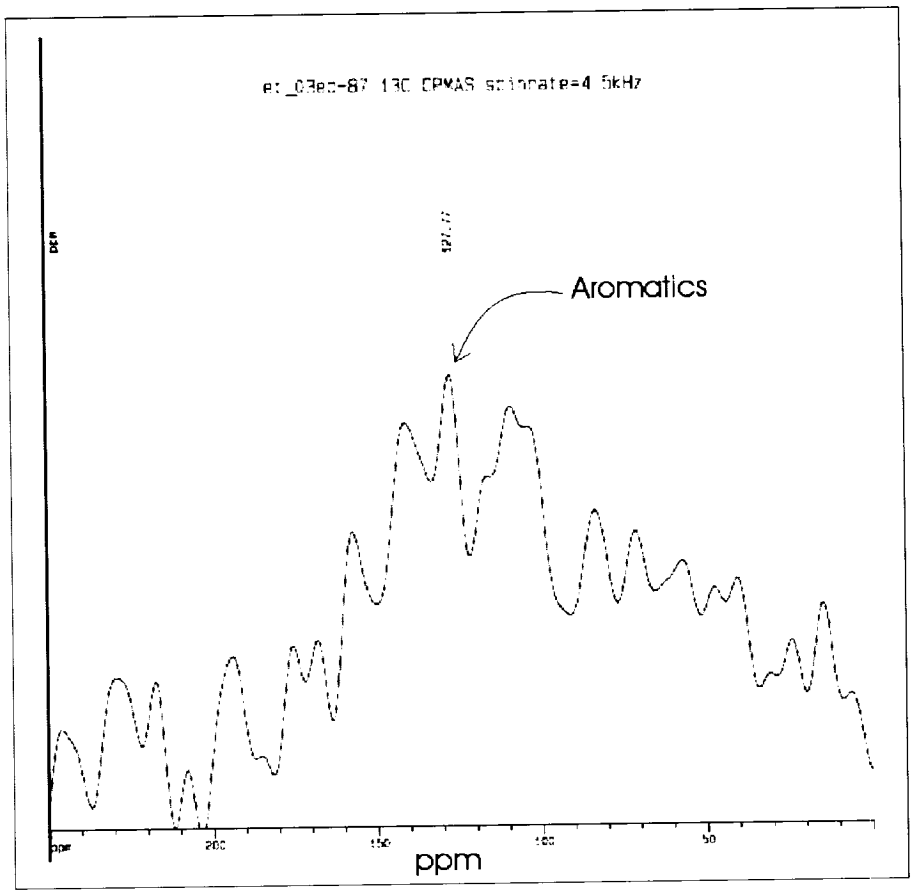

Figure 5.8 Nuclear Magnetic Resonance (NMR) C-H spectra of the graphite samples.

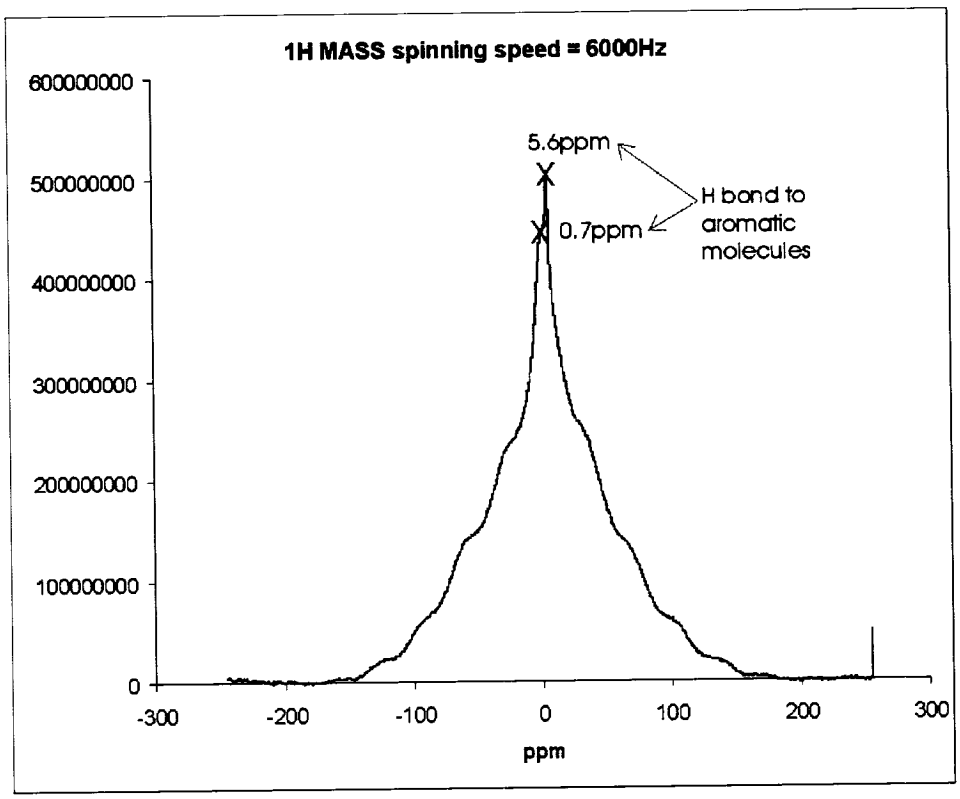

Figure 5.9 NMR Hydrogen spectra of graphite samples, showing H bond to cyclic aromatic aromatic molecules.

Albite Alteration

The albite alteration zones are characterised by 20 to 50m halos enveloping the sericite alteration zones, but also locally crosscut by sericite within the cleavage domains (S3 & S4). Typically the albite alteration is a bleached apple green colour consisting of fine grained albite in the groundmass of the volcanic rocks. In thin section it can be observed as pervasive albite porphyroblasts and spherulitic textured secondary albite (Photo 5.4).

Sodium enrichment

In geochemical terms the albite alteration is expressed by an increase in Na_2O and pronounced negative Eu anomalies in chondrite normalized REE patterns (Eu/Eu* 0.22-0.5). Figure 5.10A shows REE chondritic pattern of unaltered samples and figure 5.10B shows the REE pattern of the albite altered samples.

The Na enrichment appears to decrease approaching the vein and is replaced by an increase in K, whereas when mineralized veins are spaced closely together albite is overprinted by sericitic alteration. Interestingly, the High Mg-tholeiites are 4 times more enriched in Na than are the Fe-rich tholeiites (Dinel et al., accepted by external editor). We interpret Eu depletion to be the result of replacement of more calcic-plagioclase by albite, thus causing the release Ca and Eu from the plagioclase crystal structure (e.g., Fowler and Doig, 1983). The Ca released during albitization of relatively Ca-rich plagioglase (e.g. in basalts) was mobilized and combined with Fe and Mg and CO_2 to form carbonates (calcite, dolomite and Fe-dolomite) (see below).

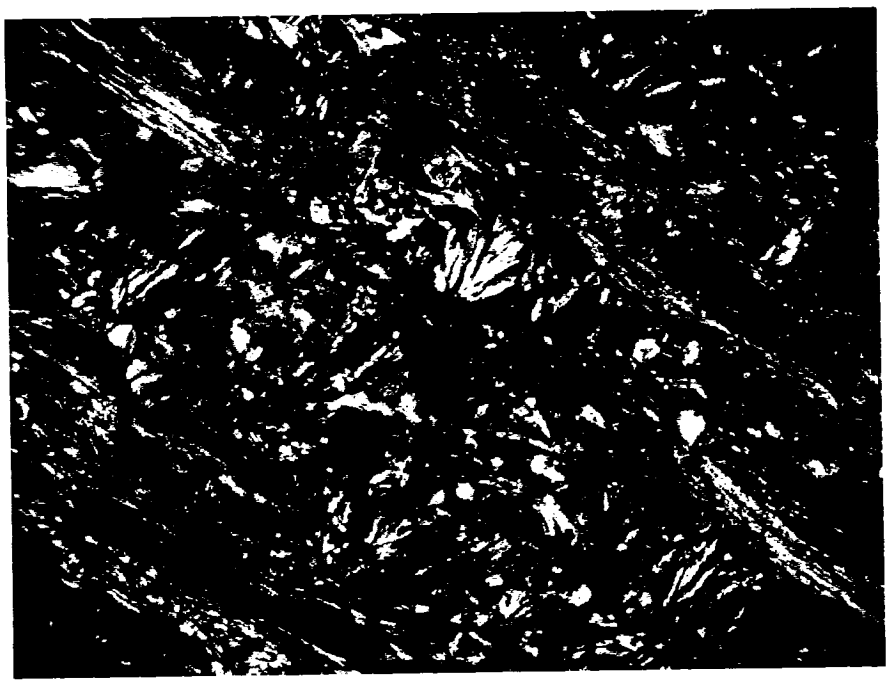

Photo 5.4 Photomicrograph of albite alteration, and secondary spherulitic albite crystal growth, cross polarized light (f.o.v.= 4mm).

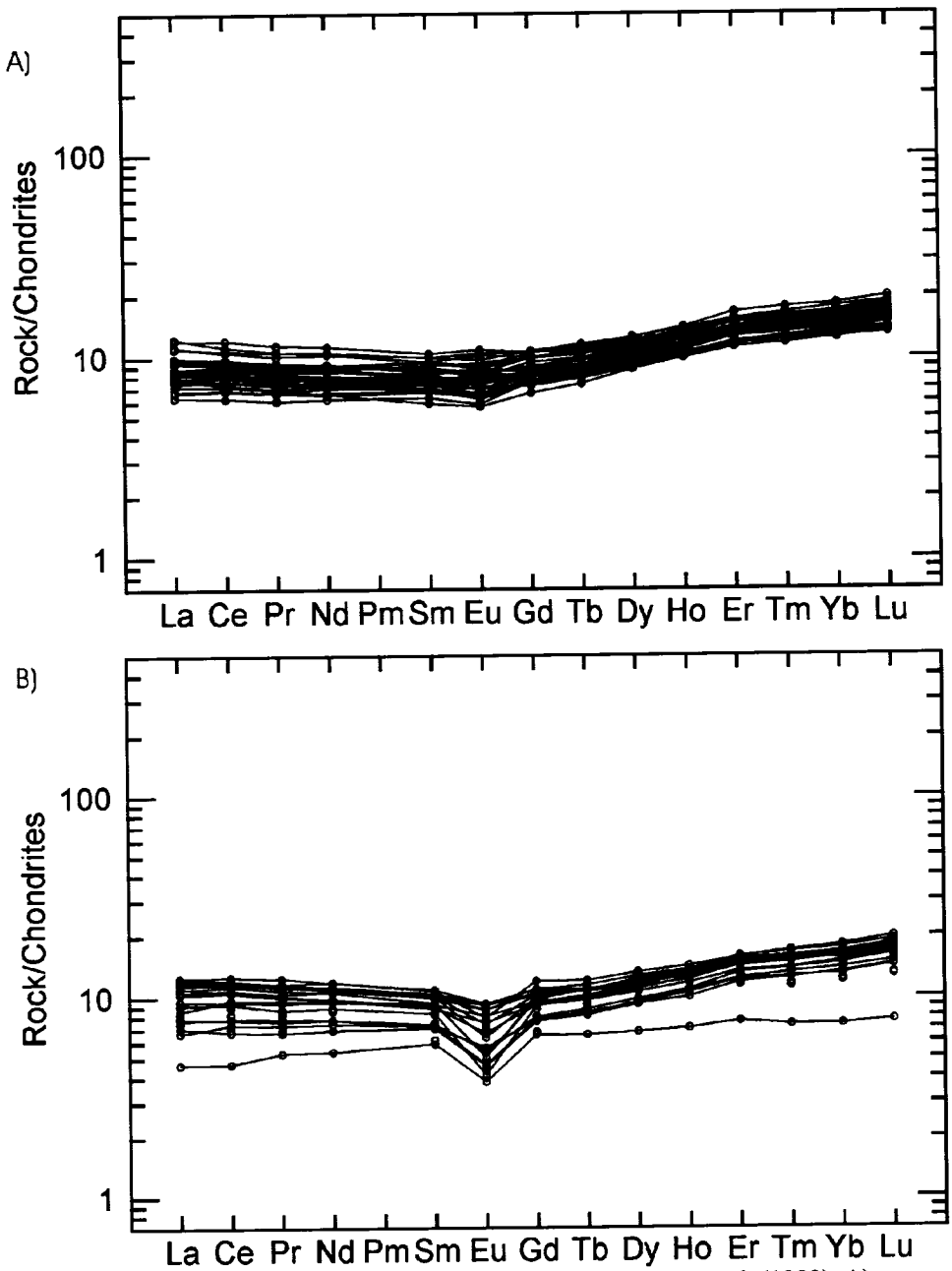

Figure 5.10 REE chondritic pattern based on Sun and McDonnough (1989), A) unaltered volcanic rock samples, B) albite altered volcanic rock samples.

Carbonate alteration

Two types of carbonate alteration occur at Hoyle Pond. Pervasive carbonate consists of calcite infillings of pillow selvages, amygdules and is interpreted to have formed during sub-seafloor metamorphism or burial metamorphism (Dinel et al., accepted by guest editor, see chapter 4). The second consists of dolomite and ferroan dolomite in cleavages and sieved-textured porphyroblasts. This type is interpreted to be associated with regional metamorphism and alteration.

The second carbonate alteration is most intense in the immediate proximity of the veins as coarse dolomite porphyroblasts (0.2 to 1.5 mm). The CO_2 enrichment associated with this alteration type is more pronounced in the high Mg-tholeiites within the 1060fz, the ultramafic rock of the CVP and the high Mg-tholeiites of the NVP. Fe-tholeiites appears to be less enriched in CO_2, but are slightly enriched in Fe-dolomite (Dinel et al. accepted by guest editor, see chapter 4.

Tourmaline and arsenopyrite alteration

Tourmaline is present in fault-fill and extensional veins, as coarse euhedral crystals (5-15 mm) or in stylolites. Needles of arsenopyrite occur in veins and their wall rocks which also contain pyrite at vein contacts. The arsenopyrite alteration is defined geochemicaly by a narrow zones (1-2 m wide) of As enrichment in the gold bearing veins selvages (Fig 5.4).

Discussion

Sources of gold, organic matter, arsenic, boron and chromium

Because the graphite has a chemical signature consistent with it having been ultimately derived from organic material, we reject the possibility that it was from mantle derived carbon. Given the fact that organic matter has been documented in black shales elsewhere in the Archean (e.g., Tait, 1987; Condie et al., 2001; Rasmussen, 2005), it is hypothesised that the organic material at Hoyle Pond, though re-mobilized into shear zones, was derived from carbonaceous sedimentary rocks. This suggests that the Porcupine and/or the Timiskaming assemblages may have been the source of carbon. Boron is significantly enriched in modern sea water (4.5 mg/g, Faure, 1998) and in sea floor sedimentary rocks

(100 to 230 ppm; Faure, 1998) whereas it is rather impoverished in mafic and ultramafic rocks (2 to 5 ppm; Faure, 1998). In fact, deep-marine sediments have the highest B content of all supracrustal material, > 100ppm (Leeman and Sisson, 1996). Thus we suggest that the B within the tourmaline in quartz veins associated with the gold mineralization throughout the Porcupine camp was leached from clay minerals and or micas (e.g. Leeman and Sisson, 1996) in these sedimentary assemblages. Similarly, we interpret that the As was also derived from these sedimentary units as Faure (1998) indicates marine sediments typically contain the highest content of As of all supracrustal rocks.

Solubility of Chromium

Chromium mobility has not been extensively studied in relevant hydrothermal systems at high temperatures although there has been some work on this in layered intrusions (e.g., Eales, 2000). However, Cr geochemistry has been widely studied in soil and groundwater systems, both for its mobility and toxicity. Chromium is commonly found in trivalent (Cr^{3+}) or hexavalent (Cr^{6+}) states. In general Cr^{3+} is not considered to be very mobile, but it can be oxidized by manganese\iron oxides or by hydroxide, to Cr^{6+} which is soluble and thus easily mobilized (e.g., Richard et al., 1991). In aqueous solution the oxidation of Cr^{3+} to Cr^{6+} increases with increasing temperature and pressure (Henry, 2000) with the oxidation rate of Cr^{3+} to Cr^{6+}increasing from 67% at 470 K (197°C) to 95% at 620 K (347°C) (Anderson, 1975).

In order to investigate the mobility of Cr under the relevant conditions of Archean "Orogenic" gold hydrothermal systems, we have modeled the solubility of Cr in aqueous solution at a temperature equivalent to greenschist metamorphism using the software Geochemists Workbench. Figure 5.10A and B, show the stability trends of $HCrO_4^-$ (chromic acid) and CrO_4^{2-} (chromate) at temperatures of 250°C and 300°C respectively, 1 atmosphere and with varying Eh and pH. These temperatures are the same order of magnitude as estimated temperatures of hydrothermal fluids responsible for gold mineralization in the Abitibi greenstone belt (Olivo et al., 2002). In general hydrothermal solutions associated with Au mineralization have nearly neutral or low pH (Seward, 1973; Hedenquist al., 2000; Groves et al., 2003). We hypothesis that the chromium

speciated as chromic acid under oxidizing conditions (see figure 5.11A and B). Note that reduction of Cr can be triggered by a reducing agent or by a drop in pH. In addition, the figure 5-10 suggests a large region on the Eh vs. pH diagram where Cr^{6+} can be in solution. In addition, potassium and sodium salts of chromate (CrO_4^{2-}) are freely-soluble in aqueous solution over pH range of 1-14 at 1 atm and 25°C (Nieboer and Jusys, 1988), although there are no data for high temperatures. Based on the above we conclude that Cr^{6+} can be mobilized in hydrothermal solutions under the appropriate condition for gold mineralization.

Hexavalent chrome can be observed in many other oxide-species. White and Roy (1975) experimentally proved the stability of various Cr species with changing oxygen pressures (Fig. 5.12). They have shown that Cr_3O_8 and Cr_5O_{12}, which correspond to source of Cr^{6+}, are stable at temperatures below 350°C and oxygen pressure varying from 0 to more than 8 kbars.

The Cr^{3+} found in chromite of ultramafic volcanic rocks could be oxidised to Cr^{6+} under aqueous conditions as follows (equations 1):

(1) $$Cr_2O_3 + 5H_2O_{(aq)} \rightarrow 2\ CrO_4^{2-}{}_{(aq)} + 10H^+ + 6e^-$$

This Cr can be transported in hydrothermal solutions, reduced and precipitated in the mineral phase (Cr-mica). The most efficient reduction agents would be Fe II (in aqueous phase) (Sass and Rai, 1987), Fe II sulfides (pyrite), Thiol (HS^-often referred to thio), hydrogen sulfides and organic matter (Zouboulis et al., 1995; Thornton et al., 1999; Szulczewski et al. 1999; Kim et al. 2001). Cr^{3+} replaces aluminium in the octahedral site of muscovite. Cr^{6+} has a tetrahedral geometry (White and Roy, 1975), and given its smaller atomic radius (Faure, 1998) would likely replace Al in the tetrahedral site of muscovite.

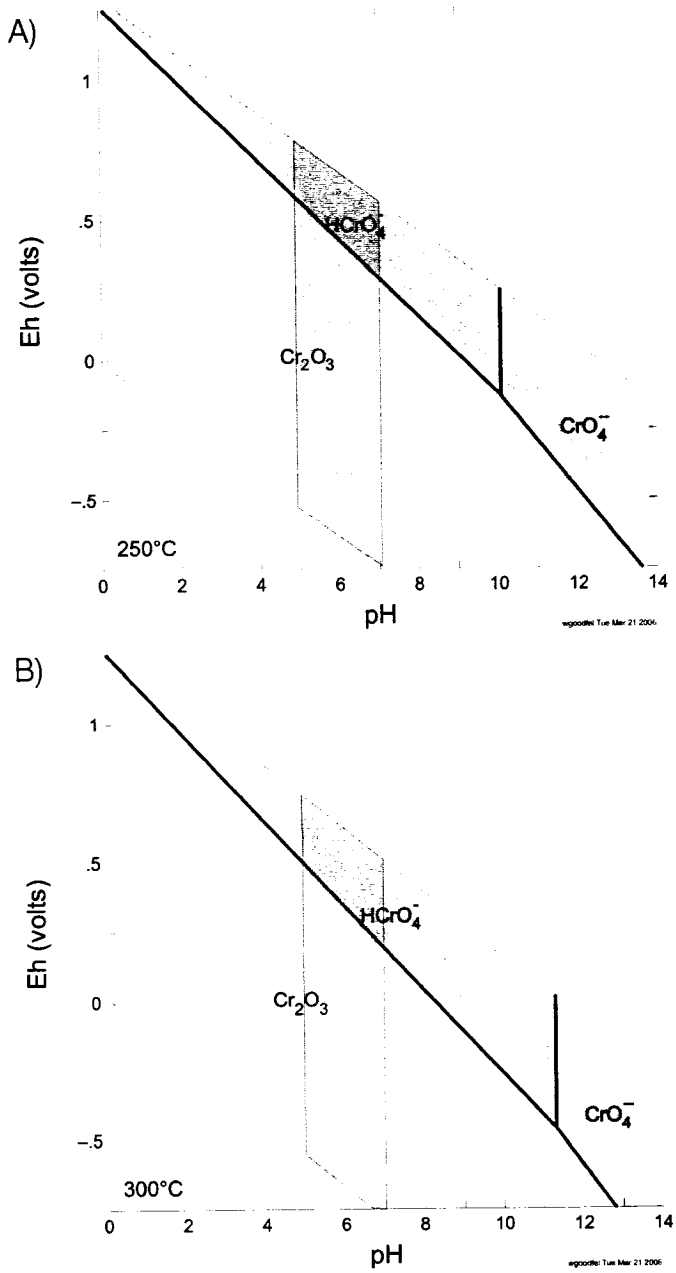

Figure 5.11 Cr species properties with respect to pH (Eh vs. pH diagrams) . Cr2O3 represent the solid state, the blue coloured area represent the aqueous stability field and the shaded area represents the pH range where Au-bearing and Cr-bearing fluids would interact. A drop in pH shifts the chemical balance to the left, a reconfiguration of the electrons in the fluid and a reduction of Cr^{6+} to Cr^{3+}. A) at 250°C , B) at 300°C

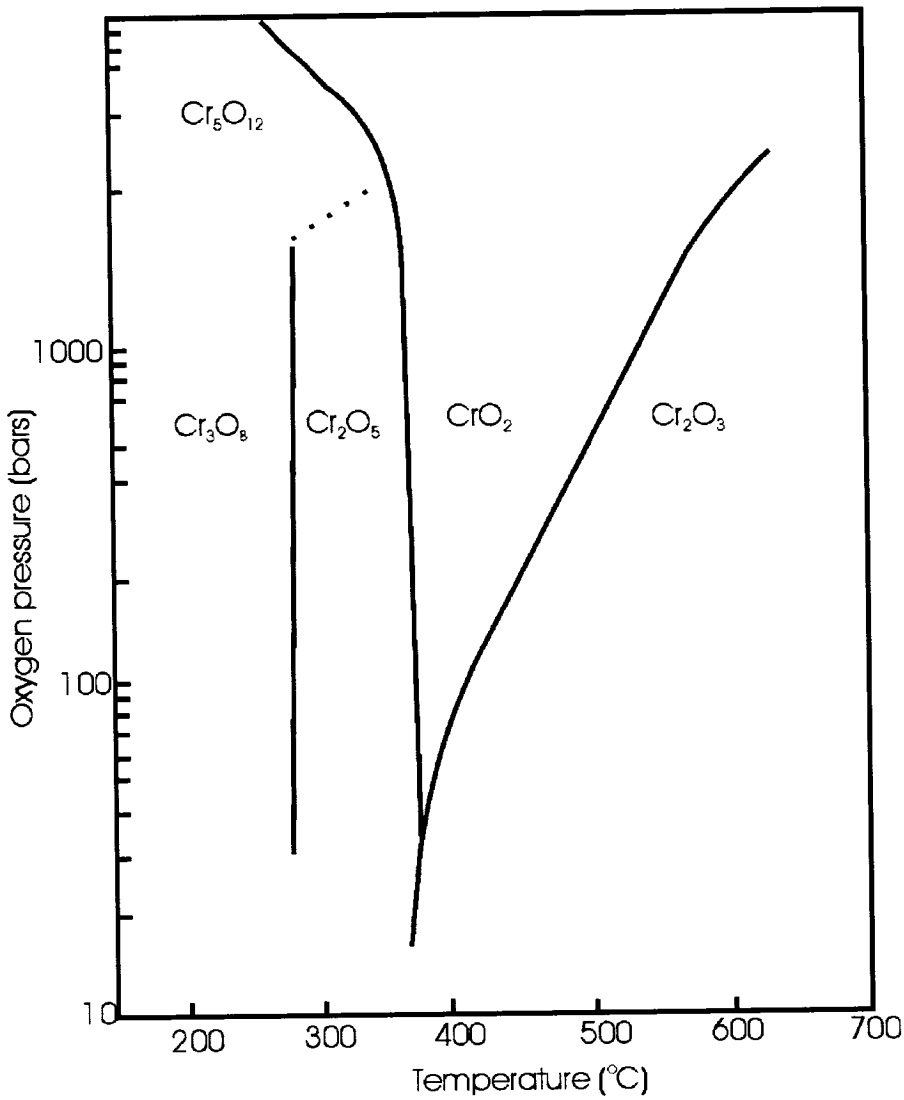

Figure 5.12 Chromium species under various oxygen pressures and temperatures (White and Roy, 1975).

Hydrothermal transport and precipitation of gold, arsnics, boron and carbon

Gold transportation and precipitation concepts are well described by Mikucki (1998) and other authors. The main mechanism of precipitation are; adiabatic and conductive cooling of the ore fluids, interaction between ore fluids and their surrounding host rocks, phase separation in response to pressure decrease during the rise or throttling of the ore fluid and, by the mixing of two or more different fluids. All four mechanisms could be responsible for gold precipitation at Hoyle Pond mine. However, in the following we will discuss our ideas concerning Au precipitation by fluid mixing.

The alteration mineralogy and chemistry at Hoyle Pond thus provide insight into the mobility of various elements. Therefore we propose a number of chemical reactions for the mineralization based upon our analyses, data from the literature and known geochemistry of the elements. Gold is known to be solubilized by thiol complexes in conjunction with other HS complexes as illustrated in Eq. 2 (Seward 1973).

(2) $Au^0 + H_2S + HS^- \leftrightarrow Au(HS)_2^- + 1/2H_2$ (from Seward, 1973).

Alternatively MacDougall and Hancock (1981) demonstrate that gold can be leached from sediments by soluble organic matter. Equation 3 suggests possible reactions for mobilizing gold with organic matter in the presence of HS.

(3) $Au + H_2O + HS^- + C_x\text{-}H_{x(aq)} \rightarrow Au\ (HS)\text{-}C_x\text{-}H_{x(aq)} + H_2O$

These reactions indicate that the gold would have been transported in a rather reducing fluid contrary to what we expect for Cr which we have illustrated is mobile in hexavalent form under oxidizing conditions.

Interestingly, thiol complexes (Au-HS-) are believed to be responsible for remobilizing gold in hydrothermal solution (eq. 2) (Seward, 1973; Böhlke, 1989; Stefansson and Seward, 2003). This could imply that the reduction of the Cr^{6+} into Cr^{3+} to form Cr-mica may be related to the precipitation of Au. Recent work on the origin of graphite alteration at Hoyle Pond mine (Downes et al., 1982; Dinel et al., under revision) has shown that

traces of organic matter are preserved in the graphite, thus suggesting that the graphite may be the result of the oxidation of the organic matter, and related to the reduction of Cr $^{6+}$ to Cr $^{3+}$.

Relatively reduced solutions containing thiol complexes, organic matter, and Au can not coexist with an oxidized fluid containing Cr^{6+} thus implying that more than one fluid was involved in the mineralization process.

Fluid mixing model

We suggest the most reasonable hypothesis is a fluid mixing model, where gold, transported as an Au-thiol-organo complex, associated with other species such as As and B, reacted with an oxidizing fluid. Migration of the oxidizing hydrothermal fluid would result in breakdown of calcic plagioclase forming albite (and carbonate?). Equation 4 models chemical reactions for albitization of anorthite during choritization of pyroxene (modified from Colvine et al., 1988).

(4) $3(Ca,Na)Al_2Si_2O_8+3CO_2+ 1/2H_2O + Fe + Mg \rightarrow (Fe, Mg, Al)_6(Si, Al)_4O_{10}(OH)_8 + 3NaAlSi_3O_8+3CaCO_3+21/2O_2$

As the oxydizing fluid migrates and interacts with wall rock , becomes saturated in K and Cr and reacts with a reduced fluid, carrying the organo-thiol-Au complexes B and As. Equation 5 propose a simplified oxidation of organic matter by CrO_4^{2-}.

(5) $CrO_4^{2-} + Au\text{-}HS\text{-}C_xH_x \rightarrow C + CO + CO_2 + H_2O + S + Au + Cr^{3+}$

The oxidation-reduction reaction between the fluids would precipitate the Au, oxidise the organic matter to graphite, and reduce the Cr $^{6+}$ to Cr $^{3+}$, which couples with K in the muscovite crystal lattice in equation 6.

(6) $NaAlSi_3O_8 + K^+ + Cr^{3+} + 2H^+ \rightarrow KNa(Cr)Al_3Si_3O_{10}(OH)_2 + SiO_2$

Reaction 5 would also release CO_2 and CO, which in turn would form more carbonate minerals. The reducing of Cr^{6+} to Cr^{3+} and oxidation of thiol, organic matter, and precipitation of Au would occur under oxidation-reduction reactions (eq. 3). Trivalent Cr would now react with wall rock, forming Cr-muscovite and sulphur to react with Fe and As forming pyrite and arsenopyrite. Figure 5.13 summarize the chemical reactions enumerate above, leading to gold precipitation.

Groves et al. (1998, 2000), Goldfarb et al. (1998) and Jia et al. (2003) have shown that Au in orogenic gold deposits could be release during orogenic heating of hydrous silicate mineral phases within accreted sedimentary rocks. At Hoyle Pond we also propose sedimentary rocks were the source of Au, B, As and organic matter. Boyle (1979) reported Au average content of deep marine sediments at 0.108ppm, Wedepohl (1995) estimate Au content of deep marine wackes to approximately be around 0.0048 ppm. If we estimate the leaching efficiency at 50%, and gold minimum solubility at 300°C of $3.42x10^{-7}$ g/l (Stefansson and Seward, 2003), it would need approximately 8.4 km^3 of sedimentary rock to form a Au deposit the size of Hoyle Pond (~2,000,000 oz). The solubility of Au increases with temperature and pressures. At 500°C and 2 kbars the solubility of Au is $7.8x10^{-6}$ g/l (Stefansson and Seward, 2003). In addition, the solubility of gold increases if the fluids contains organic matter (MacDougall and Hancock, 1981).

Estimated concentrations of 1 to 10% coarse to medium grained black tourmaline crystals within the mineralized veins and stylolites, confirms the enrichment in B. Moreover geochemical B enrichment in Au-bearing veins has been documented elsewhere in the Porcupine gold camp (e.g., King and Kerrich 1989a; Ferkous and Tremblay, 2001; Olivo and Jones, 2002; Bateman et al., 2005). Boron is insensitive to oxidation-reduction, but the trigonal or tetrahedral coordinated boron-hydroxide species is highly soluble (Palmer and Swilhart, 1996). Boron is reactive to temperature and pH of fluids and can easily be leached out of sedimentary rocks. The precipitation of B as tourmaline most likely, is the result of a pH change and/or the temperature of the hydrothermal fluids. Boron in the fluid phase is trivalent whereas B in the crystal phase is tetravalent (Palmer and Swilhart, 1996). Thus we suggest that the source for both As and B was sedimentary rocks.

Trace of organic matter in graphitic samples may indicate incomplete oxidation. The formation of graphite by oxidation suggests that the organic matter were oxidised under near anaerobic conditions, similar to incomplete combustion in a vacuum.

A number of geochemical exploration tools are evident from this work at Hoyle Pond. First, lithological contacts which are enriched in K, As and S may be pathfinders for auriferous fluid channels that could be traced along strike or dip. Secondly, high-Mg tholeiitic basalts, basaltic komatiites and komatiites are more carbonatized than Fe-rich tholeiitic basalt thus suggesting that high-Mg content volcanic rocks may have been more reactive to CO_2-rich fluid than Fe-rich tholeiitic basalts under mineralizing condition at Hoyle Pond.

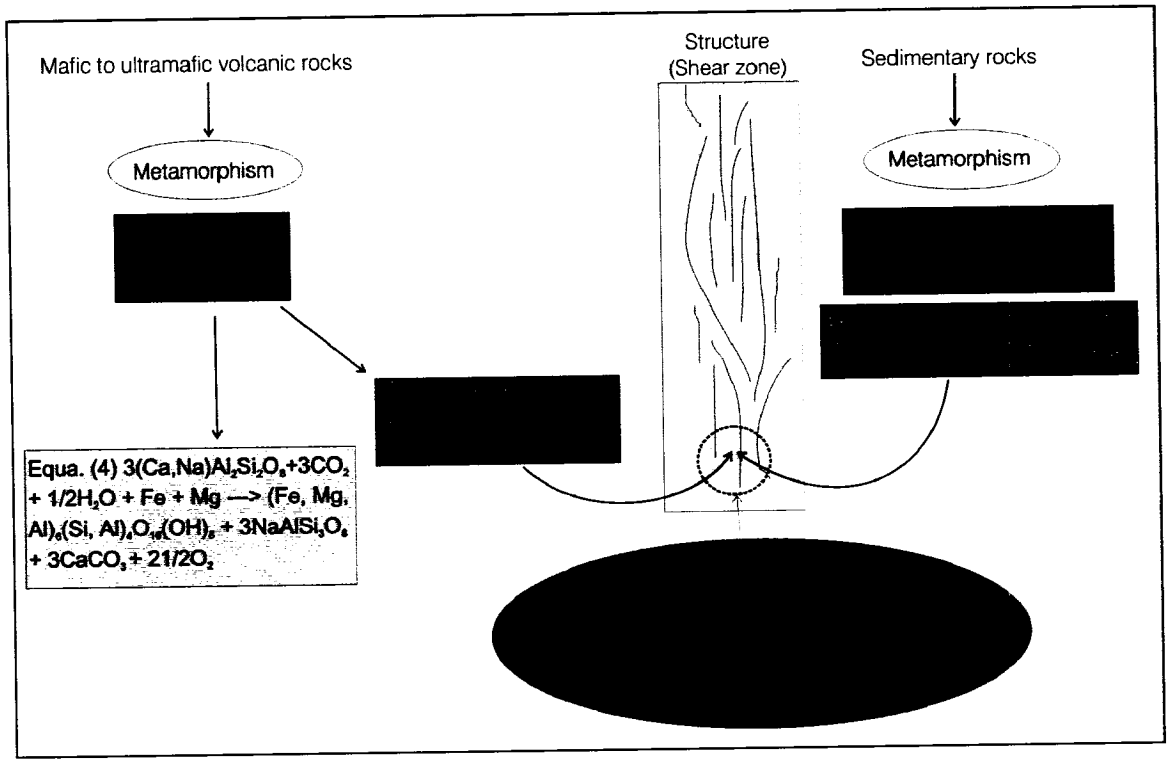

Figure 5.13 Flow chart illustrating processes and chemical reaction leading to gold precipitation.

Conclusions

Chromium mobility is relatively poorly documented in research on gold deposits. However, mine geologists in the Porcupine gold camp have reported that quartz-carbonate veins associated with Cr-muscovite wall rock alteration are generally gold bearing (Moritz and Crocket, 1991). At Hoyle Pond, Cr was mobile during mineralization. Mineralogically there is a modal increase in muscovite and Cr-muscovite associated with the sericite alteration zone in the surrounding the veins. Cr^{6+} is a known mobile species in aqueous solutions and the best known Cr^{6+} reducing agents are organic matter, thiol complexes, and Fe II. We interpret that gold was mobilized by an Au-thiol complexes and organic matter (Au-HS-C_xH_x). Cr^{6+} is a strong oxidant and suggests that more than one fluid was involved in the mineralization processes; a reducing fluid mobilizing gold along with other species such as organic matter, As and B, and a fluid with oxidizing properties, mobilizing Cr^{6+}.

Analyses conducted on graphite samples from mineralized zones have shown trace amount of complex organic matter, specifically aromatics. We suggest a possible source for the gold, organic matter, boron and arsenic was from the surrounding metasedimentary rocks of the Porcupine assemblage, located to the north and south of the mine, which would have been buried to depth during folding and thrusting (Dinel et al., accepted by guest editor, see chapter 4). Gold would have been leached from these metasedimentary rocks by a reducing fluid with dissolved organic matter. Gold precipitated in quartz carbonate veins in structures related to D3 and D4 with the likely source for Cr being locally available ultramafic and mafic volcanic rocks in the mine stratigraphy. Based on observation, data and the chemical properties of elements, we suggest a fluid mixing model which would have generated oxidation-reduction reactions. An oxidizing fluids with soluble Cr^{6+} in solutions with other alkaline elements, like K, Na, and a reducing fluid carrying organic matter, Au-thiol complex, B and As. The fluids would migrate along structures where they would mix. Cr^{6+} would then be reduced by the Au-thiol and organic matter complexes, and would result in the oxidation of organic matter and thiol-complex to form graphite and CO_2, oxidized B to form tourmaline, release S and As to form arsenopyrite and pyrite during interaction with the host rock and finally precipitate gold.

Chapter 6.0 Host rock Control?

One of the main on-going problems in gold exploration is an understanding of the controls and timing of mineralization. The controls are not clearly defined, however it is obvious in some case that Au mineralization is primarily controlled by structures, though in most of these cases the structures are located in zones of primary weakness, such as flow contacts (e.g. Hoyle Pond mine, Dinel et al., accepted by guest editor, see chapter 4, Hollinger mine, Brisbin, 1997). In the Timmins gold camp, the type of gold mineralization sought for has always been gold bearing quartz carbonate veins, which provide, in most cases highly profitable ore. Disseminated gold mineralization appears to be taboo and exploration for such deposits is under explored, however disseminated gold mineralization has been reported and mined at the McIntyre mine and in the Buffalo Ankerite-Delnite mine (Atkinson et al., 2005 and Hurst, 1935). This project has investigated numerous lithofacies associated with the Vipond Formation in the Timmins gold camp. In particular the V10b unit, which for many exploration companies has been used as a marker horizon (Fig. 6.1). The Hoyle Pond work stems from a project to understand the facies of Archean volcanoclastic rocks and their relation to gold mineralization (e.g. Ropchan et al., 2002 Scott et al., 2003). At the outset of this thesis Fowler and I along with B.Sc. students investigated numerous interesting fragmental unit in the Abitibi near known deposits, from the former Croesus mine in Munro Twp. to the Hollinger-McIntyre Mine in the Timmins area. As part of this work, a collaboration between student B.-M. Saumur, myself and Fowler resulted in a paper Dinel, Saumur, and Fowler that is currently under revision for a special volume in Economic Geology (the revised paper will appear in the final copy of the thesis). The paper formed part of Mr. Saumur's B.Sc. thesis and also forms a significant part of the work I did for this thesis and is therefore reproduced below in this chapter. In the following, we discuss the possibility of disseminated Au mineralization in primary porosity, e.g. flow breccias, hyaloclastite breccias, in secondary porosity created during deformation, in mineralization hosted in shear zones and the association between Fe/Mg ratio and gold mineralization.

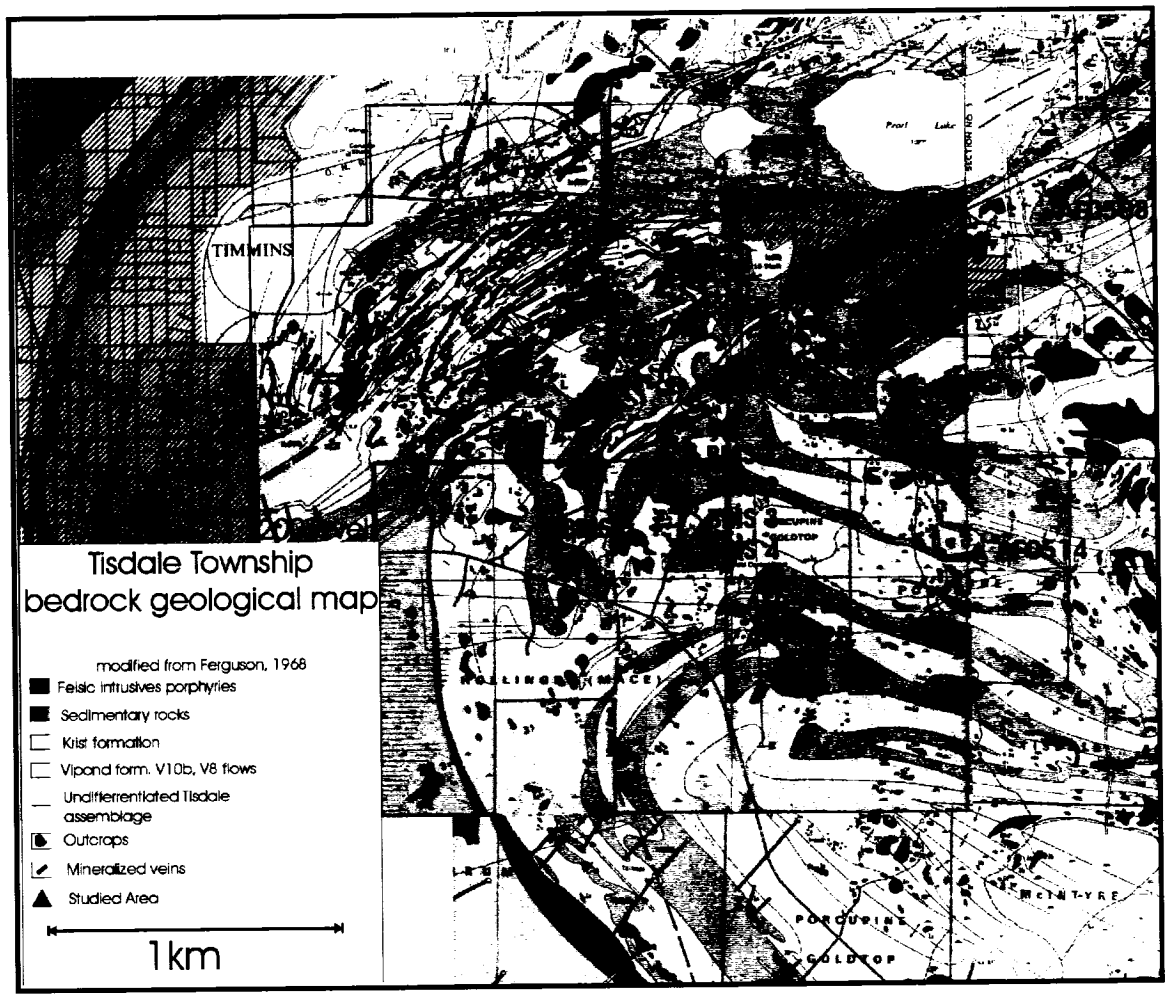

Figure 6.1 Tisdale Twp. Geological map, Timmins Ontario, modified from Ferguson 1968. Notice the distribution, continuity and spatial association of the V10b unit to the mineralized vein of the Hollinger and McIntyre mine (Dinel et al., accepted by guest editor, see chapter 4).

6.1 Tectonic induced porosity

A shear zone is a corridor in which rocks are submitted to intense deformation, forming multiple sets of fractures perpendicular to principal stress and containing minerals that are metamorphosed and rotated parallel to the main fracture plane. Passhier and Trouw (1998), define a shear zone as a "planar zone of relatively intense deformation in which progressive deformation is non-coaxial". The fracture planes or cleavage domains in shear zones or deformed terrain increase the porosity of the rock favouring the migration of fluid and increasing the surface area of the rock thus promoting reactions. Fluids can in some case remobilize economically valuable elements. Of course primary porosity in rocks can also serve as a locus for mineralization.

6.2 Primary porosity

Porosity can form by means other than tectonic deformation. The cohesive or non-cohesive nature of lavas is dependent on numerous physical parameters. The lava rheology is controlled in general by the composition of the lavas during eruption, the temperature of lavas during eruptions, the effusion rate during eruption, the paleo-surface, the environment of deposition and the volatile content of magma. Viscous felsic to intermediate "coherent" lava erupting in sub-marine or sub-aerial, will tend, as they flow, to fragment due to shearing, forming so-called autoclastic breccias. They may fragment during effusive eruptions to form pyroclastic deposits. Alternatively fresh volcanic material may be transported and sedimented to form epiclastic deposits. The term volcanoclastic is applied, particularly in the Archean, to any one of these deposits until a specific facies can be determined. Pyroclastic deposits generally form a porous network during deposition, composed of glassy fragment of various size and a finer grain matrix composed of ash to lapilli size glass particles material (Photo 6.1). Mafic magmas, tend to be less viscous, such that their volatile phases generally escape "tranquilly" precluding pyroclastic (excepting phreatic eruptions) and thus minimizing the formation of explosively primary porosity. However, quenching of the lavas and continued flow movement favours the formation of autoclastic breccia. In submarine environment, extensive deposits of "hyaloclastite" breccia form. Its formation and the generation of

cooling cracks and joint enhance porosity (Photo 6.2 and 6.3), and thus favour the migration of fluids.

Photo 6.1 Photo of a pyroclastic lapilli tuff breccia in the vicinity of the McIntyre mine, near Goldale shaft, notice the orangey colour of the plastically deformed amoboedal fragment, due to viscous deformation while hot during eruption and deposition, followed by iron carbonate alteration by hydrothermal fluids percolating through pore spaces.

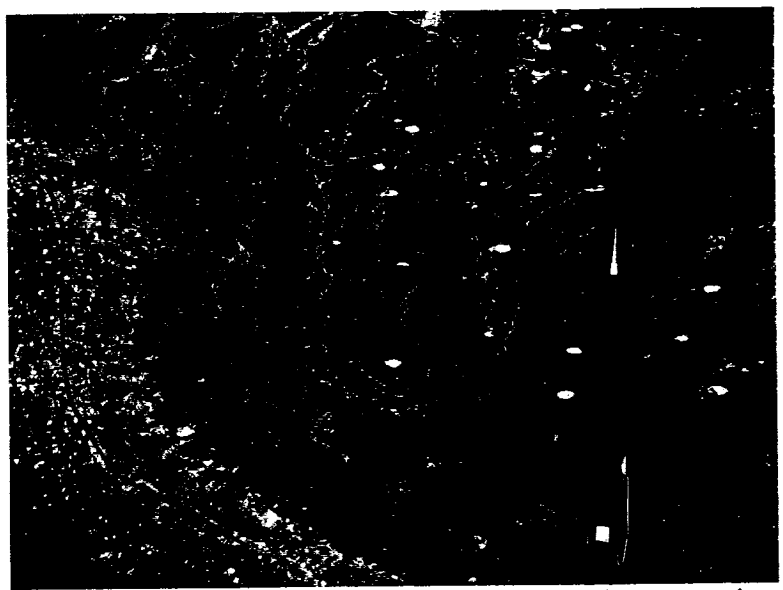

Photo 6.2 Photo of pillowed mafic volcanic flow, showing concentric and radial fracturing formed during quenching upon eruption.

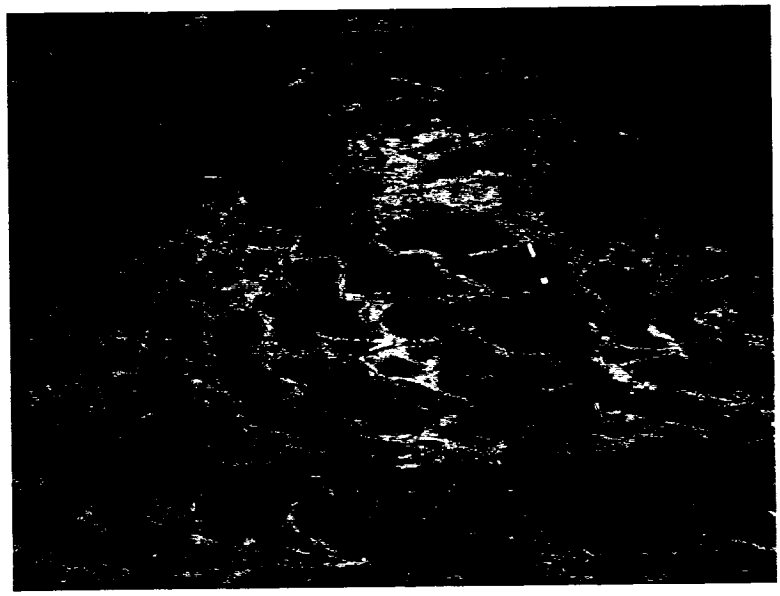

Photo 6.3 Photo of similar concentric and radial fracturing patterns in pillowed mafic volcanic flows as in photo 5.2. However, in this case it is strongly albitized and silicified along the fractures.

In the Timmins area we have focused on mapping, sampling, documenting and interpreting the eruption-time-rheology of some Archean lava flows based on the petrographic and detailed outcrop-scale observations.

The McIntyre mine and neighbouring Hollinger mine are located in a thick pile of volcanic rocks of the Vipond and Central formations (Ferguson, 1968, Brisbin, 1997). The volcanic rocks observed at the surface are characterized by submarine type deposition and have pillow and fragmental facies. The McIntyre property near the Goldale shaft shows great exposure of strongly altered volcanoclastic material (Fig. 6.1) that is rusty coloured due to an intense iron carbonate alteration. The rock contains plastically deformed amoeboid clast (1-10cm) from tuff to breccia size. The plastic deformation shows that the material was deposited hot possibly due to pyroclastic deposition, though autoclastic deposition can not be ruled out. Indeed Scott et al. (2003) have shown that similar rocks to the East in Harker Twp. were pyroclastically emplaced likely the result of submarine dome collapse. Nonetheless there is strong evidence at the Goldale shaft exposure that fluids migrated through the primary porosity, leaving an intense carbonate alteration suggesting a possibility for disseminated gold grade in this outcrop, its extension, or equivalent facies elsewhere in the region.

Another type of flow has been investigated in the area, more particularly the Vipond Formation V10b flows (Dinel et al., under revision; see below). The V10b flows are dacitic in composition and the facies observed were classified as pillow-lobes. In the following section we discuss the facies variations associated to the V10b flow at the outcrop scale, geochemistry and detailed petrography, and relate it to a possible loci for mineralization. The following paper: "**Spherulitic aphyric pillow-lobe meta-dacite lava of the Timmins area, Ontario, Canada: A new Archean facies and its implications for lode-gold mineralization**" by Dinel E., Saumur B-M and Fowler A.D. characterizes the V10b unit, and possibility to host a disseminated style of gold mineralization. The V10b flow or other fragmental flows in the area have potential for disseminated mineralization.

6.3 Spherulitic aphyric pillow-lobe meta-dacite lava of the Timmins area, Ontario, Canada: A new Archean facies and its implications for lode-gold mineralization

E.Dinel, B.-M. Saumur, and A.D. Fowler, Department of Earth Sciences, University of Ottawa, 140 Louis Pasteur, Ottawa, K1N 6N5 & Ottawa Carleton Geoscience Centre.

Abstract

In addition to a first-order structural control on the Porcupine camp gold deposits, exerted by the Porcupine Destor Deformation Zone, many of the deposits also have host-rock controls. Numerous veins are spatially associated and emplaced at contacts between lava flows of the tholeiitic rocks of the Tisdale Assemblage. In addition fragmental rocks of the V10 units of the Tisdale's Vipond formation hosted significant Au mineralization. These rocks have been previously misidentified as pillow basalts and are shown to be tholeiitic dacite in composition. Specifically the V10b is mapped as a pillow-lobe dacite. Aside from being more geochemically evolved in terms of their immobile trace elements these rocks differ from typical pillow basalts in that they has more abundant primary breccia and hyaloclastite, the pillow-lobes are misshapen, having been folded in a plastic state, and are zoned, typically having a spherulite-rich core. Moreover, the flows are aphyric, interpreted to mean that they were erupted in a superheated state. This along with their pillow-lobe nature demonstrates that at eruption they were low-viscosity melts for such silicic compositions. Interaction with water quenched the outer pillow-lobe and contributed to the formation of the abundant breccia. The fact that the melt was crystal and microlite free inhibited crystal growth such that the bulk of the lobes were quenched to crystal-free glass. Nucleation occurred only in the cores, where cooling rates were lower in comparison to the medial and exterior areas of the pillow-lobes, though here crystal growth rates were high so that abundant spherulite formation took place. The flows are exposed over a strike-length of more than 10km and are interpreted to be continuous and to have resulted from fissure eruptions. The resulting porous, permeable, high Fe/Mg ratio, high surface area glassy rocks would have been ideal for channeling and reacting with hydrothermal gold-bearing solutions. Reports on most other Archean

subaqueous felsic lobes document that the lavas were phyric and that spherulites formed near the external lobe margin, hence the zoning of the V10b pillow-lobes are different, suggesting that they constitute a new Archean facies formed from superheated melts.

Introduction

The Abitibi Sub-Province of the Superior Province of the Canadian Shield is a greenstone belt of late Archean age, elongated E-W, that extends over 700km from the Kapuskasing uplift in Ontario eastward into Québec where it is truncated by the younger high-grade rocks of the late Proterozoic Grenville Province. To the north it is bounded by granitic rocks of the Opatica Sub-Province and to the south the Pontiac Sub-Province.

Mines in the Timmins area of the Abitibi Subprovince of Ontario have been prolific gold producers, and continue to be so. The bulk of the mineralization is contained within mafic meta-volcanic rocks. Mineralization within them is primarily contained within the Tisdale Assemblage, an approximately 3km thick tholeiitic suite of 2710-2704 Ma rocks (Ayer et al. 2005) predominantly consisting of meta-basalts with intercalated meta-komatiites toward its base and intermediate/felsic rocks toward its top. There is an important structural control associated with the mineralization: much of the ore is situated in quartz-carbonate shear and extension veins in close proximity and structurally related to the Porcupine-Destor Deformation Zone (PDDZ), an extensive corridor of intense deformation, and its second order parallel shear zones.

Examination of the literature shows that there is also an intrinsic permeability control on the mineralization. For instance Brisbin (1997) wrote "Most of the large, prolific veins at the McIntyre Mine occur along flow contacts marked by carbonaceous argillite and/or hyalobreccia" and more generally "The common factor in the geological controls on gold mineralization discussed above is the affinity of hydrothermal fluids for rocks with high permeability. Vein, replacement ores and hydrothermal alteration are localized in areas of high permeability such as flow tops [...]". Ferguson et al. (1968) reported "[...] mineralization at least in part is related to flow contacts." and Dunbar (1948) wrote, "The ore favors the upper part of the Tisdale group (now Tisdale Assemblage), which has a

fragmental character." Examination of geological maps and mine locations demonstrates that the bulk of the mineralization is stratigraphically located in the Hershey Lake, Central and Vipond formations. The Hollinger-McIntyre and Dome system is located in volcanic rocks of the Vipond and Central formation (see geological map in Ferguson, 1968). Accordingly the aim of this paper is to investigate the concept of host rock control.

Moreover, here we report on pillow-lobe felsic meta-lavas of the Vipond Formation of the Tisdale Assemblage, specifically the V10b unit which is a distinctive marker horizon in the Timmins camp (e.g. Ferguson, 1968) and was well mineralized. Because the rocks are well preserved we dispense with use of the prefix "meta" from hereon. The V10b is part of a series of similar units that were collectively termed the V10 "Member" by Brisbin (1997). The unit has been variously identified as a dacite or andesite flow (e.g. Ferguson, 1968), "chicken-feed" (e.g. Brisbin, 1997), and pillow basalt (Pyke, 1982). We believe that the term "chicken-feed" does not refer to the economic significance of the formation! Indeed, the earliest reference we can find for the term (Graton et al., 1933) makes it clear that chicken-feed is a local name applied to "[...] granulated glassy material filling spaces between the pillows and are more rarely found within the pillows themselves" in other words hyaloclastite. Elsewhere the chicken-feed has been described as consisting of broken spherulites or varioles (Ferguson, 1968; Brisbin, 1997) and described by Griffis (1968) as consisting of "[...] brecciated spherules and angular porcelainic fragments or shards."

The McIntyre Mine geologists (Griffis, 1962) divided the V10 into the V10a,b,c and d, whereas at Dome Mine (Ferguson, 1968) they are loosely correlated with what are termed the Andesite, Upper Andesite and Dacite flows (V10b & V10c), these rock names being to some extent a hold-over from the early days of the mining camp. Rocks of andesitic and dacitic composition were also reported at the Hollinger mine. Indeed, Graton et al. (1933, p.3) stated that "The flows [...] are mainly of intermediate composition, ranging from albite-dacite toward andesite [...] None of the flows on the Hollinger property is basic enough to be properly called basalt." Today, through the use

of modern geochemical analyses it is evident that most of the volcanic rocks of the region are mafic and likely followed in order of abundance by lavas of ultramafic and then intermediate to felsic compositions.

We have focused on the V10b unit because it held significant mineralization and it is well exposed on surface – unfortunately access to the former underground workings at the Dome, McIntyre, Hollinger and other nearby mines is no longer possible. Accordingly our approach has been to seek out the freshest best-preserved outcrops of the V10b in order to document its volcanological features without the added complications of post emplacement strain, mineralization and alteration. We document the physical volcanology, petrography and geochemistry of these rocks and demonstrate that they are similar in appearance to pillow basalts, and how the two can be distinguished. We conjecture they are likely restricted to the Archean and speculate on their suitability as hosts for hydrothermal gold mineralization.

Review: Pillows vs. Lobes and Varioles vs. Spherulites

For clarity, we briefly review a few terms important for the work. The distinction between subaqueously formed pillow lavas and lava lobes is not sharp, for instance McPhie et al. (1993) commonly use the term "pillow lobes" (e.g. pages 58 & 59). Lava lobes (e.g. Ayres and Peloquin, 2000; De Rosen-Spence et al., 1980) are typically large-scale lenticular features with pointed terminations. De Rosen-Spence et al. (1985) describe them as "[...] folded sheets, 1-10m thick, and 10-500m long." They also describe pods as ellipsoid masses 10-100 m across, and tongues as finger-shaped masses 0.5 to 10m long, though these terms are not commonly used. Lobes are often found associated with domes and typically crop out as isolated elements within abundant surrounding hyaloclastite. Lobes are closed structures, have a distinctive zoning, (described below) and grade into hyaloclastite (McPhie et al., 1993) into which they are sometimes intrusive.

Compositionally, pillows are generally thought to be restricted to mafic systems though they have been described from felsic rocks (e.g. Bevins and Roach, 1978) and others

considered that the rhyolite lobes they mapped were essentially pillows formed at the flow front during advancement (Dimroth et al., 1979; De Rosen-Spence et al., 1980). Typically pillows (of basaltic systems) form clusters of m-scale entities that are individually molded such that the convex geometry of one pillow's side is reflected as a concave side in its immediately adjacent neighbor. They are coherent, have a distinctive cooling margin and may be zoned with respect to vesicle distributions (McPhie et al., 1993), or crystal habit (e.g. Fowler et al., 1986). In addition their surfaces may have wrinkles, corrugations, contraction or spreading cracks (McPhie et al., 1993) and more rarely they may have multiple rinds (Kawachi and Pringle, 1988). Typically, at least in ancient environments, they are associated with the distal portions of massive flows (e.g. Dimroth et al., 1978). Hyaloclastite is preserved but is far less abundant than in felsic systems. Pillows may be intrusive into unconsolidated sediment in which case they are associated with pepperite. The bulbous forms of the V10b unit that we describe contain elements of both lobes and pillows and accordingly we use the term pillow-lobes.

The term variole should refer to a cm-sized leucocratic globule within a fine-grained mafic igneous rock (see Lofgren, 1974 or Fowler et al., 1986 for details). As such it is a useful, general, descriptive, and "non-genetic field term" particularly for altered rocks. Detailed work is often necessary to characterize varioles further, for instance experience in the study of Archean basalts show they may prove to be amygdules, blotchy alteration, lapilli, spherulites, etc. Spherulites are fibrous branching mineral growths that commonly, but not necessarily, have a spherical geometry. The crystallographic orientation of each fiber within the ensemble is different from that of its neighbors; hence the branching is termed "non-crystallographic". Within Archean basalts spherulites are typically composed of plagioclase and less commonly clinopyroxene. Once a detailed textural determination has been made the field-term variole should be discarded. Varioles of Archean basalts were thought to be quenched immiscible droplets (e.g. Gélinas et al., 1976) however most commonly they are plagioclase spherulites (Fowler et *al.*, 1986). Although the term variolitic basalt is entrenched for Archean basalts that are clearly spherulitic, it makes no sense to apply the term spherulite to felsic rocks and a different term for the identical texture in mafic rocks. We have retained the word variole in this

text, chiefly when quoting or reporting on the work of others, though for the most part, the textures have been proven to be spherulitic.

Methodology

The mapping and sampling of the fire-tower outcrops in Timmins, were completed during the summer of 2004, and additional samples from other V10b outcrops were collected during June 2005. The samples were cut, crushed and powdered for analysis and polished thin sections at the University of Ottawa. The samples were crushed, to a size less than ~1cm using a steel plate Jaw Crusher and pulverized to a very fine powder using a porcelain shatter box. The powders were placed into platinum crucibles and fused into disks composed of 1g of sample mixed with 4g of flux, which consist of 78.53% lithium tetraborate ($Li_2B_4O_7$) and 21.47% lithium metaborate fused.

The major oxides were analysed by X-ray fluorescence at the University of Ottawa, using a Philips 2400 spectrometer controlled by the software XRF SuperQ. The method used for determination of iron (XRF) did not discriminate the Fe^{2+} and Fe^{3+}. However, ferrous iron was determined by the modified Wilson (1960) technique (Whipple 1974) and was completed at the Ontario Geoscience Laboratory in Sudbury. The trace elements were analyzed by means of an Inductively Coupled Plasma Mass Spectrometer (ICP-MS) at the Ontario Geoscience Laboratories in 2004. The samples collected in 2005 were analyzed at the SGS laboratory in Toronto.

In addition, a geochemical database of the Vipond formation was provided by Porcupine Joint Venture (PJV), now Goldcorp inc. Their samples (55), collected in 2001 were analysed for major oxides and traces elements by ALS Chemex laboratories. Details on the analytical techniques are contained in Saumur (2005) and Dinel (2007, see chapter 2).

Geology of the Tisdale Assemblage

The Tisdale Assemblage was subdivided into five formations, by Ferguson (1968), Dunbar (1948) and Jones (1948). The majority of the gold deposits of the Timmins area are contained within it, particularly the Vipond Formation (Brisbin 1997). It is characterized by very distinctive high-Fe tholeiitic spherulitic pillowed mafic volcanic flows, and variolitic hyaloclastic mafic flows which are intercalated with massive mafic flows and carbonaceous argillite. In addition, certain units within the Vipond serve as marker horizons within the Timmins camp notably, the V8 and V10b. The V8 is variable in terms of its thickness (e.g. Ferguson, 1968) and overall it has a striking appearance characterized by large meter sized elongated basalt pillows with thick zones (10-15cm) of hyaloclastite. The pillows are spherulitic with spherulites typically being concentrated in a ~20cm band just within the pillow margins.

Brisbin (1997) described the V10a (at McIntyre) as a fine-grained massive flow that is 12 to 35m thick and is locally underlain and overlain by carbonaceous interflow sediments. At Dome Mine the unit is termed the Andesite flow. Overlying this is the V10b (at McIntyre) described as a 20 to 40m thick unit with a distinctive chicken-feed texture, which at Dome Mine formed the upper portion of the Andesite flow. The V10c (at McIntyre) is a massive flow identical to the V10a approximately 5 to 20 m thick and correlative with the base of the Dacite flow at the Dome mine. The V10d has the same texture as the V10b and is known as the upper portion of the Dacite flow at Dome mine, where in addition to having chicken-feed texture; it has also been described as having a "ropey flow top". It appears (Holmes, 1968 (in Ferguson, 1968); Brisbin, 1997) that at the Dome Mine the Dacite flow comprises two facies of the same lava and that the Andesite flow is composed of "several flows, which lens out along strike" (Holmes, 1968 (in Ferguson, 1968)). At Hollinger the V10a and b were apparent but neither the V10c nor the V10d were recognized (Jones 1968, in Ferguson, 1968).

It is not possible to ascertain the details of the gold mineralization within the V10 units as there is no longer access to the underground workings mines, and detailed descriptions do not exist. However, Brisbin (1997) reviewed the distribution of ore in the various mines

having rocks of the V10 "Member". The V10a hosted the most important ore-bodies at the Vipond Mine whereas portions of the 92, 93 and 44 veins at Hollinger were hosted in V10a and V10b. Furthermore, the "Dacite Ore" at Dome Mine was hosted in all four of the V10 units. Typically gold mineralization is found associated with quartz-ankerite fault-fill and extensional veins that are distributed along structures or flow contacts. Hurst 1935, Graton et al. (1933) Brisbin (1997) and Ferguson (1968) all described ore either being distributed at flow contacts or in veins parallel to flow contacts. In addition, Hurst (1935) described significant gold mineralization in "pyritic orebodies" within the mines of the camp. These ore bodies have irregular geometry and disseminated mineralization associated with pyritization of the host rock. He observed a chemical control over this and the vein mineralization: "[...] the chemical composition of the wall rock, through its control over the formation of pyrite is an important factor in determining the locus of gold deposition."

Geology of the V10b unit

We inspected and sampled numerous outcrops of the "chicken-feed" V10b in and around Timmins that appear on the map of Ferguson (1968) over a strike length of more than 10 km (Fig. 6.1). The Fire-tower outcrops, where the primary features of the V10b unit are best exposed and preserved, are situated within 200m of the former Vipond Mine shaft that was part of the McIntyre system. We enlarged the area of exposure and cleaned the outcrops in 2003, and mapped them in detail in July 2004. The area is composed of three hummocky exposures that afford three-dimensional observation of the rocks. Although the rocks are strained their original textures are still well preserved. They were subjected to a penetrative deformation that produced a nearly vertical stretching lineation. The mineralogy is dominantly composed of chlorite, albite and carbonate (calcite and ankerite) typical of the low degree of metamorphism in the area.

As can be seen from the map (Fig. 6.2) and wide-angle photo (Photo 6.4), the outcrop is dominated by amoeboid shaped pillow-lobes with an abundance of intervening breccia. The pillow-lobes are in general m-scale, ranging in size from 10 cm to 4m, and weather to a pale green (chlorite) to buff (ankerite) or white (albite) color. Many of the pillow-

lobes are characterized by a highly contorted and folded geometry and some have the appearance of having been necked. The folding pattern is not consistent over the outcrop and does not coincide with regional pattern, and the foliation observed is not axial-planar to these folds it is related later regional-scale deformation. The Pillow-lobe geometry is therefore interpreted to be primary and formed as a result of plastic deformation during effusion.

V10b pillow-lobes can be classified into three types depending upon their internal components and size. However, all pillow-lobes are surrounded by massive 5 cm thick dark green colored margins composed of extremely fine-grained altered glass dominated by chlorite and carbonate (Photo 6.5). Margins are aphyric and there is a lack of primary porosity. In addition they have a "crumbled" look suggestive of *in-situ* primary brecciation related to shearing during flow. Like other pillow-lobe components, the margins have been complexly deformed while still plastic.

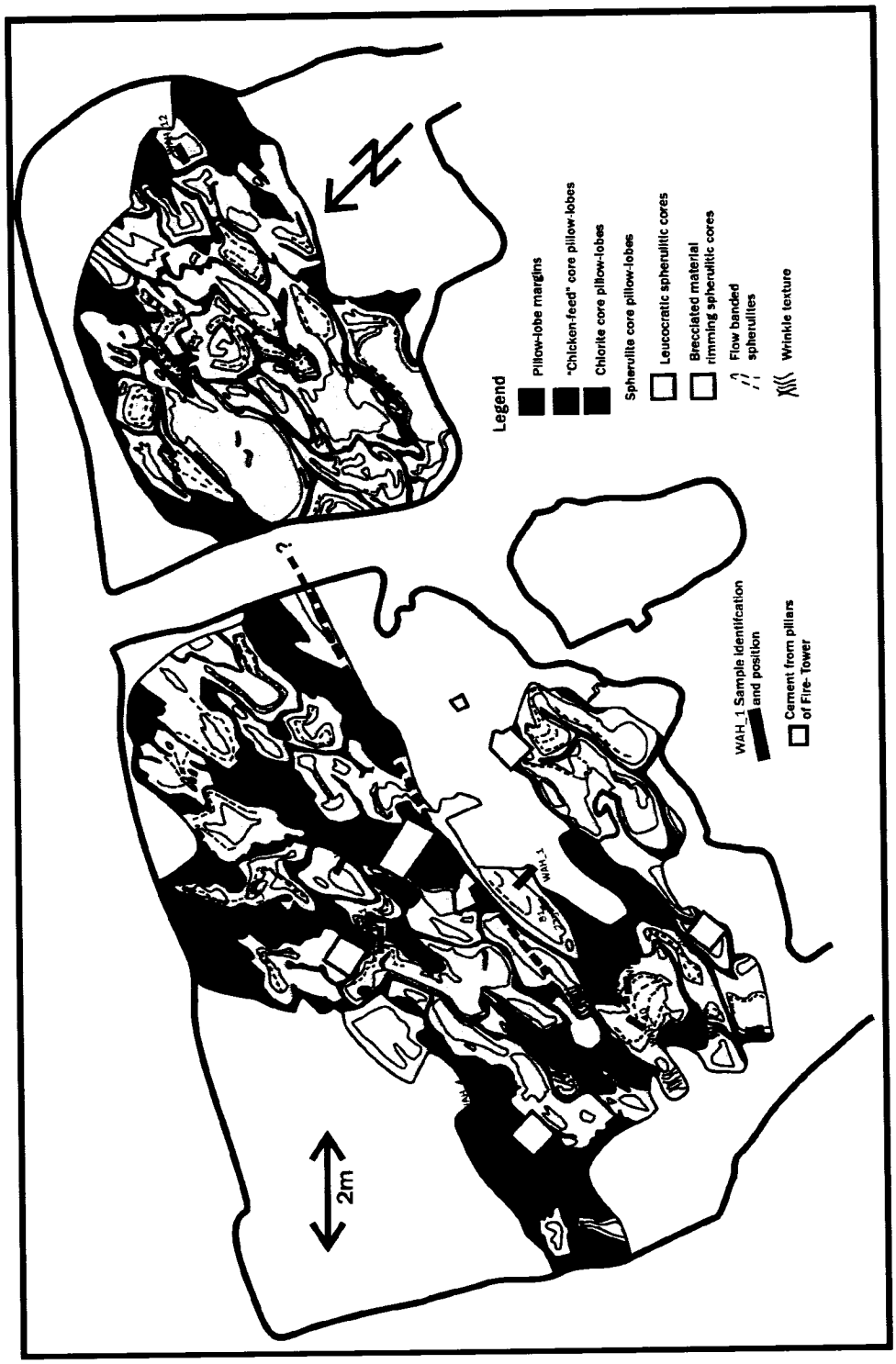

Figure 6.2 Map of the Fire-tower outcrops (after Saumur, 2005).

Photo 6.4 Wide-angle photo of a portion of the Fire-tower outcrops, field of view is ~3m

Photo 6.5 Image of large pillow-lobe (spherulite core) showing fine grained margin and breccia zone, field of view is ~1m

"Spherulite-core" pillow-lobes

In the largest pillow-lobes (≥1m), the margin gives way to a breccia zone of variable thickness (10 to 50cm) consisting of mm-scale brecciated homogeneous or flow-banded aphyric chloritized and ankeritized glass. The fragments are blocky and angular with sharp boundaries and rotated clasts. In some places jig-saw fit breccias (Photo 6.6) can be observed. Perlitic fractures (Photo 6.7) are evident in some clasts. Pore spaces between the clasts are filled with quartz, albite and carbonate minerals. Chloritized breccia appears massive on weathered surfaces, whereas ankeritized material shows a distinct mottled porous texture where clasts appear brownish white because of carbonate dissolution. The latter is the material that was named chicken-feed by Graton et al. (1933), Griffis (1968), Ferguson (1968) and Brisbin (1997). Flow banding defined by varioles (spherulites) is commonly observed in the brecciated zones and shows complex flow history and rotation (Photo 6.8). Also, a wrinkled or "ropey" structure is evident on some of the thinner extremities of the more contorted pillow-lobes (Photo 6.9).

Photo 6.6 Image of "chicken-feed" from pillow breccia zone, coin is ~1cm in diameter

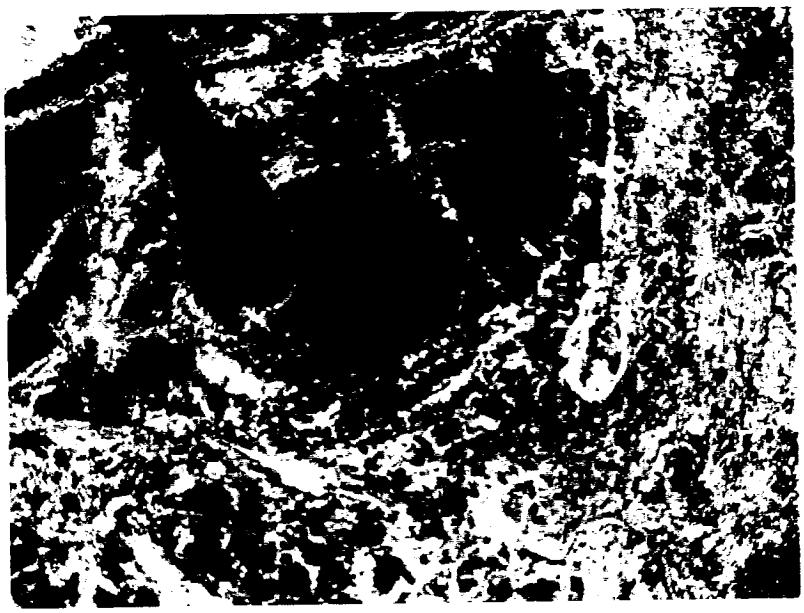

Photo 6.7 Image of perlitic fracture, field of view is 5mm

Photo 6.8 Flow banding in spherulite pillow-lobe core, field of view is 1.5m

Photo 6.9 Image of ropy wrinkles having a slight curvature associated with the pervasive foliation that is sub axial-planar to the curvature. However, the texture is primary, though deformed, coin is ~1cm in diameter

The cores of these large pillow-lobes are of variable size (50cm to 4m) and composed of altered aphyric glass containing abundant spherulites. The spherulites weather to a white color and form mm-scale positive relief mounds. In places, generally toward the centre of a particular pillow, the spherulites have coalesced and form cm to dm-scale white weathering amoeboid patches of rock (Photo 6.5). The spherulites are composed of fine radiating fibers of plagioclase in a matrix of chloritized altered glass. Rarely, they have nucleated on the margins of gas bubbles (Photo 6.10). The cores of the pillows are evidently less brecciated and altered and therefore were likely less permeable than their exteriors. Flow banding can commonly be traced within spherulitic cores. Figure 6.3 illustrates an idealized spherulitic core pillow-lobe.

"Breccia-core" pillow-lobes: Chlorite-core and Ankerite (chickenfeed) core

Smaller pillow-lobes do not have the full range of facies observed in the larger ones. Pillow-lobes ranging from 40cm to 1m in size lack a spherulitic core and have chlorite breccia identical to that of the breccia zone of spherulitic pillow-lobes. There is usually a zone of ankerite rich "chicken-feed" surrounding these chloritic cores. The outer chicken-feed zone has more primary porosity than the chlorite breccia in the cores. Chlorite-core pillows commonly contain flow-banding defined by spherulites. Hence a distinction is made between spherulites concentrated in pillow-lobe cores and spherulites defining flow banding. Only the largest of these pillow-lobes are contorted in a similar fashion to those having spherulite-cores.

The smallest pillow-lobes are typically decimeter scale brownish pods completely filled with "chicken-feed", and it is in these pillow-lobes that this texture is best developed as mm to cm scale void spaces related to primary brecciation (Photo 6.11). The perimeter walls of the void spaces are quasi-planar, stand out in relief, and meet at well-defined corners. However, the carbonate within the voids is recessively weathered forming conspicuous hemi-spherical pits giving the illusion that the texture is composed of broken spherical fragments (i.e. spherulites).

Both these pillow-lobe types are similar in the sense that they are both almost entirely composed of breccia, are smaller than, and not as deformed as, spherulite-core type. We interpret both pillow-lobe types as having had the same primary volcanic origin but alteration played a major role in determining their appearance on weathered surfaces. Penetrative chloritization is associated with regional metamorphism (Thompson, 2005), whereas ankeritization overprints it (Photo 6.12). The ankeritization is later and related to hydrothermal fluids and was evidently dependent on permeability as only the smallest of pillow lobes are completely ankeritized.

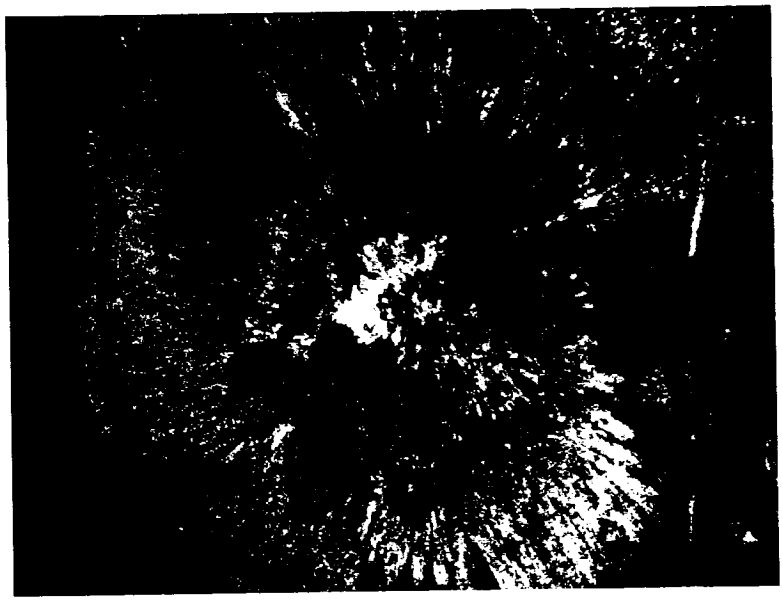

Photo 6.10 Spherulite surrounding calcite interpreted to be an amygdule, field of view = 2mm

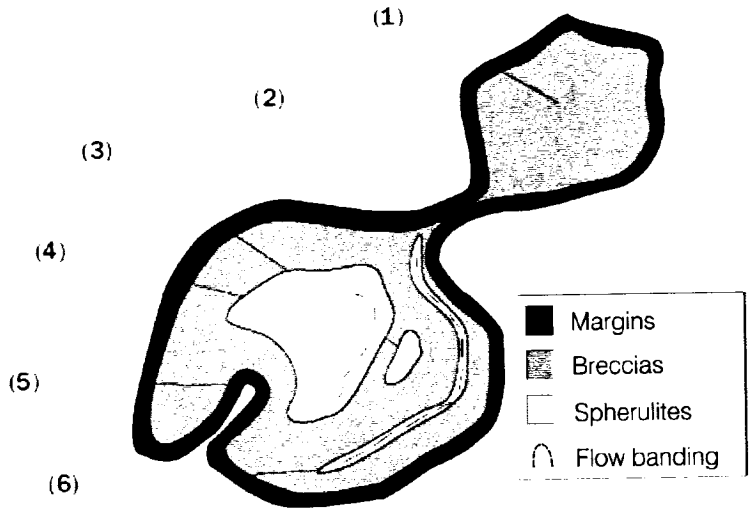

Figure 6.3 Sketch of an idealized m-scale pillow-lobe. 1) Pillow-lobe containing no spherulites. breccia may have a "chicken-feed" appearance. 2) Example of complex primary contortion and connection between two breccia zones as defined by margins (necking). 3) Observation of more than one spherulite-rich area in a pillow-lobe is common. 4) The boundary between spherulitic cores and breccia is generally diffuse: the spherulites are discrete at the core's edge and coalesced at the core's interior; and spherulite – defined flow banding is common. 5) Margins are generally severely contorted and can be in-folded 6) There is commonly flow banding in the brecciated material defined by spherulites

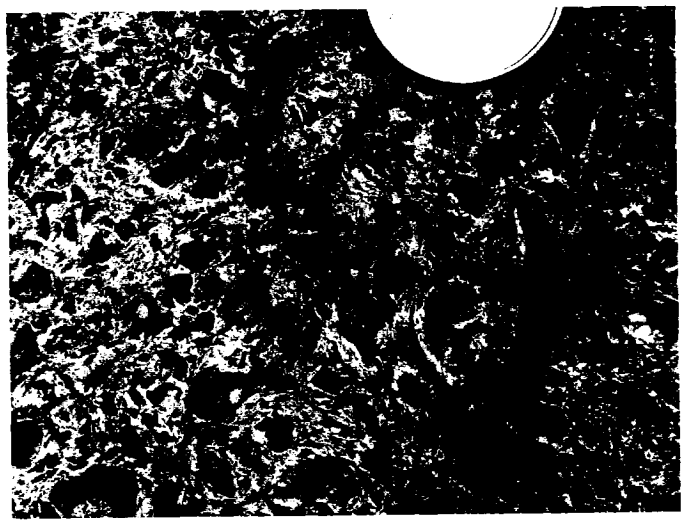

Photo 6.11 Image of chicken-feed on weathered surface, coin is 2.5cm in diameter

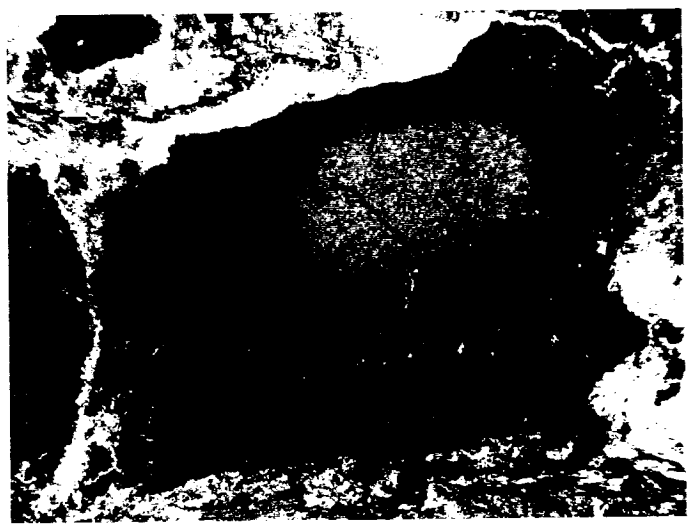

Photo 6.12 Chloritized chicken-feed clast partially replaced by ankerite, field of view = 4mm

Geochemistry of the V10b unit

Rocks of the Vipond formation are tholeiitic in composition (Brisbin, 1997) and are characterized by flat REE chondritic normalized patterns. Below we compare our samples of the V10b unit to those of the Vipond formation geochemical database provided by the Porcupine Joint Venture in order to classify the rocks. Geochemical data, sample locations and sample descriptions of the V10b specimens collected by us are given in Table 1.

Although slight LREE mobility is not uncommon REE are generally considered reliable indicators of the protolith of volcanic rocks within the Abitibi (e.g. Kerrich and Xie, 2002; Ropchan et al., 2002; Dinel et al., accepted by guest editor, see chapter 4; MacLean, 1988; MacLean and Kranidiotis, 1987). Exceptions are rocks that have been subjected to amphibolite facies, or higher metamorphism, or those that have been altered by hydrothermal fluids having a high activity of Cl^- (e.g. McCuaig and Kerrich, 1998). REE abundances have been used to determine the protolith of moderately altered rocks within the Abitibi at VMS deposits (e.g. Gibson et al. 2000) and gold deposits, (e.g. Dinel at al. (accepted by guest editor, see chapter 4), Ropchan et al.2002). MacLean 1991 has demonstrated that Ti, Al, Zr and Y are generally immobile in the volcanic rocks of VMS deposits of the area, of course these elements may also be solubilized. Indeed Hynes (1980) has demonstrated their mobility in response to carbonatization of basalts. The majority of rocks in the Timmins area are lower greenschist facies (Thompson, 2005) and the fluids associated with Archean lode gold systems do not have a high activity of Cl^-, hence we expect the REE and other "immobile" elements and oxides (Ti, Al_2O_3, Zr, Y) to be reliable indicators of lithogeochemistry. Indeed our work on mobility of elements in Tisdale assemblage rocks at the nearby Hoyle Pond mine shows that this is indeed the case (Dinel et al., accepted by guest editor, see chapter 4). There it was demonstrated that REE, Al_2O_3, Zr, TiO_2 and Y were relatively immobile with respect to alteration and can be used to identify rock type whereas, K_2O, Na_2O, Cr, Rb, CO_2, CaO, Eu, FeO, MgO and to a minor extent the LREE, were mobile. Table 1 contains the geochemical data. For completeness we present all the data we accumulated although certain data, for instance

the concentrations of alkalis and silica, are not used by us because they are notoriously mobile.

	BMS 1 Firetower 5367897N 0477565E	**BMS 2** Firetower 5367897N 0477565E	**BMS 3** Firetower 5367897N 0477565E	**BMS 4** Firetower 5367897N 0477565E	**BMS 5** Vipond Rd. 5368037N 0476983E	**AF0508** Hwy. 101 5369345N 0479066E	**AF0512A** Powerline 5367700N 0477820E	**AF0512B** Powerline 5367700N 0477820E	**AF0514** Powerline 5367665N 0478630E
Sample description	Spherulitic core of lobe	massive facies of lobe	chill margin of lobe, hyaloclastite breccia	"Chicken Feed" texture facies, highly ankeritized hyaloclastite breccia	Bulk sample	highly strained lobe and breccia in contact with the variolitic basaltic flow	lobe and breccia facies, showing margin to core transition	lobe and breccia facies, showing margin to core transition	highly strained lobe and breccia ("Chicken Feed") facies
Major element oxides (wt %)									
SiO_2	59.70	57.53	48.27	51.39	54.39	58.81	66.96	38.03	57.85
TiO_2	1.31	1.50	1.32	1.30	1.43	1.465	1.258	1.502	1.448
Al_2O_3	10.42	12.81	10.69	10.83	11.92	12.87	13.85	17.16	11.95
Fe_2O_3	1.76	1.77	3.11	2.23	2.97	11.787	7.463	21.46	13.173
FeO	4.67	10.81	17.91	12.46	13.00	-	-	-	-
MnO	0.22	0.17	0.31	0.32	0.26	0.174	0.069	0.242	0.198
MgO	1.15	2.31	3.67	2.51	3.14	2.08	2.4	6.56	1.76
CaO	6.84	3.42	5.07	7.46	3.93	3.96	0.71	4.46	3.81
Na_2O	3.81	3.89	0.19	2.11	2.41	4.4	2.69	0.31	4.85
K_2O	0.47	0.01	0.00	0.02	0.02	0.014	0.997	0.561	0.008
P_2O_5	0.46	0.51	0.47	0.46	0.51	0.52	0.11	0.14	0.52
S	0.01	0.10	0.02	0.03	0.05	-	-	-	-
CO_2	5.26	2.21	4.30	5.81	1.67	-	-	-	-
LOI	1.27	2.34	4.65	2.60	3.50	4.5	4.6	10.2	4.8
Total	97.35	99.38	99.97	99.52	99.18	100.58	101.107	100.625	100.367
Trace elements (ppm)									
Ba	158	22	24	39	89	29	464	368	25
Co	15	24	23	16	24	22	33	57	20
Cr	28	29	26	26	33	28	43	57	27
Cs	1.208	0.067	0.15	0.12	0.228	-	-	-	-
Ga	15	20	13	16	20	18	16	23	14
Hf	4.7	5.8	5	4.8	5.4	-	-	-	-
Nb	7.9	9.7	7.3	7.9	8.5	10	5	4	8
Ni	0	0	6	0	0	18	29	111	17
Pb	1	7	5	3	3	5	6	9	2
Rb	12.18	0.18	0.17	0.46	0.33	7	39	26	5
Sr	206.5	130.4	113.9	229.9	80.3	72	82	71	127
Ta	0.45	0.56	0.46	0.46	0.52	-	-	-	-
Th	0.78	1.14	0.78	0.76	0.88	8	7	9	8
U	0.228	0.467	0.232	0.223	0.257	2	3	4	2
V	31	41	45	34	41	38	278	391	42
Y	56.95	71.46	80.05	65.92	71.26	77.5	40.4	63.5	78.2
Zn	74	135	201	140	165.25	119	75	224	103
Zr	168.6	202.8	181.7	172.8	191.1	191	126	153	189
La	9.87	12.16	12.16	10.3	11.32	9.7	8.3	7.1	11.6
Ce	28.16	33.93	33.28	28.61	31.84	26.5	21.9	19.7	31.5
Pr	4.535	5.462	5.489	4.672	5.091	-	-	-	-
Nd	24.25	28.38	28.84	24.6	26.64	25.3	16.7	14.2	27.1
Sm	7.49	8.99	9.01	7.86	8.67	9.2	4.9	5	9.3
Eu	2.326	2.895	2.863	2.633	2.789	3.6	1.47	1.63	3.2
Gd	9.361	11.765	11.949	10.373	11.553	11.5	5.43	7.64	11.8
Tb	1.558	2.008	2.07	1.795	1.934	2.29	1.15	1.75	2.45
Dy	10.202	12.985	13.772	11.626	12.804	13.5	7.01	10.8	13.9
Ho	2.167	2.763	2.968	2.465	2.692	3.3	1.75	2.75	3.54
Er	6.525	8.312	8.93	7.367	8.004	9.39	5.01	7.86	9.6
Tm	0.942	1.208	1.306	1.084	1.197	1.44	0.77	1.19	1.54
Yb	6.19	7.99	8.7	7.23	7.88	8.4	4.6	7	8.8
Lu	0.932	1.194	1.328	1.102	1.199	1.46	0.82	1.2	1.58

Table 6.1 Geochemical data showing major oxides (weight %) and trace elements (ppm) with sample location given with respect Universal Trans Mercator grid NAD 27 and sample description and position in the lobe various facies

REE spectra of rocks of the tholeiitic suites of the Abitibi are typically flat, with basalts having approximately 10 to 30 times chondrites and rhyolites on the order of 100 to 400 times chondrites with slight negative Eu anomalies in the more evolved rocks (Fowler et al. 1989; Jackson et al. 1991; Hart, 2001; and Hart et al., 2004). In contrast rocks of the calc-alkaline suites typically have significant LREE enriched spectra and conspicuous negative Eu anomalies in their evolved rocks.

Data from the Vipond formation database show a wide range in REE spectra from 6 to 90 times chondrite (Fig. 6.4) with a gap between 35 and 45 times chondrites. The REE chondritic normalized plots of the V10b rocks (Fig. 6.5), are essentially "flat" with concentrations roughly 40 to 70 times chondrites and no conspicuous Eu anomalies. Most of our V10b samples plot above this gap (Fig 6.5) with the exception of two samples (sample AF0512A & B). These two samples were taken from an outcrop exposed along a power line approximately 250m south (down stratigraphy) of the fire-tower. Based on the flat REE spectra, we conclude that the V10b rocks are part of the tholeiitic suite and are intermediate in character. Because we are unaware of any specific classification scheme for the tholeiitic rocks of the area in terms of the REE, we use other elements to refine the classification before proposing a REE-based classification.

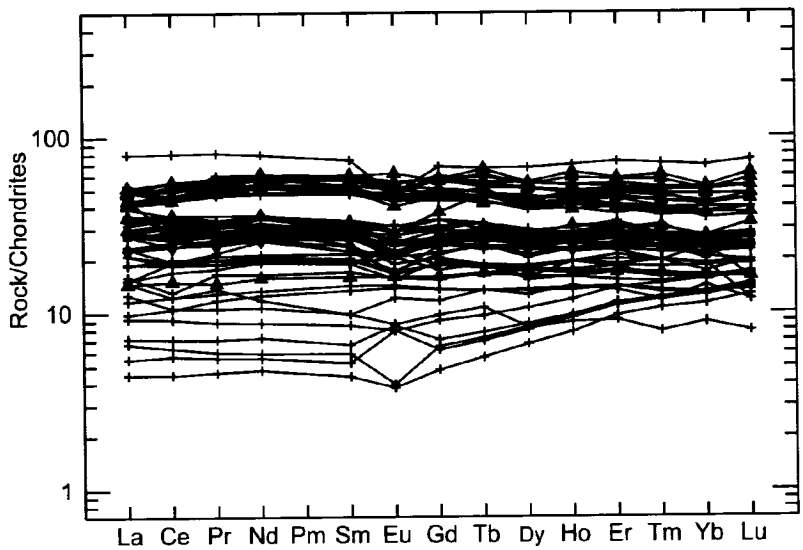

Figure 6.4 REE spectra of the Vipond Formation database, provided by the Porcupine Joint Venture. The chondrite meteorite abundance data of Sun and McDonough (1989) were used to normalize

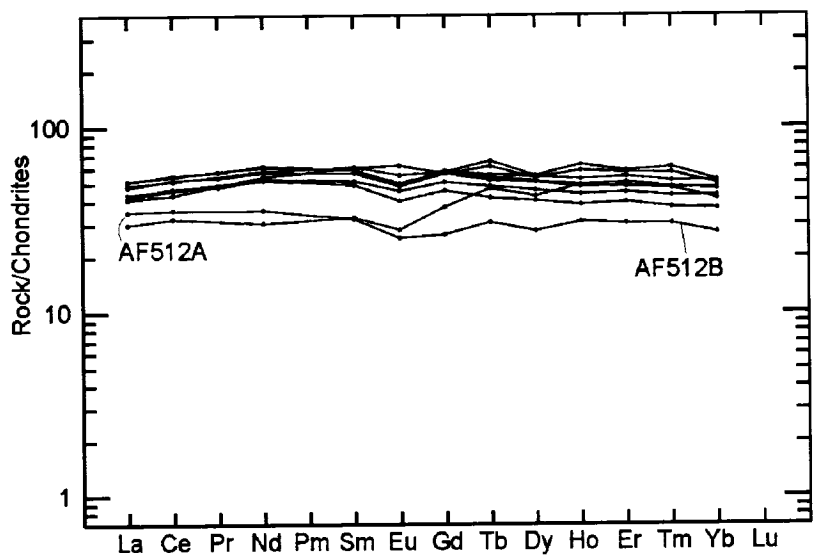

Figure 6.5 REE spectra of data from samples of the Fire-tower and other outcrops

We recognize the fact that a plethora of classification schemes exist for more modern volcanic rocks (e.g. Winchester and Floyd, 1977). However, there is no doubt that our rocks are altered hence we do not use schemes based upon mobile elements (e.g. alkalis or silica) Because one may argue that Archean volcanic rocks are not identical to their modern equivalents we believe it makes most sense to compare our rocks to nearby Archean equivalents. Accordingly we have used empirical diagrams designed by MacLean and his students (MacLean 1990, Maclean and Kranidiotis 1987) more specifically the work of Barrett et al. (1991) for similar rocks in the Abitibi from the Aldermach mine sequence Noranda. These rocks represent a suite from basalt to rhyolite, the REE spectra of which are almost flat. Although the rocks are considered "transitional" by the authors they state. "The relatively flat REE patterns indicate that the volcanic rocks are more closely related to tholeiitic than calc-alkaline magmas". Indeed their REE spectra of rhyodacite and rhyolite are approximately 60-100 times chondrites essentially flat and very similar to those of the V10b (see below). Unlike the V10b rocks the Aldermach rocks have more pronounced negative Eu anomalies possibly due to differences in igneous fractionation, though Eu unlike the other REE is fairly easily mobilized during alteration (e.g. Fowler & Doig 1983). Thus we deduce, based upon the comparison with the REE of the Aldermach rocks that the V10 B rocks are evolved and possibly dacite in composition with the exception of the samples AF0512 that appear to be less evolved.

We test this classification further by using other plots of "immobile" elements Al, Ti and Zr as used by Barrett et al (1991). A plot of the Vipond formation volcanic rocks from the Porcupine Joint venture database in Y vs. Zr space (Fig. 6.6) shows a fractionation pattern consistent with that defined by Barrett et al. (1991) for the Aldermach rocks. In addition data from 80% of the V10b rocks we sampled plot within the dacitic field. Figure 6.7 shows the TiO_2 vs. Zr diagram of Barrett et al. (1991) and their modeled fractionation trend. Most of the samples of the Vipond formation plot in the andesite field, however, the V10b samples plot closer to the dacite field, again with the exception of samples AF0512 A&B. On Barrett et al.'s (1991) Al_2O_3 vs. Zr diagram (Fig. 6.8), the Vipond formation samples are concordant with their fractionation trend (Barrett et al.,

1991), and most of the V10b analyses plot in the dacite field, excepting samples AF0512 A & B. Although there is scatter in all of these diagrams particularly in figure 6.6 with respect to the differentiation trend the "immobile" elements REE, Ti, Zr ,Y and Al_2O_3 geochemical data are consistent with the V10b rocks being part of the tholeiitic suite. The data are also consistent with the field observations of flow banding, contorted geometry, abundant breccia and lobe zonation, thus demonstrating that the rocks are for the most part dacite in composition.

As stated, we are unaware of any discrimination diagram for Archean greenschist volcanic rock types of the tholeiitic suite using REE chondritic normalized plots having been published. Accordingly, we propose a REE chondritic normalized plot to discriminate the volcanic rock of the tholeiitic suite (Fig. 6.9). This was accomplished by correlating concentration fields of Zr, Al_2O_3, TiO_2, REE and Y of Barrett et al. (1991) and our data. The diagram effectively discriminates tholeiitic volcanic rocks that have undergone greenschist metamorphism in terms of rock type.

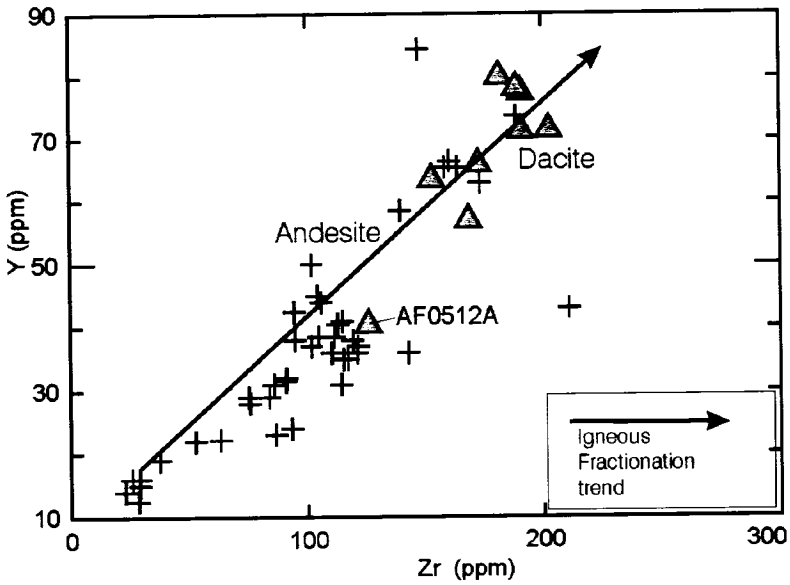

Figure 6.6 Y vs. Zr plot based on Barrett et al. (1991) The samples identified with triangles represent the V10b samples and the cross, the Vipond formation database

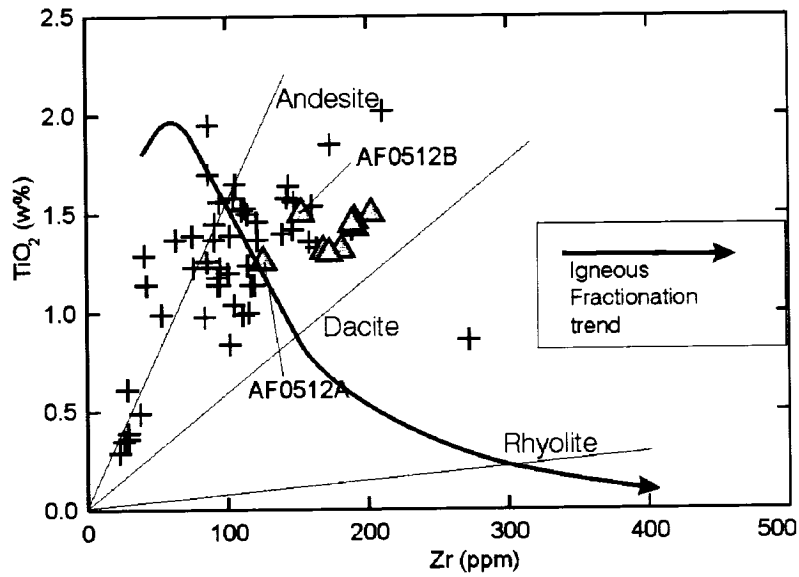

Figure 6.7 TiO_2 vs. Zr plot based on Barrett et al. (1991). The samples identified with triangles represent the V10b samples and the cross, the Vipond formation database

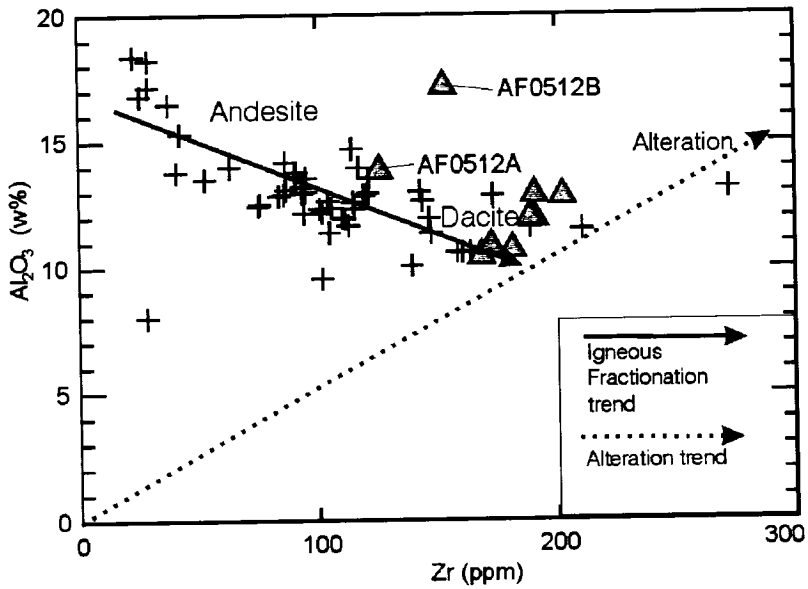

Figure 6.8 Al_2O_3 vs. Zr plot based on Barrett et al. (1991). The samples identified with triangles represent the V10b samples and the cross, the Vipond formation database

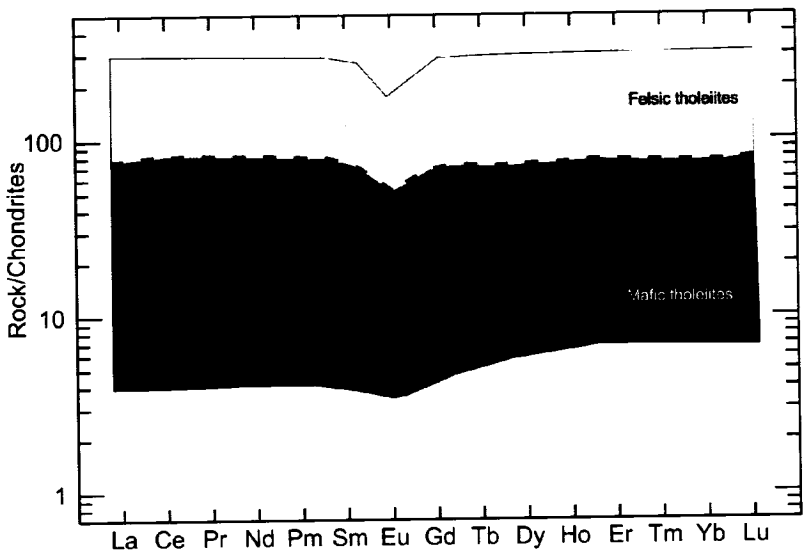

Figure 6.9 Proposed discrimination diagram for the tholeiitic suite of volcanic rock under greenschist metamorphism, based on the REE chondritic normalized fractionation pattern

Figure 6.10 is a Jensen plot (Jensen 1976) of whole-rock samples taken from the Fire-tower outcrop. This diagram is presented because of its widespread use on rocks in the Abitibi. The data span the range from high Fe-tholeiite through andesite to tholeiitic dacite. Significantly however, the data correlate with location in the pillow-lobes. The specimens with high iron content come from the ankerite-rich and porous peripheral areas of the pillows whereas the core, which is characterized by minimal porosity, is represented by the dacite composition. Thus we interpret the high-Fe data points as being an artifact of alteration (ankeritization). On figure 6.11, we show the correlation between Fe_2O_3 (total wt%) vs. TiO_2. One expects an igneous fractionation trend of a tholeiitic suite to be similar to that depicted by the solid line (i.e. Fe_2O_3 correlates directly with TiO_2). However, because TiO_2 is relatively insoluble, alteration will have preferentially affected Fe_2O_3 (and of course FeO in silicates) and has perturbed the igneous trend. The V10b samples define a trend almost orthogonal to the igneous trend, which we interpret to be due to the mobility of Fe.

Samples BMS 3 and BMS 1 show significant departure from the expected igneous trend. Sample BMS-3 is enriched in Fe and was collected from the pillow-lobe margin where brecciation and alteration (ankerite and chlorite) is strongly developed in comparison to the pillow-lobe core where sample BMS-1 was taken. The sample pair AF0512 A & B have a similar relation to position in the pillow-lobe and alteration trend.
In summary the Jensen diagram is not a reliable rock discrimination tool for highly carbonatized and chloritized rock, though the diagram shows that the low-porosity lobe-cores that have relatively little space-filling carbonate are dacite in composition.

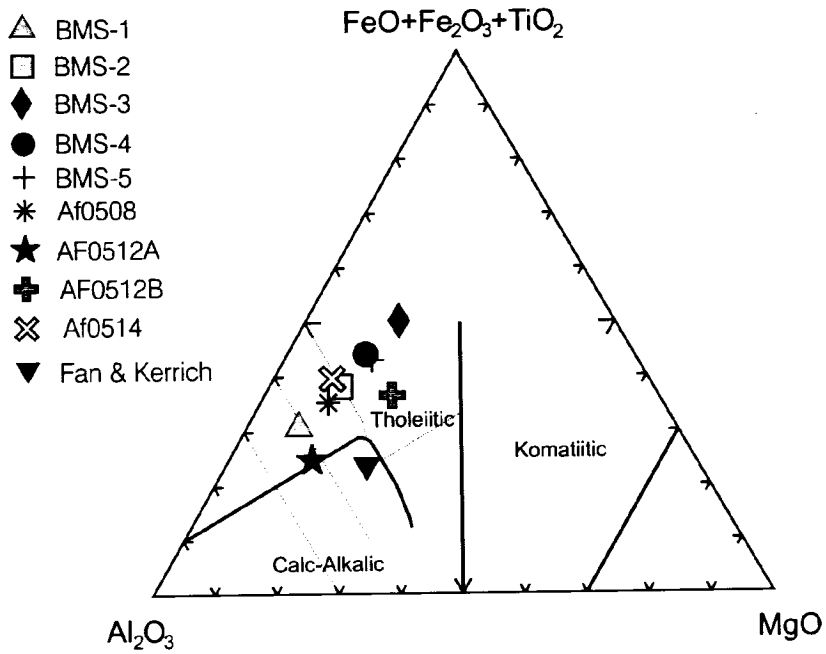

Figure 6.10 Jensen plot (Jensen 1976) of the data from samples of the Fire-tower and other outcrops

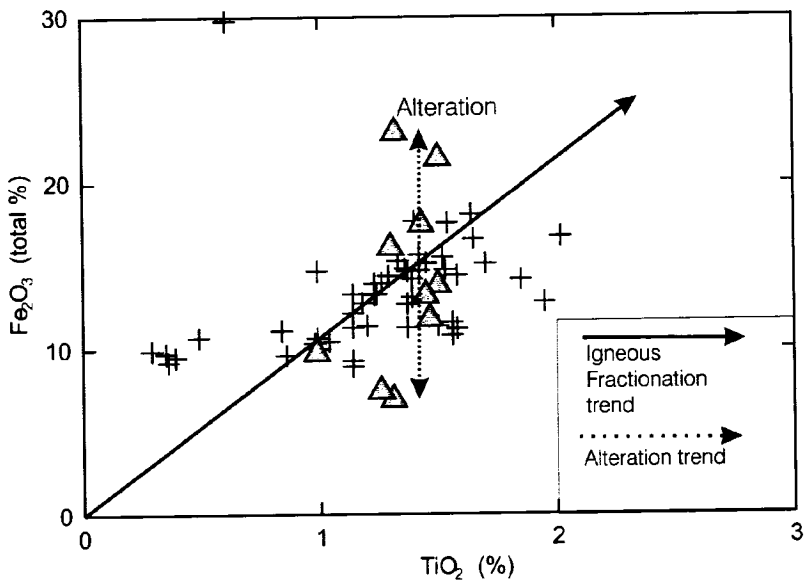

Figure 6.11 Fe_2O_3 total (w%) vs. TiO_2 plot showing their relationship in the tholeiitic suite. The samples identified with triangles represent the V10b samples and the cross, the Vipond formation database. Notice the Fe migration of some sample interpreted to represent alteration

Interpretation and Discussion

Subaqueous felsic flows have been documented by numerous authors (e.g. Cas, 1978; De Rosen-Spence *et al.*, 1980; Yamagishi and Dimroth, 1985; Kano et al., 1991; Scutter *et al.*, 1998; Waters and Binns, 1998; Ayers and Peloquin, 2000) some of whom describe pillow-like pods. For instance Bevins and Roach (1979) describe pillowed rhyodacite lavas from the Ordovician of Wales. They attribute the pillow formation to the fluid nature of the melt. The lavas contained less than 1% phenocrysts and may have been erupted on a relatively steep slope in deep water where ambient pressure would have prevented exsolution of the gas phase thereby reducing viscosity. Cas (1978) described "regionally extensive" vesicular and porphyritic dacite-andesite and rhyodacite units associated with "flysch-like" sedimentary rocks suggesting a deep-water environment of deposition. He attributed the large-scale coherent nature of the felsic flows to suppression of volatile exsolution in the deep marine environment and the concomitant reduction in melt viscosity. Scutter et al. (1998) described large (~25 km^2) submarine rhyolite flows from Ponza Italy that were emplaced over domes. They demonstrated that flow was favored where eruptive rates were high, topography steep, the cooling rate was slow and that the magma had relatively low viscosity. Manley and Fink (1987) studied sub-aerial rhyolite flows and documented an internal stratigraphy consisting of seven zones, and that the stratigraphy is quite variable. Typically the rhyolite flows have glassy margins and spherulitic cores. Kano et al. (1991) describe porphyritic rhyolites that were erupted into a sub-marine environment. These are composed of flow-banded and folded 1-15m large lobes, blocks and rhyolite breccias and are considered to be the equivalent of subaerial block lavas.

We are unaware of any previous detailed work on aphyric pillow-lobe dacitic lava facies in the Timmins area, and apparently little has been published on it elsewhere. De Rosen – Spence et al. (1980) described the various facies of rhyolite and dacite from the Quaternary of Iceland, and quartz and plagioclase phenocryst bearing rhyolite and dacite flows from the Archean of the Rouyn-Noranda area, Québec. In essence they described a core, rim, and border facies of m-scale lava pods, lobes and tongues characterized by increasing matrix crystallinity toward the core and brecciation toward the margin - the

overall architecture of the bodies being similar to young shallow endogenous cryptodomes (e.g. Goto & McPhie, 1998). Importantly their Archean rocks are described as having quartz and plagioclase phenocrysts and the lobes are characterized by an internal stratigraphy different from what we report here. They stated: "In most flows a gradation from microlitic to felsitic to spherulitic textures can be observed from the centre to the margin of the lava bodies, however, microlitic textures are present only in some of the larger lava pods and lobes." Interestingly, De Rosen – Spence et al. (1980) briefly described "unusual" spherulitic flows, however, they neither "studied the spherulitic flows in detail, because they are not very common", nor did they report the locations of the flows. We think that these "unusual" flows could be equivalent to those of this study. Péloquin et al. (1996) used the spherulitic nature and chemical composition of rhyolites in the Rouyn-Noranda area of Québec as a correlation tool with potential for VMS exploration.

In addition, Scott et al. (2001) document rocks that are similar to ours. The Héva Formation is a 25km long subaqueous spherulitic dacite lava flow in the Abitibi Greenstone Belt of Québec consisting of a massive facies, a medial lobe-hyaloclastite facies and an upper hyaloclastite facies. The flow is described as being aphanitic. They interpreted the flow to have formed in an extensional setting at elevated temperatures and discharge rates, and that the melt was of low viscosity due to high confining pressures, thus suppressing the liquidus temperature as a result of volatile solution.

Varolitic pillow basalts are ubiquitous in the region. The varioles are most prevalent as plagioclase spherulites in the Fe- rich basalts of tholeiitic suites and to a lesser extent as clinopyroxene spherulites in Mg-rich basalts. Typically the pillows are zoned with respect to their spherulite distribution. In general the spherulites are most conspicuous as cm-sized spheres within the outer 10 – 20 cm thick altered formerly glassy margin of the pillows.

Although superficially similar to basalt pillow-lavas (e.g. Pyke, 1982), we use the term pillow-lobe for the V10b rocks because there are significant morphological differences.

Although they are clustered m-scale objects and have the typical molded appearance of pillows and other features such as wrinkles and well defined margins, they are like lobes in that they have an abundance of hyaloclastite, are internally brecciated, flow-banded, and zoned in a manner different from mafic pillows.

Emplacement

We have not found exposures of the bounding facies, however previous work (described above) suggests that the four V10 units are a pair of couplets each composed of a massive (V10a & c) and chicken-feed (i.e. pillow-lobe dacitic flow V10b & d). We interpret the pillow-lobes to represent tubes and lobes formed during subaqueous flow with some brecciation and flow banding having been caused by movement during emplacement. Further brecciation was caused by thermally driven granulation. The massive flows were likely deposited first and then a transition to the pillow-lobe morphology ensued in a manner typically observed for Archean submarine basalts (e.g. Dimroth et al., 1978) possibly due to a change in slope or effusion rate or both. Given the sinuous outcrop pattern of the V10b rocks, which was likely more nearly linear pre-deformation, and that they crop out over a strike length greater than 10 km, we postulate that the lavas most likely emanated from a rift. Clearly we cannot trace the unit continuously, however it is known from previous underground work that the V10 units were continuous over distances of 100's of meters underground (e.g Ferguson, 1968). One could argue that the facies represent domes and lobes, however the outcrop pattern is not correct: the pillow-lobes are small, molded and clustered, without the zonation described by De Rosen Spence et al. (1980) and the massive unit apparently lacks brecciation or the zonation of shallow submarine cryptodomes (e.g. Stewart and McPhie, 2003; Goto and McPhie, 1998). Moreover, we have neither observed pepperites nor pyroclastic deposits in outcrops associated with this unit.

Development of Pillow-lobe zonation

Large pillow-lobes are characterized by a thin margin that gives way to a breccia zone and finally to a spherulitic core. We interpret the zones to be related to the thermal history of the melt. The contorted nature, banding and tortuous outline of many of the

pillow margins is evidence that the lava was viscous in comparison to basaltic melts, and that it most likely flowed down a reasonably steep gradient once it was erupted. It would appear that the lava cooled quickly below the glass transition, stiffened and was brecciated both by physical and thermal stresses associated with cooling by sea-water and movement.

Spherulites are most prevalent within the cores of large pillow-lobes where they coalesced to form dm to m-scale patches. Spherulites form in silicate melts and other Hi-polymers such as nylon. In volcanic rocks they are commonly associated with glass and typically grow when diffusion is sluggish (i.e. high viscosity) and the cooling is rapid. Granasy et al. (2005) demonstrate that in strongly undercooled polymeric liquids dynamic heterogeneities exist. In essence, with undercooling, the rotational diffusivity of growth-species in the melt diminishes much faster than their translational diffusivity. Thus growth-species impinge upon and adhere to an ensemble due to growth front nucleation, but with a mismatched geometry - thus explaining the characteristic non-crystallographic branching.

In common with all crystals, spherulites require nuclei from which to grow. The aphyric lava, having been superheated, contained no crystals and likely no crystal nuclei because it was at a supra-liquidus temperature. It requires a finite time to produce nuclei in the melt because molecular species of the correct composition, geometry and energy must collide and freeze in order to form a stable ensemble. If the material is extremely viscous so that diffusivities are minimal, or it is cooled very quickly, or both, there is insufficient time to form nuclei, and hence crystals - therefore a glass is formed instead. The lack of spherulites in the margin, and the paucity within the brecciated zone is different from the zonation of Archean pillow basalts (Fowler et al., 1986) and is interpreted as evidence that pillow-lobe exteriors cooled too quickly for crystal nucleation and crystal growth to occur. On the other hand the cores of the pillow-lobes have abundant spherulites. Here, one expects that the cooling rate was relatively slow in comparison to the exterior because of the thermal insulation caused by the encapsulating material. Therefore sufficient time existed during cooling of the pillow-lobe cores so that nuclei were formed

before the glass transition was crossed, however the cooling rate was still sufficiently fast, so that spherulites arose rather than more compact and closer-to-equilibrium habits such as dendrites. Also, at large undercoolings the melt can be in a state where nucleation is slow relative to crystal growth favoring the formation of few large spherulites rather than many small better-faceted crystals (see for example Fowler et al., 2002).

The breccias are in part blocky, platy and angular consistent with them having been produced by autoclastic processes i.e. they have a significant amount of hyaloclastite. In addition some are jig-saw fit breccias interpreted to be the result of thermal-contraction-granulation. The presence of sharp clast boundaries with overprinted alteration and rotated clasts precludes the textures being pseudobreccias produced by alteration (e.g. De Rosen-Spence, 1980). The pillow-lobes convoluted banding is indicative of plastic deformation during flow, and is related to the zonation of individual pillow-lobes. We interpret the V10b lavas to have been erupted in a sub-aqueous environment as coherent flows, consistent with the mafic pillow lavas that are ubiquitous within the Tisdale assemblage (Pyke, 1982; Brisbin, 1997).

We think that the core material of the large pillow-lobes remained above the glass transition during the time that the lobes were in motion and being deformed and after the main plastic deformation at the margins and brecciation had occurred. Small pillow-lobes are far less folded and are thoroughly brecciated likely because they quenched quickly to a glass.

Temporal distribution of aphyric dacites

We think that the facies is largely restricted to the Archean because the lavas were erupted in a superheated state and it is well known that the Archean thermal regime was hotter in comparison to succeeding Eras. Thus the dacites are similar to komatiites and the widespread spherulitic basalts of the Archean in the sense that they are apparently *largely*-restricted to Archean volcanic sequences. The aphyric pillow-lobe dacite lavas we describe differ from the Archean subaqueous felsic flows first described by De Rosen-Spence et al. (1980) that form lava lobes, pods, and tongues. In terms of the

composition these authors state "Some of the flows are true rhyolites, but most are probably siliceous iron-rich dacites and a few flows are silicified andesites."
In contrast to the rocks we describe, theirs contain phenocrysts, and the large lobes described by De Rosen-Spence et al. (1980) have microlitic and felsitic textures in their cores and spherulites are apparent at the margins, not the cores.

We believe that aphyric pillow-lobe dacite may have been erupted elsewhere in the Archean of the Abitibi (e.g. Scott and Mueller 2001) and that the "unusual" spherulitic flows mentioned by De Rosen-Spence et al. (1980) in the Rouyn Noranda area are likely the same. The literature (reviewed above) shows that most felsic flows contain phenocrysts and that description of dacitic lobes or pillows is rare. Although aphyric dacites and dacitic pillows have been reported elsewhere, aphyric pillow-lobes with spherulitic cores have not been described before, and in Archean rocks of the Timmins area, at least, they have been misidentified as basalts.

Recently, aphyric dacites have been reported from the Powder River Basin Wyoming, USA. These were sub-aerially erupted and formed "laterally extensive and voluminous (~4km) flows of aphyric andesite and dacite" that overlie Miocene olivine basalt (McConnell et al. 2002). In addition, Waters and Binns (1998) described using bottom-photographs and dredge samples, neo-volcanic sub-marine porphyritic and aphyric dacite lavas with contrasting morphologies from the Manus Basin, Papua New Guinea. The plagioclase-clinopyroxene-orthopyroxene-magnetite porphyritic dacitic lavas form prominent steep-sided conical peaks. In contrast the aphyric dacite lavas form a 15km long 500m high linear ridge dominantly composed of chaotic autoclastically fragmented flows, plus sheet, and lobate flows. Lobes are up to 5m in diameter and have ropey wrinkles and fractures. Unfortunately there are no petrographic details given, presumably because sampling of lobes would not have been possible. Rarely smooth to ropy sheet flows were observed near the ridge crest. The authors interpret the linear ridge, parallel the extension direction of the basin to have been formed from fault controlled fissure eruptions in which low viscosity dacite melts "were erupted at, or above, their liquidus temperatures."

Spherulite formation & preservation

Although not explicitly stated it appears that De Rosen-Spence et al. (1980) interpret the spherulites they observed to have formed through devitrification. Because diffusion is so sluggish below the glass transition, spherulite growth at ambient temperature is unlikely (Manley, 1992; Ryan and Sammis, 1981). Indeed experimental work by Lofgren (1971) demonstrates that devitrification of felsic glasses proceeds at elevated temperature and in the presence of an alkali solution. Distinguishing between primary and devitrification growth of spherulites can be difficult. We interpret the spherulites within the cores of the pillow-lobe dacites to be primary because their distribution is related to position in the pillow (i.e. cooling) and in at least one instance a spherulite was observed to have nucleated on a gas bubble. Energy required to open and maintain a bubble is taken from the melt in the form of heat, causing spherulite growth and providing a nucleation surface. Moreover, the spherulites within the pillow cores are not related to fractures. Spherulites associated with flow banding were also likely formed above the glass transition as shown for rhyolites by Manley (1992).

Clearly the rocks we describe are altered, though many primary features are well preserved. They did not contain phenocrysts and we also believe they did not contain microlites. Of course all the glass is altered, however in our experience fine wispy crystals such as microlites would, if initially present, have been preserved. Certainly the spherulites have been preserved, and we have documented microlites and spherulites in similarly altered Archean rocks (Fowler et al., 1986). Thus we think that the use of the term aphyric is justified and that the rocks were truly superheated upon eruption.

Recognition of Archean pillow basalts vs. pillow-lobe dacites

As noted the aphyric spherulitic lobate dacites have been misidentified as pillow basalts. The chief distinguishing features are the spherulite- rich cores abundance of breccia, plastic deformation, flow banding, necking, and in-*situ* shearing within the margins of the dacites. Generally within "variolitic" Archean pillow basalts the spherulites are concentrated in a cm-scale zone near and concentric with the pillow-rim whereas in the

aphyric dacite pillow-lobes the spherulites are concentrated in the cores. In addition the dacites have a much more convoluted geometry and thus far we have yet to observe any dacite pillow-lobes with the classic bulb and tail geometry visible in some pillow basalt outcrops. As demonstrated immobile elements such as the REE, Al, Ti, Y and Zr serve to classify the rocks.

Viscosity of Superheated Dacitic Lobes

One expects the viscosity of a superheated melt to be substantially less than one at sub-liquidus temperatures, particularly one carrying a large proportion of phenocrysts. However, because the V10b rocks are altered we expect that their major element geochemistry is likely no longer an accurate representation of their initial composition we cannot use any computational method to estimate their viscosity. Nonetheless, as an analogy we have computed the viscosity of a dacite from Mt. Unzen Japan (Sato et al., 1999) for various temperatures and crystal concentrations. The liquidus temperature of this material computed using MELTS (Ghiorso and Sack, 1995) is 1090° C and corresponds to a viscosity of ~$2*10^3$ Pa*s using the method of Shaw (1972). Figure 6.12 shows the results of calculations using the Einstein-Roscoe equation,

$$\eta = \eta_o(1 - \varphi/\sigma)^{-2.5} \qquad (1)$$

that allows for the computation of viscosity η of a liquid containing solids within it. η_o is the effective viscosity of the melt calculated using the method of Shaw (1972), φ the proportion of crystals and, σ is a constant whose value we set at either 0.3 or 0.6 (see below).

The data (Fig. 6.12) show a sharp increase in viscosity at the liquidus likely explaining the difference in facies between the aphyric pillow-lobe material we observe compared with the more typical phenocryst-bearing lobe facies as documented by De Rosen-Spence (1980) and of course dacitic pyroclastic deposits.

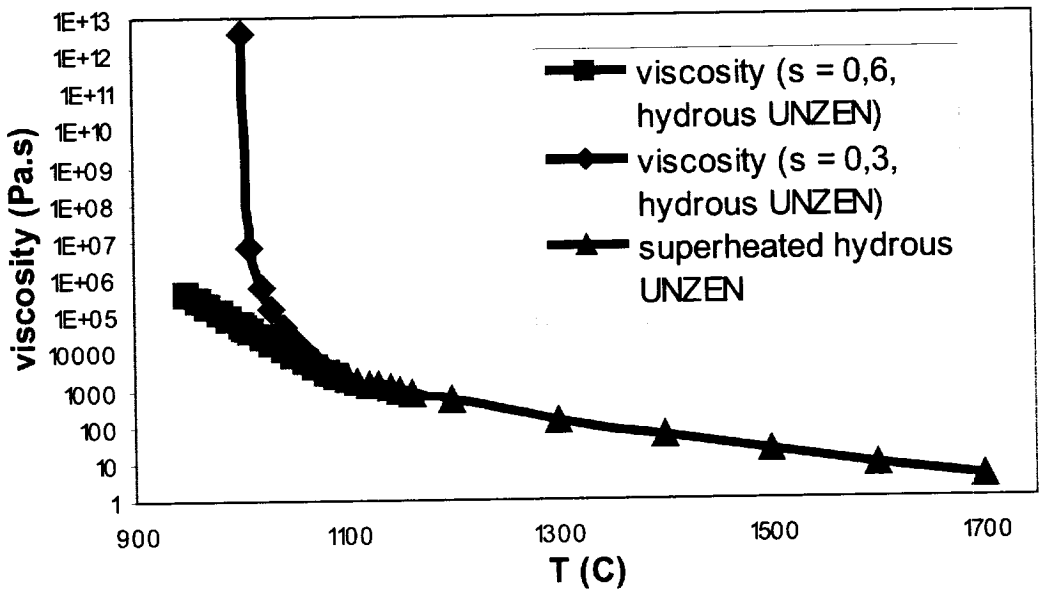

Figure 6.12 Calculated viscosity vs temperature (see text for details)

The melt viscosity calculations are only crude estimates for a number of reasons and they are used only for illustrative purposes. Because alteration of our rocks would undoubtedly have re-distributed the major elements we therefore have no means of measuring viscosity critical elements such as H, K and Na. Thus the Unzen dacite we chose to use is likely only approximately close to the composition of the V10b rocks. Also, the calculation is based on the Arrhenian model of Shaw (1972) whereas Russell et al. (2003) has demonstrated non- Arrhenian behavior in the viscosity of silicate melts. In addition the Einstein–Roscoe equation does not account for the size, shape or distribution of particles, factors that would undoubtedly affect the results. We have used two values of the constant σ (see Sato, 2005) the results of which likely bracket reality. In addition Pinkerton and Stevenson (1992) show that the Einstein-Stokes relationship fails for large crystal concentrations because of non-Newtonian behavior of the mush and variations in the activation energy for flow. Thus our results are only qualitative and a crude estimate nonetheless they serve to illustrate that the viscosity of the V10b analogue lava would be very sensitivity to change, likely about an order of magnitude within 100°C above the liquidus and more sharply below the liquidus.

It has been pointed out by Cas (1978), and others that the viscosity of silica – rich melts maybe be suppressed due to non-exsolution of volatiles resulting from submarine eruption at great depth and therefore high confining pressure. We have no evidence for the depth of emplacement of the subject rocks – though emplacement was not extraordinarily shallow. Some outcrops have thin horizons of capping carbonaceous shales but given the anoxia of the time these may have formed at depths not far below wave-base (i.e. 2-300m). Even if the rocks were erupted at depths of only a few 100m we speculate that they could have maintained dissolved volatiles and thus relatively low viscosities. Nucleation of a gas phase from a melt by homogeneous mechanisms requires significant supersaturation, at least in basaltic melts, (e.g. Bottinga and Javoy, 1990a &b) Although Bottinga and Javoy (1990a) state that most bubble nucleation is homogeneous Sparks (1978) provides evidence for significant heterogeneous nucleation that takes place on crystal surfaces. The dacite melts, being aphyric, may have reached a high-level without significant heterogeneous gas-exsolution having taken place because

heterogeneities for gas nucleation did not exist. Thus gas-retention in solution by non-nucleation may have played a role in reducing viscosity of the lava.

Gold mineralization potential

Most of the gold currently mined in Timmins is associated with quartz carbonate veins. For instance the current major producer, the Hoyle Pond Mine, exploits veins associated with regional D3-D4 structures in the Central Formation of the Lower Tisdale Assemblage (Dinel et al., accepted by guest editor, see chapter 4). However there is documentation (cited above) that mineralization occurs with in the pores of fragmental rocks in the upper part of the Tisdale and that disseminated ore was mined. We know that the V10 units were mineralised, though details were not recorded. Nonetheless we speculate that the pillow-lobe dacite likely made an excellent host for mineralization. Clearly it had an initial high porosity and permeability that left open would have been an ideal channel-way for mineralising fluids. One expects that the competency contrast between massive and fragmental flows would also yield greater permeability as a result of deformation. In addition permeable rocks present a greater surface area for chemical reaction and glass-rich units would be particularly reactive.

It has often been documented that gold-bearing veins of the area occupy the contacts between flows (e.g. Hurst, 1935) At the Hoyle Pond Mine this relationship holds true (Dinel et al., accepted by guest editor, see chapter 4), but the alteration and deformation is very intense. We have been unable to determine if the effect is a result of primary permeability (e.g. flow-top breccias) or secondary permeability caused by the mechanical response of flows of differing competency, or both

As stated earlier, Hurst (1935) reported a correlation between the Fe content of the wall rocks and gold mineralization in the camp. Ropchan et al. (2002) noted a similar relationship at the Holloway Mine further to the east in a very similar geological setting to that of Timmins, although there is no such relationship at the Hoyle Pond Mine (Dinel *et al.*, accepted by guest editor, see chapter 4). The pillow-lobe dacitic rocks are part of the tholeiitic suite and are therefore, by definition, Fe-enriched and are characterized by a

high Fe/Mg ratio. As demonstrated by Bolke (1988) an elevated Fe/Mg ratio in the host rocks favors the formation of pyrite from Au thio-complexes and the scavenging of gold from solution, whereas low Fe/Mg rocks tend to form carbonate rather than pyrite. Finally we note that gold mineralization is prevalent in volcanic rocks in other regions e.g. Red lake Ontario, and that here too brecciated (presumable autobreccia) rocks are described as "chickenfeed" leading to the possibility that pillow-lobe dacites may be widespread hosts of Archean lode gold mineralization.

Conclusions

We propose that tholeiitic aphyric pillow-lobe spherulitic dacites of the Tisdale Assemblage V10b unit represent a new facies that may very well be largely restricted to Archean rocks. The lavas were erupted in a superheated state and formed coherent flows rather than domes or pyroclastic flows. Together with massive underlying facies they were likely erupted from fissures. Pillow-lobe zoning consists of a thin rim-breccia zone and spherulite-rich core. The pillow lobes are distinguished from pillows of mafic rocks by their zoning, abundant associated hyaloclastite, flow banding, contorted outlines, necking and their felsic compositions, REE and other "immobile" element geochemistry. The V10 fragmental rocks were well mineralized in the former mines. Their high initial permeability, competency and high Fe/Mg ratios make these rocks ideal hosts for lode-gold mineralization.

6.4 Au vs. Fe/Mg ratio in disseminated Au mineralization

Disseminated gold mineralization in the Abitibi is in our view likely under explored. Thus it is possible that some non-negligible Au deposits remain undiscovered. The Holloway mine, east of Matheson (NE Ontario) is known for its gold mineralization associated with pyritization of the volcanic rocks. Here, for example 5% pyrite in the wall rock typically correlated with approximately 5g/t gold. In addition, Ropchan et al. (2002) identified a correlation of Au content with Fe/Mg ratio, and that the more evolved the rock which are part of the tholeiitic suite, the more Fe available to reduce S. They suggested based on the model of Bohlke (1989), that the higher the Fe content in rock the

more reactive it is to the hydrothermal fluid, reducing S, forming pyrite and scavenging the gold.

Some of the volcanic rocks studied in the Timmins area also have chemical affinities we consider good for disseminated style of mineralization. The rocks of the Vipond V10b flows have Fe/Mg ratio, varying from 3 to 8 (see table 6.2) in comparison to the Holloway mines where the Fe/Mg ratio varies from 0.5 to 20 and Au grade are in the range of 0 to 5g/t. Figure 6.13 & 6.14 shows a positive correlation between Fe/Mg ratio and Au grades at Holloway mine. However studies at Hoyle Pond mine have shown contrary to Ropchan et al., (2002), gold mineralization in vein setting do not appear to correlate to Fe/Mg ratio, where results show that the gold grades correlates to vein density (Dinel et al., accepted by guest editor, see chapter 4).

Samples	Fe_2O_3	FeO	MgO	Fe %	Mg %	Fe/Mg
BMS 1	1.76	4.67	1.15	4.861044	0.693491	7.009524
BMS 2	1.77	10.81	2.31	9.640728	1.393013	6.920773
BMS 3	3.11	17.91	3.67	16.09688	2.213142	7.273314
BMS 4	2.23	12.46	2.51	11.24503	1.51362	7.429228
BMS 5	2.97	13.00	3.14	12.18236	1.890518	6.443927
AF0508	11.787	-	2.08	**8.244959**	1.254315	6.573277
AF0512A	7.463	-	2.4	**5.220339**	1.447286	3.606984
AF0512B	21.46	-	6.56	**15.01118**	3.955916	3.794616
AF0514	13.173	-	1.76	**9.214461**	1.061343	8.681885

Table 6.2 Fe/Mg ratio value for the V10b unit in the Timmins area. Samples # AF0508 to AF0514, the Fe % is based on FeO total.

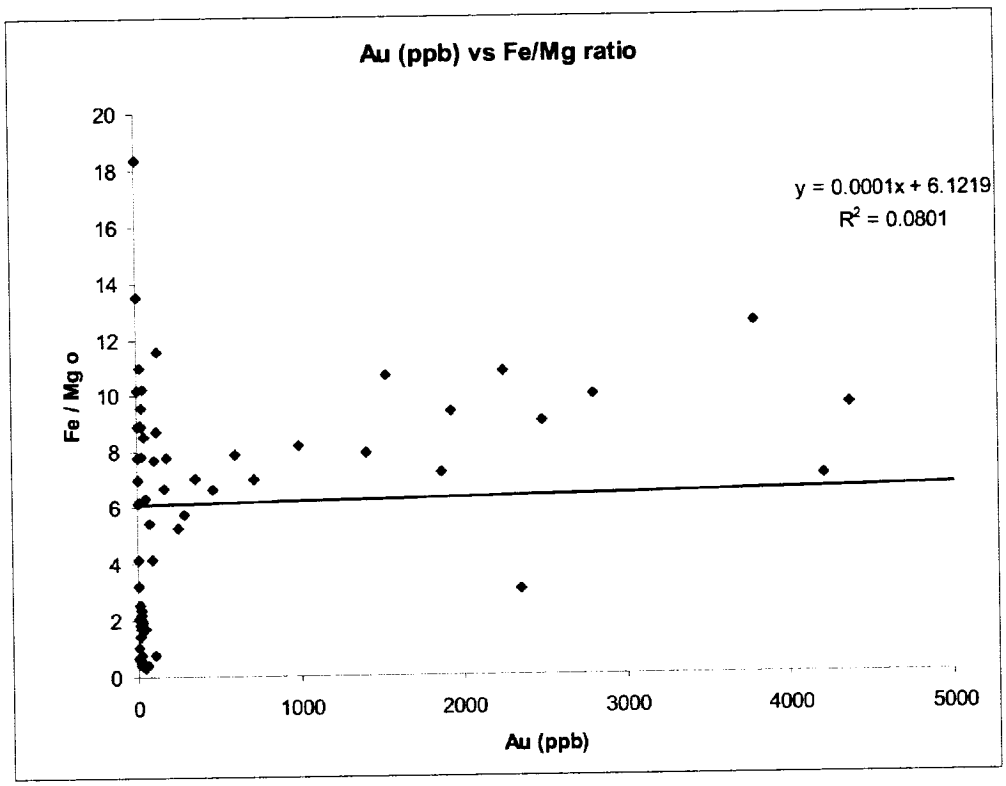

Figure 6.13 Graphic showing Fe/Mg ratio vs. Au from the Holloway mine (from Ropchan et al. 2002) for Au

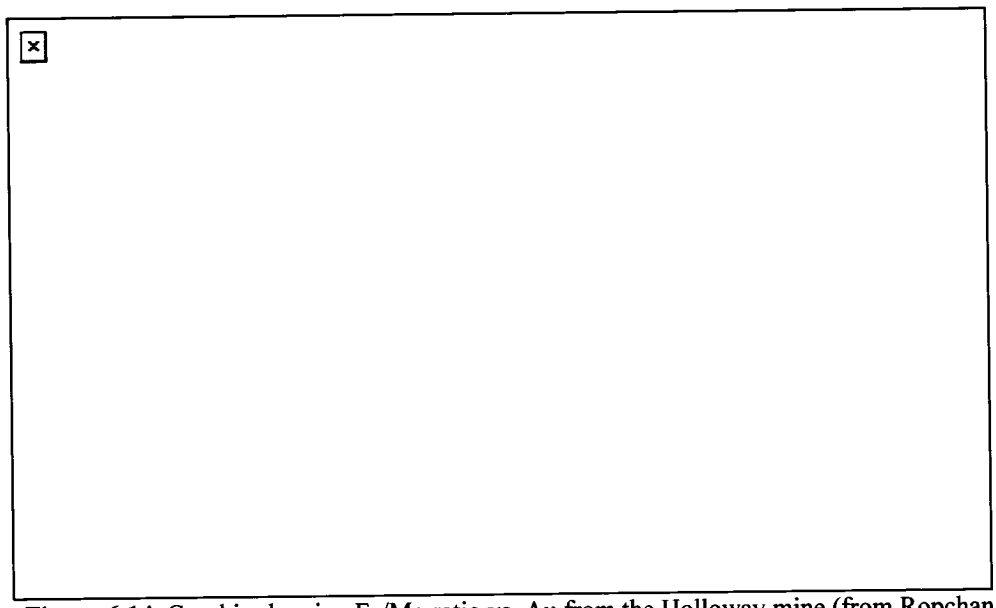

Figure 6.14. Graphic showing Fe/Mg ratio vs. Au from the Holloway mine (from Ropchan et al. 2002) for Au values above 200 ppb.

6.5 Summary

Based on the research in the Timmins area, we suggest that good host rock for disseminated Au mineralization has to possess permeability for fluids to circulate, and a geochemical composition prompt to chemical reactions to scavenge Au from fluids and reasonable proximity to a source of fluids. Disseminated gold mineralization can be form in primary porosity and secondary porosity such has shear zone. In addition, zones of porosity have to be connected to a network of structures that could canalized fluids from a source.

What is the ideal composition of the host rock? The ideal composition of a host rock is dependent on the composition of the fluids transporting Au, thus making difficult to define what would be the ideal chemical composition of the host rock. Fluids and chemical constituents of rocks will interact only if their chemical properties have affinities. However, the chemical composition of the rock may be important in terms of its physical and rheological characteristics and behaviour when submitted to stress. Less competent rock like ultramafic volcanic will deform in ductile fashion, thus creating none or minimum porosity, in more competent rock, stress will create porosity. Interestingly, to our knowledge, no gold mineralization in the Timmins area is hosted in ultramafic volcanic rock. On the other hand, there is reason to believe that the higher the Fe content in rocks, the more susceptible the rock was to chemical reactions with hydrothermal fluids and precipitating Au, based on the data from Ropchan et al. (2002) and Bohlke, (1989). However, in gold mineralization similar to the Hoyle Pond mine, there is no correlation between Fe/Mg ratio and Au content.

Chapter 7.0 Conclusion

The objectives of the project are to better understand the geology of the Hoyle Pond Mine, provide a better understanding of the formation of Archean epigenetic gold deposits and associated alteration, and to investigate the concepts of host rock and structural control on mineralization, by studying the physical and chemical properties of several key lithologies.

At the Hoyle Pone Mine the mapping and geochemistry of the rocks and the investigation of the structural geology have defined a south-facing homoclinal sequence of stacked volcanic rocks correlative with the Hershey Lake and Central formations of the Tisdale assemblage. The rocks were altered by sub-greenschist burial metamorphism, regional sub-greenschist metamorphism and hydrothermal alteration during mineralization. The hydrothermal mineralizing fluid was injected during D3 and D4 and associated with isoclinal folding, shearing, and thrusting that may be explained by compressional deformation. The two generations of fault-fill veins are present at Hoyle Pond. In the NVP, fault-fill veins are hosted in D3 structures and in the SVP, within the 1060fz, fault-fill veins occupy D4 structures emplaced at flow contacts on both limbs of isoclinal folds (e.g. B1, B1S B1N and B3 veins).

The alteration associated with Au-bearing quartz-carbonate veins is zoned and consists of an inner sericite alteration zone immediately enveloping the vein and an outer albite alteration zone. The sericite alteration zone is composed of sericite, Cr- mica "fuchsite", quartz, Fe-dolomite, arsenopyrite, pyrite, tourmaline and graphite; and has a concomitant enrichment in K_2O, Cr, SiO_2, CO_2, As, and S. The albite alteration zone is composed of albite, quartz and Fe-dolomite and has enrichment in Na_2O, CO_2 and SiO_2. The Isocon method (Grant, 1986), was used to identified the mobile and immobile major oxides and trace elements. REE, Al_2O_3, Zr, TiO_2 and Y were relatively immobile with respect to alteration and can be used to identify rock type. K_2O, Na_2O, Cr, Rb, CO_2, CaO, Eu, FeO, MgO and to a minor extent La (LREE), were mobile during hydrothermal activities and greenschist metamorphism.

The significance of chromium mobility in orogenic gold deposits and its role in the concentration of gold has previously been little-researched. Nonetheless, mining geologist have, on numerous occasions, reported that the quartz-carbonate veins associated with Cr-muscovite wall rock alteration are commonly gold bearing (e.g. Moritz and Crocket, 1991). At Hoyle Pond, Cr content increases in the vicinity of the veins, whereas Mg# and Ni concentrations stay relatively constant. Cr^{6+} is the known mobile species in aqueous solutions and the best known Cr^{6+} reducing agents are organic matter, thio complexes and Fe II. We suggest that Au was mobilized in hydrothermal solution by Au-thio complexes and organic matter. I propose a fluid mixing model in which oxidizing fluids with soluble Cr^{6+} and other elements, for instance K and Na reacted with a reducing fluid carrying gold as a thio-organic complexes (Au-HS-C_xH_x), and other elements (e.g. B and As). Cr^{6+} would have been reduced by the Au-thio and organic matter complexes, resulting in the oxidation of organic matter and thio-complexes to form graphite, CO_2, precipitating gold and the oxidation of B to form tourmaline minerals. Au, As and B were probably leached from the Porcupine assemblage sedimentary rocks by a reducing fluid that contained dissolved organic matter. The chromium in the oxidizing fluid was most likely derived from ultramafic and mafic volcanic rocks.

The Porcupine assemblage sedimentary rocks were buried to depth, folded and thrusted, during D3, and contained reduced fluids were expelled from them and migrated along D3 structures and similar process occurred during D4 deformation.

The V10b unit of the Tisdale assemblage in Timmins represent a new facies type that may be dominantly restricted to Archean rocks. These tholeiitic dacitic lavas were erupted in a superheated state and formed coherent flows rather than domes or pyroclastic flows erupted from fissures vents with the underlying massive flows. Pillow-lobe zoning consists of a thin rim breccia zone and spherulite-rich core. The pillow-lobes of the dacites are distinguished from pillows of mafic rocks by their abundant associated hyaloclastite, flow banding, contorted outlines, necking and felsic compositions. Study of

the Vipond formation V10b units has resulted in the formulation of a discrimination diagram based on the REE to help classify volcanic rocks of the tholeiitic suite that have undergone greenschist metamorphism.

The V10b fragmental rocks are economically important as the units are mineralized in the McIntyre, Hollinger and Dome mines. Their high initial permeability, competency and high Fe/Mg ratios make these rocks ideal hosts for lode-gold mineralization. At the Holloway Mine approximately 100 km east of Timmins, Ropchan et al. (2002) demonstrated that there is a sympathetic relationship between Fe/Mg ratio of the evolved rocks of the tholeiitic suite and Au content. The V10b unit contains felsic tholeiitic rocks with high Fe/Mg ratios, ranging from 3.6 to 8.7. These units are compositionally similar to units at the Holloway mine with Au concentrations of 1000 to 15,000 ppb, further suggesting that the V10B unit is a geochemically favourable host rock for gold mineralization.

At Hoyle Pond, the mafic tholeiitic volcanic rocks do not show any positive correlations between Fe/Mg ratio and gold content. Moreover, the gold mineralization is not disseminated, but is restricted to within quartz-carbonate veins. This difference in mineralization style may be related to a number of factor but perhaps principally the chemistry of the hydrothermal fluids at Hoyle Pond which contained organic matter that acted as a medium for transporting Au. In addition, here mixing of reduced and oxidized fluids is considered to be more important than fluid-wall rock interaction.

Lists of Contributions

Following is a list of contributions made during the preparation of this dissertation:

- Detailed geological mapping of the 440ml and 720ml 1060fz, and detailed sampling through the 1060fz on the 880ml and the 3level #16 vein area, Hoyle Pond mine.
- Definition of the major elements and trace elements that are immobile and mobile with respect to the alterations.
- Determination of the volcanic rock stratigraphy of the mine, by their primary lithofacies, petrology and their geochemistry.
- Demonstration of the asymmetry of the volcanic rocks on either side of the central volcanic package, ruling out the presence of an anticlinal fold in the central ultramafic volcanic rocks of the mine stratigraphy
- Demonstration that the mine stratigraphy consists of a homoclinal sequence of stacked volcanic rocks, with a general south-facing direction.
- Demonstration that the stratigraphy of the Hoyle Pond mine is correlative with rocks at the base of the Tisdale Assemblage, i.e. the Hershey Lake and Central formations.
- Demonstration of the controls on mineralization, i.e. structures focussed at contacts of lithologies or flows, and on the limbs of isoclinal F4 folds.
- Definition of the geochemical and mineralogical characteristic of the alteration zones associated with gold bearing quartz-carbonate veins.
- Investigation of the nature of the graphite alteration, demonstration of trace content of organic matter by modern analysis techniques (Nuclear Magnetic Resonance, Carbon Isotope ^{13}C and ^{14}C), and suggesting a proposed source of graphite.
- Investigation of the nature of chromium enrichment in the sericite alteration zone, demonstration, by literature review and analysis, of the mobility of Cr in hydrothermal fluids.

- Proposed model for gold mineralization, involving fluid mixing of an oxidizing and reducing fluid.
- Hypothesis that porous zones, such as flow breccia, and shear zones increased the efficiency of circulating hydrothermal fluids and increased the surface area for chemical reactions to occur
- Hypothesis that reduced organic matter transported gold in solution to zones of increased porosity where fluid mixing precipitated gold.
- Hypothesis that the sedimentary rocks of the Porcupine assemblage were a source for Au.
- Demonstration that the Au content is not correlative with Fe/Mg ratio, in vein type mineralization at Hoyle Pond, unlike Ropchan et al. (2002) observations.
- Investigation of the nature of fragmental volcanic flow facies within the V10b flows in the Timmins area; demonstrating that they were a good host rock for disseminated gold and vein gold mineralization.
- Proposal of a new discrimination diagram for Archean greenschist metamorphic volcanic rocks of tholeiitic composition, based on REE chondritic normalized plot.

Reference

Anderson, J.R., 1975. Structure of Metallic Catalyst: Academic Press Inc. New York, USA, p.469.

Arndt, N.D., 1975. Ultramafic rocks of Munro Township and their volcanic setting: Unpublished Ph.D. thesis, University of Toronto, Toronto, 192 p.

Ashworth, D.J., D.O. Adams, B.Y. Giang, M. Tunghai Cheng, and R.Y lee,1985, Carbon-13 nuclear magnetic resonance spectrometric and gas chromatography of lipids in corn suspension cells, Analytical Chemistry, vol. 57, p. 710-715.

Ayer, J.A., Amelin, Y., Corfu, F., Kamo, S., Ketchum, J., Kwok, K., and Trowell, N., 2002. Evolution of the southern Abitibi greenstone belt based on U-Pb geochronology; autochthonous volcanic construction followed by plutonism, regional deformation and sedimentation. Precambrian Research, 115(1-4), p. 63-95.

Ayer, J.A., Thurston, P.C., Bateman, R., Dubé, B., Gibson, H.L., Hamilton, M.A., Hathway, B., Hocker, S.M., Houlé, M.G., Hudak, G., Ispolatov, V.O., Lafrance, B., Lesher, C.M., MacDonald, P.J., Péloquin, A.S., Piercey, S.J., Reed, L.E. and Thompson, P.H., 2005. Overview of Results from the Greenstone Architecture Project. Discover Abitibi Initiative, Ontario Geological Survey, Open file report 6154, 175 p.

Ayer, J.A., Thurston, P.C., Dubé, B. Gibson, H.L., Hudak, G., Lafrance, B., Lesher, C.M., Piercey, S.J., Reed, L.E., and Thompson, P.H., 2004. Discover Abitibi greenstone architecture project: overview of results and belt-scale implications; in Summary of Field work and Other Activities 2004, Ontario Geological Survey, Open File Report 6145, p. 37-1 to 37-15.

Ayres, L.D., and Peloquin, A.S., 2000. Subaqueous, Paleoproterozoic, metarhyolite dome-flow-cone complex, Flin Flon greenstone belt, Manitoba, Canada. Precambrian Research, v. 101, p. 211-235.

Atkinson, B.T., Hailstone, M., Seim, G.W., Wilson, A.C., Draper, D.M., Bulman, V.J., and Pace, A., 2005. Report of Activities 2004, Resident Geologist Program, Timmins Regional Resident Geologist Report, Timmins and Sault Ste. Marie District, Ontario Geological Survey, Open File Report 6149, 93 p.

Bachmann, K., 2005. Looking back, Porcupine Goldfields, Ontario. Looking back Press, St. Catharines, Ontario, 128 p.

Barr E., 2005. Porcupine Joint Venture internal company report.

Barrett, T. J., Cattalani, S., Chartrand, F., and Jones, P., 1991, Massive sulfide deposits of the Noranda area, Quebec; II, The Aldermac Mine: Canadian Journal of Earth Sciences = Journal Canadien des Sciences de la Terre, v. 28, p. 1301-1327.

Barrie, C.T., 1999. The Kidd Munro extension project: Year 3 report. Unpublish report, 263 p.

Bateman, R, Ayer, J.A., Barr, E., Dubé, B., and Hamilton, M.A., 2003, Discover Abitibi. Gold subproject 1. Protracted structural evolution of the Timmins-Porcupine gold camp and the Porcupine-Destor deformation zone, in Summary of Field work and Other Activities, Ontario Geological Survey, Open file report 6145, p. 41-1 to 41-10.

Bateman, R., Ayer, J.A., Barr, E., Dubé, B. and Hamilton, M.A., 2005. The Timmins-Porcupine gold camp, northern Ontario: the anatomy of an Archean greenstone belt and its gold mineralization. Discover Abitibi Initiative; Ontario Geological Survey, Open File Report 6158, 90 p.

Berry, L.G., 1941. Geology of the Bigwater Lake area. Ontario Department of Mines, Annual Report, 1939, v. 48-12, 11 p.

Bevins, R.E., and Roach, R.A., 1979. Pillow lava and isolated pillow breccia of rhyodacitic composition from the Fishguard Volcanic Group, Lower Ordovician , S.W. Wales, United Kingdom. Journal of Geology, v. 87, p. 193-201.

Bleeker, W., 1995. Surface geology of the Porcupine camp, Geological Survey of Canada, Open File 3141, p. 13-47.

Bleeker, W., 1999. Structure, stratigraphy and primary setting of the Kidd Creek volcanogenic massive sulphide deposit: a semi quantitative reconstruction. Economic Geology Monograph, v. 10, p. 71-122.

Bohlke, J.K., 1988. Carbonate-sulphide equilibria and "stratabound" disseminated epigenetic gold mineralization: A proposal based on examples from Alleghany, California, U.S.A. Applied Geochemistry, v. 3, p. 499–516.

Bohlke, J. K., 1989. Comparison of metasomatic reactions between a common CO (sub 2) -rich vein fluid and diverse wall rocks; intensive variables, mass transfers, and Au mineralization at Alleghany, California. Economic Geology, v. 84, p. 291-327.

Böhm, B. and Fisher, W.R., 2004. Kinetics of chromium (III)-oxidation in top soils. Journal of Plant Nutrition and Soil Science., vol. 167, p. 22-23.

Born, P., 1995. A sedimentary basin analysis of the Abitibi greenstone belt in the Timmins area, Northern Ontario, Canada: Unpublished Ph.D. thesis, Carleton University, Ottawa, 489 p.

Bottinga, Y., and Javoy, M., 1990. Mid-ocean ridge basalt bubble degassing: Bubble nucleation. Journal of Geophysical Research, v. 95, p. 5125-5131.

Bottinga, Y., and Javoy, M., 1990. MORB degassing: Bubble growth and ascent. Chemical Geology, v.81, p. 255-270.

Boyle, R.W., 1979. The geochemistry of gold and its deposits. Geological Survey of Canada, Bulletin 280, 485 p.

Brisbin, D. I., 1997. The Geological Setting of gold deposits in the Porcupine Gold Camp, Timmins, Ontario. Unpublished Ph. D. thesis, Queen's University, Kingston, 523 p.

Buffam, B. S. W., 1948. Moneta Porcupine Mine, Ontario. *In* Economic geology of ore deposits. P. 457-464.

Burrows, D.R., Spooner, E.T.C., Wood P.C., and Jemielita, R.A., 1993. Structural controls on formation of the Hollinger-McIntyre Au quartz vein system in the Hollinger Shear Zone, Timmins, southern Abitibi greenstone belt, Ontario. Economic Geology, v. 88, p. 1643-1663.

Calvert, A. J., and Ludden, J. N., 1999. Archean continental assembly in the southeastern Superior Province of Canada. Tectonics, v. 18, p. 412-429.

Card, K. D., and Ciesielski, A., 1986. DNAG #1; Subdivisions of the Superior Province of the Canadian Shield. Geoscience Canada, v. 13, p. 5-13.

Carr, S.D., Easton, R.M., Jamieson, R.A., and Culshaw, N.G., 2000. Geologic transect across the Grenville orogen of Ontario and New York. Canadian Journal of Earth Sciences, v.37 issue 2/3, p. 193-216.

Cas, R.A.F., 1978. Silicic lavas in Paleozoic flysch-like deposits in New South Wales, Australia: behaviour of deep subaqueous silicic flows. Geological Society of America Bulletin, v. 89, p. 1708-1713.

Colvine, A. C., Fyon, J. A., Heather, K. B., Marmont, S., Smith, P. M., and Troop, D. G., 1988. Archean Lode Gold Deposits in Ontario. *in* Mines, M. o. N. D. a., ed., Ontario Geological Survey, 136 p.

Condie, K. C., Des Marais, D. J., and Abbott, D., 2001. Precambrian superplumes and supercontinents; a record in black shales, carbon isotopes, and paleoclimates?: Precambrian Research, v. 106, p. 239-260.

Corfu, F., Krogh, T.E., Kwok, Y.Y., and Jensen, L.S., 1989. U-Pb zircon geochronology in the southwestern Abitibi greenstone belt, Superior Province. Canadian Journal of Earth Sciences, v. 26, p. 1747-1763.

Davies, J.F., Whitehead, R.E.S., Cameron, R.A., and Duff, D., 1982. Regional and local patterns of CO2-K-Rb-As alteration: a guide to gold in the Timmins area. *In* Geology of

Canadian Gold deposits, Special Volume 24, The Canadian Institute of Mining and Metallurgy, 286 p.

Deer, W.A, Howie, R.A. and Zussman, J., 1992. An Introduciton to the Rock-Forming Minerals (Second Edition): Longman Scientific and Technical, New York, USA, 696 p.

De Rosen-Spence, A., Provost, G., Dimroth, E., Gochauer, K., and Owen, V., 1980. Archean subaqueous felsic flows, Rouyn-Noranda, Quebec, Canada, and their Quaternary equivalents. Precambrian Research, v. 12, p. 43-77.

Dimroth, E., Cousineau, P., Leduc, M., and Sanschagrin, Y., 1978. Structure and organization of Archean basalt flows, Rouyn-Noranda area, Quebec, Canada. Canadian Journal of Earth Sciences, v.15, p. 902-918.

Dimroth, E., Cousineau, P., Leduc, M., Sanschagrin, Y., Provost, G., 1979. flow mechanisme of Archean sub-aqueous basalt and rhyolite flows. Geological survey of Canada, Current Research part A, paper 79-1A, p. 207-211.

Dimroth, E., Imreh, L., Goulet, N., and Rocheleau, M., 1983. Evolution of the south-central segment of Archean Abitibi Belt, Quebec; Part II, Tectonic evolution and geomechanical model. Canadian Journal of Earth Sciences, v. 20, p. 1355-1373.

Dinel, E., 2001. Structural Investigation of the Echo Bay and International Properties, Timmins, Ontario: Unpublished B.Sc. thesis, University of Ottawa, Ottawa, 28 p.

Dinel, E. Saumur, B.M. and Fowler, A.D., 2005. Lobe and Breccia Facies Rhyolite and Intermediate Volcanic Rocks of the Timmins Area, Ontario, Abitibi Greenstone Belt: A Previously Unrecognized Facies. Poster and Abstract, GAC-MAC, Halifax, Nova Scotia.

Dinel, E., Fowler, A.D., Ayer, J., Still, A., Tylee, K., and Barr, E., accepted by guest editor. Litho-geochemical and stratigraphic controls on gold mineralization within the meta-volcanic rocks of the Hoyle Pond Mine, Timmins, Ontario, Economic Geology.

Dinel, E., Saumur, B-M., and Fowler, A.D., under revision, Spherulitic aphyric pillow-lobe meta-tholeiitic dacite lava of the Timmins area, Ontario, Canada: A new Archean facies and its implications for lode-gold mineralisation Submitted to Economic Geology.

Dostal, J., and Mueller, W., 1996. An Archean oceanic felsic dyke swarm in a nascent arc; the Hunter Mine Group, Abitibi greenstone belt, Canada. Journal of Volcanology and Geothermal Research, v. 72, p. 37-57.

Dostal, J., and Mueller, W. U., 1997. Komatiite flooding of a rifted Archean rhyolitic arc complex; geochemical signature and tectonic significance of the Stoughton-Roquemaure Group, Abitibi greenstone belt, Canada. Journal of Geology, v. 105, p. 545-563.

Downes, M. J., Hodges, D.J. and Derwedwen J., 1982. A free carbon - and carbonate-bearing alteration zone associated with the Hoyle Pond gold occurrence, Ontario, Canada. Gold' 82: The Geology, Geochemistry and Genesis of Gold Deposits, University of Zimbabwe. 753 p.

Dunbar, W. R., 1948. Structural relations of the Porcupine Ore deposits (Ontario). *In* Canadian Ore Deposits, vol. 1: Canadian Institute of Mining and Metallurgy, Montréal, vol. 1, p.442-456.

Eales, H. V., 2000. Implications of the chromium budget of the western limb of the Bushveld Complex. South African Journal of Geology, v. 103, p. 141-150.

Elliott, S.R., 1984. Geochemical, mineralogical and stable isotope studies at Owl Creek mine Timmins, Ontario. Unpublished Master's thesis, Department of Geology, Carleton University, Ottawa, 109 p.

Farmer, B.C., Morrison, R.I., 1960. Chemical and Infrared on phramites peat and its humic acid. Science Proceeding Royal Dublin Society. Series A1, p. 85-104.

Faure, G., 1998, Principles and Applications of Geochemistry (Second Edition): Prentice Hall, The Ohio State University, USA, 600 p.

Ferguson, S. A., Buffman, B.S.W., Carter, O.F., Griffis, A.T., Holmes, T.C., Hurst, M.E., Jones, W.A., Lane, H.C., and Longley, C.S., 1968. Geology of ore deposits of Tisdale Township, District of Cochrane. Timmins: Ontario Department of Mines, Geological Report 58, p. 117, with Map 2075, scale 1"=1000'.

Ferguson, S.A. and associated geologists, 1968. Geology and Ore Deposits of Tisdale Township. Ontario Department of Mines Geological Report 58, p.177.

Fowler, A.D., and Doig, R., 1983. The significance of Europium anomalies in the REE spectra of granites and pegmatites, Mont Laurier, Québec. Geochimica et Cosmochimica Acta, vol. 47, p. 1131-1137.

Fowler, A.D., Jensen, L.S., and Peloquin, S.A. 1986. Varioles in Archean basalts: Products of spherulitic crystallization. Canadian Mineralogist, v.25, p. 275-289.

Fowler, A.D., and Jensen, L.S. 1989. Quantitative trace element modeling of the crystallization history of the Kinojevis and Blake River Groups, Abitibi Greenstone Belt, Ontario. Canadian Journal of Earth Science v. 26, p. 1356-1367.

Fowler, A.D., Berger, B., Shore, M., Jones, M.I. and Ropchan, J. 2002. Supercooled rocks: Development and significance of varioles, spherulites, dendrites and spinifex in Archean volcanic rocks, Abitibi Greenstone Belt, Canada. Precambrian Research, v. 115, p. 311-328.

Fyon, J.A., and Crocket, J.H., 1980. Gold exploration in the Timmins District using field and lithogeochemical characteristics of carbonate alteration zones. *In* Geology of Canadian Gold Deposits. Canadian Institute of Mining and Metallurgy, Special Volume 24, p. 113-129.

Gabriel, K.R., 1971. The biplot graphic display of matrices with application to principal component analysis. Biometrika, vol. 58, p. 453-467.

Gélinas, L., Brooks, C., and Trzcienski, W.E. 1976. Archean variolites – quenched immiscible liquids. Canadian Journal of Earth Science. v. 13, p. 210-230.

Ghiorso, M.S., and Sack, Richard O.,1995. Chemical Mass Transfer in Magmatic Processes. IV. A Revised and Internally Consistent Thermodynamic Model for the Interpolation and Extrapolation of Liquid-Solid Equilibria in Magmatic Systems at Elevated Temperatures and Pressures. Contributions to Mineralogy and Petrology, v. 119, p.197-212.

Goldfarb R.J., Groves D.I., Gardoll, S., 2001. Orogenic gold and geologic time: a global synthesis. Ore Geology Reviews, vol. 18, p. 1-75.

Goodwin, A.M., 1977. Archean volcanism in the Superior province, Canadian Shield. *In* W.R.A. Barager,L.C. Coleman, & J.M. Hall (Eds.), Volcanic Regimes in Canada: The Geological Association of Canada, Special Paper 16, p. 205-241.

Goodwin, A.M., and Ridler, R.H., 1970. The Abitibi orogenic belt. *In* Symposium on Basins and Geosynclines of the Canadian Shield, Geological Survey of Canada, Paper 70-40, p. 1-30.

Goto, Y., and McPhie, J., 1998. Endogenous growth of a Miocene submarine dacite cryptodome, Rebun Island, Hokkaido, Japan. Journal of Volcanology and Geothermal Research, v. 84, p. 273-286.

Granasy, L., Puztai, T., Tegze, G., Warren, J., and Douglas, J., 2005. Growth and form of spherulites. Physical Review, v. 72, p. 011605-1 - 011605-15.

Grant, G.A., 1986. The isocon diagram –A simple solution to Gresen's equations for metasomatic alteration. Economic Geology, vol. 82, p. 1976-1982.

Graton, L.C., McKinstry, H.E. and Others, 1933. Outstanding features of Hollinger geology: The Transactions of the Canadian Institute of Mining and Metallurgy and of the Mining Society of Nova Scotia, v. 36, p. 1–21.

Gray, M., and Hutchinson, R.W., 2001. New Evidence for Multiple Periods of Gold Emplacement in the Porcupine Mining District, Timmins Area, Ontario, Canada. Economic Geology, vol. 96, p. 453-475.

Griffis, A.T., 1962. A geological study of the McIntyre Mine. The Canadian Mining and Metallurgical Bulletin, v. 55, p. 76-83.

Groves, D.I., Goldfarb, R.J., Gebre-Mariam, M., Hageman, S.G., and Robert, F., 1998. Orogenic gold deposits: A proposed classification in the context of their crustal distribution and relationship to other gold deposit types. Ore Geology Reviews, vol. 13, p. 7-27.

Groves, D.I., Goldfarb, R.J., Knox-Robinson, C.M., Ojala, J., Gardoll, S., Yun, G.Y., and Holyland, P., 2000. Late-kinematic timing of orogenic gold deposits and significance for computer-based exploration techniques with emphasis on the Yilgarn Block, Western Australia. Ore Geology Reviews, vol. 17, p. 1-38.

Groves, D.I, Goldfarb, R.J. Robert, F., and Hart, C.J.R., 2003. Gold deposits in metamorphic belts: Overview of current understanding, outstanding problems, future research, and exploration significance. Economic Geology, v. 98, p. 1-29.

Hart, T.R., 2001. Whole rock lithogeochemical data of prospective versus barren volcanic belt for volcanogenic massive sulphide (VMS) deposits, Superior province, Ontario. Operation treasure hunt: Ontario Geological Survey Miscellaneous Release of Data 085.

Hart, T.R., Gibson, H.L., and Lesher, C.M., 2004. Trace element geochemistry and petrogenesis of felsic volcanic rocks associated with volcanogenic massive Cu-Zn-Pb sulfide deposits. Economic Geology, v. 99, p. 1003-1013.

Heaman, L.M., 1997. Global mafic magmatism at 2.45 Ga: remnants of an ancient large igneous province? Geology, v.25, p. 299-302.

Henry, S., 2000. Influence de la vapeur d'eau sur l'oxydation à haute température du chrome et de quelques aciers inoxydables férritiques stabilisés: Grenoble-thèse. Micro-fiche.

Hodges, D.J., 1982. Alteration associated with gold mineralization near the Owl Creek deposit. Unpublished B.Sc. thesis, University of Waterloo, Waterloo, 39 p.

Holmes, T. C., 1948. Dome mine. in Structural Geology of Canadian Ore Deposits Canadian Institute of Mining and Metallurgy, Montreal, p. 539-547.

Houlé, M.G., Gibson, H.L., Lesher, C.M., Davis, P.C., Cas, R.A.F., Beresford, S.W., and Arndt, N.T., Accepted with revisions. Komatiitic Basalt Sills and Multi-Generational Peperite at Dundonald Beach, Abitibi Greenstone Belt, Ontario: Implications for Komatiite Volcanic-Subvolcanic Architecture and Seafloor-Subseafloor Nickel Sulfide Distribution, Economic Geology.

Humphris, S. E., Morrison, M. A., and Thompson, R. N., 1978. Influence of rock crystallisation history upon subsequent lanthanide mobility during hydrothermal alteration of basalts. Chemical Geology, v. 23, p. 125-137.

Hunt, D.S., & Maharaj, D., 1980. Hoyle Township, District of Cochrane, Ontario. Ontario Geological Survey, Preliminary map P2088, scale 1:15840.

Hurst. M.E., 1935. Vein formation at Porcupine, Ontario. Economic Geology, v. 30, p. 103-127.

Hurst, M.E., 1939. Porcupine Area, District of Cochrane, Ontario. Ontario Department of Mines map 47A. scale 1 inch to 2000 feet.

Hynes, A., 1980, Carbonatization and mobility of Ti, Y, and Zr in Ascot Formation metabasalts, SE Quebec: Contributions to Mineralogy and Petrology, v. 75, p. 79-87.

Jackson, S. L., and Fyon, J. A., 1991 The Western Abitibi subprovince in Ontario Ontario Geological Survey Special Volume, v. 4, p. 405-482.

Jackson, S.L., Fyon, J.A. and Corfu, F. 1991. Review of Archean supracrustal assemblages of the Southern Abitibi greenstone belt in Ontario, Canada: Products of microplate interaction within a large–scale plate-tectonic setting. Precambrian Research, v. 65, p.183-205.

Jackson, L.S., Fyon, J.A., and Corfu, F., 1994. Review of Archean supracrustal assemblages of the southern Abitibi greenstone belt in Ontario: product of microplate interaction within a large-scale plate-tectonic setting. Precambrian Research, v. 65, p. 183-205.

Jackson, S.L., Cruden, A.R., White, D., and Milkereit, B., 1995. A seismic-reflection-based regional cross section of the southern Abitibi greenstone belt. Canadian Journal of Earth Sciences, v. 32, p. 135-148.

Jensen, L.S., 1976. A new cation plot for classifying subalkalic volcanic rocks. Ontario Department of Mines, Miscellaneous Paper 66, p. 22.

Jensen, L. S., and Langford, F. F., 1985. Geology and petrogenesis of the Archean Abitibi Belt in the Kirkland Lake area, Ontario. Ontario Geological Survey Miscellaneous Paper 123, 130 p.

Jia, Y., Kerrich, R., and Goldfarb, R. J., 2003. Metamorphic origin of ore-forming fluids for orogenic gold-bearing quartz vein systems in the North American Cordillera; constraints from a reconnaissance study of delta (super 15) N, delta D, and delta (super 18) O. Economic Geology, v. 98, p. 109-123.

Jolicoeur, P. and Mosimann, J.E., 1960. Size and shape variation in the painted turtle: A principal component analysis. Growth, vol. 24, p. 339-354.

Jones, W.A., 1948, Hollinger Mine: In Structural Geology of Canadian Ore Deposits, Volume 1. Canadian Institute of Mining and Metallurgy, Montreal, p. 464-481.

Jones, M. I., 1992. Variolitic basalts; relations to Archean epigenetic gold deposits in the Abitibi greenstone belt: Unpublished Master's thesis, University of Ottawa, Ottawa, 143 p.

Kano, K., Takeuchi, K., Yamamoto, T., and Hoshizumi, H., 1991. Subaqueous rhyolite block lavas in the Miocene Ushikiri Formation, Shimane Peninsula, SW Japan. Journal of Volcanological and Geothermal Research, v.46, p. 241-253.

Kawachi, Y., and Pringle, I.J., 1988. Multiple-rind structure in pillow lavas an indicator of shallow water. Bulletin of Volcanology, v. 50, p. 161-168.

Kim, C., Zhou, Q., and Deng, B., 2001, Chromium (VI) reduction by hydrogen sulfide in aqueous media: stoichiometry and kinetics. Environmental Science & Technology, v. 35, p. 2219-25.

Kerrich, R., and Hodder, R.W., 1982. Archean Lode Gold and Base Metal Deposits: chemical evidence for metal fractionation into independent hydrothermal reservoirs. In: Geology of Canadian Gold deposits, Special Volume 24, The Canadian Institute of Mining and Metallurgy, 286 p.

Kerrich R., P. A., Wyman D., Hollings P., 1999. Trace elements systematics of Mg-, to Fe-tholeiitic basal suites of the Superior Province: implications for Achean mantle reservoirs and Greenstone belt genesis. Lithos, vol. 46, p. 163-187.

Kerrich, R. and Xie, Q., 2002. Compositional recycling structure of an Archean super-plume: Nb-Th-U-LREE systematics of Archean komatiites and basalts revisited. Contributions to Mineralogy and Petrology, v.142 p. 476 484

Kim, C., Zhou, Q., and Deng, B., 2001. Chromium (VI) reduction by hydrogen sulfide in aqueous media: Stoechiometry and kinetics. Environmental Science & Technology, v. 35, p. 2219-225.

King, L. H., Goodspeed, F. E., and Montgomery, D. S., 1963. A study of sedimented organic matter and its natural derivatives. Canada Deptarment of Mines and Technology Surveys, Mines Branch. Research Report. R 114, 66 p.

King, R. W., and Kerrich, R. W., 1989. Chromium dravite associated to ultramafic-rock-hosted Archean lode gold deposits, Timmins-Porcupine district, Ontario. Canadian Mineralogist, v. 27, p. 419-426..

Kretz, R., 1985. Calculation and illustration of uncertainty in geochemical analysis. Journal of Geological Education, vol. 33, p. 40-44.

Krogh, T.E., Corfu, F., Davis, D.W., Dunning, G.R., Heaman, L.M., Kamo, S.L., Machado, N., Greenough, J.D., and Nakamura, E., 1987. Precise U-Pb isotopic ages of diabase dykes and mafic to ultramafic rocks using trace amounts of baddeleyite and zircon; in Mafic Dyke Swarms, (ed.) H.C. Halls and W.F. Fahrig; Geological Association of Canada, Special Paper 34, p. 147-152.

Lafleche, M. R., Dupuy, C., and Dostal, J., 1992. Tholeiitic volcanic rocks of the late Archean Blake River Group, southern Abitibi greenstone belt; origin and geodynamic implications. Canadian Journal of Earth Sciences, v. 29, p. 1448-1458.

Lafrance, B., Mueller, W. U., Daigneault, R., and Dupras, N., 2000. Evolution of a submerged composite arc volcano; volcanology and geochemistry of the Normetal volcanic complex, Abitibi greenstone belt, Quebec, Canada. Precambrian Research, v. 101, p. 277-311.

Lawton, K. D., 1959. Geology and petrogenesis of the Archean Abitibi Belt in the Kirkland Lake area, Ontario. Ontario Geological Survey Miscellaneous Paper 123, p. 130.

Leeman, W. P., and Sisson, V. B., 1996. Geochemistry of Boron and Its Implications for Crustal and Mantle Processes. Reviews in Mineralogy, v. 33, p. 645-707.

Lofgren G.E. 1971. Experimentally produced devitrification textures in natural rhyolitic glass. Geological Society of America Bulletin, v. 82, p.111-124.

Lofgren, G. 1974. An experimental study of plagioclase crystal morphology: isothermal crystallization. American Journal of Science, v. 274, p. 243-273.

Maclean, W. H., and Kranidiotis, P., 1987, Immobile elements as monitors of mass transfer in hydrothermal alteration: Phelps Dodge massive sulphide deposit, Matagami, Québec: Economic Geology, v. 82, p. 951-962.

Maclean, W. H., 1988, Rare earth element mobility at constant inter-REE ratios in the alteration zone of the Phelps Dodge massive sulphide deposit, Matagami, Québec: Mineralium Deposita, v. 23, p. 231-238.

Manley, C.R. and Fink, J.H., 1987. Internal textures of rhyolite flows as revealed by research drilling. Geology, v.15, p. 549-552.

Manley, C.R. ,1992. Extended cooling and viscous flow of large hot rhyolite lavas: Implications of numerical modeling results. Journal of Volcanology and Geothermal Research, v. 53, p. 27-46.

Mason, R., & Melnik, N. (1986). The anatomy of an Archean gold system -The McIntyre-Hollinger complex at Timmins, Ontario, Canada. *In* Proceeding of gold '86:, An International Symposium on the Geology of Gold, Konsult International, Toronto, p. 40-55.

McConnell, V,S., Ferns, M.L., Proscal, M.A., Wacaster, S.G., Madin, I.P., and Betteridge, I.P. 2002. New mapping of a mid to late Miocene calc-alkaline volcanic field in NE Oregon: Geological Society of America, Cordilleran Section Annual Meeting. http://gsa.confex.com/gsa/2002CD/finalprogram/abstract_34192.htm

McCuaig, T.C, Kerrich, R., 1998. P-T-t-deformation-fluid characteristics of lode gold deposits: evidence from alteration systematics. Ore Geology Reviews, vol. 12, p. 381-453.

McDougall, G. J., and Hancock, R. D., 1980. Activated Carbons and Gold - A literature Survey. Minerals Science and Engineering, v. 12, p. 85-99.

McPhie, J., Doyle, M., and Allen, R., 1993, Volcanic Textures: Centre for Ore Deposit and Exploration Studies, University of Tasmania, p.197.

Melnik-Proud, N., 1992. The geology and ore controls in and around the McIntyre mine at Timmins, Ontario, Canada. Earth Sciences Unpublished Ph.D. thesis, Kingston, Queen's University, 353p.

Michard, A., Albarède, F., Michard, G., Minster, J.F. and Charlou, J.L., 1983. Rare-earth elements and uranium in high-temperature solutions from east Pacific Rise hydrothermal vent field (13°N). Nature, vol. 303, p. 795-797.

Michard, A. and Albarède, F., 1986. The REE content of some hydrothermal fluids. Chemical Geology, vol. 55, p 51-65.

Michard, A., Beaucaire, C and Michard, G., 1987. Uranium and rare earth elements in CO_2-rich waters from Vals-les-Bains (France). Geochimica et Cosmochimica Acta, vol. 51, p. 901-909.

Michard, A., 1989. Rare earth element systematics in hydrothermal fluids (Letter). Geochimica et Cosmochimica Acta, vol. 53, p. 745-750.

Moritz, R.P., and Crocket, J.H., 1991. Hydrothermal Wall-Rock Alteration and Formation of the Gold-Bearing Quartz-Fuchsite Vein at the Dome Mine, Timmins Area, Ontario, Canada. Economic Geology, vol. 86, p. 620-643.

Mueller, W., Donaldson, J. A., and Doucet, P., 1994. Volcanic and tectono-plutonic influences on sedimentation in the Archaean Kirkland Basin, Abitibi greenstone belt, Canada. Precambrian Research, v. 68, p. 201-230.

Mueller, W. U., Daigneault, R., Mortensen, J. K., and Chown, E. H., 1996. Archean terrane docking; upper crust collision tectonics, Abitibi greenstone belt, Quebec, Canada, *in* van der Pluijm, B. A., Kusky, T. M., Condie, K. C., and Coney, P. J., eds., Tectonophysics, 265, p. 127-150.

Nieboer, E., Jusys, A.A., 1988. Biologic chemistry of chromium: In: Nriagu J.O. & Nieboer E., eds. Chromium in natural and Human Environments. New York: Wiley.

Oliver, H. S., Hughes, D. J., Hall, R. P., and Johns, G. W., 2000, Lithogeochemistry of the Shining Tree area: in: Summary and Field Works an Other Activities, Ontario Geological Survey, v. Open File Report 6032, p. 6.1 to 6.14.

Olivo, G.M., and Williams-Jones, A.E., 2002. Genesis of the auriferous C quartz-tourmaline vein of the Siscoe Mine, Val d'Or District, Abitibi Subprovince, Canada: structural, mineralogical and fluid inclusion constraints. Economic Geology, vol. 97, p. 929-947.

Palmer, M. R., and Swilhart, G. H., 1996, Boron isotope geochemistry: An Overview. Reviews in Mineralogy, v. 33, p. 709-744.

Péloquin, A.S., Verpaelst, P., and Ludden, J.N. 1996. Spherulitic rhyolites of the Archean Blake River Group, Canada: Implications for stratigraphic correlation and volcanogenic massive sulfide exploration. Economic Geology, v. 96, p. 343-354.

Percival, J. A., and Card, K. D., 1983, Archean crust as revealed in the Kapuskasing Uplift, Superior Province, Canada. Geology, v. 11, p. 323-326.

Percival, J. A., and Card, K. D., 1985. Structure and evolution of Archean crust in central Superior Province, Canada, *in* Ayres, L. D., Thurston, P. C., Card, K. D., and Weber, W., eds., Special Paper - Geological Association of Canada, vol.28, p. 179-192.

Pinkerton, H. and Stevenson, R.J., 1992. Methods of determining the rheological properties of magmas at sub-liquidus temperatures. Journal of Volcanology and Geothermal Research, v.53, p. 47-56.

Polat, A., and Kerrich, R., 2001. Geodynamic processes, continental growth, and mantle evolution recorded in late Archean greenstone belts of the southern Superior Province, Canada. Precambrian Research, v. 112, p. 5-25.

Powell, W. G., Carmichael, D. M., and Hodgson, C. J., 1995. Conditions and timing of metamorphism in the southern Abitibi greenstone belt, Quebec. Canadian Journal of Earth Sciences, v. 32, p. 787-805.

Pressacco, R., 1999. Special project; ore deposit descriptions of the Timmins area.

Pyke, D.R., 1982. Geology of the Timmins Area District of Cochrane. Ontario Geological Survey Report 219, 141 p.

Rasmussen, B., 2005. Evidence for pervasive petroleum generation and migration in 3.2 and 2.63 Ga shales. Geology, v. 33, p. 497-500.

Rhys, D. A., 1999. Report on Structural Setting and Controls on Gold Deposits in the Porcupine Mining Camp, Northern Ontario, unpublished Company Report, Porcupine Joint Venture, 154 p.

Rhys, D.A., 2003a. Report on January-February 2003 Structural studies of the Hoyle Pond Mine, Timmins, Ontario, Porcupine Joint Venture, unpublished company report, p. 36.

Rhys, D.A., 2003b. Structural style and setting of gold deposits, Hollinger-McIntyre to Pamour, Porcupine mining camp; A Field trip for the Placer Dome exploration seminar, October 1, 2003.

Richard, F.C., Bourg, A.C.M., 1991. Aqueous geochemistry of chromium. A review: Water Resource, v. 25, p. 807-816.

Robert, F., 2001. Syenite-associated disseminated gold deposits in the Abitibi greenstone belt, Canada. Mineralium Deposita, vol. 36, p. 503-516.

Ropchan J.R., L. B., Fowler A.D., Benn K., Ayer J., Berger B., Dahn, R., Labine, R., and Amelin, Y., 2002. Host Rock and Structural Controls on the Nature and Timing of Gold Mineralization at the Holloway Mine, Abitibi Subprovince, Ontario. Economic Geology, v. 97, p. 291-309.

Rose, B., 1924. Murphy, Hoyle and Matheson Township: Ontario Department of Mines Report 33. p. 50-54.

Russell, J.K., Giordano, D. and Dingwell, D., 2003. High-temperature limits on viscosity of non-Arrhenian silicate melts. American Mineralogist, v. 88, p. 1390-1394.

Ryan, M.P. and Sammis, C.G., 1981. The glass transition in basalt. Journal of Volcanology and Geothermal Research, v. 86, 9519-9535.

Rye, K. A., 1987. Geology and Geochemistry of the Hoyle Pond Gold Deposit, Timmins, Ontario. Earth Sciences department, Unpublished Master's thesis, London, University of Western Ontario, 220 p.

Sangster, A. L., and Bourne, J., 1982. Geology of the Grenville Province, and regional metallogenesis of the Grenville Supergroup. Special Paper - Geological Association of Canada, v. 25, p. 91-125.

Sapek, B., Sapek, A., and Okruzko, H., 1980. Optical properties of alkaline soil extracts as a test characterizing humic substances from peat soils. *In* Proceeding of the 6th International peat society. Duluth, Minnesota, USA, August 1980, 735 p.

Sass, B.M., and Rai, D., 1987. Solubility of Amorphous Chromium (III)-Iron (III) Hydroxide Solid Solutions. Inorganic Chemistry, vol. 26, p. 2228-2232.

Sato, H., Nakada, S., Fujii, T., Nakamura, M., and Suzuki-Kamata, K., 1999. Groundmass pargasite in the 1991-1995 dacite of Unzen volcano; phase stability experiments and volcanological implications. Journal of Volcanology and Geothermal Research, v. 89, p. 197-212.

Sato, H., 2005. Viscosity measurements of subliquidus magmas: 1707 basalt of Fuji volcano. Journal of Mineralogical and Petrological Sciences, v. 100, p. 133-142.

Saumur, B.-M., 2005, The variolitic intermediate lobate breccia of the V10B flow unit (Vipond formation, Abitibi greenstone belt): a detailed study at the fire-tower outcrop, Schumacher, Ontario. Unpublished B.Sc. thesis, University of Ottawa, Ottawa, 69 p.

Scott, C.R., and Mueller, W.U., 2001. Emplacement of a voluminous subaqueous felsic lava flow, Val d'Or, Québec, Canada. Geological/Mineralogical Association of Canada Annual Meeting, St.John's, http://gac.esd.mun.ca/gac_2001/seven/sub_program.asp?sess=98&form=10&abs_no=614

Scutter, C.R., Cas R.A.F., and Moore, C.L. 1998. Facies architecture and origin of a submarine rhyolite lava flow-dome complex, Ponza, Italy. Journal of Geophysical Research, v. 103, 27 p.

Seward, T.M., 1973. Thio complexes of gold and the transport of gold in hydrothermal ore solutions. Geochimica et Cosmochimica Acta, v. 37, p. 379–399.

Shaw, H.R., 1972. Viscosities of magmatic silicate liquids: an empirical method of prediction. American Journal of Science, v. 272, p. 870-893.

Shore, M., 1996. Cooling and crystallization of komatiite flows. Earth Science department, Unpublished Ph.D. thesis, University of Ottawa, Ottawa, 251 p.

Sparks, R.S.J., 1978. The dynamics of bubble formation and growth in magma: A review and analysis. Journal of Volcanology and Geothermal Research, v. 3, p. 1-37.

Springer, J. S., 1983. Invisible gold: Ontario Geological Survey Miscellaneous Paper, v. 110, p. 240-250.

Springer, J.S., 1984a. Entrapment of gold by sulphide and carbon in Archean gold ores of Ontario, Abstracts with Programs - Geological Society of America, 665 p.

Springer, J.S., 1984b. Active carbon in Archean rocks and its effect on gold concentration. Program with Abstracts - Geological Association of Canada; Mineralogical Association of Canada; Canadian Geophysical Union, Joint Annual Meeting, v. 9, 107 p.

Springer, J. S., 1985. Carbon in Archean rocks of the Abitibi Belt (Ontario-Quebec) and its relation to gold distribution. *in* Macqueen, R. W., and Coope, J. A., eds., Canadian Journal of Earth Sciences, 22, p. 1945-1951.

Sproule, R. A., Lesher, C. M., Ayer, J. A., Thurston, P. C., and Herzberg, C. T., 2002. Spatial and temporal variations in the geochemistry of komatiites and komatiitic basalts in the Abitibi greenstone belt. Precambrian Research, v. 115, p. 153-186.

Stefansson, A., and Seward, T. M., 2003. The hydrolysis of gold (I) in aqueous solutions to 600 degrees C and 1500 bar. Geochimica et Cosmochimica Acta, v. 67, p. 1677-1688.

Stewart, A.L., and McPhie, J., 2003. Internal structure and emplacement of an Upper Pliocene dacite cryptodome, Milos Island, Greece. Journal of Volcanology and Geothermal Research, v. 124, p. 129-148.

Stone, W. E., Crocket, J. H., Dickin, A. P., and Fleet, M. E., 1995. Origin of Archean ferropicrites: geochemical constraints from the Boston Creek Flow, Abitibi greenstone belt, Ontario, Canada. Chemical Geology, v. 121, p. 51-71.

Sun, S.S., and McDonough, W.F., 1989. Chemical and Isotopic systematics and oceanic basalts; implications for mantle composition and processes, In: Saunders A.D., Norry, M.J., eds. Magmatism in the oceans basins. Boston, Blackwell Scientific, p. 315-345.

Szulczewski, M.D., Helmke, P.A., and Bleam, W.F., 2001. XANES spectroscopy studies of Cr (VI) reduction by thiol in organosulphur compounds and humic substances. Environmental Science Technology, v. 35, p. 1134-1141.

Tait, L., 1987. The character of organic matter and the partitioning of trace and rare earth elements in black shales; Blondeau Formation, Chibougamau, Quebec. Unpublished Master's thesis, Université du Quebec a Chicoutimi, 140 p.

Thompson, P. H., 2005. A new metamorphic framework for gold exploration in the Timmins-Kirkland Lake area, Western Abitbi greenstone belt: Discover Abitibi Initiative, 104 p.

Thornton, E.C. and Amonette, J.E., 1999. Hydrogen sulfide gas treatment of Cr (VI)-contaminated sediment samples from a plating-waste disposal site-implications for in-situ remediation. Environmental Science Technology, vol. 33, p. 4096-4101.

Thurston, P.C., Ayer, J.A., Goutier, J., and Hamilton, M.A., under revision. Depositional gaps in Abitibi Greenstone Belt Stratigraphy: a key to exploration for syngenetic mineralization, Economic Geology, Abitibi Special Volume.

Tomlinson, K.Y., Bowins, R., and Hechler, J., 1999. Refinement of hafnium (Hf) and zirconium (Zr) ICP-MS analysis by improvement in the sample digestion procedure. *In* Summary of Field Work ant Other Activities, Ontario Geological Survey, p. 189-192.

Vaillancourt, C., Pickett, C.L. and Dinel, E., 2001 Precambrian Geology; Timmins West-Bristol and Ogden Townships. Map-Ontario Geological Survey, Report P3436, 1 sheet.

Verpaelst, P., Peloquin, A. S., Adam, E., Barnes, A. E., Ludden, J. N., Dion, D.-J., Hubert, C., Milkereit, B., and Labrie, M., 1995. Seismic reflection profiles across the "Mine Series" in the Noranda Camp of the Abitibi Belt, Eastern Canada. Canadian Journal of Earth Sciences, v. 32, p. 167-176.

Waters, J,C. and Binns, R.A. 1998. Contrasting styles of felsic submarine volcanism, Eastern Manus Basin, Papua New Guinea. Abstracts from the 14th Australian Geological Convention, 6-10th July 1998, Townsville.
www.syd.dem.csiro.au/research/hydrothermal/jo/abstracts/AGC1998.htm.

Wedenpohl, K. H., 1995, The composition of the continental crust Geochimica et Cosmochimica Acta, v. 59, p. 1217-1232.

Whipple, E.R., 1974,. A study of Wilson's determination of ferrous iron silicates. Chemical Geology, vol. 14, pp. 119-134.

White, B. W., and Roy, R., 1975. The system chromium-oxygen at high oxygen pressures. Geochimica et Cosmochimica Acta, v. 39, p. 803-817.

Wilson, A.D., 1960. The micro-determination of ferrous iron in minerals by a volumetric and calorimetric method. Analyst, vol. 85, p. 823-827.

Wilson, G.C. 1986. A petrographic study of carbonaceous rocks in gold deposits. Geological Association of Canada / Mineralogical Association of Canada, Program with Abstract, v.11, p. 145.

Wilson, G.C., and Rucklidge, J.C. 1984. Mass spectrometric studies of carbonaceous materials from Archean gold deposits. Geological Society of America Abstracts with Programs, v. 16, 696 p.

Wilson, G.C., and Rucklidge, J.C., 1986. Lithological features and economic significance of reduced carbonaceous rocks in gold deposits. Ontario Geological Survey Miscellaneous Paper, 130, p. 177-189.

Winchester, J. A., and Floyd, P. A., 1977, Geochemical discrimination of different magma series and their differentiation products using immobile elements: Chemical Geology, v. 20, p. 325-343.

Wood, P.C., Burrows, D.R., Thomas, A., and Spooner, E.T.C., 1986. The Hollinger-McIntyre au-quartz vein system, Timmins, Ontario, Canada; geologic characteristics, fluid properties and light stableisotopes. *In* Proceeding of gold '86, An International Symposium on the Geology of Gold, Konsult International, Toronto, p. 56-79.

Wyman, D. A., 2003. Upper mantle processes beneath the 2.7 Ga Abitibi belt, Canada: a trace element perspective. Precambrian Research, vol. 127, p. 143-165.

Wynne-Edwards, H. R., 1972. The Grenville Province. Special Paper - Geological Association of Canada, v. 11, p. 263-334.

Yamagishi, H., and Dimroth, H., 1985. A comparison of Miocene and Archean rhyolite hyaloclastites: Evidence for a hot and fluid rhyolite lava. Journal of Volcanological and geothermal Research, v. 23, p. 337-355.

Zouboulis, A.I., Kydros, K.A., and Matis, K.A., 1995. Removal of hexavalent chromium anions from solutions by pyrite fines. Water Resource, vol. 29, p. 1755-1760.

APPENDIX I

The Hoyle Pond mine is hosted in volcanic rocks stratigraphicaly observed at the base of the Tisdale Assemblage. It consists of a south facing homoclinal sequence of stacked volcanic rocks of the Hershey Lake formation and Central formation (Dinel et al., 2006). The Hershey lake formation is observed in the NVP and CVP mine volcanic sequence, and consists of interbedded high-Mg tholeiitic basalts, basaltic komatiites and komatiites. The Central formation is observed in the SVP and consists of interbedded high-Mg tholeiitic basalts and Fe-rich tholeiitic basalts. The volcanic sequence is complexly folded by at least 4 deformations events (Dinel et al., 2007) (D3-D6), and consists of a 1 km scale asymmetric z-folds (F4 folds) folding a previously formed S3 fabric parallel to bedding.

The mineralization at Hoyle Pond is observed in two zones, the North Hoyle Pond zone hosted in mafic volcanic rocks of the Hershey Lake formation and in the 1060 zone hosted in volcanic rocks of the Central formation. The Hoyle Pond zone mineralization occupies D3 and D4 structures and consists of free gold in quartz-carbonate fault-fill and extensional veins. In addition, the mineralization appears to be hosted at flow contacts (see map 3level, annexe 3). The 1060zone mineralization consists of free gold in quartz-carbonate fault-fill and extensional veins. The main mineralization is hosted in D3 and D4 structures, emplaced at flow contacts and on the limbs of isoclinal F4 folds anticline (Dinel et al., 2006). The two mineralization zones occupy structures oriented 070°.

The alterations enveloping the mineralization are characterized by a zonation; a sericite alteration zones which consist of muscovite, Cr-muscovite, ferroan-dolomite, graphite, quartz, pyrite and arsenopyrite, and a albite alteration zones composed of albite and carbonates. We have proposed that the mineralization was formed by fluid mixing, from a reducing fluid carrying gold and an oxidizing fluid in which the interaction of the fluids. Based on the presence of mobile Cr, organic matter and Au transported by thio complex (Seward, 1979). We have proposed that the Cr was remobilized by an oxidizing fluid, reacted with a thio-organo-Au complex, precipitating Au, forming graphite, pyrite,

arsenopyrite, tourmaline, muscovite, Cr-muscovite, carbonate, albite and quartz (Dinel et al. 2007). Other deposits in the Timmins area have similar characteristic to the Hoyle Pond mine.

Comparison to the Hollinger and McIntyre mine

The Hollinger-McIntyre Mines in Tisdale Twp., Timmins, Ontario, Canada, are hosted in intermediate (Saumur et al., under revision) to mafic volcanic rocks of the Central Formation, the Vipond formation, the Gold Centre formation, and late felsic intrusive porphyries (Brisbin, 1997; Melnik-Proud, 1992, Pyke, 1982, Ferguson, 1968, Jones, 1948, Dunbar, 1948, Hurst, 1935). The Au mineralization is hosted in structures with an orientation of 070°, in fault-fill and extensional veins. The veins at Hollinger are in part emplaced at flow contacts (Brisbin, 1997) on the south limb of the Hollinger isoclinal anticline fold. Bateman et al., (2005) associated the Hollinger fold to the D4 event. In terms of alteration, Melnik-Proud (1992) and Brisbin (1997) described alteration mineralogy proximal to mineralization to be composed of sericite (muscovite), carbonate, quartz, tourmaline, pyrite and arsenopyrite and distal albite alteration. Brisbin (1997) also reported Au mineralization spatially associated with argilitic sediments, inter flow sediments, enrich in graphite (e.g. termed graphitic argillites). In terms of geometry, stratigraphy and alteration zonation the Hoyle Pond mine is similar to the Hollinger-McIntyre mines. The Hoyle Pond mine Au mineralization in the1060z is located in shear zone on the limbs of isoclinal anticline folds, the 1060fz is emplaced in volcanic rock of the Central formation and the alterations are similar (Dinel et al., 2006). The presence of graphitic argillite at Hollinger, reported by Brisbin (1997), also resembles the geological setting to the north thrust at Hoyle Pond where sediments of the Porcupine are graphite enriched and to the "Grey Zone" alterations observed in the mineralized zone.

Comparison to the Buffalo Ankerite- Delnite-Aunor Mines

The Buffalo Ankerite, Delnite and Aunor gold mine are located south of Timmins on an east-west segment approximately on the corridor of the Destor Porcupine Deformation

Zone (Pyke, 1982; Fyon, 1986). The mineralization is hosted in polymictic conglomerate and sandstone clastic rocks of the Timiskaming Assemblage, and in strongly carbonatized mafic-ultramafic volcanic rocks of the Hersey Lake Formation at the base of the Tisdale Assemblage (Pyke, 1982 and Fyon, 1986). Stratigraphicaly, the volcanic rocks of the Buffalo Ankerite, Delnite and Aunor Mines resembles to the rocks of the NVP and CVP at the Hoyle Pond mines. Thus the style of veining associated with mineralization is vaguely described, though some disseminated mineralization has been reported in the past (Atkinson, 2005.)

Ashanti mine (Ghana)

The Ashanti gold mine is located in Ghana (Africa) approximately 50km south of Oboasi. The area is characterized by belts of mafic volcanic rocks, unconformably underlain (thrust fault), with sedimentary rocks (Oberthuer et al., 1997) and cross cut by younger shear zones propagated from the thrust faults into the mafic volcanic rocks. The Au mineralization is emplaced in the shear zones and is enveloped by an alteration halo composed of muscovite, quartz, albite, tourmaline pyrite and arsenopyrite. In addition a significant amount of graphite was added to the host rock as a porosity filling. Oberthuer et al. (1997) suggested that the graphite was remobilised through the shear zones and originates from the sediments bounding the mafic belt.

Ste Yves deposits (Australia)

In addition, research done on the Ste-Yves gold deposit in Austrlia indicated gold mineralization associated to alteration pattern caused by oxidation-reduction chemical reaction that could be explained by fluid mixing chemical reaction (internal company report).

Cadillac-Larder Lake Fault shear zone Au mineralization

The Cheminis gold mine in King Kirland (Abitibi greenstone belt) shows similarities to Hoyle Pond associated. However, the main alteration is composed of roscoelite, a vanadium rich muscovite. The chemistry of vanadium is very similar to chromium. Vanadate solution is a very strong oxidant, like Cr^{6+}, and may play a similar role in the precipitation of gold. The precipitation of gold here could have been triggered by oxidation-reduction reactions caused by fluid mixing of reducing fluids and oxidizing fluid.

Summary

The Hoyle Pond mine shares similarities to other deposits in the Timmins gold camp. The mineralization is hosted in rocks of the same stratigraphy, in similar lithologies at the base of the Tisdale Assemblage, the Hershey Lake and Central Formation. It is hosted in structure, e.g. on the limbs of isoclinal folds at the contact of lithologies and with similar orientations. The mineral alterations enveloping the mineralization at Hoyle Pond mine is is similar to the one observed at McIntyre and Hollinger mines. In addition, the role of chrome in the mineralization process may be similar to the role of vanadium observed in V-rich muscovite in some gold deposits along the Cadillac-Larder Lake deformation zone. The graphite alteration is also spatially associated to gold mineralization at Hollinger and McIntyre mine, but also at the Ashanti mine in South Africa. Finally, the proposed model for fluid mixing of an oxidizing and reducing fluids based on the observation made at Hoyle Pond is comparable to the St-Yves gold deposits.